

SOUTHERN

~~ARIZONA~~

Land Subsidence and Earth-Fissure Formation in Eastern Phoenix Metropolitan Area, Arizona

Troy L. P  w  
Department of Geology
Arizona State University
Tempe, Arizona 85287

Richard H. Raymond
Consulting Geologist
510 E. Greenway Dr.
Tempe, Arizona 85282

Herbert H. Schumann
U.S. Geological Survey
3738 N. 16th St. Suite E
Phoenix, Arizona 85016

INTRODUCTION

Land subsidence caused by groundwater withdrawal has gained prominence in major coastal cities such as Tokyo, Venice, and Houston because of the danger of flooding from the sea. In the Central Valley of California subsidence was a factor in determining the gradient of an aqueduct system designed to provide an alternate water supply. In Arizona it was also a factor in the designing of a major aqueduct system being built to supplement the water supply, but earth fissures, which are uncommon in other subsiding areas, caused additional prob-

lems. Earth fissures are doubly terminated cracks in unconsolidated sediments that occur in areas of differential subsidence. They open only a fraction of an inch, but capture surface-water drainage, which erodes fissure-gullies commonly as much as 10 feet wide and 20 feet deep. These fissure-gullies are becoming a problem for construction in the rapidly developing urban areas of Arizona, in addition to the gradient changes in sewer lines caused by subsidence. Subsidence and future earth-fissure locations were addressed by a recently completed U.S. Geological Survey - Bureau of Re-

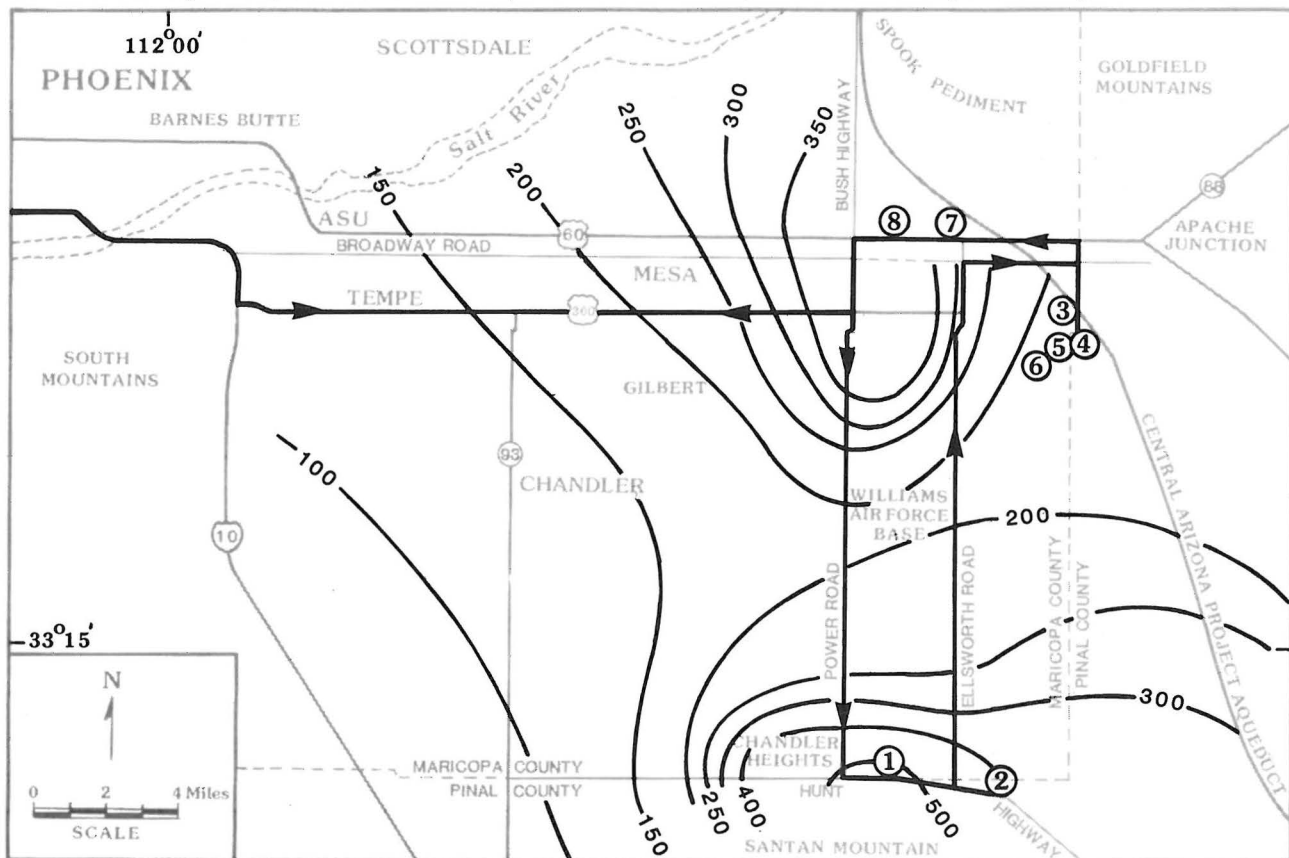


Figure 1. - Index map of southwestern Maricopa and northern Pinal Counties, central Arizona, showing location of field-trip route and stops (circled numbers) and contour lines in feet illustrating drop of water table in the area from 1900 to 1983. Water-table information from Thomsen and Baldys III (1985). Base map modified from Mesa 1:250,000 topographic map of the U.S. Geological Survey, 1969.)

clamation study for the aqueduct systems of the Central Arizona Project. Other public concerns are being addressed by an Arizona Governor's Committee headed by the Arizona Department of Water Resources. Please see Strange (1983) for a list of references and Schumann and Genualdi (1986) for a map of subsidence, earth fissures, and water-level change in southern Arizona.

Groundwater withdrawal in Arizona exceeds recharge per year by 2.2 million acre feet (Briggs, 1976). This has caused groundwater-level declines in some basins of more than 500 feet and widespread subsidence of the land surface in southern Arizona, locally up to 15 feet (oral communication, Carl Winikka, Assistant State Engineer, Arizona Department of Transportation, June 1985).

Earth fissures occur in unconsolidated sediments, typically near the margins of basins where groundwater levels have declined from 180 feet to more than 500 feet. The first surface indication of an earth fissure may be hairline cracks, a line of holes, or an already eroded fissure gully. Earth fissures in southern Arizona occur in calichified soils under tensile stress caused by differential subsidence induced by water-level declines (Raymond, 1987). Recent work utilizing geophysical and geodetic surveying techniques shows that fissure locations correspond to the locations of buried bedrock hills, ridges, or fault scarps, and that differential surface subsidence and horizontal extension occurs at these sites (Sauck, 1975; Jennings, 1977; Pankratz and others, 1978; Jachens and Holzer, 1982; Schumann and others, 1984; Larson and Péwé, 1986; Schumann and others, 1986). Fissures in some locations occur for other



Figure 2. - Low oblique air photograph of curving earth fissure crossing Hunt Highway near Chandler Heights, Arizona. See Figure 3 for exact location and configuration. See p. 111 in Raymond and others (1978) for ground photograph. (Photograph No. PK 23,275 by Troy L. Pewe, June 1982).

reasons, such as where there are lateral variations in the type and thickness of alluvium (Raymond, 1986). Determination of the subsurface geology therefore permits more accurate predictions of fissure locations.

The purpose of this field trip is to show examples of earth fissures and fissure-gullies in a rapidly developing area, some of the problems they are causing, and a subsidence-monitoring installation, and to summarize some of the research that has been done.

REGIONAL SETTING

The southeast part of Maricopa County and adjacent Pinal County, the so-called "East Valley," is one of the most rapidly developing areas in the United States (Figure 1). Until recently, the fissure hazard had been confined to outlying agricultural areas, but with rapid widespread urbanization, fissures are now being encountered in developed areas. In 1980 a 400-foot-long fissure opened in Paradise Valley at a residential construction site in northeast Phoenix (Larson and Péwé, 1986). The field-trip area lies in an alluvial basin, the Basin and Range physiographic province, and is bounded by fault-block mountains (Figure 1). The unconsolidated alluvium is about 3000 to 4500 feet thick and locally up to 9000 feet. Since 1900 the water table has declined 100 to 300 feet and locally as much as 500 feet (Figure 1). With decline of the groundwater level, the land surface just west of Apache Junction has subsided; the maximum measured subsidence between 1948 and 1981 of a bench mark near U.S. Highway 60 and the Bush Highway is 5.1 feet (Figure 1). During the same interval, probably 6.3 feet of subsidence has occurred at two bench marks near the intersection of Broadway and Power Roads (Arizona Department of Transportation, 1981).

STOP 1

The deepest and widest earth fissure yet observed in Arizona crosses the Hunt Highway near Chandler Heights (Figure 1). It is 15 feet wide and open as a small crack to a depth of at least 50 feet. It lies along a small wash, which may cause the continued erosion. It is a multiple curved fissure (Figure 2) and has been known since at least 1960. Several subparallel fissures are present (Robinson and Peterson, 1963; Raymond and others, 1978). Péwé has rephotographed the site annually since 1972. [See photograph in Raymond and others, (1978, p. 111.)] The northern part of the fissure has been filled and a mobile home was built near by. Garbage has been dumped in the southern part of the crack for many years.

The level of the water table in the immediate area has dropped 400 to 500 feet since 1900, the greatest in the Phoenix region (Figure 1). The water table has dropped below the top of the bedrock knob and also below the shallow bedrock slope of Santan Mountains. The land surface is subsiding over irregular buried-bedrock topography. The large fissures are located on the side of a buried-bedrock hill about 500 feet high (Figure 3). Differential subsidence and compaction of the sediment has developed tensile stresses resulting in formation of the original cracks.

STOP 2

About 3 mi east of STOP 1 on the Hunt Highway lies a cluster of earth fissures, which occur in caliche-cemented gravelly alluvium on the east, west, and north side of a bedrock knob almost isolated from Goldmine Mountain. It is characteristic for the fissures to be parallel or subparallel to the mountain front; these fissures maintain such

a position as they "wrap around" the bedrock extension of the mountain to surround the knoll on three sides.

The two parallel fissures on the north side show vertical displacement and have broken and displaced a concrete-lined irrigation ditch. The area between the two fissures has been displaced downward. Displacement is about 2 feet on the south side.

The fissures on the east side have cracked concrete-lined ditches north of the highway and have formed gullies 10 feet wide and 12 feet deep on the south side of the highway. Road works have filled these gullies but they continue to open, erode, and endanger the highway. Two photographs of fissures in this area are in Raymond and others (1978).

The water table in the immediate area (Figure 1) has dropped about 500 feet and much of the area near the bedrock knoll is dewatered. The drop of the water table and compaction of the overlying sediments has permitted fissuring at the "hinge-line" (see Larson and Péwé, 1986, Figure 17 for diagrammatic sketch of geologic settings of potential fissuring).

STOP 3

Two compaction recorders, also called vertical extensometers, were installed at this location in 1978 as part of the study for the Central Arizona Project by the U.S. Geological Survey and Bureau of Reclamation. A recording device measures the change in distance between the ground surface and the top of a steel pipe, which is anchored at the bottom of a cased drill hole and extends to the surface. Compaction of the alluvium between the bottom of the hole and the surface is thus recorded. The bottom of one installation was set at the top of rock at a depth of about 1200 feet (Figure 4). The other was

set at about 600 feet in alluvium. Compaction of about 0.2 feet per year has been recorded by the deeper recorder, which compares very closely to the amount of subsidence measured by surveying. Compaction measured by the other recorder was about half as much. Water-level recorders measure the change in water level inside the casing in the installations. Water level has fallen about 5 feet per year from 1976 to 1986.

STOP 4

Earth fissures were discovered here in 1976 that were only about 1500 feet from the alignment of the Central Arizona Project Aqueduct. Since then additional fissures have formed, but they have not extended closer to the aqueduct.

Extensive research was done at this site starting in 1976 on the geologic occurrence and physical behavior of earth fissures as part of the U.S. Bureau of Reclamation - Geological Survey subsidence investigations for the Central Arizona Project (Raymond, 1985). The objectives of this research were to (1) determine if there was a correlation between the location of the fissures and the subsurface geology; (2) measure the vertical and horizontal ground-surface movements associated with the fissures; (3) observe the erosional effects of water at the fissures; (4) test possible remedial measures to limit erosion; and (5) test geophysical methods for subsurface detection of fissures.

To determine the subsurface geology, refraction and reflection seismic surveys and Bouguer anomaly gravity surveys were made from near STOP 3, across the fissures, to Hawk Rock (STOP 6). Holes were drilled to crystalline rock and geophysically logged to learn the stratigraphy and calibrate geophysical models. Figure 4 illustrates the relationship of the earth fissures to the subsurface geology as

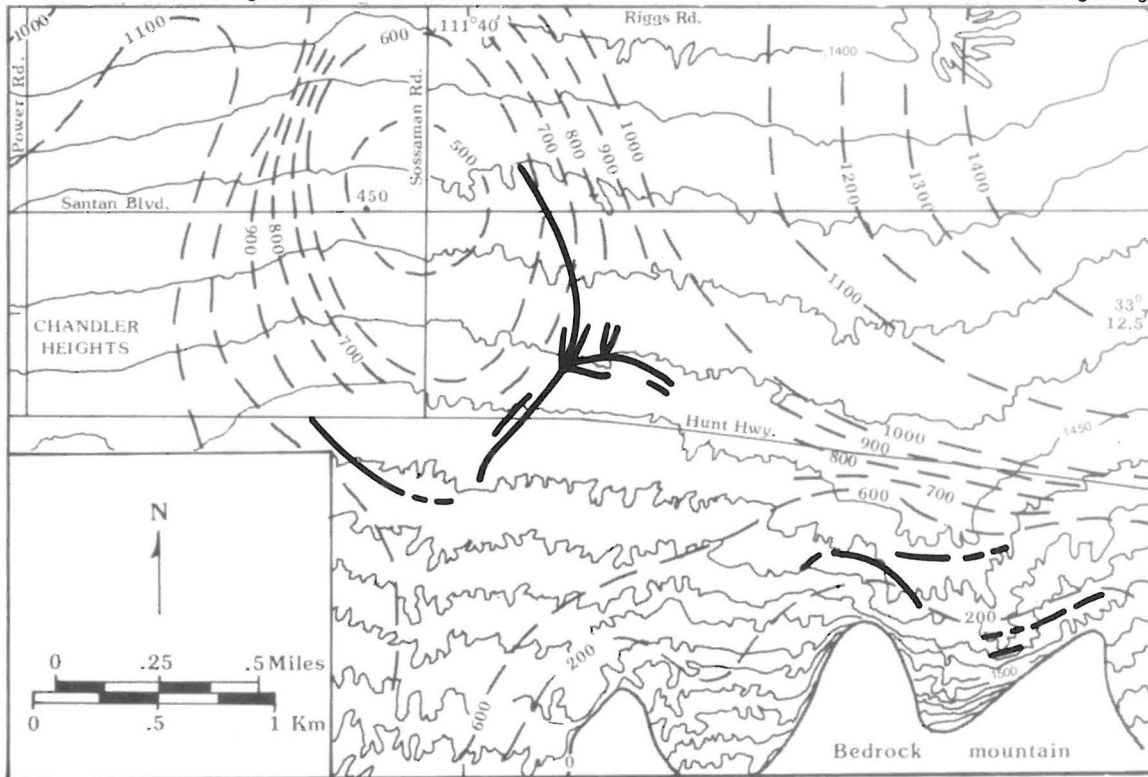


Figure 3. - Map of the Chandler Heights area, Maricopa and Pinal Counties, showing depth to bedrock in feet beneath alluvium (heavy dashed lines), surface topography in feet (light solid lines), & location of earth fissures (heavy solid lines). Depth to buried bedrock surface estimated from gravity and well data (Map slightly modified from Jennings, 1977).

interpreted from the collected data. The figure shows that Hawk Rock is the highest peak of an otherwise buried mountain. The fissures occur over buried ridges (Pankratz and others, 1978; Hassemer and Dansereau, 1980). Level data showed that differential subsidence occurred on either side of the ridge, and horizontal surveys showed that land-surface extension occurred over the ridge and normal to the fissures (Raymond and others, 1979).

Earth fissures are known to capture surface water (see Figures 5 and 6). In fact, the fissure-gully resulting from surface water erosion has sometimes been confused with the earth fissure itself. The most obvious damage that might occur to a structure would be from collapse into a fissure-gully. Water was pumped into one of the fissures at this stop to define the erosional process better. Initially the water flowed downward into the fissure, enlarging it until a cemented layer was encountered. The fissure in the cemented layer did not erode, but rather plugged up with material eroded from above. The water ponded here for a time and then piped laterally in the soil along the fissure above the cemented layer until it reached a point beyond the plug in the cemented layer. The pipe enlarged for a time as it carried more water

until it collapsed from the surface. The collapsed material plugged the fissure in the cemented layer, and piping started all over again. The collapsed pipes formed in this experiment were similar to fissure-gullies formed naturally (Raymond, 1985).

Self-potential, shear-wave, and resistivity geophysical methods were tested to determine if fissures could be detected in the shallow subsurface. The first two methods were successful, although resistivity detected a fissure when the soil was wet after recent rains but did not later after the soil had dried out.

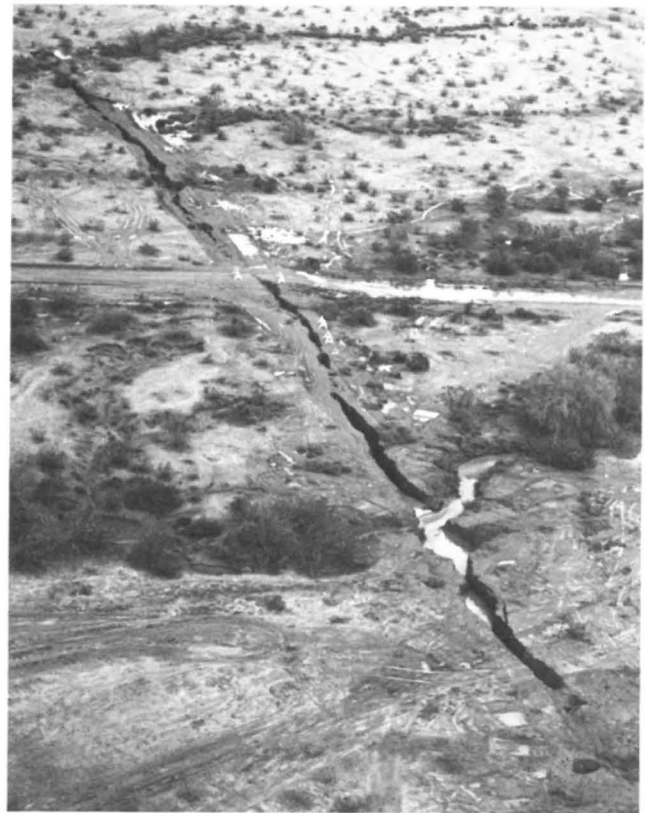


Figure 5.- Earth fissure near Apache Junction, Arizona capturing runoff from wash after a heavy rain. (Photograph No. P44-300-02501 by E. E. Hertzog, Bureau of Reclamation, March 1, 1978).

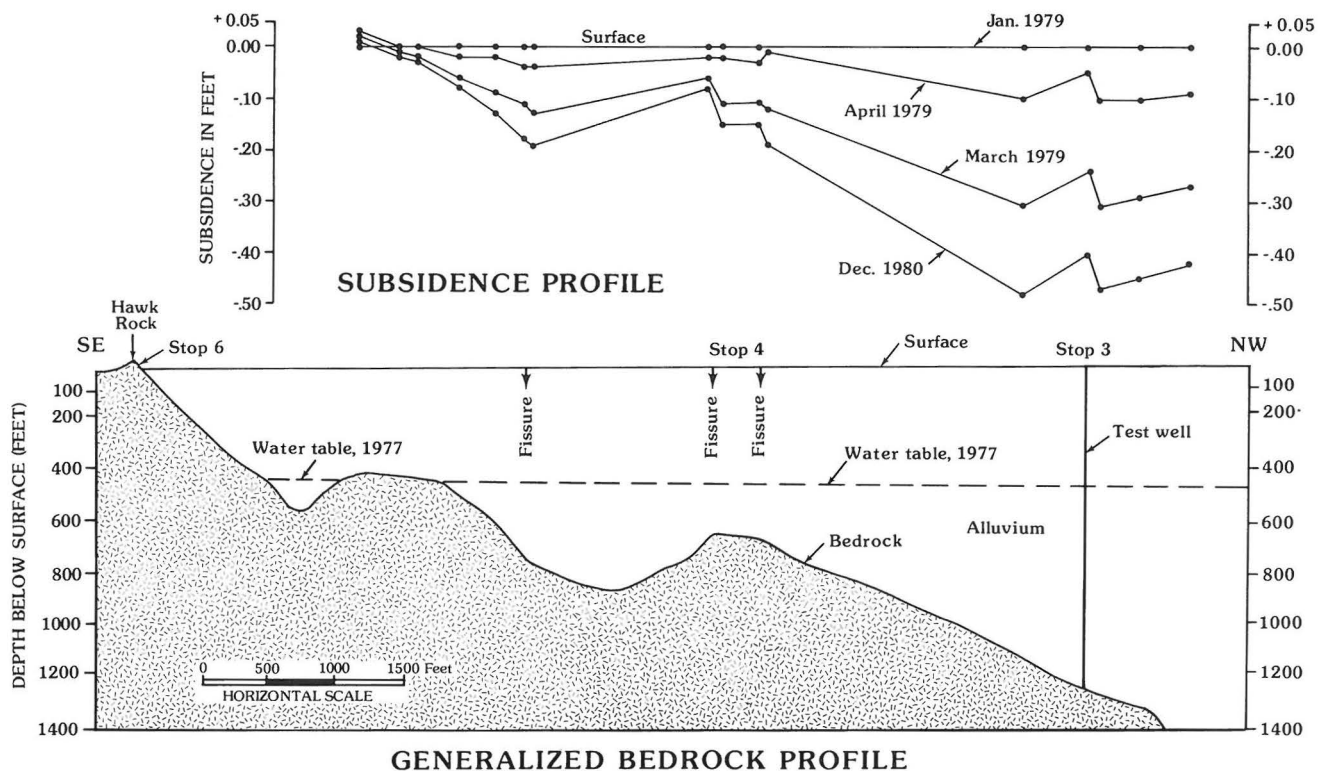


Figure 4. - Relationship of subsurface geology, water table, earth fissures, and land subsidence near Apache Junction, Arizona (Modified from Raymond, 1985).



Figure 6. - Erosion on earth fissure shown in Figure 5 after water receded.

STOP 5

A fissure-gully occurred here after very heavy rains in July 1984 (Figure 7). It was traceable as a hairline crack from about 25 feet inside the canal fence to across the road. From there to the house on the other side of the wash it was up to a few feet wide and 13.5 feet deep. The trace of the fissure appeared to pass under the corner of the house, which was under construction at the time. Water from the wash and a stock pond probably caused the fissure-gully. The owner of the house has sued the U.S. Bureau of Reclamation for directing the water into the wash. The U.S. Bureau of Reclamation has driven sheet piling 50 feet deep across the trace of the fissure to prevent a fissure-gully from forming that might damage the canal.



Figure 8. - Low oblique air view to the west of the Mesa earth fissure, Mesa, Arizona. Note fresh repair to fissure at junction of 76th Street and Albany Street (Photograph no. P25-300-7528 by E.E. Hertzog, U.S. Bureau of Reclamation, Oct. 17, 1967, 1967. See also 1971 photograph of this fissure at this locality; p. 117, Raymond and others, 1978).

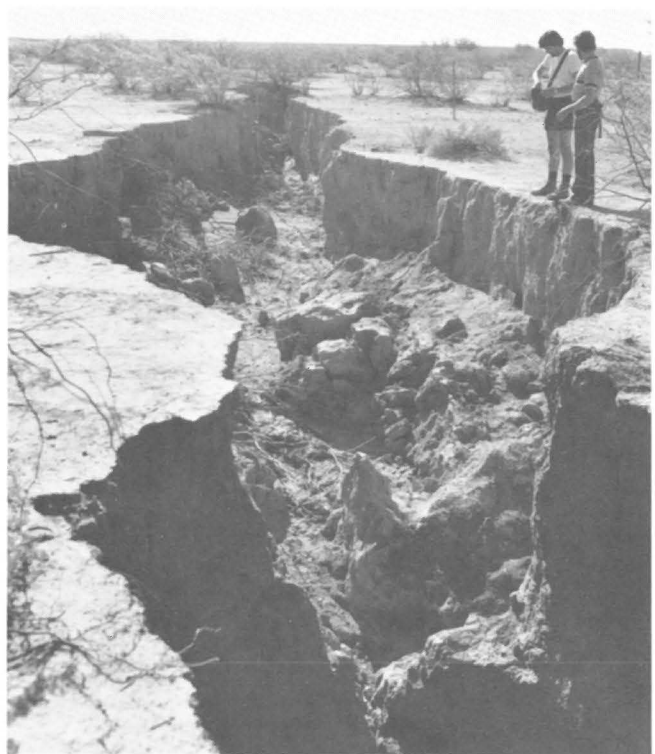


Figure 7. - This fissure formed July 18, 1984 in a matter of minutes when thousands of gallons of discharge water from a stock pond found egress into an underlying earth fissure in alluvium. The eroded fissure was about 600 feet long. Apache Junction, Arizona. (Photograph no. 4815 by Troy L. Pewe, August 25, 1984).

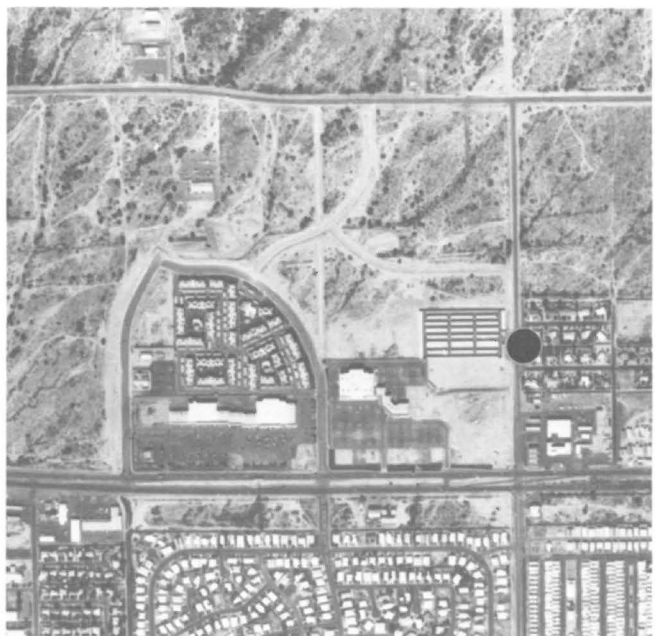


Figure 9. - Vertical air photograph of Mesa earth fissure area showing construction over and near the fissure. Black circle is near intersection of 76th Street and Albany (see Figure 8). Photograph taken Nov. 3, 1985. Courtesy Arizona Department of Transportation. (North is toward the top).

STOP 6

The two small quartzite outcrops are called "Hawk Rock." Geophysical data indicate that they are at the top of a mountain buried by alluvium (see Figure 4).

STOP 7

The fissure at this stop was first discovered in 1978. At that time it extended from the east side of 90th Street in an arcuate pattern across a vacant lot on the north side of U.S. Highway 60. Since that time it has eroded to as much as 15 feet deep and 5 feet wide in places, crossed all lanes of the highway, which had to be repaired, and connected to a new fissure on the south side of the highway. It will be interesting to see how the vacant lot is used in the future.

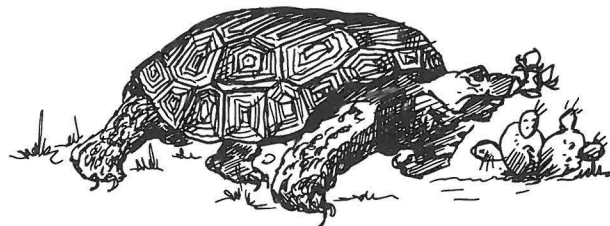
STOP 8

The earth fissure at 76th Street in east Mesa 300 feet north of the Apache Trail (U.S. Highway 60; Figure 1), earlier referred to as the Mesa earth crack (Anderson, 1973), first opened on Dec. 16, 1965 and extended about a mile to the west (Figure 8). It is as much as 3 feet wide and 15 feet deep, although it has been repeatedly filled and the area graded. The fissure is transverse to surface drainage and much runoff drains into the fissure. The groundwater table has dropped about 350 feet (Figure 1) in this area and the dewatered sediments have compacted. Gravity studies indicate that a buried bedrock ridge lies directly under the fissure.

Perhaps the most important aspect of this fissure is that land development has taken place in this area (Figure 9) and the fissure in the streets and elsewhere have been filled, patched, and covered, only to reappear (see p. 114, Raymond and others, 1978). Careful monitoring of the fissure to record reaction of buildings and other construction in the area is under way.

REFERENCES CITED

- Anderson, S.L., 1973, Investigation of the Mesa earth crack, Arizona, attributed to differential subsidence due to groundwater withdrawal, [Master's thesis]: Tempe, Arizona State University, 111 p.
- Arizona Department of Transportation, 1981, 1981 NGS level line, Apache Junction to I-10 at Miller Road, ADOT preliminary adjustment: Arizona Department of Transportation, Highways Division, Photogrammetry and Mapping Services, unpublished report, 192 p.
- Briggs, P.C., 1976, Arizona groundwater resources supplies and problems, in Proceedings, 20th Arizona Watershed Symposium, Phoenix, Report no. 8, September, 1976, p. 11-29.
- Hassemer, J.H., and Dansereau, D., 1980, Gravity survey in parts of Maricopa and Pinal Counties, Arizona: U.S. Geological Survey Open-File Report 80-1255, 65 p.
- Jachens, R.C., and Holzer, T.L., 1982, Differential compaction mechanisms for earth fissures near Casa Grande, Arizona: Geological Society of America Bulletin, v. 93, p. 998-1012.
- Jennings, M.D., 1977, Geophysical investigations near subsidence fissures in northern Pinal and southern Maricopa Counties, Arizona [Master's thesis]: Tempe, Arizona State University, 102 p.
- Larson, M.K., and Péwé, T.L., 1986, Origin of land subsidence and earth fissuring, northeast Phoenix, Arizona: Association of Engineering Geologists Bulletin, v. 23, no. 2, p. 139-165.
- Pankratz, L.W., Hassemer, J.H., and Ackermann, H.D., 1978, Geophysical studies relating to earth fissures in central Arizona [abs.]: Geophysics, v. 44, no. 3, p. 367.
- Raymond, R.H., 1985, Earth fissure investigations for Reach 2A, Salt-Gila Aqueduct, Central Arizona Project, Arizona: U.S. Bureau of Reclamation, Arizona Projects Office, internal report, 24 p.
- 1986, Seven geologic settings for earth fissures in south-central Arizona [abs.]: Journal of the Arizona-Nevada Academy of Science, Proceedings Supplement, v. 21, p. 51.
- 1987, Why land-subsidence related earth fissures are more common in Arizona than elsewhere: Geological Society of America Abstracts with Programs, v. 19, no. 6.
- Raymond, R.H., Laney, R.L., Pankratz, L.W., Riley, F.S., and Carpenter, M.C., 1979, Relationship of earth fissures in alluvial basins in south-central Arizona to irregularities in the underlying formations: Geological Society of America Abstracts with Programs, v. 11, no. 7, p. 501.
- Raymond, R.H., Winikka, C.L., and Laney, R.L., 1978, Earth fissures and land subsidence-eastern Maricopa and northern Pinal Counties, Arizona, in Burt, D.M., and Péwé, eds., T.L., Guidebook to the geology of central Arizona: Arizona Bureau of Geology and Mineral Technology Special Paper 2, p. 107-114.
- Robinson, G.M., and Peterson, D.E., 1963, Notes on earth fissures in southern Arizona: U.S. Geological Survey Circular 466, 7 p.
- Sauck, W.A., 1975, Geophysical studies near subsidence fissures in central Arizona [abs.]: EOS (American Geophysical Union Transactions), v. 56, no. 12, p. 984-985.
- Schumann, H.H., and Genualdi, R., 1986, Land subsidence, earth fissures, and water-level change in southern Arizona: Arizona Bureau of Geology and Mineral Technology Map 23, scale 1:1,000,000.
- Schumann, H.H., Laney, R.L., and Cripe, L.S., 1986, Land subsidence and earth fissures caused by groundwater depletion in southern Arizona, in Anderson, T.W., and Johnson, A.I., eds., Regional aquifer systems of United States, southwest alluvial basins of Arizona: American Water Resources Association Monograph Series no. 7, p. 81-91.
- Schumann, H.H., Tosline, D.J., and Rege, D.M., 1984, Occurrence and prediction of earth-fissure hazards caused by groundwater depletion in south-central Arizona, U.S.A. [abs.], in Replogle, J.A., and Renard, K.G., eds., Water today and tomorrow: American Society of Civil Engineers Specialty Conference, Flagstaff, July 1984, Proceedings, p. 673.
- Strange, E., 1983, Subsidence monitoring for State of Arizona: National Oceanic and Atmospheric Administration, National Geodetic Survey, 74 p.
- Thomsen, B.W., and Baldys, S., III, 1985, Groundwater conditions in and near the Gila River Indian Reservation, south-central Arizona: U.S. Geological Survey Water-Resources Investigations Report 85-21073, scale 1:250,000, 2 sheets.



Selected Hydrogeologic Problems in Central Arizona

Thomas L. Holzer
U.S. Geological Survey
345 Middlefield Road
Menlo Park, California 94025

Mario R. Lluria
Salt River Project
1500 Project Drive
Tempe, Arizona 85281

INTRODUCTION

Over the past 40 years, agricultural activities and rapid growth in central Arizona have produced accelerated depletion of ground-water supplies throughout this portion of the southern Basin and Range physiographic province. Problems associated with overdrafting of the aquifers include increased pumping lifts, changes in regional ground-water flow regimes, deterioration of ground-water quality, and land mass subsidence.

The purpose of this field trip is to offer a description of the hydrogeologic framework of this region, in addition to examining some of its problems and possible solutions being adopted to mitigate and correct overdrafting of reserves. During the morning portion of this trip, Stops 1, 2, and 4 (Figure 1), we will visit surface exposures of rock units that host various segments of the alluvial aquifer system. Stop 3 is the pilot-project test site for the City of Phoenix Cave Creek Recharge Project.

Within the Phoenix metropolitan area, artificial ground-water recharge studies are being conducted in order to evaluate replenishment of aquifers, storage and recovery of imported water, subsidence control, and remediate ground-water contamination. At present, four major recharge projects are under investigation for this area. They include City of Phoenix Cave Creek Recharge Project, City of Scottsdale Recharge Project, Arizona Municipal Water Users Association Recharge Project, and Maricopa County Flood Control District Recharge Project.

HIGHLIGHTS EN ROUTE TO STOP 1

The trip this morning will commence in downtown Phoenix, northward towards Camelback Mountain. We will cross the historic Grand Canal, an unlined, open channel that conveys water from the Salt River to agricultural areas in western Phoenix and Glendale.

STOP 1. CAMELBACK MOUNTAIN

The Phoenix metropolitan area is located within the Basin and Range physiographic province. In this region of central Arizona, ground water is produced from alluvial aquifers contained within deep structural basins. The formation of these basins commenced during mid-Tertiary time, approximately 25 Ma. At that time a prevailing extensional regime generated low-angle normal faults, which in turn produced listric normal faults that originated basins. This period was followed by one of high-angle faulting with the generation of numerous horst and graben structures. These were superimposed on the earlier structures and created the present-day basins. (Figure 2).

Erosion of the ranges into the basins created during these tectonic events of Tertiary age produced the sedimentation of the geologic units that constitute the aquifers of this region. Each phase of the tectonic evolution is reflected in the physical character of the corresponding unit and consequently in the hydraulic properties of the aquifers. These units range from the poorly sorted, coarse-grained, high-energy fanglomerates with high permeability and storage, to the very fine grained, low-energy lacustrine sediments with good storage capabilities but poor transmissive properties. Predominantly andesitic to basaltic

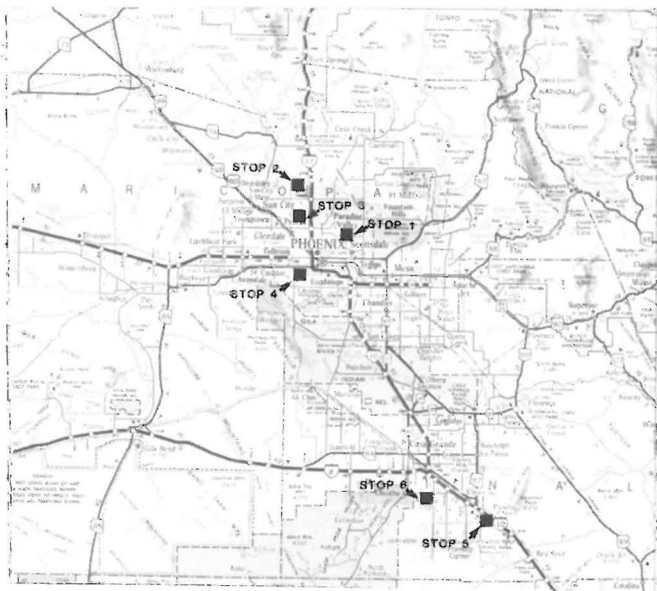


Figure 1. Road map of the Phoenix and Casa Grande areas showing the location of the stops for the Selected Hydrogeologic Problems in Central Arizona Field Trip.

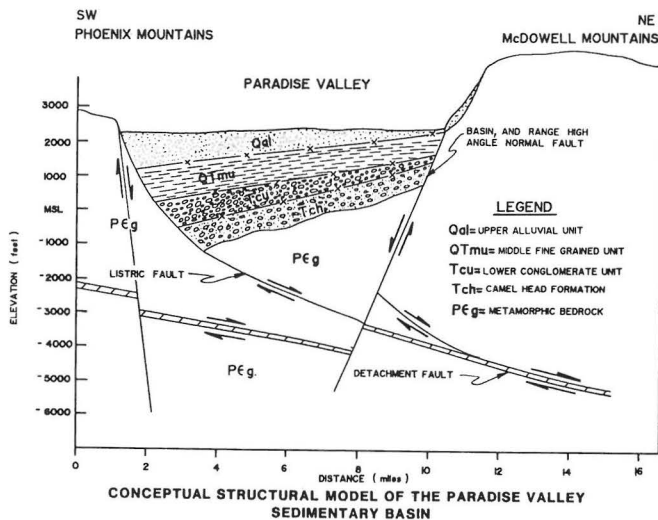


Figure 2. Conceptual model of basin formation in the Southern Basin and Range Province.

contemporaneous volcanic activity, as well as the formation of more areally restricted salt deposits, is an important modifier for the local ground-water hydrology.

The stratigraphic units that constitute the various components of the aquifer system of this region are, from older to younger, Camel Head formation, Lower Conglomerate Unit, Middle Fine-Grained Unit, and Upper Alluvial Unit. Figure 3 shows schematically the depth and distribution of these units within a structural basin of central Arizona. The texture, degree of consolidation, and relative position in the stratigraphic column determines the type of aquifer hosted in each unit (Table 1).

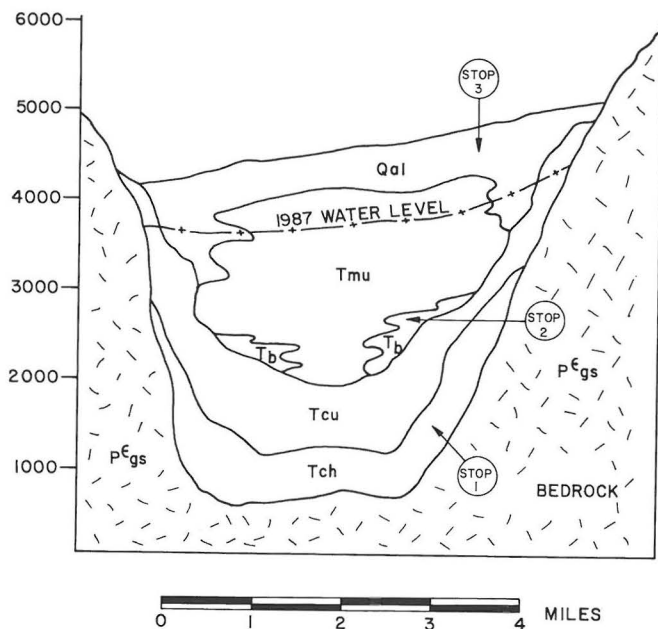


Figure 3. Depth distribution of sedimentary units that constitute the components of the aquifer system of a typical basin of central Arizona. Bedrock: pCgs; Camel Head formation: Tch; Lower Conglomerate Unit: Tcu; basalt flows: Tb; Middle Fine-Grained Unit: Tmj; Upper Alluvial Unit: Qal.

At this stop outcrops of the Camel Head formation exposed in the northwestern flank of Camelback Mountain will be examined and the aquifer characteristics of this unit will be discussed.

The Camel Head formation, frequently recognized by local well drillers as the Red Unit, is the lowermost unit of the aquifer system of this region. It rests unconformably on intrusive and metamorphic rocks of Precambrian age, which most commonly constitute bedrock in the basins of this area. At Camelback Mountain, this contact is very well exposed in Echo Canyon Park, where in places it is a low-angle normal fault. The Camel Head formation is composed of consolidated alluvial and landslide deposits of early to mid-Miocene age (Cordy, 1978). Four members have been recognized in this formation.

TABLE 1
STRATIGRAPHIC UNITS HOSTING THE AQUIFERS
OF THE EAST CENTRAL SOUTHERN BASIN AND RANGE PROVINCE

UNIT	PREDOMINANT LITHOLOGY	AGE	TYPE	RAISE OF THICKNESS (ft)	TYPE OF AQUIFERS	STRUCTURAL ASSOCIATION
Upper Alluvial Unit	Unconsolidated Sand and Gravel	Pleistocene-Recent	Alluvial	0-300	Unconfined Perched	Present Erosional Cycle
Middle Fine Grained Unit	Clays, Silts, Evaporites, Sulfates in Lower Section	Pliocene-Pleistocene	Lacustrine	0-2,000	Semi-Confined to Confined	Basin and Range Disturbance; Basin Subsidence
Lower Conglomerate	Semi-Consolidated Sand and Gravels	Miocene-Pliocene	Fanglomerate	0-2,000	Confined (Unconfined lens not overlain by Fine-Grained Unit)	Basin and Range Disturbance; Horst and Graben
-----Unconformity-----						
Camel Head Formation	Conglomerate and Breccia	Miocene	Fanglomerate	0-3,000	Confined	Mid-Tertiary Orogeny; Listic Faults

Deep wells in the eastern and western Salt River Valley produce water from the Camel Head formation. Ground-water in this unit is normally under confined conditions.

HIGHLIGHTS EN ROUTE TO STOP 2

As we proceed east and north into the city of Scottsdale, we will cross Indian Bend Wash and the Granite Reef Aqueduct, a feature of the Central Arizona Project (CAP). North of this canal and behind the Paradise Valley Flood Detention Dike is the site of the projected Artificial Recharge Project of the city of Scottsdale. A combination of basins, dry wells, and deep wells will be employed to recharge 12 Mm³ of CAP and runoff water at this site (Lluria and Jeffries, 1986).

STOP 2. HEDGPETH HILLS

Basalts have been recognized as excellent aquifers in the Salt River Valley basins. Several City of Phoenix wells produce in excess of 0.16 m³/s (2,500 gal/min) from this type of aquifer. There are several flow events of this type of unit in late Tertiary and Quaternary time. The most productive basalt unit is in the lower section of the Middle Fine-Grained Unit. Primary porosity and permeability of the basalt units can be considerable in the amygdaloidal facies. However, the principal water storage and transmissive characteristics are imparted by fracturing. A construction trench in the Hedgpeth Hills exposes basalt of Tertiary age that has been rotated by a normal Basin and Range fault. Intense fracturing has resulted. This exposure shows conditions similar to those in the basalt aquifers of the

HIGHLIGHTS EN ROUTE TO STOP 3

Adobe Dam, a 3-km-long structure north of the Hedgpeth Hills, renders flood protection to the new subdivisions along Skunk Creek. The route to Stop 3 is along a portion of Phoenix underlain by the Cave Creek subbasin.

STOP 3. CITY OF PHOENIX WELL 217

The Cave Creek Artificial Recharge Project of the city of Phoenix is the first municipal supply recharge and recovery project in Arizona. A study of all surface and subsurface geologic, hydrologic, and environmental data of the Cave Creek subbasin determined that artificial recharge is a cost-effective method to store and recover excess Central Arizona Project water (Lluria, 1987). The use of deep recharge wells was selected as the best method to recharge under the prevailing local hydrogeologic, environmental, and engineering conditions (Lluria, 1985). Recharge wells will be used for this project and treated CAP water will be injected. City of Phoenix Well 217 was selected to test the aquifer conditions during recharge and the injection system. CAP water flows along two tubes that discharge below the water level at 150 m (Figure 4). Local transmissive and storage characteristics of the sediments of Tertiary age have proven to be very favorable for the pilot test. Well 217 produces 0.06 m³/s (1,050 gal/min) and the recharge rate exceeds 0.04 m³/s (650 gal/min). Buildup of the cone of impression during the test has been very modest, indicating high transmissivity. This has been corroborated by the results of the pumping tests, which showed values exceeding the original estimate of 744 m³/d. The ground-water quality in the area of the pilot test is good, with total dissolved solids content under 500 mg/L.

HIGHLIGHTS EN ROUTE TO STOP 4

Proceeding south towards the Salt River takes us across what very few years ago was a well-developed agricultural area. Ground water was the principal source of irrigation, supplemented by Salt River water, conveyed via the Arizona and Grand Canals. Water-level declines in this area has exceeded 60 m during the last 40 years.

STOP 4. GRAVEL PIT

The Upper Alluvial Unit is composed of gravel, sand, and silt. These sediments are predominantly unconsolidated and exhibit considerable hydraulic conductivity. Measurements in recharge basins near the Salt River showed a hydraulic conductivity for these sediments of up to 85 m³/d horizontally and 5.5 m³/d vertically. Layers of caliche, which act as effective aquicludes, are frequently developed in this unit and, along with thin clay layers, cause perched conditions at several locations in the Salt River Valley. At Stop 4 we will examine the characteristics of a part of the Upper Alluvial Unit which, in the early days of development in this area, supplied most of the ground water used for municipal and agricultural needs.

CAVE CREEK RECHARGE PROJECT
TENTATIVE INJECTION SYSTEM DESIGN

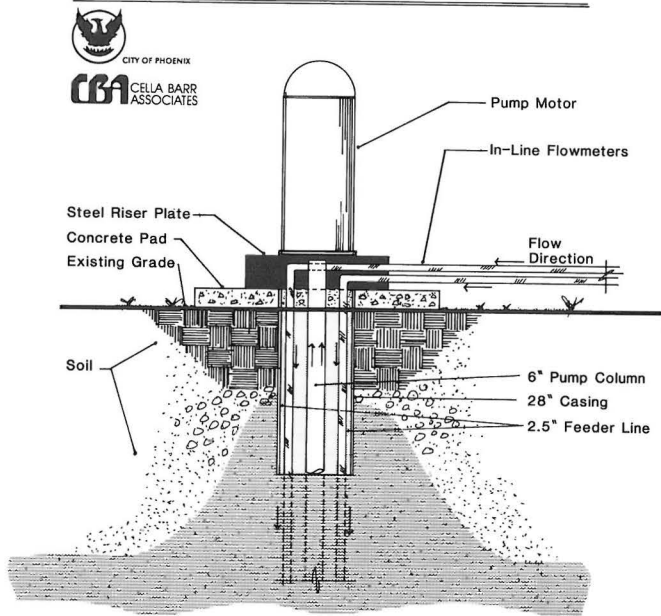


Figure 4. Recharge system installed on City of Phoenix Well 217 for a pilot test. Injection is along two 2.5-inch-diameter PVC pipes that discharge under the phreatic level. The pump is for development of the well and for production.

HIGHLIGHTS EN ROUTE TO STOP 5

The afternoon portion of the field trip, Stops 5 and 6, visits the Picacho basin, which is a deep alluvial basin in the southern part of the Basin and Range physiographic province. Massive mining of ground water in the basin created the first examples in Arizona of land subsidence and ground failure caused by withdrawal of ground water. About 1,200 km² of land in the basin have subsided more than 30 cm and at least 18 areas are affected by ground failure. The failures include reactivated faults and km-long earth fissures. The stops provide the opportunity to examine both types of failure where the mechanisms of failure have been identified.

As we cross the Gila River on I-10, off to our right in the distance is Snaketown, location of the remains of a village of the extinct Hohokam Indians who extensively irrigated with surface flow from the river. It is ironic that we pass this former village on our way to one of the world's classic examples of ground-water mining. Hohokam is a Pima Indian word meaning "all used up." We enter the Picacho basin as we pass by the Sacaton Mountains. Note the broad flat alluvial surface and inselbergs around the basin margin. Burial of inselbergs has controlled the location of many of the earth fissures found in the basin.

STOP 5. PICACHO FAULT

Modern surface faulting is associated with subsidence caused by withdrawal of ground water in at least seven areas in the United States. The faulting occurs by aseismic creep along

preexisting geologic faults. Only a few of the ground failures in south-central and southeast Arizona that are associated with withdrawal of ground water have shown significant vertical offset and similarity to surface faults in other subsidence areas in the United States. The longest of these is the 15.8-km-long Picacho fault (Figure 5; Holzer and others, 1979). Height of the scarp ranges from 0.2 to 0.6 m. At this stop, we will examine the fault where it has offset Interstate Highway I-10 and trace it southward into the desert where it has not been modified by construction.

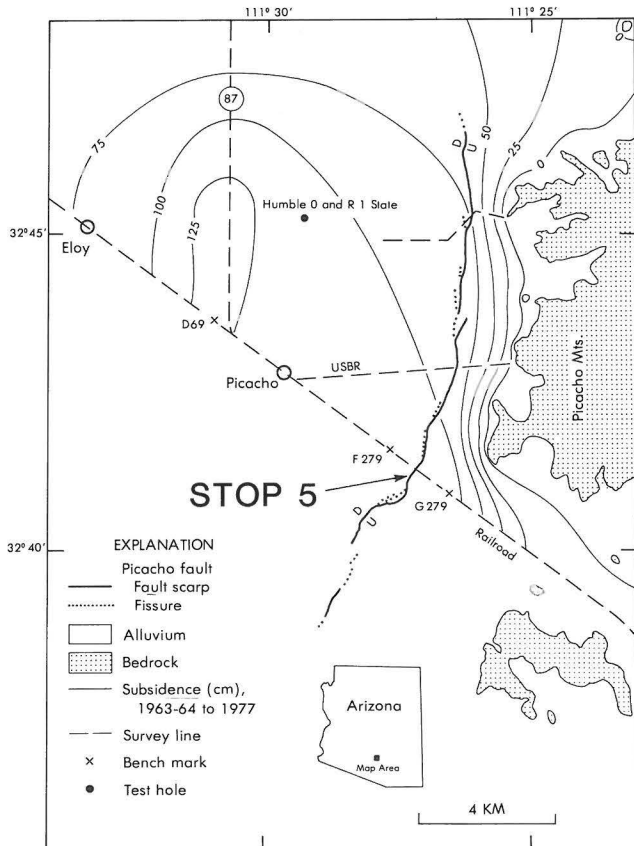


Figure 5. Map of Picacho fault and contiguous earth fissures as of May 1976. Interstate Highway I-10 parallels and is essentially adjacent to the railway survey line.

The boundary between the Picacho basin and the adjacent Picacho Mountains to the east is probably a fault zone. There is a very steep gradient in the regional gravity and relief on the bedrock surface is about 4000 m. Detailed seismic refraction and gravity surveys (Pankratz and others, 1979) across the boundary near the midpoint of the Picacho fault, approximately 3.5 km north of the highway, indicate that the fault boundary may be a complex zone. Three significant basement faults, downdropped to the west, were identified over a horizontal distance of about 2 km. The Picacho fault overlies the easternmost of the three preexisting faults where alluvium is about 300 m thick. Exploratory borings near the fault and monitoring of piezometers installed in the borings suggest that there is a preexisting normal fault in the alluvium with a 77°W dip that offsets alluvial units to within at least 40 m of

the surface and that behaves as a partial ground-water barrier (Holzer, 1978). Piezometers on opposite sides of the fault showed a seasonal water-level difference of 24 m in 1978.

The preexisting fault appears to be tectonically inactive. Naturally occurring tectonic faulting and uplift in south-central Arizona occurred relatively early in late Cenozoic time (Eaton, 1972) and the area is seismically inactive or nearly so (Sturgal and Irwin, 1971). The fault has no expression on 1936 aerial photographs or topographic maps.

The history of water-level decline west of the fault is summarized in Figure 6. The cone of depression probably reached the fault in about 1935 (Holzer, 1984). Subsidence in the basin began between 1934 and 1948. Regional subsidence in the general vicinity of the fault can be mapped in broad detail north of the interstate highway for the time period 1963-64 to 1977 (Figure 5). Total subsidence at the fault near the highway is about 2 m.

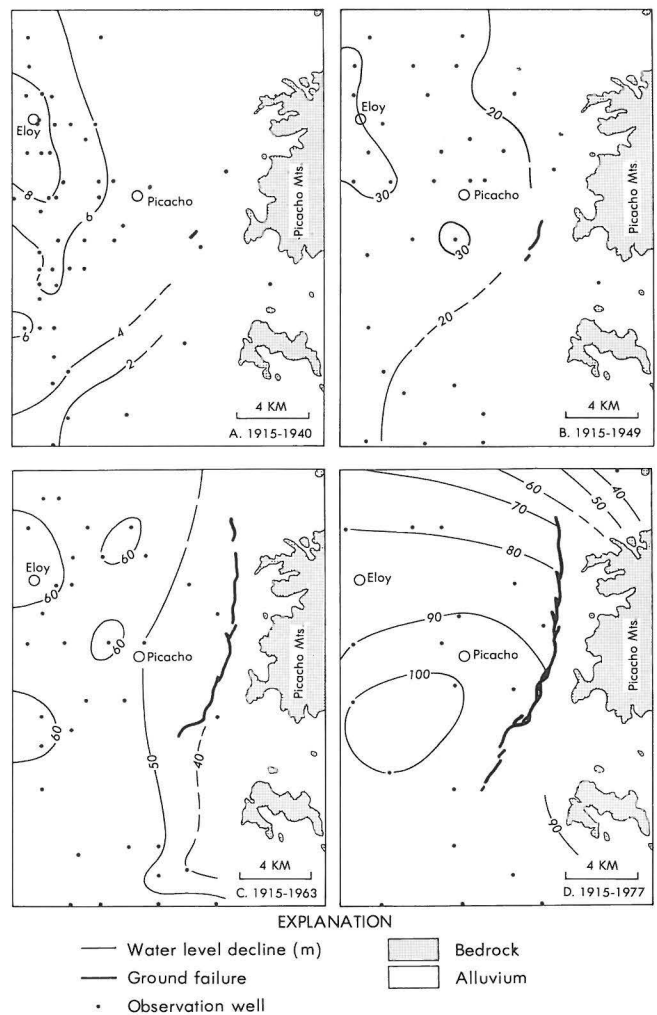


Figure 6. Map of water-level declines and Picacho fault ground failure during successive periods. Panel A shows 1927 earth fissure.

The first ground failure on the present-day trace of the fault was an earth fissure in 1949

(Figure 6B) that intersected the trace of the future roadway of the interstate highway. Differential vertical displacement across it was not detected. The 1949 fissure is the earliest ground failure in the Picacho basin that can be attributed to the withdrawal of ground water. An earlier 300-m-long fissure on September 11, 1927 that was 0.87 km northwest of the 1949 failure (Figure 6A), probably was of natural origin (Holzer, 1984).

Vertical offset across the 1949 fissure was first observed in 1961 at the interstate highway. Peterson (1962) had inspected the fissure in 1959 and described it as inactive and weathered. Hairline cracks began to appear during May 1961, and by July 1, 1961, a bump was noticeable on the newly built interstate highway. The scarp initially grew in height at a rate of 60 mm/yr, and then slowed to a rate of 9 mm/yr from 1975 to 1980 (Holzer, 1984). Scarp growth is by slow creep, but has a seasonal periodicity. It grows during the spring-summer period of water-level decline and stops or slows during the fall-winter period of water-level recovery (Holzer, 1978; Holzer and others, 1979).

The history of fault-associated vertical displacements near the fault can be inferred from two leveling lines, USBR and Railroad (Figure 5), that cross the fault. The USBR line was established in 1964 with bench marks closely spaced near the fault scarp. Rather than a step-like offset in the subsidence profiles across the fault, tilting of the land surface above the footwall and hanging wall blocks were observed from 1964 to 1977. Holzer and others (1979) concluded that pre-1964 vertical deformation near the fault consisted of a flexure in the desert floor. This flexure began to transform into a scarp in about 1964. The post-1964 vertical deformation may be modeled after elastic dislocation theory if it is assumed subsurface normal faulting extended to a depth of 190 m and occurred along a shear plane with a dip of 70° (Holzer and others, 1979). Differential vertical and horizontal displacements measured across the fault confirm the high-angle normal sense of faulting.

The mechanism of the modern faulting was attributed by Holzer (1978) to differential compaction caused by differential water-level declines localized across the preexisting fault in the alluvium. The 1949 fissure formed during bending of the land surface. As subsurface deformation continued, shear failure occurred along the preexisting fault, and surface faulting began.

HIGHLIGHTS EN ROUTE TO STOP 6

Our route along I-10 takes us across the center of the largest subsidence area in Arizona. The center of the subsidence area is near the town of Picacho. Compaction of the aquifer system has been a significant source of ground water and its omission from ground-water models has introduced errors in model-based prediction of water-level declines in the basin.

STOP 6. EARTH FISSURES -- CASA GRANDE MOUNTAINS

Tensile failure, commonly known as earth fissures, are associated with withdrawal of ground water from unconsolidated sediment in more than 19 subsidence areas in Arizona, California, Idaho,

Nevada, and Utah. Fissures are usually hundreds of meters long and typically are enlarged by erosion into wide deep gullies. The complex system of earth fissures east of the Casa Grande Mountains (Figure 7) provides a well-studied example of fissures caused by differential compaction. Precise and detailed gravity surveys by Jachens and Holzer (1982) indicate that the fissures overlie convex-upward irregularities on a buried erosional bedrock surface at the base of the unconsolidated alluvium. At this stop we will walk out part of the fissure systems C and D, starting at their south ends (Figure 7), and observe how they formed and have evolved.

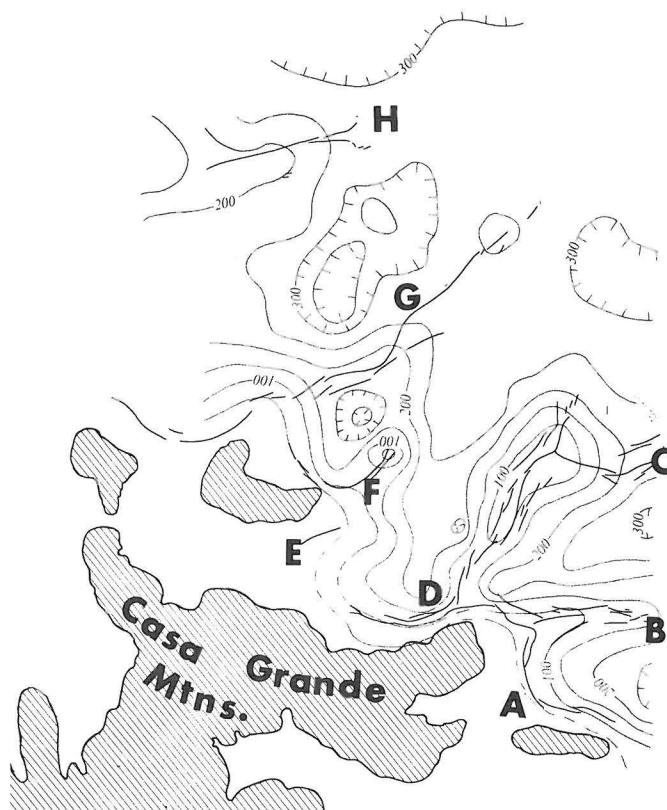


Figure 7. Map of earth fissures as of April 1980 and depth to bedrock in meters on east side of Casa Grande Mountains.

Stratigraphy of the unconsolidated alluvium is partly known from logs of wells drilled nearby. The wells penetrated 75 to 100 m of coarse-grained sediment overlying a thick clay unit.

Water levels began to decline in the area about 1940 and declined about 40m as of 1962, at which level they stabilized. Natural static water levels were about 18 m below the land surface. Subsidence began after 1948. Rates of subsidence were constant until the early 1960's, when they decreased. The continued subsidence after the stabilization of water levels probably is caused by dissipation of residual pore pressures in the thick clay.

Locations of fissure zones are determined by relief on the buried bedrock surface (Figure 7). Fissure zones B, C, D, E (southern half), G, and H

all occur almost directly over the crests of buried bedrock ridges. Other fissures overlie convex-upward irregularities on buried, gently sloping bedrock surfaces. This applies particularly to fissure zones such as A that approximately parallel the intersection of the land surface with the bedrock-alluvium contact.

Differences in cross sections and dimensions of fissures are due primarily to modification by erosion and deposition and to the amount of tensile strain relieved by each fissure. Many fissures appear to still be active, that is, horizontal opening is continuing on the basis of cracking and collapse of old sediment infilling the fissures. One of the zones (C in Figure 7) first failed before February 1956 and therefore has been active for more than 30 years.

The degree of activity probably depends on the rate of differential compaction. Active fissures occur where the water table is above the bedrock surface and differential compaction presumably is still occurring. Inactive fissures occur where the water table has dropped below the inferred bedrock and differential compaction has presumably slowed. Relations between fissure activity and bedrock depth and water-table depth are not simple, however. Active and inactive fissures lie adjacent to each other in some zones.

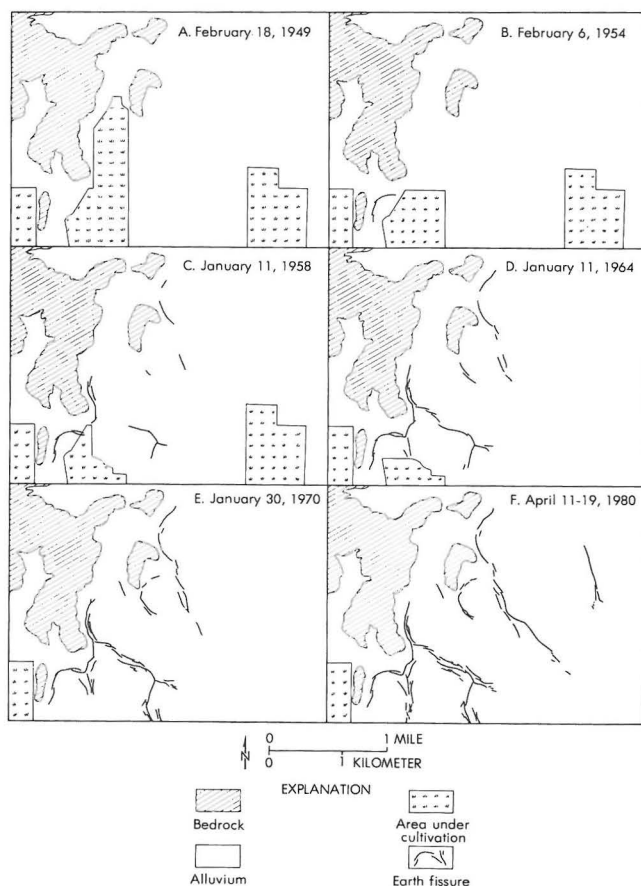


Figure 8. Chronology of fissure formation east of Casa Grande Mountains.

The sequence of fissure formation (Figure 8) in general agrees with that predicted by a differential compaction mechanism. For example, fissure zone G (Figure 7), which is over an irregularly shaped bedrock ridge, developed in a spatially and temporally discontinuous manner for more than 30 years (Figure 8); the first ground failure (1954-1958) occurred above the sharpest section of the ridge, whereas the last ground failure (1975-1979) occurred above the most subdued parts of the ridge.

Horizontal strain at failure was estimated by Jachens and Holzer (1982) who used finite element theory to model the alluvium as a beam with differential vertical displacements applied along its base. The computed horizontal surface strains at failure ranged from 0.02 to 0.2 percent, which agrees with the strains at failure inferred from geodetic surveys (Holzer and Pampeyan, 1981).

REFERENCES CITED

- Cordy, G.E., 1978, Environmental geology of the Paradise Valley quadrangle, Maricopa County, Arizona; part 2 [M.S. thesis]: Tempe, Arizona State University, 89 p.
- Eaton, G.P., 1972, Deformation of Quaternary deposits in two intermontane basins of southern Arizona, U.S.A., in Proceedings, International Geological Congress, 24th, Montreal, Section 3: Quebec, Harpell's Press, p. 607-616.
- Holzer, T.L., 1978, Results and interpretation of exploratory drilling near the Picacho fault, south-central Arizona: U.S. Geological Survey Open-File Report 78-1016, 17 p.
- , 1984, Ground failure induced by ground water withdrawal from unconsolidated sediment, in Holzer, T.L., ed., Man-induced land subsidence: Geological Society of America Reviews in Engineering Geology, v. VI, p. 67-105.
- Holzer, T.L., Davis, S.N. and Lofgren, B.E., 1979, Faulting caused by ground water extraction in south-central Arizona: Journal of Geophysical Research, v. 84, no. B2, p. 603-612.
- Holzer, T.L., and Pampeyan, E.H., 1981, Earth fissures and localized differential subsidence: Water Resources Research, v. 17, no. 1, p. 223-227.
- Jachens, R.C., and Holzer, T.L., 1982, Differential compaction mechanism for earth fissures near Casa Grande, Arizona: Geological Society of American Bulletin, v. 93, no. 10, p. 998-1012.
- Lluria, M.R., 1985, City of Phoenix Cave Creek Recharge Project; technical aspects, in Proceedings, Second Symposium on Artificial Recharge in Arizona, Tempe: Tucson, University of Arizona, p. 82-111.
- , 1987, Artificial ground water recharge in the Phoenix metropolitan area; a cost-effective solution to the storage of surplus water supplies, in Proceedings of Water Resources Planning and Management: American Society of Civil Engineers, 14th Annual Conference, Kansas City (in press).
- Lluria, M.R., and Jeffries, R.B., 1986, Preliminary evaluation of ground-water recharge for the city of Scottsdale: City of Scottsdale unpublished report, 75 p.

- Pankratz, L.W., Ackerman, H.D., and Jachens, R.C., 1979, Results and interpretation of geophysical studies near the Picacho fault, south-central Arizona: U.S. Geological Survey Open-File Report 78-1106, 17 p.
- Peterson, D.E., 1962, Earth fissuring in the Picacho area, Pinal County, Arizona [M.S. thesis]: Tucson, University of Arizona, 35 p.
- Sturgal, J.R., and Irwin, T.D., 1971, Earthquake history of Arizona and New Mexico, 1850-1966: Arizona Geological Society Digest, v. 9, p. 1-39.

The Archaeological Geology of Paleo-Indian Sites in Southeastern Arizona

Michael R. Waters
Departments of Anthropology and Geography
Texas A&M University
College Station, Texas 77843

C. Vance Haynes, Jr.
Departments of Anthropology and Geosciences
University of Arizona
Tucson, Arizona 85721

INTRODUCTION

A complex late Quaternary geologic history is preserved in the sediments in the San Pedro Valley and the Sulphur Springs Valley in southeastern Arizona. These sediments are host to some of the oldest archaeological remains in North America.

The purpose of this trip is to compare and contrast the late Quaternary geology and archaeology of the San Pedro Valley and adjacent Sulphur Springs Valley. During the first day, the alluvial stratigraphy, geochronology, Paleo-Indian archaeology, and vertebrate paleontology will be examined at the Murray Springs Clovis site exposed in Curry Draw, the Escapule mammoth site, and other localities in the San Pedro Valley (Figure 1). On the second day, participants will visit Whitewater Draw in the southern portion of the Sulphur Springs Valley to examine the alluvial stratigraphy and the context of the early archaic Cochise Culture and megafaunal remains at the Double Adobe and Skeleton (AZ FF:10:14) sites (Figure 1). At the final stop participants will examine the lacustrine features and geoarchaeology of ancient Pluvial Lake Cochise in the northern portion of the Sulphur Springs Valley (Figure 1).

SAN PEDRO VALLEY (DAY 1)

Curry Draw, a typical discontinuous gully, is an easterly flowing tributary of the upper San Pedro River in Cochise County, Arizona (Figure 1). The arroyo, which appears as an unnamed drainage on the Lewis Springs 7.5-minute quadrangle, exposes the Murray Springs Clovis site in the SW¹/₄ of the SE¹/₄ of Section 26, R21E, T21S (31°34'13"N, 110°10'40"W). The site, where the stratigraphy is best exposed, is reached on foot by following the draw downstream 1 km from where it crosses Moson Road or by following the abandoned Southern Pacific railroad grade that parallels the draw on the north side. The site is on property of the Bureau of Land Management, and permission to visit it must be obtained from the Safford District Office, 425 East 45th Street, Safford, Arizona 85546.

The stratigraphy and geomorphology of Curry Draw reveal an unusually complete record of late Quaternary depositional, pedological, and erosional events controlled by changing climate. If water-table levels with respect to channel configuration and sediments can be taken as approximate indicators of climatic change, some gross indications of late

Quaternary change can be read from the alluvial stratigraphy.

The Murray Springs Clovis site is unique in that it contains three distinct activity areas where a band of Clovis hunters killed a mammoth and several bison and occupied a small campsite during two or three brief visits 11,000 years ago (Haynes, 1968, 1973, 1974, 1976, 1978, 1979, and 1980). The buried occupation surface is clearly displayed in the arroyo walls as an erosional contact at the base of a distinctive black organic mat that preserved artifacts and extinct animal bones in their original position, and mammoth tracks, just as they were left 11,000 years ago (Haynes and Hemmings, 1968). The late Quaternary stratigraphic framework (Figure 2), more complete than at any of the dozen known Clovis sites in stratigraphic context, is impressive to see because of the marked color contrasts of the sedimentary units and the excellent exposures along 2.6 km of arroyo walls between the site and the San Pedro floodplain to which the stratigraphy is directly traceable. Correlations throughout the upper San Pedro Valley are augmented by more than 100 radiocarbon dates.

The valley of Curry Draw is cut into early Pleistocene alluvial and lacustrine deposits of the St. David formation (TQsd; Gray, 1967; Johnson and others, 1975; Haynes, 1981). Gravel straths of the Nexpa formation (unit Qne), inset into the St. David formation, are probably middle Pleistocene and appear to represent a long period of net degradation following the Brunhes/Matuyama paleomagnetic boundary. The Millville formation (unit Qmi), which is beyond the limit of radiocarbon dating, contains the remains of Rancholabrean fauna scattered among poorly sorted, muddy sand-and-gravel alluvium reflecting episodes of high-energy stream discharge (Haynes, 1980). In cross section, the eroded Millville formation is no thicker than the Holocene alluvium but occupies a channel three to five times wider than the Holocene channels, suggesting the erosion of a much broader valley floor.

The Murray Springs formation (unit Qms), unconformably overlying the Millville, consists of a basal olive-green, laminated, lacustrine mudstone, the Sobaipuri mudstone member (Qso), conformably overlain by the white, lacustrine Coro marl member (Qco). A basal sand, the Moson member (Qmo), is mainly confined to spring feeders as facies of the Sobaipuri member and extends downward into older units. The springs indicate groundwater support of a late Pleistocene lake in Curry Draw. The mudstone, up to 1 m thick, contains a dark gray to black

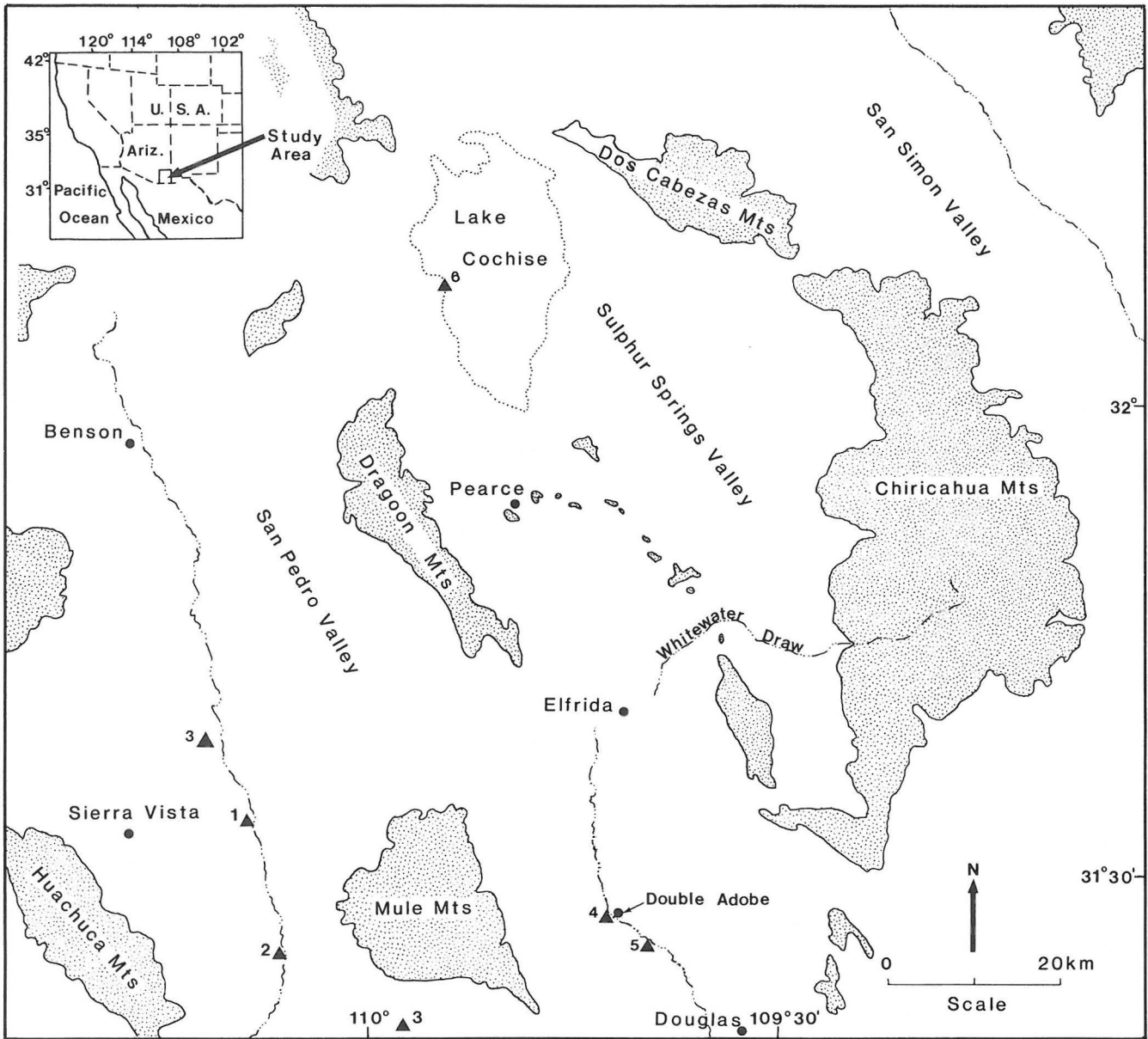


Figure 1. Location of towns, archaeological and geological sites, and physiographic features in southeastern Arizona that are mentioned in the text. The maximum extent of ancient Lake Cochise is shown by a dotted line. Mountain areas are shaded. Sites are indicated by solid triangles: 1) Murray Springs Clovis site and Curry Draw; 2) Lehner Clovis site; 3) Escapule mammoth site; 4) Double Adobe site; 5) AZ FF 10:14; 6) Lake Cochise Stop. (adapted from Waters, 1985a).

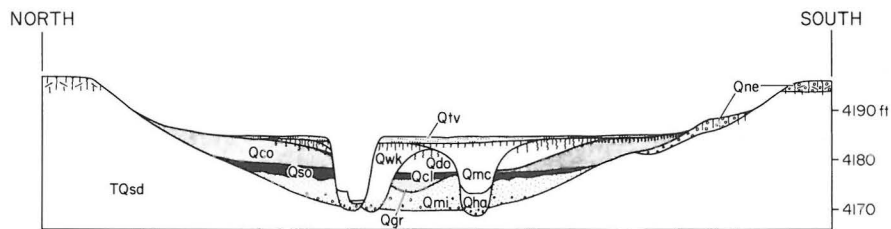


Figure 2. Generalized geologic cross section of Curry Draw showing stratigraphic relationship of units.

organic band that radiocarbon dates the upper 10 cm to 29,000 ± 2000 B.P. (A-896). Squeeze-ups into the overlying marl occur at several places, and 2- to 5-mm-thick mudstone partings, commonly accompanied by concentrations of gastropod and pelecypod shells, occur in the lower half of the marl. In some areas the Moson sand member extends horizontally within the top of the Millville formation, along the Millville-Sobaipuri contact, and cuts across the contact in a few places, indicating formation after deposition of the Millville and Sobaipuri units. It is believed to be due to the subsurface flow of groundwater leaving a lag accumulation as finer grained clasts were removed by subsurface discharge.

The Murray Springs formation, with RanchoLabrean faunal remains, has yielded radiocarbon dates on both carbonate and organic fractions that indicate Coro marl deposition occurred between 27,500 and 12,000 B.P. The late Wisconsinan along Curry Draw was a time of emergent groundwater and very low gradients. Ecological conditions were more mesic than at any time since (Martin, 1963). Mammoths, camels, horses, and bison were abundant in the area, but evidence of early man is lacking.

The Coro marl (Qco) is unconformably overlain by the Lehner Ranch formation (Qle), which represents the early Holocene. A small channel, saucer-shaped in cross section and truncating the Murray Springs formation, contains medium to coarse channel sand, the Graveyard Gulch member (Qgr), with abundant charcoal that produced radiocarbon dates between 13,000 and 10,900 B.P. A black organic algal mat, the Clanton Ranch mudstone member (Qcl), conformably overlies the channel sand, but is unconformably in contact with the Murray Springs and older units. The black mat, as much as 0.3 m thick in low areas, pinches out upslope and interfingers with a white marl pond facies in a few low areas. Both organic and carbonate radiocarbon dates indicate deposition between 10,800 and 9,700 B.P. in local ponds and groundwater seeps.

Clovis artifacts, bones of their prey, and charcoal from their fires are concentrated in the upper 10 cm of the Graveyard Gulch channel sand and along the erosional contact at the base of the Clanton Ranch mudstone that perfectly preserves and demarks the Clovis occupation surface. Thousands of artifacts and waste flakes were found exactly as they had been left by the Clovis people about 11,000 years ago. Eight radiocarbon dates on the Clovis-age charcoal, identified as ash (*Fraxinus*), average 10,900 ± 50 B.P.

In the mammoth kill area, numerous elephant-sized, shallow depressions, presumably mammoth footprints, occurred in a swath along the right bank, across the channel sand, and up the left bank to where the partially articulated skeleton of an adult female mammoth lay surrounded by Clovis artifacts. The near perfect preservation of these mammoth tracks in the soft channel sand indicates a lack of discharge sufficient to erase the tracks. The discharge must have been nil, yet subsequent deposition of the black algal mat and white marl facies indicates seepy ground and shallow ponds. This microstratigraphy suggests that a brief drop in the water table 11,000 years ago led to a dry or nearly dry streambed that was followed by a gradual rise in the water table soon after the mammoth crossing. Fossil pollen from the same level at the Lehner Clovis site, 16 km to the south (Figure 1), indicates that the water-table rise was a regional event (Mehring and Haynes, 1965). Growth of the black mat was such that the mammoth tracks were preserved essentially intact. The edges and squeezed-up ridges were only slightly rounded before burial. The indicated drop and rise

in the local water table is probably the result of changes in local base level and/or climatic change rather than tectonic activity.

The Clanton Ranch member of the Lehner Ranch formation is conformably overlain, except for localized disconformities, by the Donnet Ranch member (Qdo), a massive, silty, fine sandy loam that is believed to have been deposited by slope washing of aeolian silt and sand from adjacent valley slopes. Deposition took place between 9,500 and 8,000 B.P. with no distinct channel in evidence. This lack of a channel facies indicates that aggradation occurred gradually over a grassy swale topography. Alluvial pollen studies of the same unit at the Lehner site indicate that floodplain vegetation became increasingly more xerophytic as aggradation progressed (Mehring and Haynes, 1965; Mehring, 1967). This, plus the stratigraphic-sedimentologic evidence, suggests that the less effective moisture conditions were the results of a falling regional water table.

The Lehner Ranch formation is unconformably overlain by the Escapule Ranch formation (Qes) consisting of three middle to late Holocene alluvial-fill members, each separated by paleosols and arroyo-type erosional contacts (units Qwk, Qha, and Qmc). Each member is further subdivisible into two or three subunits separated by similar erosional contacts. The lower Weik Ranch member (Qwk) fills the first true arroyo channel of the late Quaternary stratigraphic record. Its deposition between 6500 and 4300 B.P. began a cyclical regime of arroyo cutting and filling that has continued up to the present time.

The lower part of the Weik member consists of channel sands, gravels, and chunks of older bank materials overlain by interbedded pond and slope-wash deposits with pollen, indicating more mesic floodplain conditions between 6500 and 4500 B.P. than at any other time in the Holocene record (Martin, 1963; Mehring and Haynes, 1965). The paucity of alluvial fills between 8000 and 6500 B.P. has prevented the recovery of alluvial pollen for this erosional hiatus, but pollen from dune facies in New Mexico suggests drier conditions with less effective moisture around 7000 B.P. (Mehring, personal communication; Schoenwetter, personal communication). The trend toward more xeric conditions appears to have started during the latter phases of deposition of the Donnet Ranch member and culminated with arroyo cutting soon after 8000 B.P. The filling that began 6500 B.P. appears to have coincided with a net rise of the water table and may have been in response to it by promoting the growth of vegetation that trapped sediment in the channel. The 1500- to 1000-year hiatus between 8000 and 6500 B.P. was a period of erosion and channel widening during which much of the Murray Springs and Lehner formations were removed.

Each Holocene alluvial fill is made up mostly of slope-wash alluvium locally interbedded with pond deposits in part derived from slope wash but representing the winnowed fines. These fluvio-lacustrine deposits give way in the upper parts of the fills to loamy slope wash showing various degrees of pedogenesis and bioturbation, and pollen that indicates increasingly more xeric floodplain vegetation (Mehring, personal communication). It is clear that down-valley transport of sediment, predominant in the early history of arroyo aggradation, gave way to predominantly slope-wash alluvium derived from adjacent or nearby slopes in the later history of each alluvial fill, the upper few decimeters of which reflect the onset of the driest or most xeric part of the preserved alluvium. The subsequent hiatus may represent an even drier

part of the alluvial cycle, but pollen-bearing sediments have not been preserved.

During the final half of each aggradational part of the cycle, fluvial discharge down Curry Draw was inadequate for removing slope wash faster than it was accumulating. As net aggradation ensued, the valley cross section became progressively less steep-sided (less arroyolike) as the shallow swale configuration developed. Thus, discharge became less confined as aggradation progressed and enhanced further aggradation. During the same time, a falling water table may have caused a reduction of grass cover. The combination of reduced vegetative cover and the lower water table set the stage for the next episode of arroyo cutting by lowering the threshold for erosion.

The modern episode of arroyo cutting began in 1916 when excessive runoff deepened the ruts of a wagon road that led down a grassy swale where the Murray family had pastured dairy cows before 1911. Up to 0.5 m of sand-and-gravel alluvium, the Teviston formation (Q_{tv}), covering the historic swale (floodplain) was flushed from a headcut about 1 km upstream of that at the Clovis site. Thus Curry Draw is a typical discontinuous gully whose floodplain was an undissected grassy swale at the beginning of the 20th century. The remains of a protohistoric bison cow and fetal calf were found between the Teviston and Escapule Ranch formations (Agenbroad and Haynes, 1975). Two main tributaries of Curry Draw, the east and west swales, remain essentially undissected, but aerial photography reveals that headcuts started up the east swale as soon as the main headcut reached it shortly before 1955.

Curry Draw today does not extend to the Huachuca Mountains. Instead, the channel becomes broader and shallower in the headward reach until it becomes imperceptible about 5 km from the base of the mountains. Uplands along the draw are relatively flat interfluvial remnants of the middle Pleistocene pediment surface extending from the Huachuca Mountain front to the San Pedro River. Some broader interfluves have a thin (up to 20 cm) veneer of late Pleistocene to Holocene silty loam believed to be an accumulation of windblown silt. Grass "circles," very shallow circular depressions up to 300 m in diameter, on some of the broader flats are filled with up to 1 m of this silty loam bearing a dark-gray to black paleosol and overlying a much stronger red calcic paleosol of late Pleistocene age. The Holocene paleosol has produced bulk-sample radiocarbon dates indicating minimum ages of pedogenesis of between 3000 and 6000 B.P. The paleosol is overlain by up to 5 cm of gray powdery silt representing the latest Holocene increment of eolian deposition. This thin unit is observed on most of the grassy swales of the area and on many uneroded terrace flats along the San Pedro River. It is buried by the Teviston formation in some places, and a similar unit is buried by the McCool member (Q_{mc}) of the Escapule formation in others.

From these observations it is apparent that there has been significant contributions of eolian silt to the landscape at various times throughout the Holocene and probably the late Pleistocene. This material has been washed from valley slopes at various times to become significant components of the valley fills. It appears to have been a major component of the Donnet and Clanton members indicating that a thicker eolian blanket was deposited during late Wisconsinan time than at anytime since. This veneer of eolian silt mixed with slope wash and its loss by erosion has exerted a pronounced edaphic effect on vegetational changes during the past 10,000 years, and perhaps before. The

thicker silty loam accumulations today, as exemplified by the grass circles, preserve the mesquite-grassland community as "islands" surrounded by the Chihuahuan desert-scrub community where the silty loam has been removed, leaving a substrate of caliche or older units impregnated with calcium carbonate. The cycles of upland deposition and erosion implied by the alluvial cycles must, at times, have had a profound influence on the changes of vegetation as the substrate changed. Vegetational changes would, in turn, strongly influence infiltration and slope erosion. Valley sides covered by desert grassland would have a dramatic effect on geohydrologic processes along Curry Draw compared to today's desert scrub on the highly calcareous substrate. This edaphic influence was undoubtedly a major factor in affecting the modern episode of arroyo cutting and the changing landscape (Hastings and Turner, 1965).

The sand and gravel of the Millville formation occupies a channel several times larger than the modern arroyo. Therefore, much larger ephemeral discharges appear to be represented for the period immediately preceding 30,000 B.P. The Murray Springs formation, consisting of springlaid sand, paludal mudstone, and lacustrine marl, indicates a rising piezometric surface from about 30,000 B.P. to about 27,000 B.P. and quasi-stability from 27,000 to 16,000 B.P., followed by a falling water table and degradation from perhaps 14,000 to 13,000 B.P. when the Pleistocene lake dried up and the Murray Springs formation was entrenched by a small seep-fed stream.

The Lehner Ranch formation represents a transition during the early Holocene from the high effluent (perennial) flow conditions of the late Pleistocene to the ephemeral (influent) flows of the middle to late Holocene. A brief but significant fluctuation of the water table indicating a relatively wet-dry-wet sequence is indicated by the detailed stratigraphy at the Murray Springs Clovis site where the Clovis occupation coincides with the relatively dry episode. The subsequent wet episode was accompanied by aggradation on a grassy swale kept moist by a shallow water table until about 9000 B.P. when a trend toward less effective moisture and a falling water table ensued. Concomitant loss of erosion-inhibiting vegetation and the development of soil cracks along grassy swales led to instability. This was culminated by arroyo cutting about 7500 B.P. Cycling between arroyo filling, quasi-stability, and arroyo cutting continued with increasing frequency during the next 7000 years in response to climatically controlled water-table levels fluctuating between influent and effluent flow conditions.

Misuse of floodplains, beginning during the 19th century, may have augmented erosional instability and triggered arroyo cutting sooner than it would have occurred otherwise, but the frequency of the preceding two cycles indicates that entrenchment was within a few decades of occurring anyway. Several 1 to 2 m terraces inset within Curry Draw today could be the result of complex response to base-level lowering (Schumm and Parker, 1973), but aggradation of each major Holocene fill to or near the level of the previous fill is more likely related to Holocene climatic fluctuations.

Since the beginning of excavations at the Murray Springs site in 1966, the south headcut has cut headward 35 m in 19 years at an average rate of 1.8 m/yr. This is roughly half the rate of the previous 47 years as measured from aerial photography. The reduction in the rate of cutting is due to three factors: an earthen dam for a stock pond was completed 2.8 km upstream in 1966, a dam for a wastewater evaporation pond 1.2 km upstream was

completed in 1978, and a backhoe stratigraphic trench excavated and filled in 1970, having eroded since, has diverted all but the highest discharges to the north headcut. Whereas this has reduced the rate of headward erosion at the site, it will eventually lead to bank erosion of the western end by the creation of a sharp bend.

The stratigraphy of the Lehner Clovis site (Figure 1) 18 km SSE of Murray Springs (Hauray and others, 1959), though nearly identical to that of Curry Draw, is not as well exposed. On the other hand, fluvial sand radiocarbon dated at between 13,000 and 14,000 B.P. in Lehner Arroyo (Haynes, 1982, unit E₁) is not represented in Curry Draw. Other Clovis sites and potential Clovis sites in the upper San Pedro Valley include (1) Naco Clovis site (Hauray and others, 1953), 2) Leikum mammoth site (Haynes, 1968) and Navarrete mammoth site, 3) Hargis bison site (Haynes, 1968), 4) Escapule Clovis site (Hemmings and Haynes, 1969), 5) Schaldack mammoth site, 6) Donnet mammoth site, and 7) Grey-Seff site (Gray, 1967; Haynes, 1968).

THE SULPHUR SPRINGS VALLEY (DAY 2)

The Sulphur Springs Valley is part of a northeast-trending structural trough within the Basin and Range physiographic province. A surface drainage divide, formed by low volcanic hills near Pearce, separates the Sulphur Springs Valley into two basins: the northern Willcox basin and the southern Douglas basin. The former is a closed basin in which ancient Lake Cochise formed during the late Pleistocene (Meinzer and Kelton 1913; Schreiber 1978). Whitewater Draw is located in the southern part of the Sulphur Springs Valley.

Geology of Whitewater Draw

A complex sequence of late Quaternary alluvial strata is exposed in Whitewater Draw, an arroyo in the semiarid Sulphur Springs Valley, southeastern Arizona (Figure 1). Whitewater Draw drains an area of 3100 km² north of the Mexican border and flows south to join the Rio Yaqui, which ultimately flows to the Gulf of California.

No single exposure in Whitewater Draw reveals a complete section of the upper Quaternary alluvial stratigraphy. As a result, the arroyo banks 10 km upstream and downstream from Double Adobe, Arizona, were examined, and eight geological and archaeological sites were investigated in detail. An ordering of geologic events for the past 15,000 yr was achieved by correlation from one radiocarbon-dated locality to another. Sixteen upper Quaternary alluvial units were defined and labeled C through P, from oldest to youngest. Figure 3 shows the stratigraphic relations among the alluvial units of Whitewater Draw and selected radiocarbon dates associated with those deposits. Detailed descriptions of the geologic units mentioned in the text and the stratigraphy at individual sites are given in Waters (1985a, 1985b).

Thirty-three radiocarbon dates on charcoal have been obtained from the alluvial units and provide the absolute chronological framework. Charcoal samples were collected from archaeological (hearths and dispersed from hearths) and natural contexts. All samples were pretreated to remove calcium carbonate and soluble organic contaminants. Twenty-seven samples received corrections for carbon isotope fractionation. Redeposition of older charcoal into younger alluvial deposits is not a problem in Whitewater Draw. All samples from a given stratigraphic unit at a specific site yielded

consistent dates, and all dates are stratigraphically consistent (see Waters, 1985a).

The oldest dated upper Quaternary alluvium (unit D) in Whitewater Draw unconformably overlies a late Tertiary or early Pleistocene age basin fill (unit A) and is inset against terrace sediments (unit B) and marl (unit C) of Pleistocene age. Unit D is a massive gravel overlain by sand containing interbedded silt and clay lenses. Massive clay deposits fill abandoned channels within the highly permeable gravels. Eighteen radiocarbon dates place these deposits between 15,000 and 8000 B.P. These sediments were deposited in a braided stream that shifted position over a 0.65-km wide floodplain. Massive clay deposits in the permeable gravels and cottonwood and hickory charcoal in the sand and gravel indicate an associated high water table. Periods of reduced flow are documented by the deposition of silt and clay in charcos or scours in the sandy channel.

A sandy clay (unit E) with coarse prismatic structure overlies the unit D alluvium and is dated to approximately 7600 B.P. A shallow channel was incised into unit E after 7600 B.P., and before 7000 B.P. it became filled with a laminated and massive marl (unit F). Degradation and aggradation again occurred between 7000 and 6800 B.P., when a narrow channel was incised into the older units. This channel became filled with clay and was overlain by a thick, laterally extensive deposit of clay having strong soil structure (unit G). A shallow channel cut into unit G around 6750 B.P. and was filled with a clayey sand (unit H). These units were deposited in the vegetated shallow channels and margins of a cienega or marsh (Melton, 1965; Hendrickson and Minckley, 1984).

Sometime after 6750 B.P. and before 5500 B.P., a large channel was incised to a depth of 4.3 m into the older deposits. It became filled with gravel, cross-bedded sand, and a fining-upward sequence of horizontally laminated very fine sand and silt, which, in turn, was overlain by a clay deposit having strong soil structure (unit I). Deposition of the unit I channel alluvium occurred in a discontinuous arroyo. The channel alluvium appears to have been deposited rapidly, probably during large floods. The overlying clay was deposited in a cienega.

Four distinct periods of shallow channel incising, filling, and pedogenesis within a cienega depositional environment occurred between 5500 and 3500 B.P. and produced deposits J, K, L, and M. From 3500 to 750 B.P. the fluvial system was characterized by continued clay and silty clay deposition and soil formation (units N and O) within cienegas. The period after 750 B.P. is characterized by the cutting and filling of small draws and the deposition of a large sheet of flood silt (unit P). The modern arroyo formed between A.D. 1885 and 1910.

The alluvial record of Whitewater Draw contains numerous cutting and filling events. The major shifts in depositional environments recognized in Whitewater Draw--changes from a braided stream, to a cienega environment, to an arroyo, and back to a cienega environment--appear to correlate with major changes in climate documented by paleoecologists. However, the complex degradation and aggradation documented during apparently stable climatic periods must have been dominantly controlled by intrabasin geomorphic parameters and processes operating independently of major climatic shifts.

The deposition of gravel and sand in a braided stream from 15,000 to 8000 B.P. corresponds to the mesic climatic interval defined by Spaulding and others (1983) for the Southwest. On the basis of analysis of pack-rat middens, they have suggested that

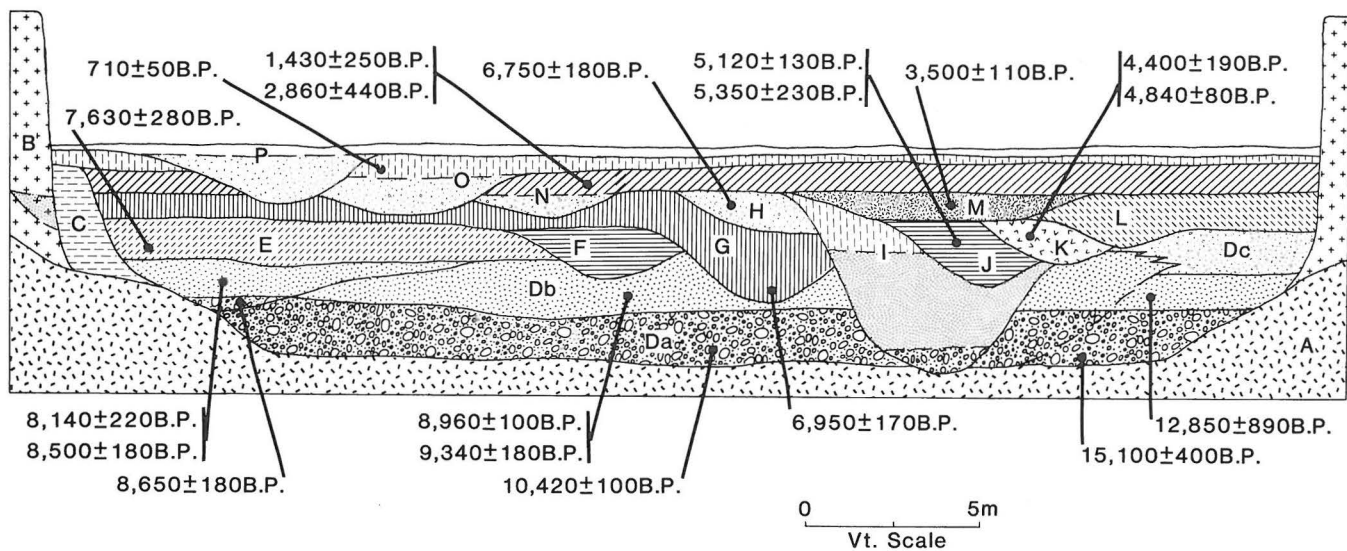


Figure 3. Generalized geologic cross section of Whitewater Draw showing stratigraphic relationship of units. Position of selected radiocarbon dates shown. Modern arroyo not shown. (from Waters, 1985a).

prior to 8000 B.P. the climate of the Sonoran and Chihuahuan deserts was characterized by cool, drier summers and wetter, milder winters. Because the Sulphur Springs Valley lies between these two deserts, similar conditions are presumed to have prevailed in the Sulphur Springs Valley. If so, braided stream deposition from 15,000 to 8000 B.P. in the Sulphur Springs Valley appears to correlate with the mesic conditions of the late Pleistocene and early Holocene.

Deposition in cienegas dominates the alluvial record of Whitewater Draw after 8000 B.P. Numerous cycles of erosion and deposition are documented between 8000 and 6750 B.P. and from 5500 B.P. to the historic period. This change in depositional environments corresponds to the introduction and persistence of the modern arid desert climatic pattern. Paleoeologists (Spaulding and others, 1983) have suggested that after 8000 B.P. modern airflow circulation and precipitation patterns were emplaced. Therefore, the replacement of the braided stream environment by a cienega depositional environment seems to correlate with the introduction of semiarid conditions at 8000 B.P.

The only interruption in the cycles of erosion and deposition in cienegas after 8000 B.P. was the middle Holocene arroyo cutting and filling episode. In the Sulphur Springs Valley an arroyo was cut to a depth of 4.3 m after 6750 B.P. and filled with clastic alluvium and a cienega clay before 5500 B.P. This arroyo cutting and filling event correlates to a regional climatic perturbation defined by Antevs (1955, 1983; Sayles and Antevs, 1941) as a time of greater aridity, known as the Altithermal.

Therefore, major shifts in the environments of deposition recorded in the alluvial record of Whitewater Draw appear to correspond to large-scale climatic changes documented by paleoenvironmental evidence. However, there is no correlation between climate and the numerous cycles of degradation and aggradation documented within the stratigraphic sequence of cienega deposits. There were four cycles of erosion and cienega deposition between 8000 and 6750 B.P., four cycles between 5500 and 3500 B.P., and numerous cycles of erosion and deposition through the historic period. Although the precise mechanism cannot be determined for these cutting and filling cycles, it is likely that intrabasin geomorphic

parameters and processes such as threshold erosional events (Schumm, 1977) and ensuing complex response depositional cycles (Patton and Schumm, 1981) are more plausible than a climatic explanation. Thus, the late Quaternary alluvial history of Whitewater Draw supports the idea that the major components of an alluvial record will reflect climatic shifts, but that the details of the record are the results of geomorphic parameters (Patton and Schumm, 1981).

Archaeology of Whitewater Draw

The Sulphur Spring stage of the Cochise Culture of southeastern Arizona has been a source of controversy for five decades. In Whitewater Draw, Sayles and Antevs (1941) reported that Sulphur Spring stage ground stone artifacts were associated with extinct megafaunal remains and concluded that the Sulphur Spring stage dated between 12,500 and 11,000 B.P. (Sayles, 1983). Based on the apparent age of the Sulphur Spring stage and acceptance of its association with extinct megafauna, some researchers (Martin and Plog, 1973; Haury, 1983) have suggested that the Sulphur Spring stage sites may represent specialized plant-processing stations of the Clovis Culture. However, other archaeologists (Willey and Philips, 1958; Whalen, 1971; Irwin-Williams, 1979) have questioned the validity of the association between extinct fauna and artifacts of the Sulphur Spring stage and see no relationship to the Clovis Culture. Geoarchaeological investigations of Whitewater Draw were undertaken in 1982-1983 to resolve this controversy (Waters, 1985a, 1986).

Sulphur Spring artifacts are found at four sites in Whitewater Draw. Artifacts occur in secondary contexts within correlative fluvial sand-and-gravel deposits (Units Da and Db) at three sites (AZ FF:6:9, AZ FF:6:8, and AZ FF:10:1 Double Adobe site) and within less disturbed sediments (unit Dc) at AZFF:10:14 (Figure 1). Early Cochise Culture artifacts have also been recovered from the Lehner site in the adjacent San Pedro Valley (Haynes, 1982).

Ground stone artifacts, milling stones, and handstones, are the most common element of the Sulphur Spring assemblage and outnumber flaked-stone tools at most sites (Sayles and Antevs, 1941; Sayles, 1983). Flaked-stone artifacts are predominately unifacially worked flake scrapers, plano-convex

scraper-cores, and core choppers. Bifacial flaking is rare and only four biface fragments have been recovered from Sulphur Spring stage contexts.

Twelve radiocarbon dates on charcoal from deposits containing artifacts at four sites and 10 additional dates from the alluvium allow temporal placement of the Sulphur Spring stage. Four radiocarbon dates from the alluvium (units Da and Db) containing Sulphur Spring artifacts at AZ FF:6:9 range from $8,390 \pm 190$ B.P. (A-3233) to $8,650 \pm 180$ B.P. (A-3232). The Sulphur Spring artifact-bearing sand (Unit Db) at AZ FF:6:8 dates between $8,140 \pm 220$ B.P. (A-3277) and $9,340 \pm 180$ B.P. (A-3238) and the underlying artifact-bearing gravel (Unit Da) is undated. At AZ FF:10:1 dates of $8,840 \pm 310$ B.P. (A-3377) and $8,760 \pm 210$ B.P. (A-3379) are associated with artifacts in the upper sand (Unit Db). Ten additional dates from correlative deposits at Double Adobe range from $8,270 \pm 250$ B.P. (A-188c) and $9,120 \pm 270$ B.P. (A-2235) (Waters, 1985a, 1986). Artifacts have also been recovered from the underlying undated gravel (Unit Da). A date of $10,420 \pm 100$ B.P. (A-1152) was reported from a similar gravel 240 m downstream from the site AZ FF:10:1 and is associated with mammoth (*Mammuthus*) remains, but no artifacts (Damon and Long, 1972; Sayles, 1983). This date may be applicable to the artifact-bearing gravel at AZ FF:10:1 (Double Adobe) and AZ FF:6:8. Two radiocarbon dates, $9,860 \pm 80$ yr B.P. (SMU-197) and $9,900 \pm 80$ B.P. (SMU-204), are associated with Cochise Culture artifacts at the Lehner site, Arizona (Haynes, 1982), which directly overlie the Clovis horizon. Therefore, radiocarbon dates from strata containing Sulphur Spring artifacts place this stage between approximately 8,000 and 10,000 B.P. and possibly as early as 10,400 B.P., based on the single date from the gravel near Double Adobe (Waters, 1985a, 1986).

No extinct faunal remains were found in Sulphur Spring artifact-bearing deposits at AZ FF:6:8, or AZ FF:6:9 or AZ FF:10:14. The only association between extinct fauna and Sulphur Spring artifacts occurs at AZ FF:10:1, where mammoth (*Mammuthus*), camel (*Camelops*), horse (*Equus*), dire wolf (*Canis dirus*), and bison (*Bison*) remains have been recovered from the alluvium and artifacts of the Sulphur Spring stage (Sayles and Antevs, 1941; Sayles, 1983).

Fossils from the alluvium from the Double Adobe area are mostly isolated disarticulated finds, but two discoveries of articulated remains have been reported: (1) Haury (1960) recovered articulated camel leg bones in the sand from which Sulphur Spring artifacts had previously been recovered, and (2) Windmiller (see Sayles, 1983) uncovered the remains of a single mammoth (two lumbar vertebrae articulated) in gravel 240 m downstream from AZ FF:10:1. A radiocarbon date on charcoal collected from the gravel near the mammoth is $10,420 \pm 100$ B.P. (A-1152) (Damon and Long, 1972). Because the bones are articulated, they are considered to lie in primary association within the alluvium dated to approximately 10,400 B.P. However, the bones recovered from the alluvium in radiocarbon-dated contexts between 8,000 and 9,400 B.P. are probably reworked from older deposits. They are not articulated and there are abundant older sediments from which they could have been dislodged.

Therefore, megafaunal remains are not in primary association with Sulphur Spring stage artifacts in the alluvium dated between 8,200 and 9,400 B.P. However, it is possible that Sulphur Spring people did temporally overlap with relict populations of Pleistocene megafauna during the terminal Pleistocene. This question, however, remains unresolved, because no direct association of

articulated megafaunal remains and Sulphur Spring artifacts have been found.

In summary, radiocarbon dates place the Sulphur Spring stage of the Cochise Culture between 8,000 and 10,000 B.P. and probably to 10,400 B.P. Evidence suggest that the Sulphur Spring people did not temporally overlap with Pleistocene megafauna except possibly during the terminal Pleistocene. Failure to find diagnostic artifacts of the Clovis Culture and Sulphur Spring stage mixed on a site, their superposition at the Lehner site, and the chronological placement of the Sulphur Spring stage show that they are not temporally equivalent.

Lake Cochise

The Willcox basin is a closed basin in the northern portion of the Sulphur Springs Valley, Arizona (Figure 1). Streams from the surrounding mountains flow into the center of the basin where the water collects in Willcox Playa. In the past, the basin was occupied by a larger, more permanent body of water known as Lake Cochise. Strong winds traverse the basin and have eroded preexisting deposits and are responsible for the accumulation of large dunes on the northeast side of the playa. As a result, the Willcox basin has a complex history of alluvial, lacustrine, and eolian deposition.

A prominent singular shoreline of ancient Lake Cochise occurs at an altitude of approximately 1274 m (4180 ft) and was first reported by Meinzer and Kelton (1913). The shoreline features are well-preserved and are very prominent on the west and east sides of the basin. To the north and south the shoreline has been obliterated by recent erosion. This lake had a surface area of more than 190 km² and a maximum depth of 11 m. Lake Cochise was a pluvial lake that formed in a closed basin as a result of increased precipitation and decreased evaporation brought about by the cooler and wetter Pleistocene climate. Few data are available on the lacustrine chronology of Lake Cochise (when it existed, fluctuations, and most importantly its last high stand). Long (1966) proposed that Lake Cochise existed between 30,000 and 13,000 B.P. and possibly as late as 11,500 and 10,500 B.P. Haynes and Long (1987) obtained a radiocarbon date of $12,970 \pm 480$ B.P. (AA-866) from beach sediments on the western side of the lake.

The Willcox Playa now occupies the former lake bed of ancient Lake Cochise in the central portion of the basin. The Willcox Playa is an ephemeral desert lake covering 130 km², with a surface elevation of approximately 1260 m (4135 ft). The Willcox Playa is dry for most of the year and portions of the playa will fill with water only after large rainstorms.

ACKNOWLEDGMENTS

Geological and archaeological investigation at the Murray Springs Clovis Site and Curry Draw were supported by the National Geographic Society and the National Science Foundation. Geological and archaeological investigations of Whitewater Draw were supported by the Wenner-Gren Foundation. The Section on the San Pedro Valley of this guidebook was written by Haynes. The sections on the Sulphur Springs Valley were written by Waters.

REFERENCES CITED

- Agenbroad, L.D., and Haynes, C.V., Jr., 1975, Bison bison remains at Murray Springs, Arizona: The Kiva, v. 40, p. 309-313.

- Antevs, E., 1955, Geologic-climatic dating in the West: *American Antiquity*, v. 20, p. 317-335.
- _____, 1959, Geologic age of the Lehner mammoth site: *American Antiquity*, v. 25, p. 31-34.
- _____, 1983, Geologic dating, in Sayles, E.B., Cochise cultural sequence in southeastern Arizona: *University of Arizona Anthropological Papers*, 42, p. 26-43.
- Damon, P.E., and Long, Austin, 1972, Arizona radiocarbon dates III: *Radiocarbon*, v.4, p. 239-249.
- Gray, R.S., 1967, Petrology of the upper Cenozoic non-marine sediments in the San Pedro Valley, Arizona: *Journal of Sedimentary Petrology*, v. 37, p. 774-789.
- Hastings, J.R., and Turner, R.M., 1965, The changing mile; an ecological study of vegetation change with time in the lower mile of an arid and semiarid region: Tucson, University of Arizona Press, 317 p.
- Haury, E.W., 1960, Association of fossil fauna and artifacts of the Sulphur Spring Stage, Cochise Culture: *American Antiquity*, v. 26, p. 609-610.
- _____, 1983, Concluding remarks, in Sayles, E.B., Cochise cultural sequence in southeastern Arizona: *University of Arizona Anthropological Papers*, 42, p. 158-160.
- Haury, E.W., Antevs, Ernst, and Lance, J.R., 1953, Artifacts with mammoth remains, Naco, Arizona: *American Antiquity*, v. 19, p. 1-24.
- Haury, E. W., Sayles, E.B., and Wasley, W.W., 1959, The Lehner mammoth site: *American Antiquity*, v. 25, p. 2-30.
- Haynes, C.V., Jr., 1968, Preliminary report on the late Quaternary geology of the San Pedro Valley, Arizona: *Arizona Geological Society, Southern Arizona Guidebook III*, p. 79-96.
- _____, 1973, Exploration of a mammoth-kill site in Arizona: *National Geographic Society Research Reports*, v. 7, p. 125-126.
- _____, 1974, Archaeological investigations at the Clovis site at Murray Springs, Arizona, 1967: *National Geographic Society Research Report*, v. 8, p. 145-147.
- _____, 1976, Archaeological investigations at the Murray Springs site, Arizona, 1968: *National Geographic Society Research Society Research Reports*, v. 9, p. 165-171.
- _____, 1978, Archaeological investigations at the Murray Springs site, Arizona, 1969: *National Geographic Society Research Reports*, v. 10, p. 239-242.
- _____, 1979, Archaeological investigations at the Murray Springs site, Arizona, 1970: *National Geographic Society Research Reports*, v. 11, p. 261-267.
- _____, 1980, Archaeological investigations at the Murray Springs site, Arizona, 1971: *National Geographic Society Research Reports*, v. 12, p. 347-353.
- _____, 1981, Geochronology and paleoenvironments of the Murray Springs Clovis site, Arizona: *National Geographic Society Research Reports*, v. 13, p. 243-251.
- _____, 1982, Archaeological investigations at the Lehner site, Arizona, 1974-75: *National Geographic Society Research Reports*, v. 14, p. 325-334.
- Haynes, C.V., Jr., and Hemmings, E.T., 1968, Mammoth-bone shaft wrench from Murray Springs, Arizona: *Science*, v. 159, p. 186-187.
- Haynes, C.V., Jr., and Long, Austin, 1987, Radiocarbon dates at Willcox Playa, Arizona, bracket the Clovis occupation surface: *Current Research in the Pleistocene*, v. 4 (in press).
- Hemmings, E. T., 1970, Early man in the San Pedro Valley, Arizona [Ph.D. thesis]: Tucson, University of Arizona, 236 p.
- Hemmings, E. T., and Haynes, C.V., Jr., 1969, The Escapule mammoth and associated projectile points, San Pedro Valley, Arizona: *Journal of Arizona Academic Science*, v. 5, p. 184-188.
- Hendrickson, D.A., and Minckley, W.L., 1984, Cienegas--vanishing climax communities of the American Southwest: *Desert Plants*, v. 6, p. 129-176.
- Irwin-Williams, C., 1979, Post-Pleistocene archaeology, 7000-2000 B.C., in Ortiz, ed., *Handbook of North American Indians, Southwest*: Washington, D.C., Smithsonian Institute, p. 31-42.
- Johnson, N.M., Opdyke, M.D., and Lindsay, E.H., 1975, magnetic polarity stratigraphy of Pliocene-Pleistocene terrestrial deposits and vertebrate faunas, San Pedro Valley, Arizona: *Geological Society of America Bulletin*, v. 86, p. 5-12.
- Long, Austin, 1966, Late Pleistocene and recent chronologies of playa lakes in Arizona and New Mexico [Ph.D. thesis]: Tucson, University of Arizona, 141 p.
- Martin, P.S., 1963, The last 10,000 years, a fossil pollen record of the American Southwest: Tucson, University of Arizona Press, 87 p.
- Martin, P.S., and Plog, F., 1973, The archaeology of Arizona: Garden City, Doubleday/Natural History Press, 422 p.
- Mehring, P.J., Jr., 1967, Pollen analysis and the alluvial chronology: *The Kiva*, v. 32, p. 96-101.
- Mehring, P.J., Jr., and Haynes, C.V., Jr., 1965, The pollen evidence for the environment of early man and extinct mammals of the Lehner mammoth site, southeastern Arizona: *American Antiquity*, v. 31, p. 17-23.
- Mehring, P.J., Jr., Martin, P.S., and Haynes, C.V., Jr., 1967, Murray Springs, a mid-postglacial pollen record from southern Arizona: *American Journal of Science*, v. 265, p. 786-797.
- Meinzer, O.E., and Kelton, F.C., 1913, Geology and water resources of the Sulphur Spring Valley, Arizona: U.S. Geological Survey Water-Supply Paper 320, 231 p.
- Melton, M.A., 1965, The geomorphic and paleoclimatic significance of alluvial deposits in southern Arizona: *Journal of Geology*, v. 73, p. 1-38.
- Patton, P.C., and Schumm, S.A., 1981, Ephemeral-stream processes; implications for studies of Quaternary valley fills: *Quaternary Research*, v. 15, p. 24-43.
- Sayles, E.B., 1983, The Cochise cultural sequence in southeastern Arizona: *Anthropological Papers of the University of Arizona*, 42, 179 p.
- Sayles, E.B., and Antevs, E., 1941, The Cochise Culture: *Gila Pueblo Medallion Papers* 29, 81 p.
- Schreiber, J.F., Jr., 1978, Geology of the Willcox Playa, Cochise County, Arizona: *New Mexico Geological Society, 29th Field Conference, Guidebook*, p. 277-282.
- Schumm, S.A., 1977, *The fluvial system*: New York, John Wiley & Sons, 327 p.
- Schumm, S.A., and Parker, R., 1973, Implications of complex response of drainage systems for Quaternary alluvial stratigraphy: *Nature*, v. 243, p. 99-100.
- Spaulding, W.G., Leopold, E.B., and Van Devender, T.R., 1983, Late Wisconsin paleoecology of the American Southwest, in Wright, H.E., Jr., and Porter, S.C., eds., *Late Quaternary environments of the United States; the late Pleistocene*: Minneapolis, University of Minnesota Press, p. 259-293.

Waters, M.R., 1985a, The geoarchaeology of Whitewater Draw, Arizona: Anthropological Papers of the University of Arizona, 45, 81 p.

_____, 1985b, Late Quaternary alluvial stratigraphy of Whitewater Draw, Arizona; implications for regional correlation of fluvial deposits in the American Southwest: *Geology*, v. 13, p. 705-708.

_____, 1986, The Sulphur Spring stage and its place in New World prehistory: *Quaternary Research*, v. 25, p. 251-256.

Whalen, N.B., 1971, Cochise Culture sites in the central San Pueblo drainage, Arizona [Ph.D. thesis]: Tucson, University of Arizona, 325 p.

Willey, G.R., and Phillips, P., 1958, *Method and theory in American archaeology*: Chicago, University of Chicago, 216 p.

Terraces of the Lower Salt River Valley in Relation to the Late Cenozoic History of the Phoenix Basin, Arizona*

Troy L. Péwé
Department of Geology
Arizona State University
Tempe, Arizona 85287

INTRODUCTION

The terraces of the lower Salt River Valley offer fine examples of physiographic features, with pediments and caliche formation, that illustrate late Cenozoic events in the Phoenix Basin and adjoining mountains. The area is characterized by fault-block mountains with intervening basins filled with thousands of feet of unconsolidated sediments shed from the mountains. All major rivers and most other streams entering the basin from the north and east are flanked by sets of paired river terraces, many of which are strath terraces. The terraces range from 10 to 300 feet above the river, and are floored with coarse, rounded river gravel.

RIVER TERRACES

Terraces that typify the important nonparallel sets and that are at right angles to the trend of the mountain range are those mapped eastward from

Tempe to Stewart Mountain Dam along the Salt River (Figure 1). Four paired terraces are present (Figure 2). Reconnaissance work indicates that these same terraces extend farther east to Roosevelt Lake. The lowest terrace, named the Lehi Terrace (Péwé, 1971) is only 5 feet above the present river level near Lehi and rises to about 20 feet above the river 15 miles upstream.

A higher terrace, the Blue Point Terrace, grades from 10 to 80 feet above the river between Tempe and Stewart Mountain Dam. The most prominent

*Field stops are numbered from an earlier guidebook to these terraces. Only a selection of the STOPS with a brief description and updates are included in the guide for this trip. More lengthy descriptions, maps, diagrams, and photographs are in the earlier report (Péwé, 1978).

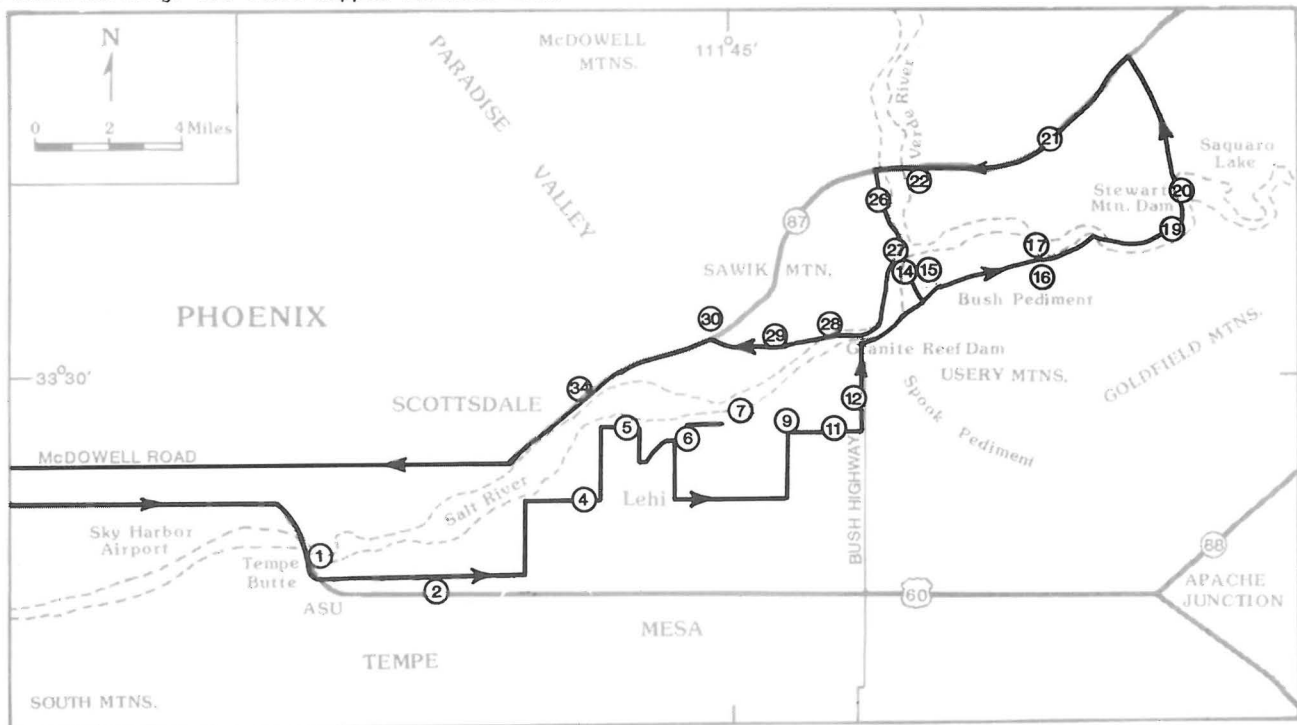


Figure 1. - Index map of lower Salt River Valley, central Arizona, showing location of field trip route and selected stops (circled numbers). Base map modified from Mesa 1:250,000 topographic map of the U.S. Geological Survey, 1969.

terrace is the Mesa Terrace (Péwé, 1971), an old, extensively dissected surface extending from Tempe, where it is 10 feet above the river, to near Stewart Mountain Dam where it is 220 feet above the river, and eastward to Roosevelt Dam where it is more than 300 feet above the river. Here it is believed to be truncated by a fault (Péwé, 1978).

The gravel of the Mesa Terrace is strongly indurated by caliche. Unlike the gravel of the younger Blue Point Terrace, which has cobbles slightly cemented, the older gravel is completely plugged by calcium carbonate and well-developed laminar layers are formed.

The Sawik Terrace (Péwé, 1971) is the highest terrace and the most fragmentary and lies 235 feet above the river at the mountain front. It decreases to an elevation of about 50 feet above the river in Scottsdale where it passes under the alluvial fan deposits shed from the Phoenix and McDowell Mountains. The gravel of the terrace is very strongly calichified. Both the Sawik and the Mesa Terraces have thick, well-calichified gravel layers near or at the surface.

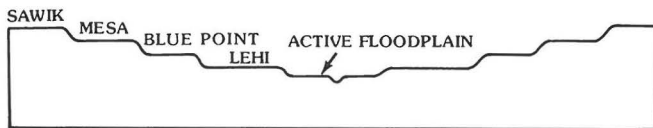


Figure 2.- Diagrammatic transverse profile of paired terraces on the lower Salt River Valley.

CALICHE

Stream terraces and alluvial fans on the edges of the Phoenix Basin expose sediments cemented by CaCO_3 - caliche. Caliche is a near-surface accumulation of CaCO_3 common to soils of low and middle latitudes in arid and semiarid regions throughout the world. This "lime" accumulation transforms otherwise unconsolidated sand and gravel to "concrete," much to the disgust of "users of the soil."

Caliche deposits in general are sheetlike and form roughly parallel to the ground surface. They undulate with topography and vary laterally in thickness. These lateral variations in thickness are the result of various factors, including differences in permeability, topography, and nature of the host material. Caliche deposits progress through a developmental sequence with time, as do other soil processes (Figure 3).

The ultimate source of CaCO_3 in caliche in noncarbonate sediments has been a topic of great interest since these occurrences were first observed. In areas of carbonate bedrock or alluvial gravels derived from carbonate bedrock, no real problem is encountered in terms of source. Some of the concepts for origin of caliche in noncarbonate rocks include chemical weathering of noncarbonate Ca-bearing parent material with additions of CO_3 from air and rain water, leaching of CaCO_3 from dust collected at the surface, and from the accumulation of Ca and CO_3 ions in water.

During the last few years some observers have suggested an eolian source from CaCO_3 . The writer strongly believes in such a source inasmuch as wind-blown dust is quite common and deposited in enormous amounts annually (Péwé and others, 1976). Analyses of the dust in the Phoenix area based on 15 samples collected over an 18-month period give a percentage

of CaCO_3 of from 1.2 to 3.8 (Péwé and others, 1981).

Although the details are not completely known, it appears that many of the grains and cobbles and perhaps even boulders in the calichified sand and gravel are in some instances completely surrounded by CaCO_3 . They float in the matrix of calcite and are not in contact with each other. In most areas the simple fillings of the voids in the parent materials by CaCO_3 cannot account for the amount of CaCO_3 present. It is believed by many that there is as much as 25% expansion of the unconsolidated sediments with the crystallization of the CaCO_3 .

A great number of fractured pebbles and cobbles appear on the surface of the older two of the terraces in the Phoenix Basin and on very old alluvial fans (Figure 4). Cobbles on these terraces show postdepositional fracturing in which the CaCO_3 apparently invaded previously existing cracks, and permeable zones in the cobbles forcing them apart below the surface. Frequently, cobbles can be found in place with major cracks revealing as much as 2 inches of separation. This is more normally characteristic of the finer grained rock types. Young (1964) concludes that crystallization forces of CaCO_3 that result in a volume increase are responsible and notes that the role of CaCO_3 in the disintegration of bedrock and surface deposits in semiarid and arid lands may be underestimated.

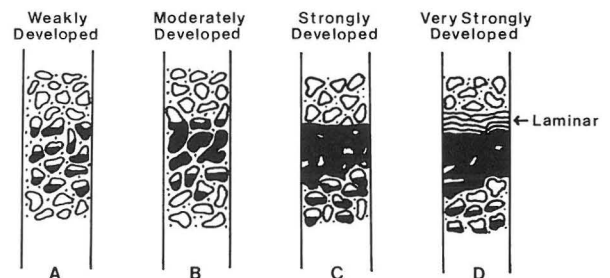


Figure 3. - Development stages of caliche surrounding the pebbles and cobbles in gravelly sediment (After Gile, 1975).

ORIGIN, AGE, AND TECTONIC SIGNIFICANCE OF TERRACES ALONG STREAMS ENTERING THE PHOENIX BASIN

It is apparent from the study of the converging terraces on the streams flowing out of the mountains and entering the Phoenix Basin from the north and east that the mountain ranges in that area are undergoing a slow regional uplift, apparently periodically. It also is apparent that the stream terraces converge on the edge of the basins and disappear under the valley-fill deposits. It would appear that there has been slow down-dropping and filling of the basins during the last 2 or 3 million years, perhaps longer, and the river gravels are present at some depth in the basin. The exact depth is not known, but in the city of Tempe, gravel at the top of the Mesa Terrace is anywhere from 10 to more than 30 feet deep, becoming deeper toward the southern part of the city. South of Mesa the coarse river gravel is at least 600 feet below the surface.

GEOLOGY FIELD TRIP ALONG THE LOWER SALT RIVER, ARIZONA FROM TEMPE BUTTE, TEMPE TO SAGUARO LAKE AND RETURN

The numbered stop locations are on U.S. Geological Survey topographic quadrangle maps. These maps should be consulted for a clearer understanding of the discussion. See Burt and Péwé (1978) for maps.

STOP 1. ARIZONA STATE UNIVERSITY (Tempe Quadrangle, 1952). On edge of river scarp near railroad track at Arizona State University. The fraternity houses to the east are on the Lehi Terrace of the Salt River which is part of the floodplain. However, they are not on the active part of the floodplain and were not flooded in 1966, 1978, 1979, or 1980. The scarp at STOP 1 is about 10 ft above the active floodplain. The terrace upon which Arizona State University is built is part of the Mesa Terrace, which is well displayed at STOP 2 in Mesa, 3 mi to the east.

The modern Salt River flows between Tempe Butte on the south and the Papago Pediment on the north. The bedrock is very shallow at this narrow constriction and actually crops out locally in the bottom of the floodplain. In the geologic past the Salt River flowed to the west by going south of Tempe Butte and South Mountains (Figure 1) (Davis, 1892; Lee, 1904). At least four terraces are present on the Tempe Quadrangle geologic map (Péwé and others, 1986a); they all have low scarps and appear to terminate in the vicinity of the western part of the map (Tempe Butte). No prominent terraces of the Salt River are exhibited downstream. On the ASU campus there are 3 to 6 feet of river silt overlying coarse, rounded river gravel of the Mesa Terrace. This gravel is exposed in the basements of most of the buildings constructed on the campus.

STOP 2. TERRACE SCARP. One of the best western exposures of the prominent Mesa Terrace that extends unbroken from here eastward 10 miles to the Utery Mountains (Figure 1). Gravel crops out and the terrace scarp here is 20 feet above the active floodplain.

As for all the major terraces, the overbank silt, or silt from the surrounding mountains that overlies the gravel, has been washed away at the terrace scarp, and it is here that the caliche-cemented gravel is well exposed.

STOP 4. VILLAGE OF LEHI. This lower terrace is named the Lehi Terrace (Péwé, 1971) from the village of Lehi (Figure 1). The village was established in 1877 by the Mormons and was the first settlement in this immediate area. The term Lehi comes from the Biblical prophet of 600 B.C. who took his family into the wilderness to escape the destruction of Jerusalem. The name has great antiquity, but the terrace is undoubtedly older. The terrace here is about 10 ft above the modern floodplain and was not flooded by recent floods. However, these floods did not reach their possible maximum height because of storage provided by the six reservoirs on the Verde and Salt Rivers. The largest known flood in the Salt River Basin occurred in February 1891 when a flow of 300,000 cubic feet per second (cfs) was recorded. Flood waters at that time invaded most of the downtown area of Phoenix and covered the Lehi Terrace.

From old records of the towns of Lehi and Mesa we learn that on February 19, 1891 the Salt River reached the highest point that could be remembered by the settlers and did considerable damage to their crops and buildings. However, 3 days later the river rose an additional 3 feet, completely engulfing the

bottomland. It is reported that five Indians were drowned, but all the white settlers escaped to the mesa where they remained for 2 weeks. Most of the Indians and settlers lost nearly all their personal possessions in the flood and the canals were badly damaged. The water in Lehi was described as being waist deep, or belly deep to a pony.

Two hundred yards southeast from STOP 4, on Keal Road, Mr. Roger Sattler came across the remains of a fossil in an excavation for a septic tank. The writer investigated the site and recovered a fine carapace and plastron of a desert tortoise 14 by 10 inches, which was at the top of the river gravel beneath 90 in. of top-stratum silt.

Brad Archer, Dept. of Geology, Arizona State University, has reconstructed the fossil and identified the tortoise as *Gopherus* sp., a late Pleistocene animal not living in central Arizona today and larger than the modern *Gopherus* species. This Pleistocene fossil and a Pleistocene fossil horse tooth from the Lehi Terrace near Sky Harbor Airport (Nations and Lindsay, 1976) suggest that this terrace is late Pleistocene in age.

STOP 5. SCARP OF LEHI TERRACE ABOVE MODERN SALT RIVER FLOODPLAIN. Beneath 3 or 4 ft of top stratum silt is a coarse, rounded river gravel with clasts about 4 in. in diameter. There is no cementation by caliche whatsoever, but there is a very thin film of caliche completely surrounding the larger cobbles in the silty matrix. In the upper 2 ft of the section there are characteristic pot sherds of Hohokam culture, as well as lithic artifacts.

STOP 6. LOW TERRACE SCARP OF BLUE POINT TERRACE. The gravel terrace scarp, 3 to 6 ft above the Lehi Terrace, appears along the road to the south in this area. This is probably the most western exposure of the Blue Point Terrace. From this STOP one can see 1/2 mi to the south the prominent scarp of the Mesa Terrace, the top of which is here 60 ft above the modern floodplain. To the north one can see the counterpart of the 60-ft terrace across the Salt River Valley.

STOP 7. BLUEPOINT TERRACE SCARP (Buckhorn Quadrangle, 1956). This is the scarp of the Blue Point Terrace. It lies below the Mesa Terrace but above the modern floodplain and the Lehi Terrace. The terrace scarp is about 20 ft above the modern floodplain of the Salt River and at an elevation of 1,300 ft at this spot. The terrace, poorly developed and partly covered with colluvium, is termed the Blue Point Terrace (Péwé, 1971) after Blue Point Picnic Area near where it is well-exposed on the south side of the Salt River, 8 to 10 mi upstream from this spot.

Caliche is poorly developed in the gravelly alluvium of this terrace. The cobbles and pebbles may have a caliche rind of about 1/8 inch, but there is no massive cementation of the pebbles or cobbles.

Kokalis (1971) made detailed analyses of the size-grade distribution of the sediments of the terraces as well as the modern floodplain. The sediments can be classed as gravels to sandy gravels. He concluded that the average medium diameter of the terrace sediment is -4.0ϕ and that of the modern floodplain sediments is -3.4ϕ . He further states that the average of the most coarse 1 percentile illustrates this difference because that of the terrace sediments is -7.4ϕ , whereas the average for the modern floodplain gravels is -7.0ϕ . His analyses indicate that for all practical purposes the size distribution of the sediments on the terrace is the same as that of the floodplain. However, there is a slight difference, and the regimen of the Salt River in the past may have

been slightly more rigorous during the time that the high terraces were produced than during the time of the modern floodplain.

Kokalis (1971) was able to demonstrate that in the reach of the Salt River from Stewart Mountain Dam to its mouth there was no change in size distribution of the sediments. Also, it was not possible to distinguish one terrace from another by size grade analyses alone.

STOP 9. ROAD CUT IN MESA TERRACE ON HIGLEY ROAD. This is the surface of the Mesa Terrace. The road cut has exposed highly calichified coarse gravel with lenses of silt and sand. The plug stage of the caliche growth (Figure 3) is well exhibited on both sides of the road cut and especially on the small new cut on the south end of the east wall of the road. Many fractured cobbles and boulders can be seen with caliche-filled fractures. In many places on Mesa Terrace the fractured parts of the cobbles have been displaced as much as 2 inches. At this locality, laminar caliche is well developed (Figure 4). As much as 1 or 2 feet of laminar caliche can be seen, especially in finer material. The development of caliche indicates great antiquity of the terrace, and the surface of the Mesa Terrace is surely quite old; very early Pleistocene if not Pliocene.

STOP 11. PEDIMENT WASH (GRUS) OVERRIDING SAWIK TERRACE GRAVEL. At an elevation of about 1,433-1,438 feet in the SE $\frac{1}{4}$ Sec. 26, the edge of the "pediment wash" sediments can be seen and the underlying rounded caliche-cemented gravels of the Sawik Terrace are exposed in shallow washes (Péwé, 1978).

STOP 12. SPOOK PEDIMENT. The broad pediment cut on granite rocks is named Spook Pediment (Péwé, 1971) from Spook Hill, a well-developed inselberg projecting 300 feet above the gently sloping pediment surface in the northern part of the Buckhorn Quadrangle. Part of the pediment is graded to remnants of the Sawik Terrace, but most is graded to the Mesa Terrace in this area. Bedrock crops out along Bush Highway at this locality and in stream cuts to the east and west. The typical gently sloping, smooth-looking pediment is gullied with shallow stream incisions 1 to

5 feet deep. The surface of the Spook Pediment in this area slopes about 100 feet per mile to the west and southwest.

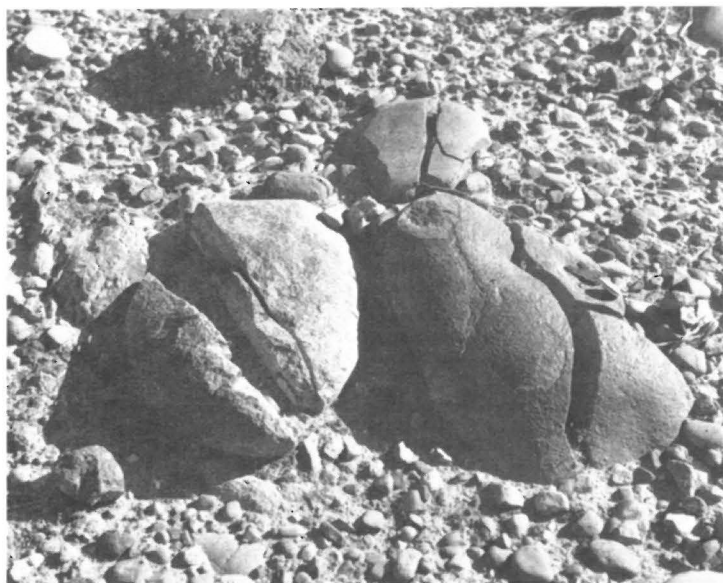
STOP 14. PHON D. SUTTON RECREATION AREA. This picnic area is on a low terrace of the Salt River about 40 feet above the river. It is part of the Blue Point Terrace. Note that the Blue Point Terrace, as well as the Mesa and Sawik Terraces, are increasingly higher above the modern floodplain as one goes upstream.

STOP 15. COON BLUFF. A remnant of Mesa Terrace overlies bedrock at an elevation of 1,480-1,550 feet at this locality. The surface is 160-180 feet above the modern river (Drosendahl, 1987). A great many of the large boulders have been fractured in place with displacement of 2 to 6 inches. Such fracturing appears to be present only of clasts on the Mesa and Sawik Terraces. The fracturing and displacement is by caliche formation while in the caliche level. Subsequent erosion and carbonate solution has exposed fractured boulders and cobbles.

It can be here noted that many of the boulders, especially the quartzite boulders, have well-developed impact scars or percussion marks, the result of large boulders saltating along the river bottom under high-velocity flows of the stream. Such marks are well developed on the boulders of the Mesa and Sawik Terraces but poorly developed or absent on the lower terraces, although large boulders are present in all terraces. This may suggest a stronger stream regimen during the time of deposition of the upper terrace gravels.

The rock types represented by the cobbles and boulders of the Mesa Terrace are typical both of the deposits of the terraces and those of the active floodplain of the lower Salt River Valley. Kokalis (1971) examined 5,900 samples and determined that 15% of the clasts were from the Precambrian basement complex of igneous rocks; 36% were of the volcanic rocks of Tertiary age; and 48% were sedimentary rocks of Precambrian age. The two most common rock types in the terrace deposits are orthoquartzite and rhyolite (metarhyolite). The larger the boulder the more likely it is to be one or another of these two types of rock.

Figure 4. - Caliche-split cobbles of quartzite on gravel surface of Mesa Terrace. Near Thomas and Higley Roads, Arizona (Photograph No. 4141 by Troy L. Péwé, September 17, 1977).



Proceed from STOP 15 to STOP 16 on the Bush Highway across the lower edge of the pediment. The well-developed pediment extending north from the Uesery Mountains to the Salt River in this area is termed the Bush Pediment (Péwé, 1971) from the new and old Bush Highways, which traverse the pediment from north to south and east to west. The pediment today is, for the most part, graded to the Blue Point Terrace, although it is now being cut below this level in an attempt to be graded to the modern Salt River floodplain.

STOP 16. MESA TERRACE REMNANT (Stewart Mountain Quadrangle, 1964). A bedrock remnant about 200 feet above the Salt River is capped with weathered, caliche-cemented gravel, which is part of the Mesa Terrace. Characteristics of the gravel here are similar to those described on Coon Bluff. A higher level gravel which is part of the Sawik Terrace lies on bedrock 40 or 50 feet above this surface.

Looking south from this remnant up the Bush Pediment one can realize that at one time the Bush Pediment was graded to the Sawik Terrace level and then later to the Mesa Terrace level. Subsequently, with the lowering of local base level (the downcutting of the Salt River), the pediment has been regraded from the Mesa Terrace level to the Blue Point Terrace level, and is now being worn down even lower. Undoubtedly, the removal of such a large amount of granite has taken a considerable amount of time and supports the suggestion of considerable antiquity for the ages of the upper terraces.

STOP 17. LONE CREEK CROSS SECTION. An exposure on the left limit of Lone Creek from the Bush Highway north to the Salt River exhibits a thick deposit of pediment wash coming off the Bush Pediment. About 200 feet north of the Bush Highway the pediment wash deposit can be seen overlying a more or less horizontal gravel surface of the Blue Point Terrace gravel. Further downstream the gravel is exposed overlying bedrock on the left limit of the Salt River at the junction of the stream and the river. A climb to the top of the terrace surface across the exposed gravel indicates that there is very little caliche in the coarse gravel. A view upstream from this vantage point (the junction of Lone Creek and the Salt River) shows the scarp of the Blue Point Terrace on the south side of the Salt River; one-half mile southeast are bedrock knobs capped with gravel patches of Mesa and Sawik ages. Far to the southeast lies the front of the Goldfield Mountains, which consists of volcanic flows and ejecta.

From STOP 17 to 1 mile east, the terrace is covered with a colluvial apron of grus (granitic weathering debris) coming from the south, an apron which has been dissected by downcutting streams as local base level has been lowered since Blue Point Terrace time. These streams have not only cut through the grus cover, but through the gravel and into the underlying bedrock, which is exposed on the terrace scarp and also in the small drainageways traversing the terrace.

STOP 19. BEDROCK CLIFF OVER RIVER. Here the grus cover is thin or absent, and gravels of the Blue Point Terrace crop out over bedrock cliffs 40 to 50 feet high above the river.

Upstream from STOP 19 a large alluvial fan from a small stream to the north deflects the Salt River to the south to cut into rocks of the Goldfield Mountains. A guest ranch, which lies immediately upstream from this fan in the right limit of the river, is on the Blue Point Terrace.

STOP 20. SAGUARO LAKE RECREATION FACILITY. From the restaurant an excellent view can be obtained to the north, south, and east. To the north one can see a colorful volcanic tuff layer from the Superstition Mountain area overlying the granite. To the south is Stewart Mountain Dam (Tilford, 1966; Anderson and others, 1986) holding in Saguaro Lake. A long finger of land stretching from the Goldfield Mountains to the dam has a relatively flat-topped area, which is the surface of the Mesa Terrace at an elevation of 1,620 feet or about 220 feet above river level. When the lake is drained, a well-developed surface of the Blue Point Terrace that is present under most of the lake adjacent to this facility is visible.

STOP 21. TERTIARY VALLEY FILL. Poorly consolidated, poorly rounded material of fairly local origin is exposed in road cuts along the highway; however, when a weathered lag gravel appears on the interfluves, it can be confused with terrace gravel of the Salt or Verde Rivers. Kokalis (1971), as well as Pope (1974), have demonstrated that there is a distinct difference in rock types between the Salt River gravel, Verde River gravel, and the Tertiary valley-fill deposits.

STOP 22. HIGH TERRACE REMNANT ALONG VERDE RIVER. Well-preserved remnants of the high Mesa Terrace lie adjacent to the Beeline Highway, both to the north and south on the east side of the Verde River. The rounded river gravel of the Verde River overlies Tertiary valley-fill deposits. The 20 or 30 feet of thickness of river gravel is exceedingly well cemented by caliche and forms a resistant caprock. The upper surface of the terrace has well-developed laminar caliche several inches thick. The surface of the terrace lies approximately 150-160 feet above the Verde River and additional terrace remnants occur on the east side of the Verde River, downstream near its junction with the Salt River. Remnants of the Mesa Terrace also occur on both sides of the river upstream as far as Bartlett Dam, 15 miles to the north. These terraces are the continuation of the Mesa Terrace surface of the Salt River.

STOP 27. FILTRATION PLANT. Across the road from the filtration plant, a small knob of Camels Head Formation (Péwé and others, 1986) (arkose conglomerate) crops out. The gravels of the Blue Point Terrace lap around this bedrock knob except on the river side where the river has steepened the slope exposing the bedrock.

The discussion point here involves taffoni. Taffoni are purse-shaped pockets or cavities 2 inches to 60 feet in diameter weathered in granitelike rocks in arid regions. They are common in all the major deserts of the world and are extremely well developed in the lower Sonoran desert of Arizona. Although debates still occur concerning the origin of taffoni, the writer believes they are due to differential weathering caused by the decay of feldspars and associated minerals. It is thought that the development of these erosional cavities takes an extremely long time and work is currently in progress by the writer and associates to obtain information along this line. The question at this locality is whether the taffoni developed before or after the formation of the Blue Point Terrace. If the taffoni formed after the Blue Point Terrace was dissected, it would appear that the terrace is of considerable antiquity because taffoni 9 feet across have formed in this arkose conglomerate.

STOP 28. MESA TERRACE AT GRANITE REEF DAM. This stop is at the edge of the mountains; downstream from here the Salt River spread out into the broad valley. At

the time of the formation of the Mesa Terrace, the river spread very widely north and south, from the edge of the McDowell Mountains to the edge of the Utery Mountains. The gravel here on the Mesa Terrace surface is on granitic bedrock. To the west, the surface has been cut on alluvial fill. The surface of the terrace is 80 to 100 feet above the river at this spot. A well-developed Mesa Terrace scarp can be seen in the distance several miles to the southwest.

In 1977 a deep cut was made across the terrace north to south at this locality to accommodate the Central Arizona Project siphon that goes under the Salt River. The cut was 50 feet deep, mostly in granite. On the south edge of the terrace at this locality there are about 8 or 9 feet of calichified terrace gravel over granite. This is a buried granite hill because as one proceeds 3 feet to the north, the hill disappears and the cut, to depths of at least 40 ft, is entirely in Mesa Terrace gravel. The cut exposed about 3 or 4 feet of a reddish soil and 11 feet of highly calichified gravel; beneath was typical coarse Salt River gravel with crossbedded sands and gravel with clasts up to 2 feet in diameter.

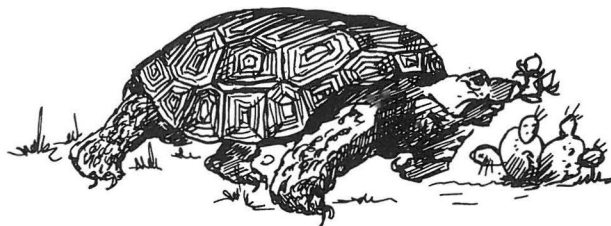
STOP 29. ALLUVIAL FAN OVER BLUE POINT TERRACE (Sawik Mountain Quadrangle, 1964). This locality is in the center of a large alluvial fan about 10 mile square which emanates from a dissected pediment to the north and covers the widespread Blue Point Terrace here with silt and colluvium from 1 to 30 feet thick. Toward the distal end of the fan, remnants of the Blue Point gravel surface are exposed. The size of this fan indicates that a long period of time must have elapsed since the cutting of the Blue Point Terrace.

STOP 30. MESA TERRACE. The Arizona Canal makes a very sharp southward bend near this top to accommodate a small fan coming from Sawik Creek; the small fan is part of the overall fan described at STOP 29. The Mesa Terrace is well developed at this locale and is about 100 feet above the modern floodplain. The terrace is entirely cut in alluvium and stands above the alluvial fan described earlier. The gravel is highly calichified and a great number of split boulders are exposed on the edge of the terrace.

STOP 34. HOHOKAM CANAL (Mesa Quadrangle, 1952). Near the edge of the Mesa Terrace are remnants of ancient canals built by the Hohokam Indians about 800-1,000 years ago. Parts of the old Indian canals have been destroyed by the shifting of the Salt River in the last 1,000 years. The terraces were evidently hacked out of the caliche-cemented gravel by hand with crude stone implements. An extensive array of these canals existed in the valley many years ago.

REFERENCES CITED

- Anderson, L.W., Piety, L.A., and Hansen, R.A., 1986, Seismotectonic investigation, Stewart Mountain Dam, Salt River Project, Arizona: U.S. Bureau of Reclamation, 41 p.
- Burt, D.M. and Pêwê, 1978, Guidebook to the geology of central Arizona: Arizona Bureau of Geology and Mineral Technology, Paper No. 2, 176 p.
- Davis, A.P., 1897, Irrigation near Phoenix, Arizona: U.S. Geological Survey Water-Supply Paper 2, 98 p.
- Drosendahl, J.K., 1987, Environmental geology of the Rio Salado Development District, eastern part [Masters thesis]: Tempe, Arizona State University, 124 p.
- Gile, L.H., 1975, Holocene soils and soil geomorphic relations in an arid region of southern New Mexico: *Quaternary Research*, v. 5, p. 321-360.
- Kokalis, P.G., 1971, Terraces of the lower Salt River Valley, Arizona [Masters thesis]: Tempe, Arizona State University, 102 p.
- Lee, W.T., 1904, Underground waters of Salt River Valley, Arizona: U.S. Geological Survey Water-Supply Paper 136, 196 p.
- Nations, J.D., and Lindsay, E., 1976, Pleistocene Equus from Salt River terrace gravels, Phoenix, Arizona: *Journal of the Academy of Science*, v. 11, p. 27-28.
- Pêwê, T.L., 1971, Guidebook to the geology of the lower Salt River Valley: unpublished guidebook, 21 p.
- 1978, Terraces of the lower Salt River Valley in relation to the late Cenozoic history of the Phoenix Basin, Arizona, in Burt, D.M., and Pêwê, T.L., Guidebook to the geology of central Arizona: Arizona: Arizona Bureau of Geology and Mineral Technology Special Paper 2, p. 1-46.
- Pêwê, T.L., Pêwê, E.A., and Pêwê, R.H., 1976, Rate of desert dust deposition [abs.]: *Journal of the Arizona Academy of Science*, v. 11, proc. suppl., p. 95-96.
- Pêwê, T.L., Pêwê, E.A., Pêwê, R. H., Journaux, A., and Slatt, R.M., 1981, Desert dust; characteristics and rates of deposition in central Arizona, U.S.A., in Pêwê, T.L., ed., *Desert dust; origin, characteristics and effect on Man: Geological Society of America Special Paper 186*, p. 169-190.
- Pewe, T.L., Wellendorf, C.S., and Bales, J.T., 1986, Environmental geology of the Tempe Quadrangle, Maricopa County, Arizona, geologic cross sections of Papago Park pediment: Arizona Bureau of Geology and Mineral Technology, Geologic Investigation Series Map GI-2-C, scale 1:24,000.
- Pope, C.W., 1974, Geology of the lower Verde River Valley, Maricopa County, Arizona [Masters thesis]: Tempe, Arizona State University, 104 p.
- Tilford, N.R., 1966, Engineering geology-Stewart Mountain Dam Site, Arizona [Masters thesis]: Tempe, Arizona State University, 42 p.
- Young, R.G., 1964, Fracturing of sandstone cobbles in caliche cemented terrace gravels: *Journal of Sedimentary Petrology*, v. 39, no. 4, p. 205-886.



Late Cenozoic Deposits, Vertebrate Faunas, and Magnetostratigraphy of Southeastern Arizona

Everett H. Lindsay
Department of Geosciences
University of Arizona
Tucson, Arizona 85721

Neil D. Opdyke
Geology Department
University of Florida
Gainesville, Florida 32611

Noye M. Johnson
Earth Science Department
Dartmouth College
Hanover, New Hampshire 03755

INTRODUCTION

The purpose of this trip is to examine some of the principal reference sections for late Cenozoic continental sedimentation in the southwestern United States, especially those that have yielded abundant vertebrate fossils and have provided a magnetic reversal sequence. Participants will examine the Gila Conglomerate at 111 Ranch in the Safford basin of Graham County, Arizona and the St. David Formation at Curtis Ranch in the San Pedro Valley of Cochise County, Arizona. Vertebrate biostratigraphy and magnetostratigraphy of both those deposits have been published in the GSA Bulletin (Johnson and others, 1975; Galusha and others, 1984). We will visit several of the sites discussed in those papers. Some of the illustrations from both papers have been copied in this trip guide.

Our itinerary (see Figure 1) for the first day takes us east from the Phoenix area, leaving the Salt River drainage to enter the Gila River drainage. We will travel to the south of the Superstition Mountains, cross over the Pinal Mountains, then follow the Gila River to Safford. After lunch, we will visit the 111 Ranch to the east of Safford, and will then return to Safford for the evening. On the second day we will leave Safford after breakfast, driving south on the western side of the San Simon Valley, then west to the Sulphur Springs Valley and Willcox Playa, later pass-

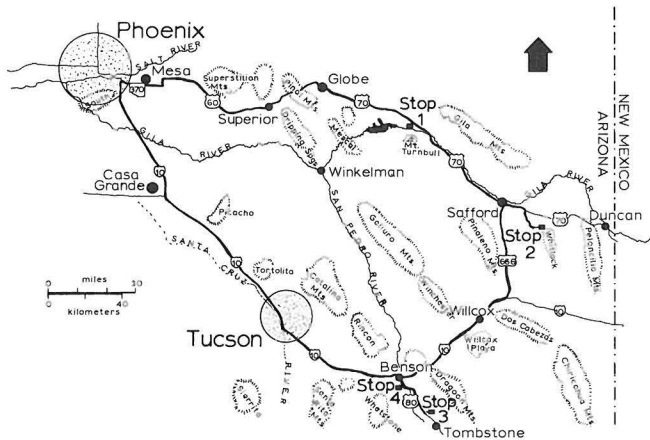


Figure 1. Field-trip route.

ing between the Dragoon Mountains and Little Dragoon Mountains into the San Pedro Valley. In the San Pedro Valley we will walk about 2 miles through the Curtis Ranch section, take our lunch there, and then drive west to Tucson, passing between the Whetstone and Rincon Mountains. Participants may leave the trip at Tucson International Airport about 6 p.m., or continue on to Phoenix, arriving there about 8:30 p.m.

Figure 2 shows the correlation of late Cenozoic fossil sites in the San Pedro Valley, Safford basin, and Duncan basin with the magnetic polarity time scale.

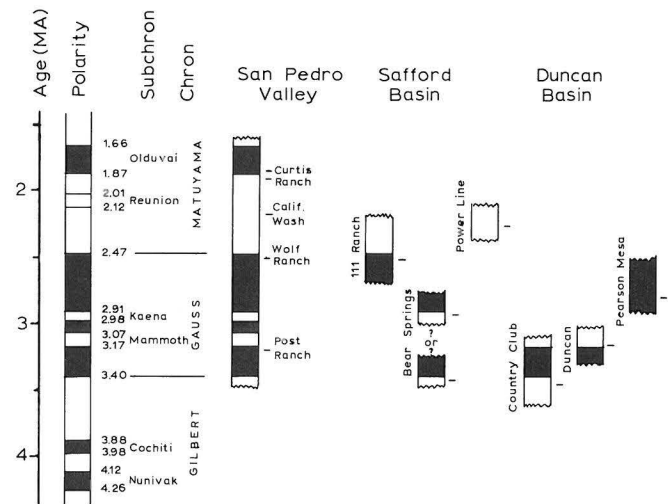


Figure 2. Magnetic polarity sequence and correlations, San Pedro Valley, Safford Basin and Duncan Basin. (Modified from Y. Tomida, 1985).

GEOLOGIC HIGHLIGHTS EN ROUTE TO STOP 1

Terraces along the lower Salt River Valley near Phoenix have been studied intensively by Péwé (1971, 1978). Péwé (1971) mapped four terraces between Phoenix and the Stewart Mountain Dam, east of Phoenix. These are (lowest to highest) Levi Terrace, Blue Point Terrace, Mesa Terrace, and Sawik Terrace. The age of these terraces has never been determined, but Péwé (1978) noted they are younger than 16 Ma and could be as old as 5 Ma. Péwé pointed out that the development of thick caliche deposition (45 feet thick

on Sawik Terrace) indicates a significant antiquity to the higher terraces. As we drive east from Phoenix, much of the residential development between Phoenix and Mesa is constructed on the Mesa Terrace, the most prominent terrace in the Phoenix area.

As we drive south of the Superstition Mountains and beyond the town of Superior, we will see silicic volcanic tuffs and ash-flow sheets of the Superstition-Superior volcanic field. These mid-Tertiary volcanics have been described by Ransome (1903), N.P. Peterson (1962), D.W. Peterson (1966, 1969), Sheridan and others (1970), and Sheridan (1978). As noted by Sheridan (1978), tuffs associated with this silicic volcanic field cover an area of approximately 100 km. Three separate volcanic centers produced these deposits between 15 and 22 Ma, with most of the volcanic activity occurring between 18 and 21 Ma (Shafiqullah and others, 1980). Sheridan (1978) recognized two main stratigraphic units, the (lower) Superstition Tuff and the (upper) Geronimo Head Formation, in the Superstition Mountain sequence. All of these volcanic rocks predate the basin-fill deposits loosely termed "Gila Conglomerate" or equivalent rocks.

As we pass through Miami and Globe, seeing the extensive mine tailings, we are reminded of the importance of copper mining in this area. Fellows (1984) noted that in 1981 Arizona led the nation in value of nonfuel minerals produced and that only one nation (Chile) produced more copper than Arizona. Copper mining in the U.S. dropped drastically in 1982 and has not recovered, although many copper mines in Arizona have reopened on a limited basis. Two old and productive copper mines close to our route are the Ray mine, located south of our route near Superior, and the Inspiration mine, located north of our route near Miami. Mining at Ray began in 1870, long before silver was discovered at Tombstone by Ed Schieffelin (in 1879), which brought many treasure-seekers and gamblers to Arizona.

The term Gila Conglomerate has been applied to late Cenozoic valley-fill deposits of southeastern Arizona since Knechtel (1938) described the deposits of the Gila and San Simon Valleys, which we will examine later today. The term was originally coined by Gilbert (1875) for coarse fluvial conglomerates along the Gila River near the Arizona/New Mexico border. It had been used by Ransome (1919) for steeply dipping deposits along the Gila River near Superior. Knechtel (1936, 1938) noted the similarity of fauna derived from sediments in the Gila and San Simon Valleys compared to fauna from the San Pedro Valley, e.g., the Benson fauna of Gidley (1922, 1926). Heindl (1963) described late Cenozoic deposits along the San Pedro River near Mammoth and suggested the term "Gila" be raised to Group status to include all valley-fill sediments in southeastern Arizona younger than middle Tertiary volcanic rocks, such as the Superstition-Superior volcanic field, and older than late Quaternary deposits. No formal recognition of Gila Group has been adopted, primarily because many of the discrete sediments, such as the 111 Ranch beds, have never been characterized lithologically or formally named.

Assembly and Departure

Our trip will assemble at the Phoenix Civic Plaza (the specific location will be given in the GSA program) before 8 a.m., departing at 8. We will proceed from the Phoenix Civic Plaza to the junction of Interstate 10 and the Superstition Freeway (State Route 360), a distance of about 9 miles. Distances for day 1 are given in miles from that junction.

Total mileage for day 1 is about 200 miles.

Miles		
Interval	Total	
0	0	Junction of Interstate 10 with Superstition Freeway (State Route 360). Proceed east on Superstition Freeway to Power Road (or farther if the freeway continues). The Superstition Mountains appear ahead of us in the distance. We will be following Highway 60 along the south margin of the Superstition Mountains.
16	16	Power Road. Turn left on Power Road and drive to the junction with Highway 60 (about 2 miles).
2	18	Highway 60. Turn right and continue heading east on Highway 60 toward Apache Junction and Globe.
8.2	26.2	Junction with State Route 88 (in Apache Junction). Continue on Highway 60 toward Globe. Multiple units of the Superstition Tuff and overlying Geronimo Head Formation are exposed along the front of the Superstition Mountains, to our left, as we drive between Apache Junction and Florence Junction.
16.2	42.4	Junction with Highway 89 (to Florence) at Florence Junction. Continue on Highway 60 toward Globe. Between Florence Junction and Superior (a distance of about 16 miles) we will see remnants of Miocene dacitic flows underlain by Precambrian granites and schists. Dromedary Peak (south of the highway near milepost 217) is one of these Miocene volcanic remnants. We pass through roadcuts of Precambrian granites near Gonzalez Pass, about 7 miles east of Florence Junction. Picket Post Mountain (south of the highway about 7 miles west of Superior) surrounds a volcanic vent that produced some of the Miocene flows.
14.6	57.0	Entering Superior. We continue on Highway 60 toward Globe. Clifty exposures to the east of Superior are tilted Paleozoic sediments that are overlain by thick Tertiary ash-flow sheets. The fault that brings these Paleozoic sediments to the surface is called the Concentrator fault; we cross this fault about where we intersect Highway 177 on the east side of Superior. The prominent cliff south of Superior (and east of the fault) is called Apache Leap. About a mile east of Superior we encounter a massive sheet of welded tuff, pass under the tuff in the Queen Creek tunnel, and over the tuff to about the Gila County line (almost 9 miles east of Superior). Between the Gila County line and Miami the highway crosses the early Tertiary

Schultze Granite. To the south we see more exposures of the Schultze Granite, and beyond the granite, Precambrian schists of the Pinal Mountains.

- 16.2 73.2 Cross Bloody Tanks Wash and enter town of Miami. Continue on Highway 60 toward Globe. Mine tailings form high banks to the left of the highway. Several copper mines are located near Miami; the price of copper has been depressed, resulting in virtual closure of these mines. Buildings of the Inspiration Consolidated Copper Company are visible on the hill to the left of the highway as we drive through Miami.
- 5.9 79.1 Enter Globe. Continue on Highway 60 to the east of Globe where we intersect Highway 70.
- 3.4 82.5 Separation of Highways 60 and 70. Continue straight ahead on Highway 70 to Safford; Highway 60 turns left (north), heading for the Salt River Canyon and the White Mountains. East of this junction we enter the San Carlos Valley, near Gibson Wash (about 8 miles east of the Highway 60 and 70 separation). Sediments exposed in roadcuts as we enter the San Carlos Valley have been called the Gila Conglomerate. However, these sediments are much coarser than the Gila Conglomerates we will see at Stop 1 and in the Safford Valley. Note that the sediments become less coarse as we approach the center of the valley.
- 19.2 101.7 Junction with State Route 170 to San Carlos. Continue on Highway 70 to Safford. We cross the San Carlos River about one-half mile east of this junction. San Carlos Reservoir is about 6 miles south of this junction. Mount Turnbull is the impressive peak on the south side of the

Gila Valley (to the south and east). The Gila Mountains form the northern border of the Gila Valley, with discontinuous terraces composed of Gila Conglomerate remaining near their base. The Gila Mountains are composed of mid-Tertiary volcanic rocks. We pass through excellent exposures of Gila Conglomerate along the highway for about 10 miles. Note that some of these sediments have been folded slightly. Some of the sediments lap onto local volcanic flows, and some have large blocks of volcanic debris interbedded with fine sediments. None of these sediments have yielded fossils. Presumably they are about the same age as the Gila Conglomerate near Safford. We will stop and examine similar beds of Gila Conglomerate at Stop 1.

- 10.5 112.2 STOP 1. We will stop to the east side of Salt Creek, between mile post 281 and 282, to stretch our legs and look more closely at the Gila Conglomerate (see Figure 3). Apparently these sediments were laid down as carbonate-rich muds in a lacustrine environment, with subsequent (but incomplete) alteration to cherts. Note the small irregular and curving "channels" in the cherty limestones that may be root casts. Dr. J.F. Schreiber, Jr., University of Arizona, X-rayed a sample from these exposures, reporting a strong calcite and weaker quartz peak. The diffractogram also showed the characteristic "humping" for amorphous silica but no strong indication for the transformation to opal-cristobalite. Is "bedding" in these cherty limestones primary or diagenetic? Do the "bands" of similar lithology in these exposures reflect climatic episodes in the history of these lakes? Cherty limestones like these can be found in exposures at 111 Ranch, but they are less well developed there.



Figure 3. Outcrop exposure of Gila Conglomerate at Stop 1.

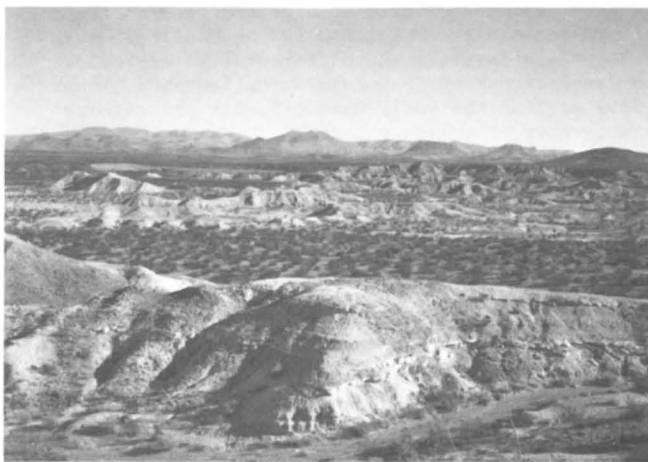


Figure 4. Outcrop exposure of Gila Conglomerate at Stop 2. Sigmodon Ravine at 111 Ranch. Dry Mountain ash is exposed in middle of bluff at center foreground.

The Safford Valley is visible to the east, Mount Turnbull is to the south, and we can barely see the fringe of the Pinaleno Mountains behind Mount Turnbull. We continue east to the Safford Valley, north of the Pinaleno Mountains.

GEOLOGIC HIGHLIGHTS EN ROUTE TO STOP 2

The most definitive study of the Gila Conglomerate was that of Knechtel (1936), in which he described the Gila Conglomerate as valley fill having a finer grained lacustrine central facies and coarser grained lateral facies of more fluvial nature. Both facies are usually flat-lying or with slight initial dip and are capped by dissected terraces having coarser, poorly indurated pediment gravels of variable thickness. Locally, the valley fill might dip toward the center of the valley, reflecting renewed uplift along mountain-front faults that formed the valleys. Conceptually, this younger valley fill represents local sedimentation coincident with and following an interval of extensional faulting that marks the development of the present "basin-and-range" topographic features of this area. The lacustrine facies in the central part of these younger valley fills, along with well-developed terraces flanking the margins of the valleys, suggest that drainage was disrupted and later reintegrated following an interval of internal drainage. During our trip we will see several valley-fill sequences in varying degrees of drainage integration. The Safford Valley represents a valley with well-integrated drainage but with well-displayed remnants of terraces and exposures of lacustrine facies. The San Simon Valley represents a valley with integrated drainage, but with terraces dissected and exposures of lacustrine facies poorly developed. Tomorrow we will visit the Sulphur Springs Valley and the San Pedro Valley. The Sulphur Springs Valley has internal drainage in the northern half where we will cross it, and poorly integrated drainage in the southern half. The San Pedro Valley has through-drainage, with very dissected terraces, plus well exposed lacustrine facies. This simplistic model of post-"Basin and Range" deposition does not (or should not) imply that sediments in the Safford, San Simon, Sulphur Springs, and San Pedro Valleys are lithologically and chronologically equivalent. However, the vertebrate faunas and the magnetostratigraphic sequence of chronologically similar deposits in the Safford and San Pedro Valleys can be compared, to evaluate similarities and differences in ecological and depositional environments. For instance, Tomida (1985) studied the small-mammal faunas and magnetostratigraphy of the Bear Springs fauna in the Safford Valley, the Power Line fauna in the San Simon Valley, and several valley-fill sequences in the Duncan Valley, east of the Safford Valley. He concluded (see Figure 2) that all these valley-fill sequences overlap in age, primarily in the interval between about 1.5 and 3.5 Ma, and they can be correlated very securely with similar deposits and faunas of the San Pedro Valley.

We will follow the Gila River from Stop 1 to Safford, passing through the towns of Pima and Thatcher along the way. Note that as we leave the San Carlos Valley and approach the Gila River the sediments become more coarse and fluvial in character.

Miles
Interval Total

- | | | |
|------|-------|---|
| 11.2 | 123.4 | Cross the Gila River. Continue on Highway 70 to Safford. Mount Turnbull is now southwest of us and the Pinaleno Mountains are directly ahead. The floodplain of the Gila River in the Safford Valley produces rich farmland. As we head east on the south side of the Gila River, notice that the Gila Conglomerate is more reddish brown. Mudstones and siltstones similar to those exposed near the highway have produced the Red Knolls fauna (near the highway) about 23 miles east of the river crossing, and Bear Springs fauna (about 7 miles south of the highway), both reported by Knechtel (1936). |
| 33.3 | 156.7 | Enter the town of Safford. We will rendezvous in Safford with vehicles from Tucson that carry our lunch, before heading east to the 111 Ranch. If we have time for a pit stop, we will take it at the city park in Safford. We continue east on Highway 70 toward the 111 Ranch. |
| 6.5 | 163.2 | Cross San Simon Creek. Continue heading east on Highway 70. The San Simon Valley is south of us, between the Pinaleno Mountains (to our west) and the Whitlock Mountains (to our east). The 111 Ranch beds are developed on the north end of the Whitlock Mountains. Note the high, more or less continuous terrace on the north side of the Gila River, and the lower, irregular terrace on this side of the river. We ascend the terrace about 2 miles east of San Simon Creek and will turn off about a quarter mile east of the agriculture inspection station. |

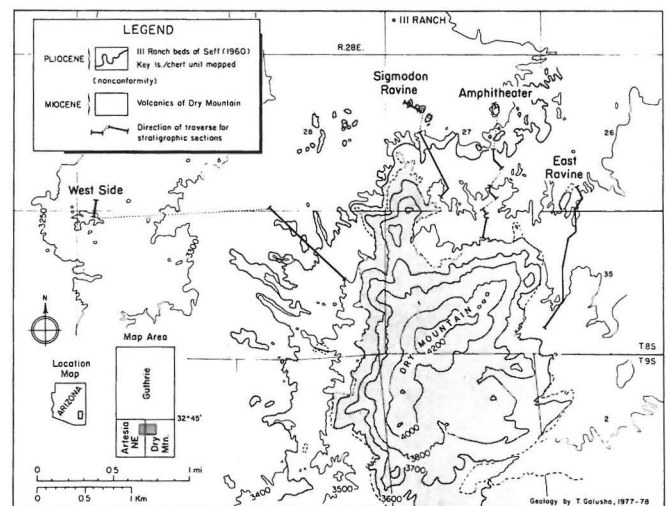


Figure 5. Location of magnetostratigraphic sections at 111 Ranch. (From Galusha and others, 1984, Figure 1)

4.2 167.4 TURN RIGHT ON UNMARKED GRAVEL ROAD. We will drive about 9.5 miles on this gravel road toward the Whitlock Mountains to the southeast. We will stop and have lunch before we reach the fossil exposures; after lunch we will transfer to the vehicles from Tucson for the final 5 miles. Stratigraphy of the 111 Ranch area was studied by Seff (1960), and fossils from 111 Ranch were described by Downey (1962), Wood (1962), Cantwell (1969), and Tomida (1985).

5.0 172.4 STOP 2. 111 RANCH. We will spend about 2-3 hours in this area, and will drive to three sections (Sigmodon Ravine, East Ravine, and West Side) before returning to the bus. Fossil sites, magnetic reversals, volcanic ashes, and lithologic changes will be pointed out in these sections. Figures 4, 5, 6, and 8 show these sections. Table 1, faunal list for 111 Ranch, is taken from Galusha and others (1984) and Tomida (1985). Figure 7 gives the stratigraphic range of selected taxa from 111 Ranch. We plan to be back at the bus about 4 p.m. so we can check into our motel about 5 p.m. Stay with the same vehicle until we get back to the bus.

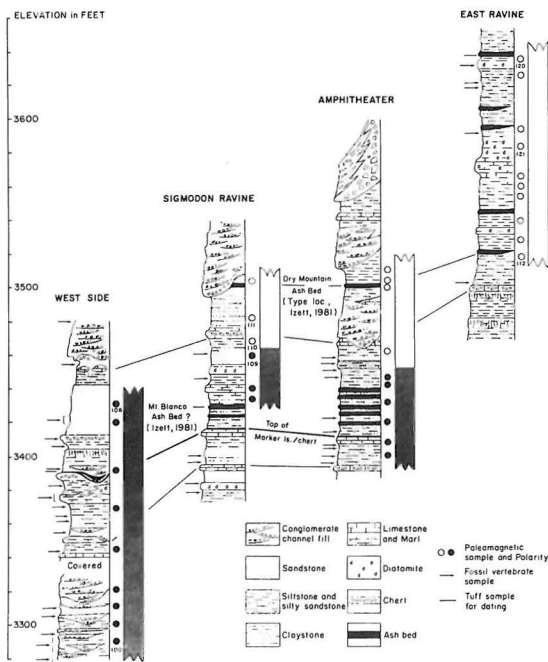


Figure 6. Magnetostratigraphic sections at 111 Ranch. (From Galusha and others, 1984, Figure 2)

TABLE 1. FAUNAL LIST, 111 RANCH, SAFFORD VALLEY

Insectivora
 Soricidae
Sorex sp. (shrew)
 Chiroptera
 Vespertilionidae (bat)

Edentata
 Glyptodontidae
Glyptotherium texanum (glyptodont)
 Megalonychidae
Megalonyx sp. (ground sloth)
 Mylodontidae
Glossotherium chapadmalensis (ground sloth)
 Lagomorpha
 Leporidae
Hypolagus arizonensis (rabbit)
 ?Hypolagus virginiae (rabbit)
Hypolagus sp. (rabbit)
Sylvilagus or Lepus sp. (rabbit)
 new gen. & sp.
 Rodentia
 Sciuridae
Spermophilus sp. (ground squirrel)
 Geomyidae
Geomys (Nerterogeomys) cf. persimilis (gopher)
Geomys sp. (gopher)
 Heteromyidae
Perognathus gidleyi (pocket mouse)
Perognathus sp. (pocket mouse)
Prodipodomys sp. (kangaroo rat)
Dipodomys hibbaridi (kangaroo rat)
Dipodomys cf. gidleyi (kangaroo rat)
 Cricetidae
Onychomys pedroensis (grasshopper mouse)
Peromyscus hagermanensis (deer mouse)
Peromyscus sp. (deer mouse)
Baiomys cf. brachygnathus (pigmy mouse)
Baiomys sp. (pigmy mouse)
Reithrodontomys rexroadensis (harvest mouse)
Reithrodontomys n. sp. (harvest mouse)
Calomys (Bensonomys) arizonae (cotton rat)
Sigmodon medius (cotton rat)
Neotoma (Paraneotoma) taylori (pack rat)
Repomys n. sp. (pack rat)
 Hydrochoeridae
Neochoceros dichroplax (capybara)
 Carnivora
 Canidae
Urocyon sp. (gray fox)
Canis cf. irvingtonensis (wolf)
Canis cf. cedazoensis (wolf)
Borophagus sp. (bone-crushing dog)
 Mustelidae
Mustela sp. (weasel)
 Procyonidae
 ?Bassariscus sp. (ring-tail)
 Felidae
Felis sp. (cat)
 ?Homotherium sp. (stabbing cat)
 Proboscidea
 Gomphotheriidae
Cuvieronius sp. (short-jawed gomphothere)
Rhynchotherium sp. (break-jawed gomphothere)
 Perissodactyla
 Equidae
Nannippus phlegon (three-toed horse)
Equus (Equus) simplicidens (horse)
Equus (Asinus) cf. scotti (horse)
Equus (Asinus) sp. (horse)
 Artiodactyla
 Tayassuidae
Platygonus sp. (javelina)
 Camelidae
Hemiauchenia sp. (llama)
Camelops cf. traviswhitei (llama)
Titanotylopus sp. (cameline)
 Antilocapridae
Capromeryx arizonensis (pronghorn)

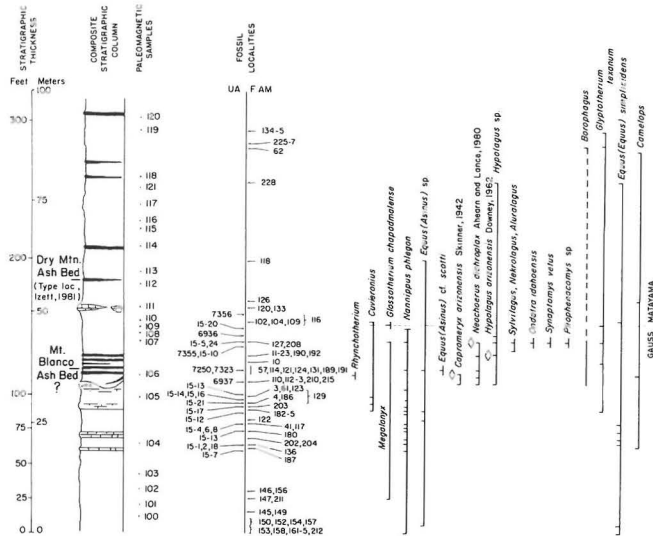


Figure 7. Biostratigraphy of vertebrate faunas and local range zones of selected taxa, 111 Ranch area. (From Galusha and others, 1984, Figure 5). Local range zones shown by heavy vertical bar and individual occurrences shown by short horizontal line joining vertical bar. UA = University of Arizona localities; F:AM = Frick Collection, AMNH localities.

Return to the bus and retrace our path to Safford and the Desert Inn Motel. The distance to the motel is about 20 miles. END OF DAY 1. The total mileage traveled during Day 1 is about 200 miles.

ROAD LOG, DAY 2

We will assemble and load into the bus after breakfast, planning to leave about 8 a.m. The road log for day 2 starts at the intersection of Highways 70 and 666 in Safford. We will head south on Highway 666 to join Interstate 10, then will follow Highway I-10 west, crossing the Sulphur Springs Valley and Willcox Playa, then descending through Texas Canyon into the San Pedro Valley. We will turn south on Highway 80 at Benson and continue on Highway 80 to the Curtis Ranch section, north of Tombstone. We will walk up the Curtis Ranch section, meet the vehicles that contain our lunch, and return to the bus, which will take us to Tucson via Highways 80 and I-10. We plan to arrive at the Tucson International Airport about 6 p.m. Participants with scheduled departures from Tucson will leave us there, and participants continuing on to Phoenix will reload the bus for the trip to Phoenix. The bus should arrive in Phoenix by 8:30 p.m.

GEOLOGIC HIGHLIGHTS EN ROUTE TO STOP 3

As mentioned in the roadlog for day 1, the San Simon Valley has younger valley-fill deposits approximately the same age as those of the Safford Valley, but drainage in the San Simon Valley was integrated less rapidly than that in the Safford Valley. We can see exposures of valley fill at the base of the Whitlock Mountains in the distance. Knechtel (1936) considered the San Simon deposits equivalent to those in the Safford Valley. Vertebrate fossils recovered from exposures at several sites along the western and



Figure 8. Outcrop exposure, upper Sigmodon Ravine, 111 Ranch area. Sigmodon locality is at top of lower bench to right of wash; Gauss/Matuyama magnetic reversal occurs below white marker bed to left of wash.

southern rim of the Whitlock Mountains are comparable to those from 111 Ranch.

Similar valley-fill deposits occur in the Sulphur Springs Valley, but drainage in the Sulphur Springs Valley is internal where we cross it. Sediments are still aggrading, with virtually no exposure of valley-fill sediments like those seen in the Safford Valley. A well penetrated the middle of the Willcox Playa to a depth of 43 m (140 feet), yielding only black clay and mud; another well drilled on the north edge of Willcox to a depth of 146 m (480 feet) included a black clay-mud thickness of 107 m (350 feet) (Schreiber, 1978). Carbon-14 samples from the playa sediments yielded ages as young as 8615 ± 110 radiocarbon years for surficial samples and exceeded the range of ^{14}C dating with depth (Long, 1966). Rancho-labrean vertebrates (*Mammuthus*, *Equus*, *Camelops*, and box turtle) were recovered from sand and gravel pits located about 5 miles west of Willcox (Lindsay and Tessman, 1974). These are the only vertebrates recovered from the Willcox Playa.

The San Pedro Valley, on the other hand, has extensive exposures of valley-fill sediments, named the St. David Formation by Gray (1967). Gray (op. cit.) described three divisions of the St. David Formation, a lower red-bed division, a middle carbonate-enriched division, and an upper carbonate soil-forming division. Fossils have never been found in the lower red-bed division. Blancan fossils are common in the middle carbonate-enriched division, Irvingtonian fossils occur in the upper part of the middle division plus the lower part of the carbonate soil-forming division, and Rancho-labrean fossils occur in overlying alluvial deposits. Indeed, the better exposures, greater fossil productivity, and longer stratigraphic sections make the San Pedro Valley a prime reference sequence for valley-fill deposits in this part of the U.S. Also, the redefined Pliocene/Pleistocene boundary is readily identified in the San Pedro Valley because of the magnetostratigraphic sequence established by Johnson and others (1975); that boundary has never been securely identified in other valley-fill sequences of the Basin and Range.

Miles					
Interval	Total				
0	0	Intersection of Highways 70 and 666 in Safford. Proceed south on Highway 666 toward Willcox. As we leave Safford we ascend an alluvial terrace from Mount Graham (about milepost 119). We see Mount Graham to the west, the Whitlock Mountains to the east, and the Dos Cabezas Mountains in the distance ahead of us (to the south). Farther to the south we can see the San Simon Valley between us and the Whitlock Mountains, and the Peloncillo Mountains to the east and south of the Whitlock Mountains. The Arizona-New Mexico border crosses the San Simon Valley about where Interstate 10 enters Arizona. Note the large dissected alluvial terraces along the base of Mount Graham. These are composed primarily of Gila Conglomerate, like that seen yesterday at 111 Ranch and on the north side of the Pinaleno Mountains along the Gila River. The terraces are capped by pediment gravels, which we also saw yesterday. Some of these sediments are exposed in roadcuts along Highway 666 south of Safford. South of the junction with Highway 266 (to Fort Grant), 16.6 miles from our starting point, roadcuts in Precambrian granite and Tertiary volcanics are encountered. The Fisher Hills, composed of Tertiary volcanics, are located east of the highway where we enter Cochise County.	11.0	56.0	Junction with Highway 666. Stay on Highway I-10, heading west toward Benson. If there is any water in the Willcox Playa, it is usually visible from this area as we ascend a low divide between the Gunnison Hills (to the south) and the Steele Hills (to the north). We cross the southern end of the Little Dragoon Mountains.
			9.6	65.6	Summit of Texas Canyon. Elevation 4975 feet. We enter the San Pedro Valley between the Dragoon Mountains (to the south) and the Little Dragoon Mountains (to the north). The Huachuca Mountains are visible ahead of us, across the San Pedro Valley. As we descend into Texas Canyon, we can see the Whetstone Mountains ahead of us on the other side of the valley, with the Rincon Mountains north of Highway I-10, and the Huachuca Mountains south of the Whetstone Mountains. The U.S.-Mexican border crosses the southern end of the Huachuca Mountains. You have probably seen the picturesque granite boulders of Texas Canyon many times before in western movies. Between mileposts 312 and 308 we see good exposures of the St. David Formation on both sides of the San Pedro River.
			13.8	79.4	Pomerene Road-Benson Turnoff. Turn right, leaving Highway I-10, taking I-10 Business into Benson. Turn left at the stop sign, pass under the freeway, then turn right toward Benson.
33.5	33.5	On-ramp for Interstate 10 West. Turn right and proceed toward Willcox (west) on Interstate 10. Our route takes us around the north end of the Dos Cabezas Mountains into the Sulphur Springs Valley.	0.4	79.8	Cross the San Pedro River east of Benson. Turn left (sharp turn) in about one-half mile onto Highway 80 south toward Tombstone and Douglas. Near milepost 295, about 2 miles south of the junction with Highway 80, we see the Post Ranch Amphitheater and Post Ranch. Most of the Benson fauna reported by Gidley (1922, 1926) and Gazin (1942) was collected from the Post Ranch Amphitheater.
11.5	45.0	Outskirts of Willcox. Continue on Highway I-10 toward Benson. Willcox is located on the northeast side of the Willcox Playa, which should be visible toward the south near and west of milepost 339. The Dos Cabezas Mountains and the Chiricahua Mountains (farther south) are located east of the Sulphur Springs Valley; the Winchester Mountains (north of the highway) and Dragoon Mountains (south of the highway) are located west of the Sulphur Springs Valley. To the south we can see the Swisshelm Mountains in the Sulphur Springs Valley, and farther south is the Mexican border.	8.7	88.5	Cross San Pedro River north of St. David. Continue south on Highway 80 through the town of St. David toward Tombstone. The Dragoon Mountains appear in the distance beyond the town of St. David. The rugged exposures of granite visible ahead of us in the Dragoon Mountains are called Cochise Stronghold. This was a favorite campsite of the Chiricahua Apache Indians. We approach the Curtis Ranch Amphitheater to the left (east) of the highway, about 4 miles south of St. David.

6.8 95.3 STOP 3. CURTIS RANCH SECTION. Pull off and park on the right side of the road, near the sign "Littering Highways Unlawful." We will walk up the section on the east side of the highway and have lunch before returning to the bus. Figure 9 is a view of the Curtis Ranch section from the highway. Fossil sites, magnetic reversals, and stratigraphic marker beds (in Figure 10) will be pointed out. Table 2 is a list of the mammals recorded from the St. David Formation. Figure 11 shows the sequence of fossil sites in the San Pedro Valley, and Figure 12 shows the magnetic polarity sequence in the San Pedro Valley along a N-S transect with the Curtis Ranch section near the center of that transect.



Figure 9. Outcrop exposure of lower Curtis Ranch section near Highway 80. Marl 2 in center foreground; marl 5 and 6 in middle distance.

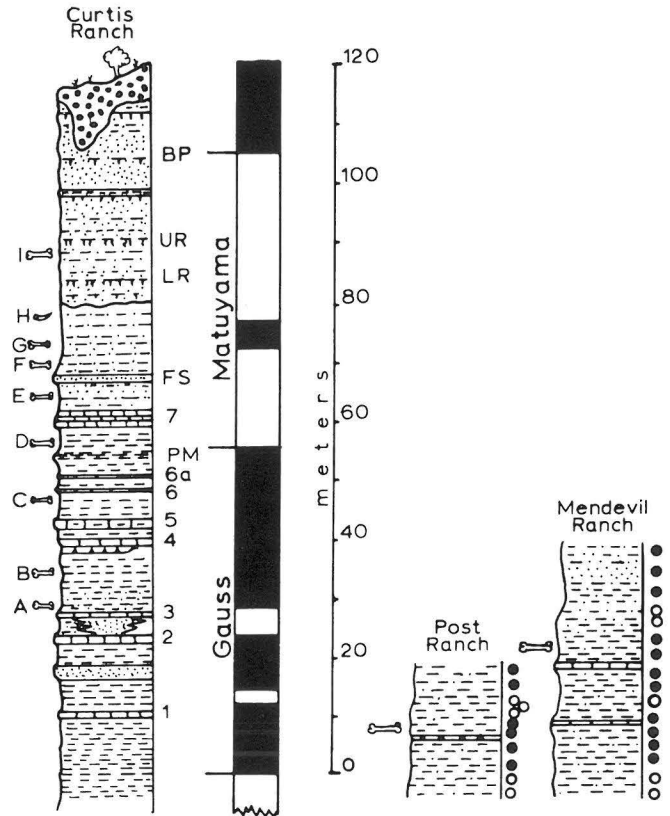


Figure 10. Stratigraphic and magnetic polarity sequence of Curtis Ranch, Post Ranch, and Mendevil Ranch, San Pedro Valley. (From Lindsay and others, 1975) Fossil levels in Curtis Ranch section: A = Bonanza; B = Honey's Hummock; C = Horsey Green; D = Cal Tech; E = Johnson Pocket; F = Gidley site; G = Glyptotherium; H = Tusk; I = Prospect. Marker beds: 1-7 = marls; PM = Powder marl; FS = Flaggy Ss.; LR = lower red; UR = upper red; BP = Brunhes Paleosol.

TABLE 2. FAUNAL LIST, ST. DAVID FORMATION, SAN PEDRO VALLEY

Insectivora	Geomyidae
Soricidae	<u>Geomys minor</u> (gopher)
<u>Sorex</u> sp. (shrew)	<u>Geomys persimilis</u> (gopher)
Chiroptera	<u>Cratogeomys bensoni</u> (gopher)
Vespertilionidae	Heteromyidae
<u>Simonycteris stocki</u> (bat)	<u>Perognathus</u> sp. (pocket mouse)
<u>Eptesicus</u> sp. (brown bat)	<u>Prodipodomys minor</u> (kangaroo rat)
Edentata	<u>Prodipodomys idahoensis</u> (kangaroo rat)
Glyptodontidae	<u>Dipodomys gidleyi</u> (kangaroo rat)
<u>Glyptotherium arizonae</u> (glyptodont)	Cricetidae
Lagomorpha	<u>Onychomys bensoni</u> (grasshopper mouse)
Leporidae	<u>Onychomys pedroensis</u> (grasshopper mouse)
<u>Notolagus</u> sp. (rabbit)	<u>Peromyscus</u> sp. (deer mouse)
<u>Aluralagus</u> sp. (rabbit)	<u>Baiomys minimus</u> (pygmy mouse)
<u>Nekrolagus</u> sp. (rabbit)	<u>Baiomys brachygnathus</u> (pygmy mouse)
<u>Sylvilagus</u> sp. (rabbit)	<u>Calomys (Bensonomys) arizonae</u> (cotton rat)
<u>Sylvilagus</u> or <u>Lepus</u> sp. (rabbit)	<u>Sigmodon medius</u> (cotton rat)
Rodentia	<u>Sigmodon minor</u> (cotton rat)
Sciuridae	<u>Sigmodon curtisi</u> (cotton rat)
<u>Spermophilus bensoni</u> (squirrel)	<u>Neotoma fossilis</u> (pack rat)
<u>Spermophilus cochisei</u> (squirrel)	<u>Neotoma</u> sp. (pack rat)
Castoridae	<u>Synaptomys (Metaxomys) sp.</u> (lemming)
<u>Castor</u> sp. (beaver)	<u>Pliophenacomys</u> sp. (pine vole)
	<u>Ondatra idahoensis</u> (muskrat)

- Erethizontidae
 - Coendou sp. (porcupine)
- Hydrochoeridae
 - Neochoerus sp. (capybara)
- Carnivora
 - Canidae
 - Canis edwardii (coyote)
 - Canis sp. (dog)
 - Borophagus sp. (bone-crushing dog)
 - Mustelidae
 - Spilogale pedroensis (spotted skunk)
 - mustelid (weasel)
 - Felidae
 - Felis sp. (cat)
 - Panthera sp. (jaguar)
- Proboscidea
 - Gomphotheriidae
 - Cuvieronius sp. (short-jawed gomphothere)
 - Stegomastodon sp. (short-jawed gomphothere)
- Perissodactyla
 - Equidae
 - Nannippus phlegon (three-toed horse)
 - Equus sp. (horse)
- Artiodactyla
 - Tayassuidae
 - Platygonus sp. (javelina)
 - Camelidae
 - Hemiauchenia sp. (llama)
 - Camelops sp. (llama)
 - Cervidae
 - Odocoileus sp. (deer)
 - Antilocapridae
 - Capromeryx gidleyi (pronghorn)

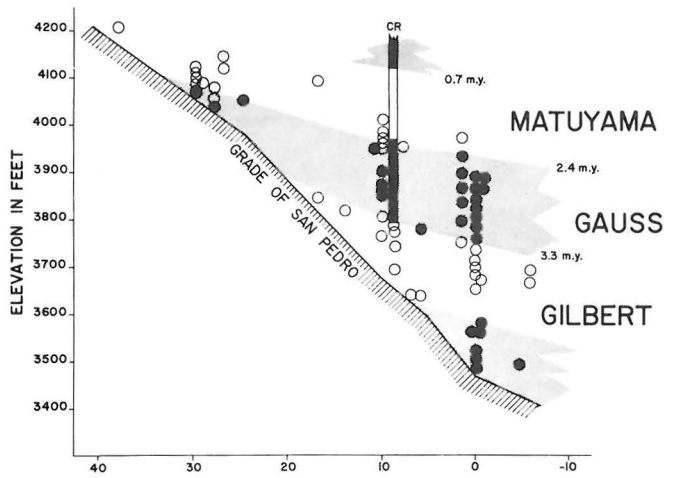


Figure 12. Distribution of magnetic polarity zones within the St. David Formation, San Pedro Valley along a N-S transect (N to right). Horizontal scale is in miles with Benson at 0. Curtis Ranch section marked CR. (From Johnson and others, 1975, Figure 10).

Miles		
Interval	Total	
6.8	102.1	Cross the San Pedro River near St. David. Continue heading north on Highway 80 toward Benson. The Whetstone Mountains appear to the north and west.
3.2	105.3	Post Ranch Road. STOP 4 (OPTIONAL). TURN LEFT ON POST RANCH ROAD AND DRIVE TO BUILDINGS. We will walk about one-half mile to the Post Ranch Amphitheater where the magnetic reversal sequence, the Post Ranch ash, and the Benson faunal site will be pointed out. The Post Ranch magnetic sequence is shown in Figure 10. After Stop 4 return to Highway 80 and continue heading north toward Benson. We get another view of the Post Ranch Amphitheater to the left. The Post Ranch ash, dated 3.1 Ma and located at the level of the Benson fauna, helped constrain placement of the San Pedro Valley paleomagnetic sequence.
2.2	107.5	Highway I-10 interchange in Benson. Continue on I-10 Business to the west through the town of Benson. As we leave the town of Benson, and before we enter the Highway I-10 interchange, we pass the Tucson Bowl on the right. The curved roof of the Tucson Bowl approximates the elevation of the base of the Gauss magnetic chron in this area, e.g., the same magnetic reversal (3.4 Ma) that we crossed at the highway when we walked up the Curtis Ranch section this morning.

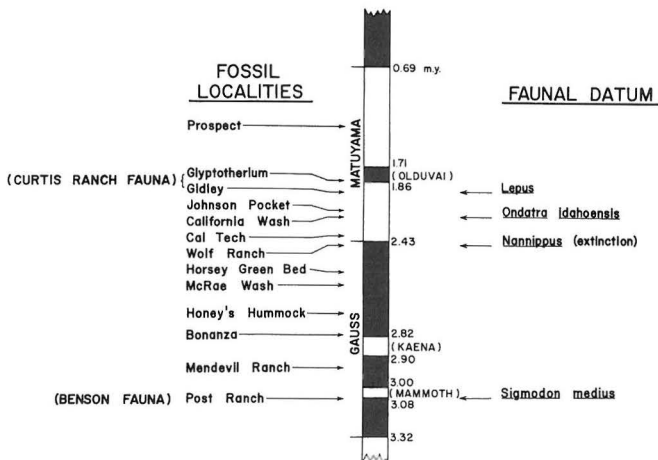


Figure 11. Biostratigraphic-magnetostratigraphic correlation and faunal datum events in the San Pedro Valley. (From Johnson and others, 1975, Figure 11).

If time permits we will stop at Post Ranch and walk to the paleomagnetic section that includes the Post Ranch ash (dated 3.1 Ma by fission tracks in zircons) and the Benson fauna. This stop would require a minimum of 1 hour, so is optional, depending on how much time we have. The Benson fauna is Blancan land mammal age; it was described by Gidley (1922, 1926) and Gazin (1942).

Reassemble at the bus and retrace our route from Benson, heading north on Highway 80.

2.0 109.5 Merge with traffic on Highway I-10 and continue to the west. The Whetstone Mountains are still on our left. The Rincon Mountains are on our right to the north, and the Santa Rita Mountains, south of Tucson, are ahead in the distance.

regrouping before continuing. If time permits, refreshments may be purchased.

GEOLOGIC HIGHLIGHTS EN ROUTE TO TUCSON

As we drive west on Highway I-10 toward Tucson, we cross the early Tertiary Pantano Formation. The Pantano Formation is one of the better exposed and readily accessible older valley-fill deposits in southern Arizona. By definition, older valley-fill sediments were deposited prior to Basin and Range extensional tectonism. Therefore, they are usually deformed, fault-bounded, and covered by younger sediments. Excellent exposures of the Pantano Formation occur along Cienega Creek north of Highway I-10, but fossils have never been recovered from the Pantano Formation. We will cross a welded tuff, interbedded with Pantano sediments, that yielded ages of 37.6 Ma (sanidine) and 33.6 Ma (biotite) (Damon and Bikerman, 1964). Another tuff and basaltic flow interbedded with the Pantano Formation and exposed along Cienega Creek to the north have yielded ages of 29.9 Ma and 24.9 Ma, respectively (Shafiqullah and others, 1978), suggesting that deposition of the Pantano Formation (or Pantano-like deposits) spanned an interval of 12 to 15 m.y. We find it amazing that this relatively well-exposed deposit, formed over a relatively long interval, should leave such a poor fossil record.

- 2.0 150.7 RETURN TO HIGHWAY I-10 VIA TUCSON BOULEVARD. Drive north on Tucson Boulevard, which will merge with Highway I-10 Business.
- 3.3 154.0 Tucson Boulevard curves to the left (west), crosses Irvington Road, and is then marked Benson Highway (which is I-10 Business). Continue heading west on the Benson Highway.
- 5.1 159.1 Park Avenue. Turn right and pass under the freeway; turn left at the stop light and proceed on Highway I-10 on-ramp. Continue heading north and west on I-10. Sentinel Peak (A Mountain) and Tumamoc Hill are west of the freeway; Tucson Community Center and downtown Tucson are right of the freeway.
- 9.7 168.8 Cross Speedway Boulevard. Continue heading north on Highway I-10. Our route parallels the Santa Cruz River, on the left. The Santa Cruz River is dry during most of the year.
- 6.1 174.9 Cross the Rillito River. Continue heading north on Highway I-10. The Rillito enters the Santa Cruz River just west of the highway. When the rivers are not running, this is a prime location for sand and gravel used in construction. Our route continues to parallel the Santa Cruz River, with the Tucson Mountains across the river. We leave the Tucson Mountains about 2 miles north of the Rillito River crossing and enter the Avra Valley.
- 30.9 205.8 Picacho Peak Turnoff. Continue heading north on Highway I-10. Picacho Peak (to the west) looks like it should be an exhumed volcanic neck. Detailed study, however, indicates it is more likely a fault-bounded block from the flank of a volcano (Dohms and others, 1980).
- 20.5 226.3 Interchange of Highways I-8 and I-10. Continue on Highway I-10 toward Phoenix. The Casa Grande Mountains are ahead and west of the highway. Our route continues to the northwest, across the broad Gila River valley.
- 26.4 252.7 Cross the Gila River near Gila Butte. Continue on Highway I-10 toward Phoenix. South Mountain is ahead in the distance, with Phoenix on the other side of South Mountain. Our route takes us to the right side (east) of South Mountain.
- 18.1 270.8 Cross Baseline Road. Continue on Highway I-10 toward Phoenix. The road log will end where it began, at the junction of Highway I-10 and the Superstition Freeway.

Miles
Interval Total

- 14.3 123.8 Cross Cienega Creek, which drains into the Tucson basin. Continue on Highway I-10 toward Tucson. We see exposures of the Oligocene Pantano Formation and the more indurated Cretaceous Bisbee Group for the next 5 miles. We cross a volcanic welded tuff in the Pantano Formation near milepost 288. Sediments exposed in roadcuts west of Davidson Canyon are generally younger than the Pantano Formation; they have not yielded fossils. We can now see the Catalina Mountains in the distance to the north, beyond the Rincon Mountains. The Empire Mountains (and the Santa Rita Mountains in the distance) are to the south and the Tucson Mountains appear ahead of us.
- 21.7 145.5 Valencia Road off-ramp. Turn off Highway I-10 on the outskirts of Tucson and continue west on Valencia Road to Tucson International Airport. We will make a left turn onto Valencia Road after leaving the highway. On a good day we can see the outline of telescopes at Kitt Peak Observatory on the Baboquivari Mountains ahead in the distance.
- 3.2 148.7 Turn left on Tucson Boulevard toward Tucson International Airport. Participants leaving us here will be let off at the airport. We will park in a hotel parking lot adjacent to the airport for a brief clean-up and/or

0.7 271.5 Junction of Highway I-10 with the Superstition Freeway. END OF ROAD LOG.

CITED REFERENCES

- Cantwell, R.J., 1969, Fossil *Sigmodon* from the Tusker locality, 111 Ranch, Arizona: *Journal of Mammalogy*, v. 50, p. 375-378.
- Damon, P.E., and Bikerman, M., 1964, Potassium-argon dating of post-Laramide plutonic and volcanic rocks within the Basin and Range province of southeastern Arizona and adjacent areas: *Arizona Geological Society Digest*, v. 7, p. 63-78.
- Dohms, P.H., Dunn P.G., Harding, L.E., Lundin, R.J., Lynch, D.J., Reynolds, S.J., and Teet, J.E., 1980, Geologic road logs, 1979 Arizona Geological Society Spring field trip; Tucson-Yuma-Quartzsite-Buckeye, *in* Jenney, J.P., and Stone, Claudia, eds., *Studies in western Arizona*: Arizona Geological Society Digest, v. 12, p. 290-322.
- Downey, J.S., 1962, Leporidae of the Tusker local fauna from southeastern Arizona: *Journal of Paleontology*, v. 36, p. 1112-1115.
- Fellows, L.D., 1984, Mineral and energy resources; assessing Arizona's potential: Arizona Bureau of Geology and Mineral Technology Fieldnotes, v. 14, no. 1, p. 1-9.
- Galusha, T., Johnson, N.M., Lindsay, E.H., Opdyke, N.D., and Tedford, R.H., 1984, Biostratigraphy and magnetostratigraphy, late Pliocene rocks, 111 Ranch, Arizona: *Geological Society of America Bulletin*, v. 95, p. 714-722.
- Gazin, C.L., 1942, The late Cenozoic vertebrate faunas from the San Pedro Valley, Arizona: U.S. National Museum Proceedings, v. 92, p. 475-518.
- Gidley, J.W., 1922, Preliminary report on fossil vertebrates of the San Pedro Valley, Arizona: U.S. Geological Survey Professional Paper 131-E, p. 119-131.
- _____ 1926, Fossil Proboscidea and Edentata of the San Pedro Valley, Arizona: U.S. Geological Survey Professional Paper 140-B, p. 83-95.
- Gilbert, G.K., 1875, Report on the geology of portions of New Mexico and Arizona: U.S. Geographic and Geologic Survey west of the 100th Meridian (Wheeler), v. 3, p. 501-567.
- Gray, R.S., 1967, Petrography of the upper Cenozoic non-marine sediments in the San Pedro Valley, Arizona: *Journal of Sedimentary Petrography*, v. 37, p. 774-789.
- Heindl, L.A., 1963, Cenozoic geology in the Mammoth area, Pinal County, Arizona: U.S. Geological Survey Bulletin 1141-E, 41 p.
- Johnson, N.M., Opdyke, N.D., and Lindsay, E.H., 1975, Magnetic polarity stratigraphy of Pliocene-Pleistocene terrestrial deposits and vertebrate faunas, San Pedro Valley, Arizona: *Geological Society of America Bulletin*, v. 86, p. 5-12.
- Knechtel, M.M., 1936, Geological relations of the Gila Conglomerate in southeastern Arizona: *American Journal of Science*, 5th ser., v. 31, p. 81-92.
- _____ 1938, Geology and ground-water resources of the valley of Gila River and San Simon Creek, Graham County, Arizona: U.S. Geological Survey Water Supply Paper 796-F, 42 p.
- Lindsay, E.H., Johnson, N.M., and Opdyke, N.D., 1975, Preliminary correlation of North American land mammal ages and geomagnetic chronology, *in* Smith, G.E., ed., *Studies on Cenozoic paleontology and stratigraphy in honour of Claude W. Hibbard*: University of Michigan Papers on Paleontology, no. 12, p. 111-119.
- Lindsay, E.H., and Tessman, N.T., 1974, Cenozoic vertebrate localities and faunas in Arizona: *Journal of Arizona Academy of Sciences*, v. 9, p. 3-24.
- Long, A., 1966, Late Pleistocene and Recent chronologies of playa lakes in Arizona and New Mexico [Ph.D. thesis]: Tucson, University of Arizona, 141 p.
- Peterson, D.W., 1966, Geology of Picket Post Mountain, northeast Pinal County, Arizona: *Arizona Geological Society Digest*, v. 8, p. 159-176.
- _____ 1969, Geologic map of the Superior quadrangle, Pinal County, Arizona: U.S. Geological Survey, Geologic Quadrangle Map GQ-818, scale 1:24,000.
- Peterson, N.P., 1962, Geology and ore deposits of the Globe-Miami district, Arizona: U.S. Geological Survey Professional Paper 342, 151 p.
- Péwé, T.L., 1971, Guidebook to the geology of the lower Salt River Valley: unpublished manuscript, 21 p.
- _____ T.L., 1978, Terraces of the lower Salt River Valley in relation to the late Cenozoic history of the Phoenix Basin, Arizona, *in* Burt, D.M., and Péwé, T.L., eds., *Guidebook to the geology of central Arizona*: Arizona Bureau of Geology and Mineral Technology Special Paper 2, p. 1-45.
- Ransome, F.L., 1903, Geology of the Globe copper district, Arizona: U.S. Geological Survey Professional Paper 12, 168 p.
- _____ 1919, The copper deposits of Ray and Miami, Arizona: U.S. Geological Survey Professional Paper 115, 192 p.
- Schreiber, J.F., Jr., 1978, Geology of the Willcox Playa, Cochise County, Arizona, *in* Callender, J.F., and others, eds., *Land of Cochise*: New Mexico Geological Society, 29th Field Conference, Guidebook, p. 277-282.
- Seff, P., 1960, Preliminary report of the stratigraphy of the 111 Ranch beds, Graham County, Arizona: *Arizona Geological Society Digest*, v. 3, p. 137-139.
- Shafiqullah, M., Damon, P.E., Lynch, D.J., Kuck, P.H., and Rehrig, W.A., 1978, Mid-Tertiary magmatism in southeastern Arizona, *in* Callender, J.F., and others, eds., *Land of Cochise*: New Mexico Geological Society, 29th Field Conference, Guidebook, p. 231-241.
- Shafiqullah, M., Damon, P.E., Lynch, D.J., Reynolds, S.J., Rehrig, W.A., and Raymond, R.H., 1980, K-Ar geochronology and geologic history of southwestern Arizona and adjacent areas, *in* Jenney, J.P., and Stone, Claudia, eds., *Studies in western Arizona*: Arizona Geological Society Digest, v. 12, p. 201-260.
- Sheridan, M.F., 1978, The Superstition cauldron complex, *in* Burt, D.M., and Péwé, T.L., eds.: *Guidebook to the geology of central Arizona*: Arizona Bureau of Geology and Mineral Technology, Special Paper 2, p. 85-96.
- Sheridan, M.F., Stuckless, J.S., and Fodor, R.V., 1970, A Tertiary silicic cauldron complex at the northern margin of the Basin and Range province, central Arizona: *Bulletin of Volcanology*, v. 34, p. 649-662.
- Tomida, Y., 1985, Small mammal fossils and correlation of continental deposits, Safford and Duncan basins, Arizona [Ph.D. thesis]: Tucson, University of Arizona, 253 p.
- Wood, P.A., 1962, Pleistocene fauna from 111 Ranch area, Graham County, Arizona [Ph.D. thesis]: Tucson, University of Arizona, 121 p.

Caldera Structures Along the Apache Trail in the Superstition Mountains, Arizona

Michael F. Sheridan
Department of Geology
Arizona State University
Tempe, Arizona 85287

INTRODUCTION

The purpose of this field trip is to examine the various structures and rocks that occur along the margins of the Goldfield, Superstition, and Tortilla calderas in central Arizona. The volcanic rocks of this area belong to the Superstition volcanic field that covers nearly 10,000 km². The Apache Trail weaves a path that transects the margins of at least three calderas or volcano-tectonic depressions (Sheridan and others, 1970; Sheridan, 1978). Hence, the stratigraphy and structures accessible by short hikes from the road are complex. The field trip stops are illustrated in Figure 1.

We will spend one day examining features that are characteristic of caldera margins in this area. There are two main questions that we will address: (1) Are the low-angle faults that mark the caldera margins related to local volcanism or to regional tectonism? (2) What are the typical products of caldera-rim volcanism in this area?

Geologic information for the Superstition and Goldfield Mountains comes from many sources including

several geology theses from Arizona State University. Most of these studies have been topical, their purpose being to understand the petrology and genesis of rocks from the Superstition volcanic field; a general synthesis of the stratigraphy and structure of the entire volcanic field does not exist.

Detailed mapping along the entire route of the Apache Trail was done at a scale of 1:10,000 by five successive Advanced Field Geology classes at Arizona State University. Many of the features seen on this excursion would have gone unrecognized without such detailed mapping. The geology illustrated in this guide is a generalized representation of the above mentioned detailed maps.

BACKGROUND

Rock Compositions

The volcanic rocks of the Superstition and Goldfield Mountains form a coherent chemical pattern that extends from basalts to high-silica, high-K rhyolites (Stuckless and O'Neil, 1973; Sheridan and Prowell,

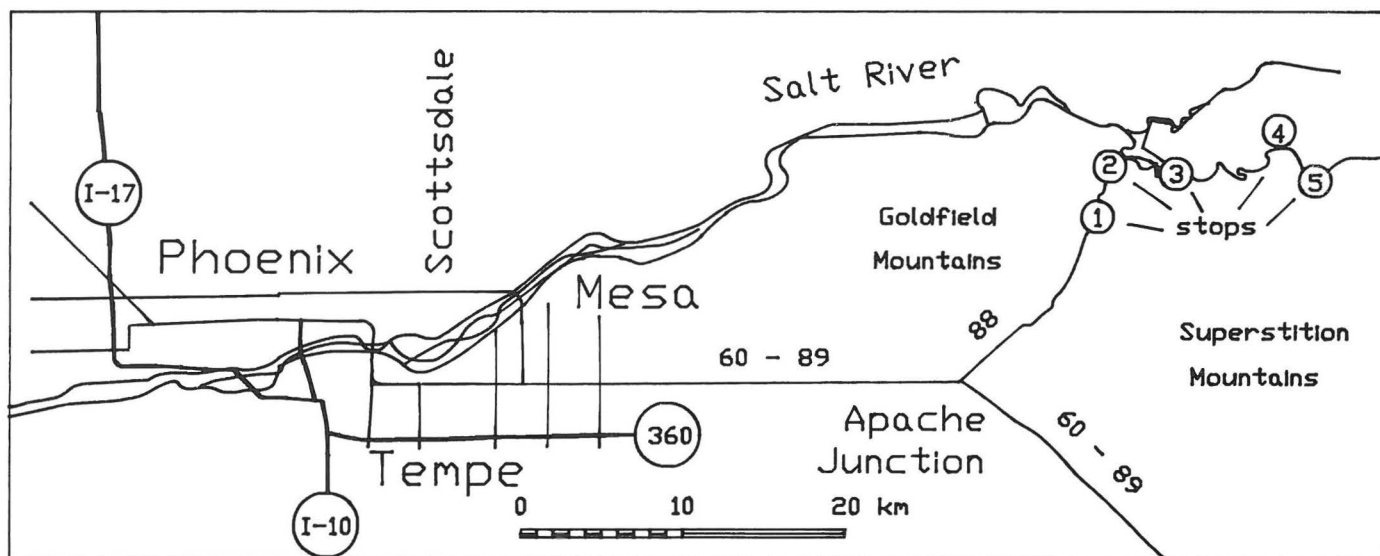


Figure 1. Index map showing the location of the Superstition and Goldfield Mountains relative to Phoenix and other valley cities. The five stops for this field trip are located along the Apache Trail (highway 88).

1986). There is a pronounced silica gap in the compositional range that corresponds to the absence of andesites in this sequence. The least evolved rocks of the silica-rich trend are high-K andesites or latites that typically contain 10 to 20% of normative quartz and have subequal amounts of alkali feldspar and plagioclase in the norms.

The rocks belong to an older and younger series divided at 16 Ma (Sheridan and Prowell, 1986). Both series have similar compositions and trends on variation diagrams. The older series eruptions appear to have been larger, forming regional ash-flow sheets, calderas, and composite volcanoes. The younger series erupted from local vents related to northwest-trending faults. Their vents commonly are surrounded by tuff rings and contain flow-dome complexes. Hydromagmatism was more prevalent during the later period.

Structures

The structural geology of the Superstition Mountains is very complex due to the interference of several calderas and the overprint of regional tectonism. There are several series of faults of various ages that cut the volcanic rocks (Prowell, 1984). The oldest set of faults in the vicinity of Goldfield trend to the northeast and parallel a basin in which the Whitetail Conglomerate accumulated.

The next chronological set of faults are low-angle (20° to 50° dip) faults with well-developed slick faces. The traces of these faults are curvilinear and they occur in concentric and en-echelon sets. This type of fault is associated with each of the three postulated calderas (Sheridan, 1978). They are assumed to be slip surfaces along which large blocks slid into the collapsed areas. Another possible origin for these faults is a thin-skin distension of the area due to regional extension. We will examine several faults of this type during this field excursion to consider their origin.

A later set of faults has a N-S to NW trend. These faults are high-angle normal types. They seem to be the loci for the volcanic vents of lavas younger than 16 Ma. They define a series of elongate horsts and graben in the northern part of the volcanic field. These faults are locally cut by WNW-trending right-lateral faults.

Systematic northeastward tilting of coherent fault blocks exposed along the Apache Trail has generally placed the oldest formations to the southwest and the youngest units to the northeast. An exception is at Horse Mesa where the oldest units are exposed at the northeastern edge of the volcanic field.

ROCK UNITS

A brief summary of the stratigraphic units, from the top of the section downward, follows. Not all of the units described below will be examined on this trip, although they can be seen from the road. The general relationship of these rocks is given in Figure 2.

Mesquite Flat breccia (Tmb). This unit (Stuckless and Sheridan, 1971; Rettenmaier, 1984) consists of lahars with bed thickness on the scale of centimeters to meters. Locally it contains thin ash-flow tuffs or coarse breccias. It has a tan to yellowish color and forms a prominent cliff along the northern edge of Canyon Lake. Large (dm) lithic clasts are set in a matrix of volcanic ash. The source is from rhyolitic dome complexes on either side of Mesquite Flat.

Younger basalt lava (Tyb). Both above and below the Mesquite Flat breccia are thin (a few meters thick) bluish basalt flows that have an alkali olivine

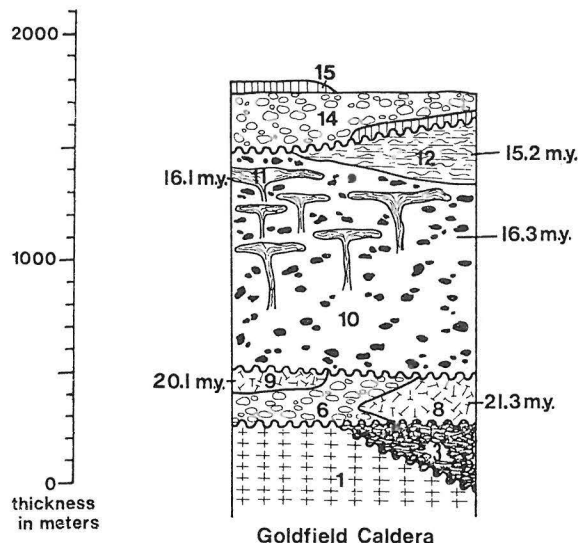


Figure 2. Generalized stratigraphic column of rock units seen on this field trip: (1) Precambrian granite (Pcg), (3) latite of Government Well (Tgl) and latite of Fish Creek, (6, 8, & 9) Apache Gap rhyodacite (Tard) lava and breccia, (10 & 11) First Water rhyolites (Tfw) tuffs and lavas, (12) Canyon Lake (Tcl) Tuff, (14) Mesquite Flat breccia (Tmb), and (15) younger basalts (Tyb). Designation of map units refers to this column.

basalt composition (Suneson, 1976). Reddish altered olivine phenocrysts are visible in hand specimens. A prominent horizon of this unit is visible to the north of the Apache Trail near Tortilla Flat.

Canyon Lake Tuff (Tcl). This rhyolitic welded tuff is composed of at least two cooling units (Stuckless and Sheridan, 1971). Locally in Bulldog Canyon it contains multiple vitrophyres and exhibits reomorphic folds in thick sections. The base is nonwelded and vitric, but generally the degree of devitrification and vapor-phase alteration is high. Nonwelded parts are yellowish due to zeolites, but the devitrified part is gray to reddish. Phenocrysts (quartz, plagioclase, sanidine, and biotite) are fairly abundant (15 to 20%) and flattened pumice can be recognized in some samples. The age is 15 Ma.

Rhyolite of First Water Canyon (Tfw). This unit was formerly included in the Geronimo Head Formation (Stuckless, 1969; Stuckless, 1971; Stuckless and Sheridan (1971), but it has now been separated because it is older than the sequence exposed at Geronimo Head. It is a thick (more than 1,000 m) deposit of tuffs and lavas of phenocryst-poor rhyolite (Fodor, 1969; Suneson, 1976). The tuffs are yellow and generally exhibit thin bedding. The lavas are commonly glassy and range from black (obsidian), to gray (perlite), to reddish (devitrified). The pyroclastic units consist of breccias, surge deposits, ash-flow tuffs, and pumice fall beds. Numerous eruptive centers occur throughout the area, principally near the margins of calderas. The age is 16 Ma (Stuckless and Sheridan, 1971).

The Geronimo Head Formation more properly applies to a group of slightly younger domes and tuff rings termed the Peters Canyon complex (Prowell, 1984). These domes and the ones to the north near Coronado Mesa (Isagholian, 1983) were the source for the Mesquite Flat breccia lahars and tuffs. Several small rhyolitic dome complexes that have similar compositions and ages extend in a belt toward the southeast through Music Mountain as far as Picketpost Mountain (Peterson, 1966).

Rhyodacite of Apache Gap (Tard). This unit (Stuckless and Sheridan, 1971) consists of a lava that is rich in phenocrysts (about 25%) and local pyroclastic breccias. The lava is black where it is glassy, but it may consist of a gray perlite matrix where hydrated or have a salt-and-pepper appearance where devitrified. Flow banding is locally common in the vicinity of vents. The associated tuffs and breccias may be ash flows, surges, or lahars. Locally a thin basalt flow lies between the base of the lava and the underlying tuff. Most exposures of the lava exhibit strong evidence of magma mixing with this basalt. The age of this unit is 20 to 21 Ma. This unit was probably erupted following collapse of the Superstition caldera.

Bronco Butte Lahar. This epiclastic volcanic breccia on Horse Mesa is about 60 m thick (Malone, 1972). It appears to grade into the dacite lava that caps the ridge near Bronco Butte, and hence may be equivalent to lahars that underlie the Rhyodacite of Apache Gap (21 Ma age) in other parts of the Superstition Mountains. It is pale yellow in color, stratified, and contains inclusions of dacite and basalt.

Superstition Tuff. This thick (more than 600 m) welded tuff makes up the main part of Superstition Mountain, where it fills a caldera (Stuckless, 1969, 1971; Stuckless and Sheridan, 1971). It is generally strongly welded and devitrified and contains about 25% phenocrysts of quartz, sanidine, plagioclase, and biotite. Flattened pumice is easily recognized in most samples. Tuffs from this formation have been dated at 22 to 25 Ma. The Apache Leap Tuff (Peterson, 1961, 1968, 1969) has a similar appearance and composition, but it is somewhat younger (about 20 Ma).

Latites of Fish Creek and Latites of Government Well (Tgl). These units occur in stratigraphically equivalent positions in the western (Malone, 1972) and eastern (Hillier, 1978; Kilbey, 1986) parts of the Apache Trail, respectively. They consist of lahars, breccias, and lavas of intermediate (latite) composition (Kilbey, 1986). Interbeds of basalt are common in these formations. Because they formed central volcanoes, their thickness is variable (from 600 m down to the thickness of a single flow) and depends on the distance from the vent. Generally these rocks are rich in phenocrysts, especially large plagioclase and hornblende crystals. Pyroxene is a minor phase. These units have ages between 25 and 29 Ma.

Older basalt (Tob). This unit consists of several thin basalt flows and local scoria cones. The lavas are black to gray and contain olivine phenocrysts, but most are highly altered. The oldest unit in the vicinity of Goldfield may be a basaltic andesite, but all of the others are alkali olivine basalts (Kilbey, 1986). Interbedded with the basalts in the Goldfield mining district are a number of latitic to rhyolitic tuffs (Kilbey, 1986). Some of these units are coarse breccias with boulders of granite supported by an ash matrix. Surge beds and welded tuffs are also present.

Whitetail Conglomerate (Twc). This unit consists of coarse-grained red beds. The thickness of this unit depends on previous topography. It is thickest in paleovalleys and is absent on paleohills. The unit is thick bedded and mainly contains clasts of granite. Locally a few limestone boulders are present.

Precambrian granite (Pcg). This rock is the basement of the area. It is deeply weathered and hence has a thick development of guss on its surface. The rock contains subequal amounts of large quartz, plagioclase, and K-spar crystals with lesser amounts of biotite and hornblende. The age of this rock is about 1.4 b.y. (Stuckless and Naeser, 1972). A local pluton of diorite exists to the south of the Goldfield Mountains and a complex Precambrian stratigraphy occurs to the south of the Superstition Mountains.

GEOLOGIC HIGHLIGHTS EN ROUTE TO STOP 1

Phoenix occupies a broad basin at the northern margin of the Basin and Range Province. The northern skyline consists of North Phoenix Mountains (Pc schists), Camelback Mountain (Pc granite), and the McDowell Mountains (Pc granites, schists, and quartzites). Local exposures of Tertiary redbeds crop out at the Camelhead, Papago Park, and Red Mountain near the Salt River. South Mountain is a metamorphic core complex with minor Tertiary igneous units.

The Goldfield and Superstition Mountains form prominent volcanic topography to the east of the Phoenix basin. We will drive due east into this caldera complex along one of the main highways. After we turn northeast onto the Apache Trail, the main buttress of the Superstition resurgent core is an obvious feature on the east. The lower cliffs consist of domes of Government Well latite and the capping layers consist of the Superstition Tuff. Along the west side of the Apache Trail is the trace of the main bounding fault for the Goldfield caldera that separates the Precambrian basement rocks from the Tertiary volcanic sequence.

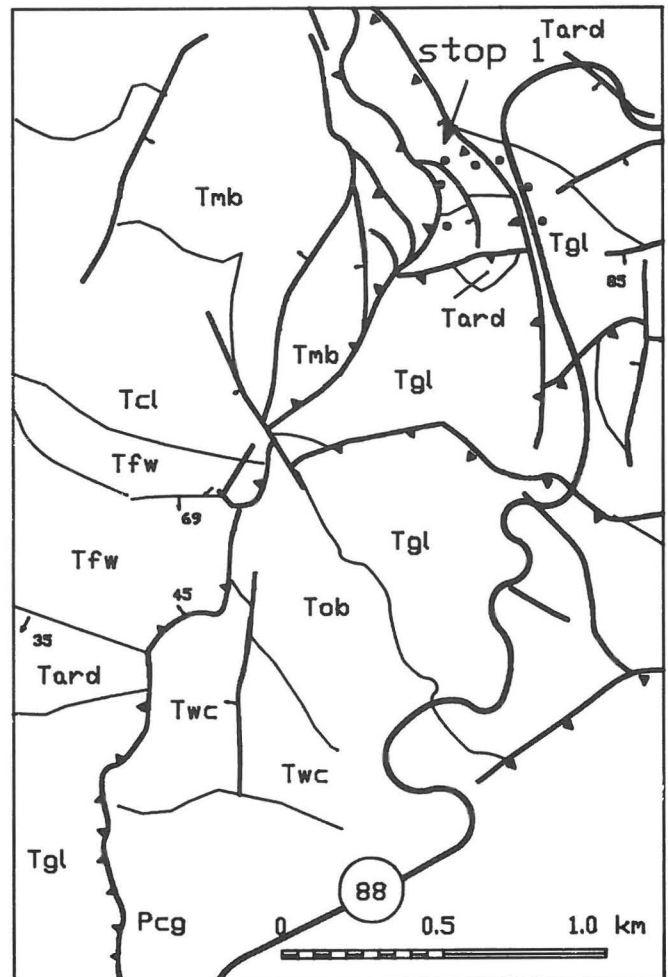


Figure 3. Geologic map of the Apache Gap area. At stop 1 we will examine low-angle faults (shown with teeth on hanging wall) along eastern margin of the Goldfield caldera. Dots indicate the path that we will hike.

STOP 1

The purpose of this stop is to examine the structures at the eastern margin of the Goldfield caldera. At this location the main caldera-bounding fault changes its trend from northward to northwestward. This fault (shown with teeth in Figure 3) splays into a series of splinter faults with greater displacement generally taken up by the more northerly faults. The stratigraphic displacement across the fault zone is approximately 1 km. This fault can be traced along strike for about 10 km. At either end there is a large ramp structure with an offset of 1 to 2 km to another caldera-bounding fault. This family of faults forms a ring of 270° surrounding the Goldfield caldera.

We will begin our traverse by walking northward along the Apache Trail (Highway 88) in the Government Well latites. We will cross a splay of the fault into the Apache Gap rhyodacite and climb up onto the rim of the caldera within the Mesquite Flat breccia. From this vantage point, we have an excellent view into the caldera as well as along the caldera-bounding fault to the south. The type locality for the Apache Gap rhyodacite is the elongate dome complex to the north. We will return to the bus along a south-facing low-angle fault related to another structure.

STOP 2

This stop is located approximately 2 km north of stop 1. Here we will walk about 700 m southeast from the Apache Trail along an apparent late-stage strike-slip fault that cuts all other structures in this area (Figure 4). The objective at this stop is to examine an imbricate set of south-dipping low-angle faults with apparent movement into the Superstition caldera. Along the trail we will see the contact of the Apache Gap rhyodacite with the First Water tuffs to the north. This is the type locality of the First Water tuffs.

At the end of the trail we will see an excellent example of the flow structures in the Apache Gap rhyodacite where it forms a large bulbous dome to the north of the canyon. This unit is decapitated and repeated by low-angle faults that can be traced along the mountainside to the east. The stop is at the complex intersection of the low-angle faults, late north-trending normal faults, and the even later strike-slip fault. If time and interest permit, we can see good evidence for magma mixing in the rhyodacite in outcrops along the road.

GEOLOGIC HIGHLIGHTS BETWEEN STOPS 2 AND 3

As the Apache Trail drops down to Canyon Lake we will be able to see the Canyon Lake Tuff exposed in roadcuts to the south. The cliff-forming unit to the north of the road is the Mesquite Flat breccia. This area represents a transition between the Goldfield and Tortilla calderas.

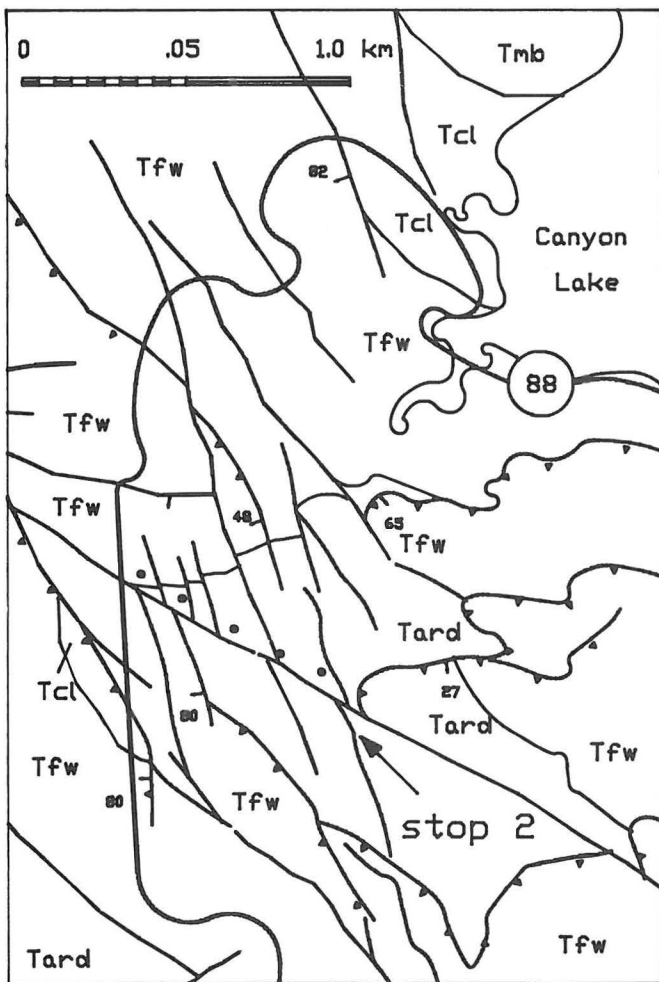


Figure 4. Geologic map of the First Water Canyon area. At stop 2 we will examine low-angle faults that slid to the south into the Superstition caldera. Dots indicate path we will follow.

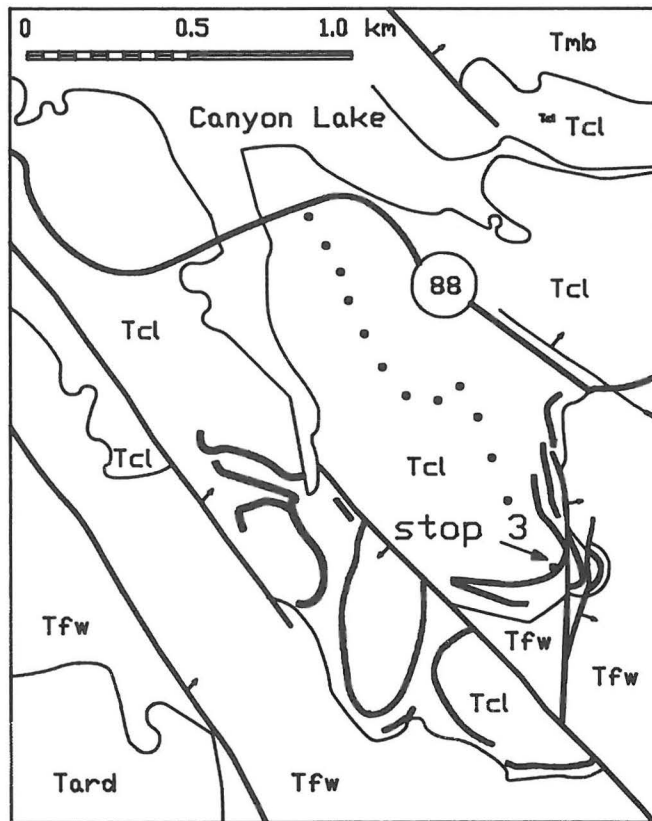


Figure 5. Geologic map of the Boulder Canyon area. At stop 3 we will examine vitrophyres in the Canyon Lake Tuff and discuss the possible postwelding movement of this unit. Dots indicate the 1.5-km hike at this location.

STOP 3

At this stop we will examine the multiple vitrophyres associated with the Canyon Lake welded tuff. We will follow a hiking path from the east end of the bridge by the marina for about 1.2 km to the crest of a ridge to the southeast (Figure 5). The only unit along the path is the Canyon Lake Tuff. At cliff faces along the eastern edge of this unit are multiple vitrophyres with complex structures. We will examine two of these vitrophyres to determine if there has been rheomorphic deformation of the unit.

From the vantage point of stop 3 it will be obvious that the Canyon Lake Tuff filled a northwest-trending valley. Relationships along the south wall of this valley suggest that faulting accompanied or shortly followed the emplacement of the tuff. Breccias and slump blocks slid onto unconsolidated tuff in those areas. Was there also rheomorphic slumping of the tuff on the north side of the valley in response to faulting contemporaneous with emplacement?

GEOLOGIC HIGHLIGHTS BETWEEN STOPS 3 AND 4

At Tortilla Flat is the eastern limit of the Canyon Lake Tuff. Its source is probably in the Peters Canyon dome complex to the east (Prowell, 1984). To

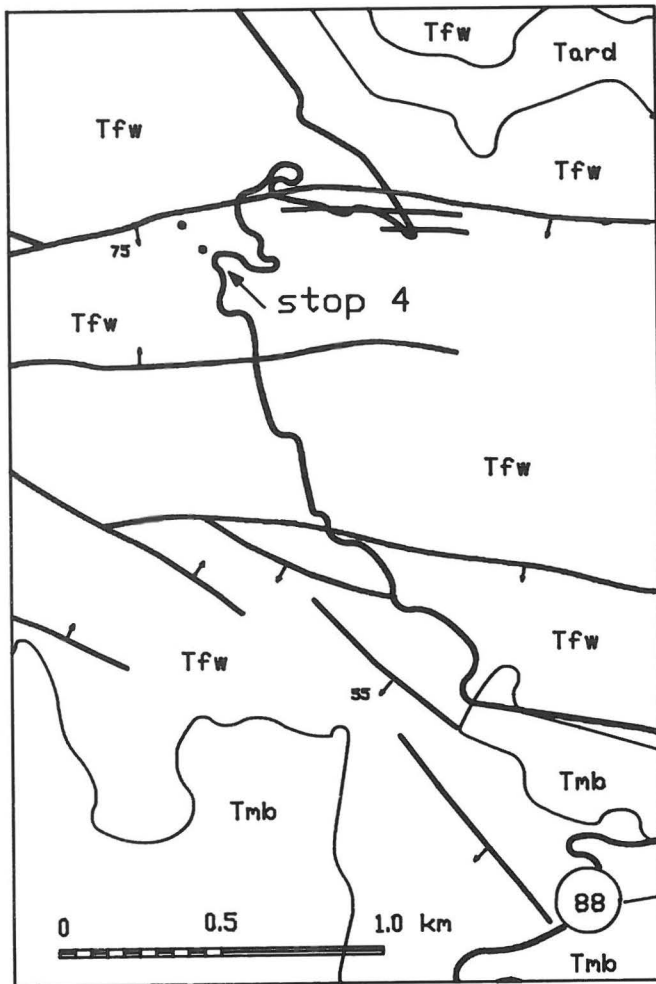


Figure 6. Geologic map along the Horse Mesa Dam access road. At stop 4 we will examine the fault that marks the northern boundary of the Tortilla caldera. Dots indicate direction to walk.

the northeast we will pass over a flat region that is the type locality of the Mesquite Flat breccia. This broad plateau is interpreted as the structural moat for the Tortilla caldera. Peters Canyon complex to the south could be a resurgent dome complex. The topographic rim of the Tortilla structure is visible to the west, north, and east. As we drive along the Horse Mesa access road we can see huge sandwave structures in surge beds related to a vent in the Coronado Mesa dome complex to the north.

STOP 4

The objective at this area is to observe the main caldera-bounding fault at the northern edge of the Tortilla structure and to examine the nature of caldera-rim volcanism. The bus will stop along the Horse Mesa Dam road at the southern edge of Fish Creek Canyon. The First Water rhyolite at this locality consists of a sequence of surge beds, pumice breccias, tuffs, and lavas that are common to the zone along the main caldera-bounding faults.

Lavas and surge beds are rare outside of the calderas, but they are common in the ring zone. In the canyon wall to the northeast of this stop it is possible to see at least five dome complexes stacked one upon another at the caldera rim. However, at a distance of 1 or 2 km north of the rim, the sequence consists only of tuffs with no vent deposits. We will examine surge beds related to a small vent at Coronado Mesa to the south.

From the stop point (Figure 6) we will take a short walk to the north to examine the nature of the caldera fault in detail. Here the fault has only about 200 m of vertical displacement, but it is continuous

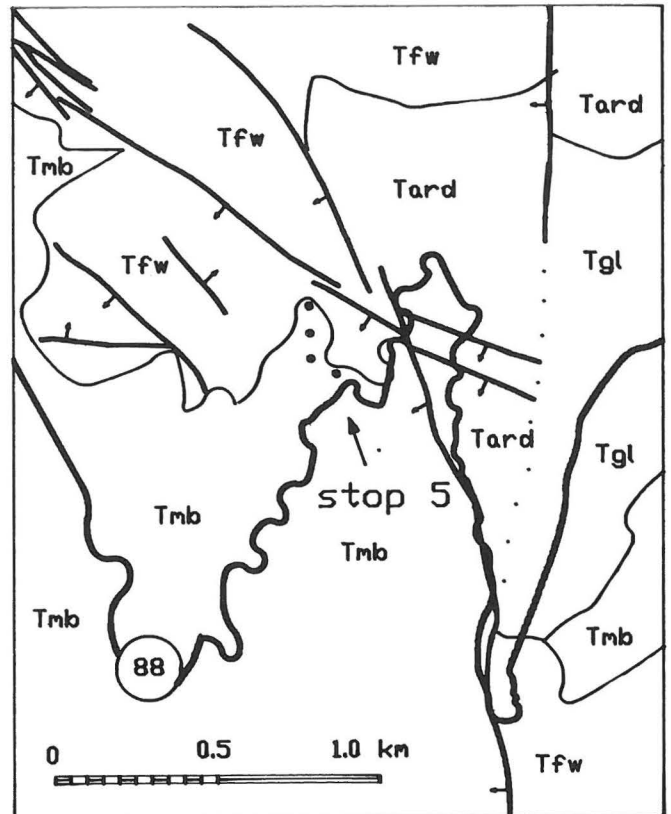


Figure 7. Geologic map of the Fish Creek overlook. At stop 5 we will inspect the faulting at the northeast margin of the Tortilla caldera.

along strike for at least 6 km in an east-west direction. This fault is nearly vertical, in contrast to the previous caldera-bounding faults, which were low angle. Locally there is silicified breccia along the fault and there are several small splays on the south side.

STOP 5

The purpose of this stop is to examine the features at the northeastern margin of the Tortilla caldera. At this stop we will walk out along a ridge composed of Mesquite Flat breccia to examine the contact of this laharic unit with the underlying First Water rhyolite (Figure 7). The caldera-bounding fault passes about 200 m to the east of this ridge where the Mesquite Flat breccia is placed into contact with the Apache Gap rhyodacite with about 1 km of stratigraphic displacement. This type of contact is similar to what we saw at stop 1, but the fault system here has a nearly vertical dip.

If time permits, we can walk down the Apache Trail to the east to examine the caldera-bounding fault. From this vantage point it is possible to see the underlying latites and a series of at least four step faults that make up the caldera rim at this location.

To the north is an excellent exposure of a typical rhyolitic dome complex that is bisected by Fish Creek. Here the First Water rhyolite rests conformably on the Apache Gap rhyodacite (actually the Bronco Butte lahar). The base of the dome complex consists of surge beds that are overlain by lava breccia. The core of the complex consists of a lava dome with a central vitrophyric member and an envelope of hydrated lava breccia. There are four sequences of tuffs exposed in the cliff face to the east. Each of these is probably related to a similar dome complex.

REFERENCES

- Fodor, R.V., 1969, Petrology and petrography of the volcanic rocks in the Goldfield Mountains, Arizona [M.S. thesis]: Tempe, Arizona State University, 66 p.
- Hillier, M.R., 1978, A geochemical study of the latite of Government Well, Superstition Mountains, Arizona [M.S. thesis]: Tempe, Arizona State University, 69 p.
- Isagholian, V., 1983, Geology of a portion of Horse Mesa and Fish Creek Canyon areas, Arizona [M.S. thesis]: Tempe, Arizona State University, 71 p.
- Kilbey, T.R., 1986, Geology and structure of the Goldfield mining district, Maricopa and Pinal Counties, Arizona [M.S. thesis]: Tempe, Arizona State University, 254 p.
- Malone, G.B., 1972, The geology of the volcanic sequences in the Horse Mesa area, Arizona [M.S. thesis]: Tempe, Arizona State University, 68 p.
- Peterson, D.W., 1961, Dacite ash-flow sheet near Superior and Globe, Arizona [Ph.D. thesis]: Stanford, Stanford University, 130 p.
- 1966, Geology of Picket Post Mountain, northeast Pinal County, Arizona: Arizona Geological Society Digest, v. 8, p. 159-176.
- 1968, Zoned ash-flow sheets in the region around Superior, Arizona, in Titley, S.R., ed., Southern Arizona Guidebook III: Arizona Geological Society, p. 215-222.
- 1969, Geologic map of the Superior quadrangle, Arizona: U.S. Geological Survey Geologic Quadrangle Map GQ-818, scale 1:24,000.
- Powell, S.E., 1984, Stratigraphic and structural relations of the north-central Superstition volcanic field [M.S. thesis]: Tempe, Arizona State University, 122 p.
- Rettenmaier, K.A., 1984, Provenance and genesis of the Mesquite Flat breccia, Superstition volcanic field, Arizona [M.S. thesis]: Tempe, Arizona State University, 181 p.
- Sheridan, M.F., 1978, The Superstition cauldron complex, in Burt, D.M., and P  w  , T.L., eds., Guidebook to the geology of central Arizona: Arizona Bureau of Geology and Mineral Technology Special Paper no. 2, p. 85-96.
- Sheridan, M.F., and Powell, S.E., 1986, Stratigraphy, structure, and gold mineralization related to calderas in the Superstition Mountains, in Beatty, B., and Wilkinson, P.A.K., eds., Frontiers in geology and ore deposits of Arizona and the Southwest: Arizona Geological Society Digest, v. 16, p. 306-311.
- Sheridan, M.F., Stuckless, J.S., and Fodor, R.V., 1970, A Tertiary silicic cauldron complex at the northern margin of the Basin and Range province, central Arizona, U.S.A.: Bulletin Volcanologique, v. 34, p. 649-662.
- Stuckless, J.S., 1969, The geology of the volcanic sequence associated with the Black Mesa caldera, Arizona [M.S. thesis]: Tempe, Arizona State University, 79 p.
- 1971, The petrology and petrography of the volcanic sequence associated with the Superstition caldera, Superstition Mountains, Arizona [Ph.D. thesis]: Stanford, Stanford University, 106 p.
- Stuckless, J.S., and Naeser, C.W., 1972, Rb-Sr and fission-track age determination in the Precambrian plutonic basement around the Superstition volcanic field, Arizona: U.S. Geological Survey Professional Paper 800-B, p. B191-B194.
- Stuckless, J.S., and O'Neil, J.R., 1973, Petrogenesis of the Superstition-Superior volcanic area as inferred from the strontium and oxygen isotope studies: Geological Society of America Bulletin, v. 84, p. 1987-1998.
- Stuckless, J.S., and Sheridan, M.F., 1971, Tertiary volcanic stratigraphy in the Goldfield and Superstition Mountains, Arizona: Geological Society of America Bulletin, v. 82, p. 3235-3240.
- Sunesson, N.H., 1976, The geology of the northern portion of the Superstition-Superior volcanic field, Arizona [M.S. thesis]: Tempe, Arizona State University, 123 p.

Field Guide to Lower- and Upper-Plate Rocks of the South Mountains Detachment Zone, Arizona

Stephen J. Reynolds
Arizona Bureau of Geology and Mineral Technology
845 N. Park Ave.
Tucson, Arizona 85719

Gordon S. Lister
Bureau of Mineral Resources, Geology, and Geophysics
P.O. Box 378
Canberra, A.C.T., 2601 Australia

INTRODUCTION

Detachment zones are major, normal-displacement shear zones that formed with an originally low dip. They are regional to subregional in extent, have generally accommodated 5 to 50 km of normal slip, and juxtapose structurally dissimilar upper- and lower-plate rocks. Structures in lower-plate rocks commonly represent a complete continuum of deformation from early ductile mylonitization to late-stage brittle faulting. In contrast, most upper-plate rocks lack detachment-related mylonitic fabrics, but are brittlely distended into tilted fault blocks bounded by high- to low-angle normal faults.

The structural evolution of detachment zones (also referred to as metamorphic core complexes) is now interpreted in terms of an evolving-shear-zone model (Wernicke, 1981; Reynolds, 1982, 1985; G. H. Davis, 1983; G. A. Davis and others, 1986; Reynolds and Lister, 1987). According to this model, normal displacement on a gently dipping shear zone produces mylonitic fabrics below the brittle-ductile transition and brittle fabrics at shallower crustal levels. As the wedge-shaped upper plate brittlely distends and is tectonically denuded, lower-plate rocks become less deeply buried and more brittle with time. In this manner, lower-plate rocks originally subjected to mylonitization below the brittle-ductile transition are successively overprinted by more brittle fabrics as they are tectonically transported toward the surface.

The South Mountains, located directly south of Phoenix (Figure 1), afford an excellent opportunity to examine structures formed during ductile-to-brittle evolution of a detachment zone. The area is ideal because the entire progression from ductile mylonitization to brittle cataclasis can be observed within a single rock type (middle Tertiary granodiorite). Access is excellent because most of the range is contained within the City of Phoenix South Mountain Park. In addition, typical upper-plate structures and rock types are well exposed in parks adjacent to the South Mountains (Figure 1).

This field-trip guide outlines a one-day field excursion into the South Mountains to examine a broad spectrum of ductile-to-brittle detachment-related structures. An additional stop in Papago Park north of the South Mountains provides an example of upper-plate rock types, including middle Tertiary syn-tectonic clastic rocks and sedimentary breccias. All roads traveled are suitable for ordinary passenger cars and most hiking is along trails that require only light boots or sneakers.

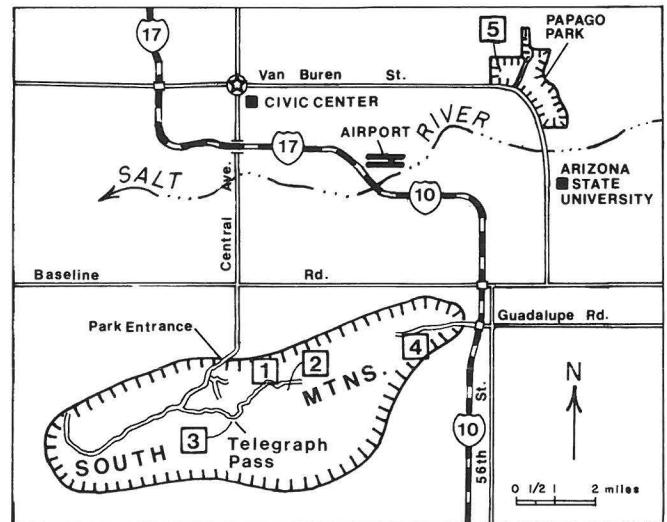


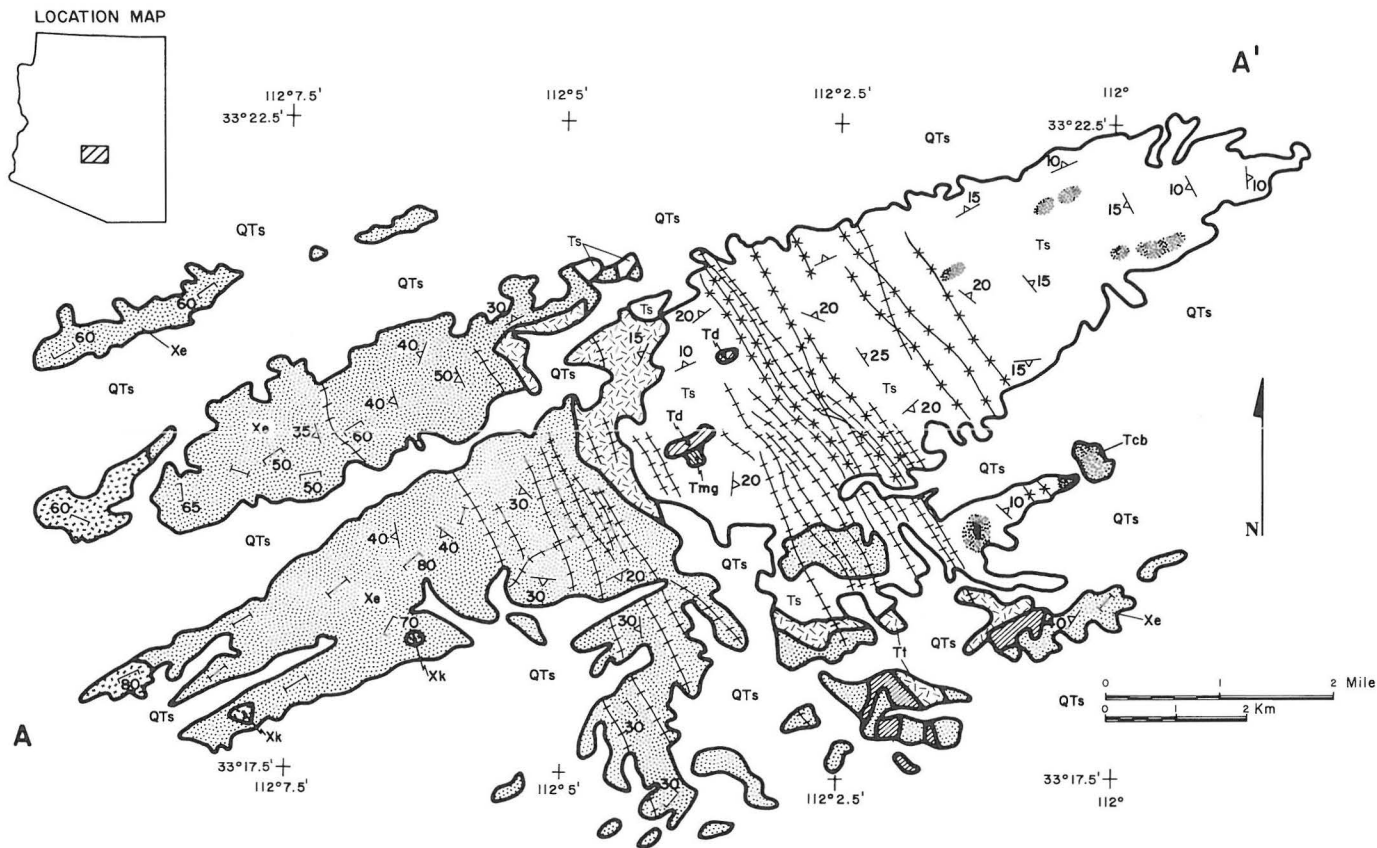
Figure 1. Location map of field-trip stops (numbered boxes).

GEOLOGIC OVERVIEW

In the South Mountains, structures that formed in a middle Tertiary detachment zone have overprinted a basement terrane composed of Proterozoic crystalline rocks and a composite middle Tertiary pluton (Reynolds and Rehrig, 1980; Reynolds, 1982, 1985; Koenemann, 1986; Reynolds and others, 1986; Reynolds and Lister, 1987 and in review). The Proterozoic rocks, exposed in the western half of the South Mountains (Figure 2), consist of amphibolite-grade Estrella Gneiss and a foliated granite. Proterozoic metamorphism and deformation produced a steeply dipping, east- to northeast-striking crystalloblastic foliation in both rock types.

The composite Tertiary pluton occupies most of the eastern part of the range and has three main phases (Figure 2). The oldest and most extensive phase is South Mountains Granodiorite. The granodiorite is intruded by and locally grades into Telegraph Pass Granite, a north-northwest-trending intrusion near the center of the range. The third phase, Dobbins Alaskite, is commonly a fine-grained border phase of the granite.

The Tertiary pluton and Proterozoic wall rocks have been intruded by two series of north-northwest-



ROCK UNITS

SYMBOLS

- Quaternary and Late Tertiary
 - QTs - surficial deposits
- Middle Tertiary
 - Tcb - chloritic breccia
 - Tmg - mylonitic gneiss and schist
 - Td - Dobbins Alaskite
 - Tt - Telegraph Pass Granite
 - Ts - South Mountains Granodiorite
- Early Proterozoic
 - Xk - Komatke Granite
 - Xe - Estrella Gneiss

- contact
- intermediate to felsic dike of middle Tertiary age
- microdiorite dike of middle Tertiary age
- 80 - strike and dip of Proterozoic crystalloblastic foliation
- 20 - strike and dip of mylonitic foliation
- strike of vertical crystalloblastic foliation
- Estrella Gneiss in upper plate of detachment fault

Figure 2a. Generalized geologic map of the South Mountains (from Reynolds, 1985).

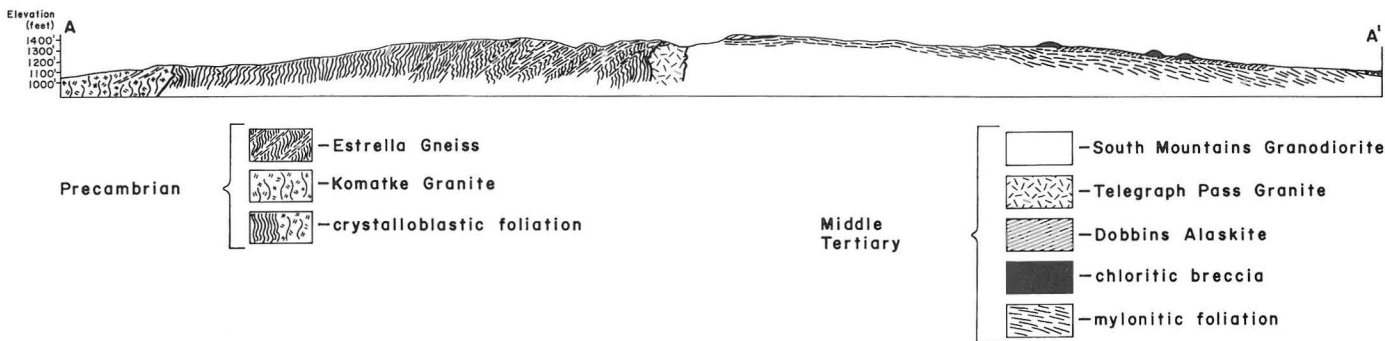


Figure 2b. Generalized cross section of the South Mountains (from Reynolds, 1985).

WSW

ENE

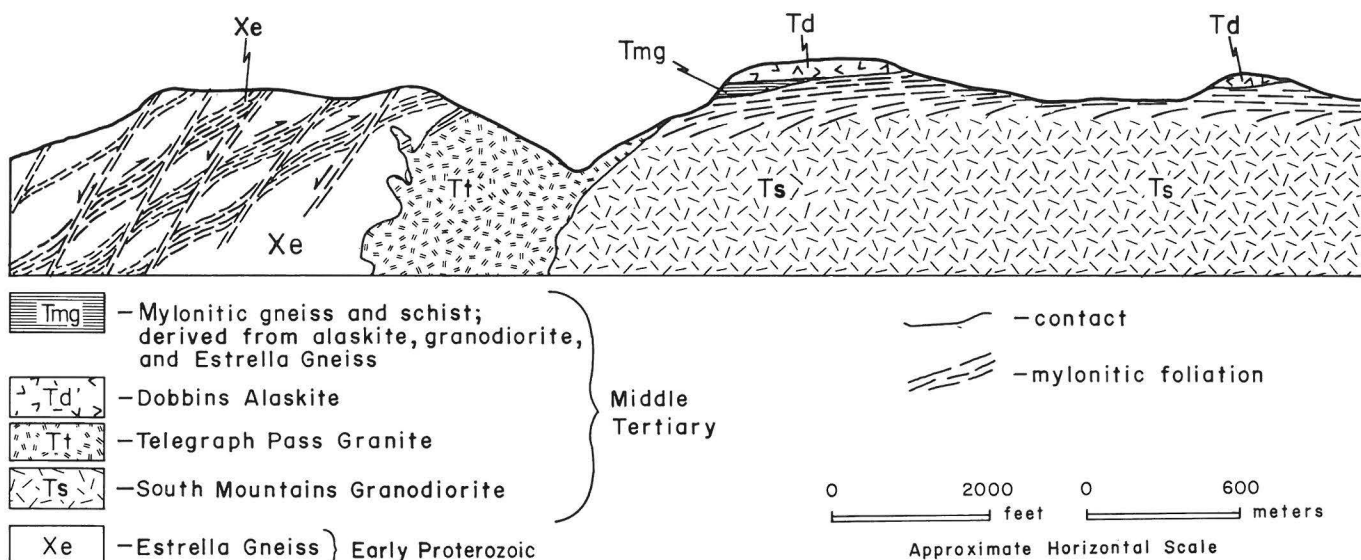


Figure 3. Schematic cross section of Telegraph Pass (Stop 3), Mount Suppoa (the high central peak), and Dobbins Lookout (the eastern peak of alaskite; Stop 1). Mylonitic front (Stop 3) is shown schematically in Proterozoic Estrella Gneiss (modified from Reynolds, 1985).

trending dikes: older fine- to medium-grained, intermediate to felsic dikes and younger dioritic dikes. The pluton was emplaced at 22 to 25 Ma, followed by intrusion of both series of dikes prior to 20 Ma (Reynolds and others, 1986).

The Proterozoic rocks, Tertiary pluton, and older series of dikes have been widely overprinted by middle Tertiary mylonitic Proterozoic with a characteristic N. 60° E.-trending stretching lineation. This detachment-related mylonitic fabric occurs in two structural settings: (1) a main, gently dipping shear zone that is 50 to 100 m thick and is best developed structurally high in the Tertiary pluton in the eastern half of the range; and (2) a more diffuse, moderately southwest-dipping mylonitic zone, or mylonitic front, that cuts through Proterozoic rocks in the western half of the range (Figure 3). The main, gently dipping mylonitic zone was formed by east-northeast-directed shear parallel to the stretching lineation. Most penetrative mylonitic fabric in the mylonitic front was also formed by northeast-directed shear, but this fabric now dips southwest and is cut by thin, late-stage shear zones that dip southwest and have normal (top-to-the-southwest) displacement. The southwest dip of the mylonitic front and the development of late-stage, antithetic shear zones are interpreted as reflecting upwarping (folding) of the shear zone due to isostatic rebound during tectonic denudation (Reynolds and Lister, in review).

Mylonitic fabrics in the main shear zone were overprinted by successively more localized and more brittle structures that formed within the same top-to-the-northeast kinematic regime as mylonitization, but at lower temperatures and pressures. Brittle and brittle-ductile deformation produced breccia, microbreccia, and brittle-ductile shear zones in the footwall of the South Mountains detachment fault on the eastern end of the range. The detachment fault dips gently to the northeast and projects beneath moderately southwest-dipping middle Tertiary sedimentary and volcanic rocks (Figure 4) that have been transported to the northeast relative to lower-plate

rocks. The subsurface continuation of the fault to the east has been recognized on seismic-reflection profiles (Frost and Okaya, 1986).

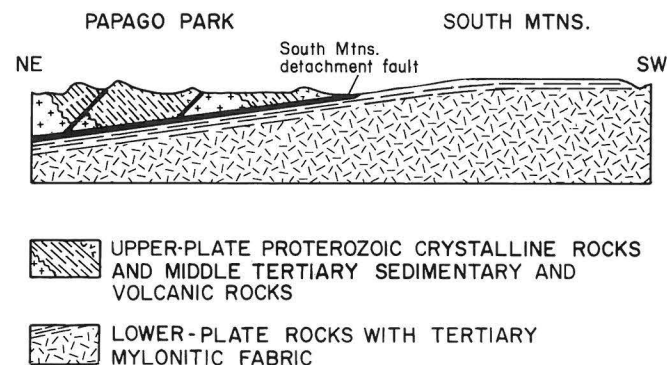


Figure 4. Schematic, interpretive cross section showing relation between South Mountains detachment fault and upper-plate rocks in Papago Park (Stop 5).

PHYSIOGRAPHY

The South Mountains have a distinctive archlike physiography with a central topographic notch, known as Telegraph Pass (Figure 2). The archlike physiography is best developed in the eastern half of the range, where topography mimics the attitudes of (1) mylonitic foliation in the granodiorite and (2) the South Mountains detachment fault. The planar profile along the crest of this part of the range reflects the gentle northeast dip of the South Mountains detachment fault and the large difference in erodibility between the nonresistant breccia zone (largely removed) and the underlying unbrecciated granodiorite. Several hills of breccia protrude above the otherwise planar

profile. Mount Suppoa, the high peak with the communication towers, is composed of flat-lying sheets of mylonitic Dobbins Alaskite and Telegraph Pass Granite (Figure 3).

Telegraph Pass is underlain by hydrothermally altered and easily eroded Telegraph Pass Granite. West of the pass, Proterozoic Estrella Gneiss is cut by the mylonitic front, which consists of a series of southwest-dipping mylonitic zones that form small ledges in the gneiss. The smooth topographic profile of the western half of the range is thought to mimic the warped geometry of the South Mountains detachment fault as it continued over this part of the range (Reynolds and Lister, in review).

FIELD GUIDE

Directions and Geologic Highlights En Route to Stop 1

The trip starts at Phoenix Civic Center (Figure 1). Proceed south on Central Avenue, which leads directly into South Mountains Park. Once inside the park, follow the main or "Summit" road by going straight ahead at the junction just inside the old park entrance (marked by an abandoned guard shack) and by veering left at the "Y" intersection 1.5 mi past the old entrance. Between this intersection and Telegraph Pass, the road traverses eastward through dark-colored Proterozoic Estrella Gneiss and light-colored Telegraph Pass Granite. The gneiss has southwest-dipping middle Tertiary mylonitic fabric that cuts and retrogresses higher grade Proterozoic crystalloblastic fabric. Just east of Telegraph Pass, the road crosses the contact between Telegraph Pass Granite and more gray-colored South Mountains Granodiorite and remains within variably mylonitic granodiorite most of the way to Stop 1. Continue on the main road, which leads to Dobbins Lookout.

Stop 1: Dobbins Lookout

Dobbins Lookout is located within the main shear zone, which here has been overprinted on flat-lying sheets of Dobbins Alaskite that overlie South Mountains Granodiorite along a subhorizontal contact (Figure 3). Mylonitic fabric in the granodiorite is best developed at structurally high levels near the contact and dies out downward, generally within 50 to 100 m. The sheets of alaskite are strongly mylonitic and contain small-scale shear zones that span the ductile-to-brittle continuum and are locally flanked by injection veins of pseudotachylite. The purpose of this stop is to provide an overview of the South Mountains, to traverse to the north down through the main shear zone into less deformed granodiorite, and to examine the entire spectrum of ductile-to-brittle structures, including those indicative of sense of shear (S-C fabrics, etc.).

Stop 2: Mylonitic Dikes and Fish Flash

Start back down the main road from Dobbins Lookout, but take the first left turn on a paved road toward Hidden Valley, continuing 0.7 mi and parking along a small dirt road on the left. Hike a short distance to the north and examine dikes cutting mylonitic South Mountains Granodiorite. The oldest dikes are strongly mylonitic, but successively younger dikes are less mylonitic or undeformed. The dikes were clearly emplaced during mylonitization and all trend north-northwest, perpendicular to the mylonitic stretching lineation (Reynolds, 1985).

This locality is where we first discovered the fish-flash technique for determining the sense of shear in micaceous mylonitic rocks. Mica phenocrysts

in some dikes have been deformed into mica fish with a strongly asymmetrical preferred orientation with respect to foliation. The fish-flash technique involves cleaving the sample and holding it right-side up with the lineation parallel to the sun azimuth, preferably with the sun behind the viewer. While looking parallel to lineation, the viewer tilts the sample backward (not past 90°) until the number of sun reflections off the mica (001) is maximized. The sample is then rotated, commonly on the palm of the hand, 180° about an axis perpendicular to foliation (maintaining the same foliation orientation). The number of reflections is then qualitatively compared with the number previously observed. The fish flash will be greatest when the viewer is looking in the same direction as the sense of shear. An alternative method is to maximize the number of reflections, but to note the angle of incidence.

Stop 3: Telegraph Pass and Traverse Through Mylonitic Front

Return to Telegraph Pass via the main road, park along the road near the pass, and climb the trail uphill to the west. At the ridge crest, follow the trail to the north and then west along the northern ridge until it crosses the mylonitic front, just east of the highest point on the ridge.

The traverse starts in Telegraph Pass and crosses the intrusive contact into Proterozoic Estrella Gneiss (Figure 3) with mylonitic fabric that is subhorizontal, has a northeast sense of shear, and projects into the main shear zone in the Tertiary pluton east of the pass. Further to the west along the trail, this fabric gradually dips more steeply southwest and cuts through the gneiss as a diffuse shear zone (the mylonitic front). Within the mylonitic front are mylonitic zones that are several meters thick, dip approximately 30° southwest, and have a northeast sense of shear; these are interpreted to represent a segment of the originally northeast-dipping main shear zone that has been subsequently folded. These northeast-directed shear zones are cut by thinner ductile and ductile-brittle shear zones that dip more steeply southwest, are marked by retrogression, and have a southwest, or antithetic, sense of shear. These late-stage antithetic shear zones resulted from and helped accommodate folding of the shear zone. They demonstrate that folding of the shear zone about an axis perpendicular to lineation started during the late stages of mylonitization.

Stop 4: Directions and Comments

Follow the main road out of the park and north on Central Avenue. Turn east (right) on Baseline Road and then south (right) on 56th Street (Avenida del Yaqui), the first major street east of Interstate 10. Drive south on 56th Street for 1 mi, turn west (right) on Guadalupe Road (Calle Guadalupe) for 1.5 mi, and park along the side of the dirt road. Lock your car and hike up the ridge to the south.

This traverse crosses the transition from mylonitic granodiorite upward into chloritic breccia and microbreccia derived from the granodiorite in the footwall of the South Mountains detachment fault. Structurally lowest exposures of the granodiorite are mylonitic, but are not brecciated or chloritic, except along widely spaced dilatant and shear fractures. The granodiorite is progressively more fractured, brecciated, and mineralogically altered up-section until it ultimately grades into chloritic breccia, microbreccia, and ductile-brittle fault rocks. Remnants of mylonitic foliation in the breccia generally dip southwest due to antithetic rotation during detachment

faulting. Fractures and normal faults within the breccia generally strike northwest and contain northeast-trending striations that are statistically parallel to mylonitic lineation (Reynolds, 1985). Injection veins and selvages of microbreccia and pseudotachylite occur along the flanks of some faults and ductile-brittle shear zones. Ledges of microbreccia (cataclasite) that cap and occur around the flanks of the hill mark discrete low-angle fault surfaces. One such fault in the southern foothills of the range dips gently to the northeast and places Proterozoic gneiss over chloritic breccia derived from South Mountains Granodiorite. A higher unexposed fault probably separates these rocks from moderately tilted Tertiary sedimentary and volcanic rocks present at the next stop (Figure 4).

Stop 5: Upper-Plate Sedimentary Rocks

Turn around and proceed east on Calle Guadalupe, north (left) on 56th Street (Avenida del Yaqui), east (right) on Baseline Road for 1.4 mi, and north (left) on Mill Avenue past Arizona State University. Approximately 0.5 mi north of the Salt River, bear right toward Van Buren Street, continue another 0.5 mi to Galvan Parkway and turn north (right). Drive north for 0.3 mi, turn west (left) for 0.05 mi, and turn north (right) for 0.4 mi. Lock your car and hike to the small ridge west of the road. The northern part of this ridge is composed of middle Tertiary conglomerate and sedimentary breccia that dip moderately to the southwest and that elsewhere depositionally overlie Proterozoic crystalline rocks (Péwé and others, 1987). The southern part of the ridge is composed of highly shattered Proterozoic granite and metarhyolite, which we interpret to be a megabreccia block intercalated within the Tertiary section. Such megabreccia blocks, representing catastrophic debris avalanches, are widespread in half-graben deposits in the upper plates of other detachment zones in Arizona.

The Tertiary section and depositionally underlying Proterozoic rocks are broken into a series of tilted fault blocks by northwest-trending, northeast-dipping normal faults (Péwé and others, 1987). The normal faults and southwest tilt of the rocks reflect distension and antithetic rotation during north-eastward transport above the South Mountains detachment fault (Figure 4; Reynolds, 1985).

Return to the cars and drive south on the Galivan Parkway, west on Van Buren, and south on Central Avenue back to the Convention Center.

REFERENCES CITED

- Davis, G. A., Lister, G. S., and Reynolds, S. J., 1986, Structural evolution of the Whipple and South Mountains shear zones, southwestern United States: *Geology*, v. 14, p. 7-10.
- Davis, G. H., 1983, Shear-zone model for the origin of metamorphic core complexes: *Geology*, v. 11, p. 342-347.
- Frost, E. G., and Okaya, D. A., 1986, Application of seismic reflection profiles to tectonic analysis in mineral exploration, in Beatty, Barbara, and Wilkinson, P. A. K., eds., *Frontiers in geology and ore deposits of Arizona and the Southwest*: Arizona Geological Society Digest, v. 16, p. 137-150.
- Koenemann, Falk, 1986, Microtextural study and axial distribution analysis for quartz in a deformed granite [M.S. thesis]: Davis, University of California, 129 p.
- Péwé, T. L., Wellendorf, C. S., and Bales, J. T., 1987, Environmental geology of the Tempe quadrangle, Maricopa County, Arizona: Arizona Bureau of Geology and Mineral Technology Folio Series No. 2, scale 1:24,000.
- Reynolds, S. J., 1982, Geology and geochronology of the South Mountains, central Arizona [Ph.D. thesis]: Tucson, University of Arizona, 220 p.
- _____, 1985, Geology of the South Mountains, central Arizona: Arizona Bureau of Geology and Mineral Technology Bulletin 195, 61 p.
- Reynolds, S. J., and Lister, G. S., 1987, Structural aspects of fluid-rock interactions within detachment zones: *Geology*, v. 15 (in press).
- _____, in review, Ductile-to-brittle evolution of the South Mountains detachment zone: submitted to *Journal of Structural Geology*.
- Reynolds, S. J., and Rehrig, W. A., 1980, Mid-Tertiary plutonism and mylonitization, South Mountains, central Arizona, in Crittenden, M. D., Jr., and others, eds., *Cordilleran metamorphic core complexes*: Geological Society of America Memoir 153, p. 159-175.
- Reynolds, S. J., Shafiqullah, M., Damon, P. E., and DeWitt, Ed, 1986, Early Miocene mylonitization and detachment faulting, South Mountains, central Arizona: *Geology*, v. 14, p. 283-286.
- Wernicke, Brian, 1981, Low-angle faults in the Basin and Range Province--nappe tectonics in an extending orogen: *Nature*, v. 291, p. 645-648.

Structural Geology of the Rincon and Pinaleno Metamorphic Core Complexes, Southeast Arizona

George H. Davis
Department of Geosciences
The University of Arizona
Tucson, Arizona 85721

Stephen J. Naruk
Department of Geosciences
The University of Arizona
Tucson, Arizona 85721

Charles H. Thorman
U.S. Geological Survey
Denver, Colorado 80225

INTRODUCTION

Purpose of Trip

Interpretations of the characteristic structures of metamorphic core complexes generally fall into three broad categories: (1) Sevier-Laramide mylonitic thrust zones with superimposed mid-Tertiary low-angle normal faults (detachment faults; e.g., Drewes, 1977; Thorman, 1977); (2) mid-Tertiary, pure-shear extension zones in which the detachment fault marks a rheological transition between lower ductile extension and upper brittle extension (e.g., Rehrig and Reynolds, 1980; Miller and others, 1983); and (3) mid-Tertiary, simple-shear extension zones in which the detachment faults and mylonite zones represent the correlative upper- and lower-crustal levels of continuous, crustally penetrative, brittle-ductile shear zones (e.g., Davis, 1983, 1987a; Wernicke, 1985). Interpretations (1) and (3) are not mutually exclusive. Most workers now agree that the low-angle detachment faults are mid-Tertiary extensional phenomena and that the crystalline cores of the metamorphic core complexes contain Sevier-Laramide compressional structures. However, there is little consensus as to the relationships between the compressional and extensional structures, and it is largely this that continues to make the core complexes "a very . . . special and enigmatic tectonic response of obscure significance" (Coney, 1980). In this trip, we will examine the structural characteristics of two well-studied metamorphic core complexes and discuss their tectonic significance.

Summary of Geology

The Pinaleno Mountains are composed primarily of Proterozoic igneous and metamorphic rocks (Thorman, 1981a,b; Figure 1). Mylonites form a thin, northwest-striking zone along the northeastern flank of the range (Davis, 1980; Thorman, 1981a,b; Naruk, 1986a). Both the mylonitic foliation (S-surfaces) and the mylonite-zone lower boundary dip northeast, but the boundary dips 10°-15° more steeply than the foliation. Mineral lineations within the mylonites trend N40°-50°E. Structures within the mylonite zone consistently indicate a top-to-the-northeast sense of shear. Generally the mylonites are unconformably

overlain by Quaternary-Tertiary gravels, although a few breccia outcrops are locally exposed. Integration of the shear strain within the zone indicates that the hanging wall has moved a minimum of 7 km northeast relative to the footwall (Naruk, 1987).

The Eagle Pass detachment fault is a gently southwest-plunging, spoon-shaped fault at the northwestern end of the Pinaleno Mountains (Figure 1) (Blacet and Miller, 1978; Davis, 1980; Davis and Hardy, 1981). A mirror-image detachment fault occurs along the northeastern flank of the Jackson Mountains (Blacet and Miller, 1978; Davis, 1980; Simons, 1987; Simons and others, 1987). The footwall of the Eagle Pass detachment consists of microbrecciated, but non-mylonitic, Proterozoic granodiorite. The hanging wall consists of southwest-dipping, mid-Tertiary andesites, rhyolites and volcaniclastics (Davis and Hardy, 1981). Kinematic indicators along the fault indicate N40°-50°E transport of the hanging-wall, parallel to the mineral lineation and to the direction of shear in the Pinaleno mylonites (Davis and Hardy, 1981). Correlation of a depositional contact within autochthonous rocks in the Galiuro Mountains west of Eagle Pass, with its allochthonous counterpart in the detachment fault upper plate, indicates that the upper plate has moved 6-9 km (Naruk, 1987).

Thorman interprets the Pinaleno shear zone and the Eagle Pass detachment as unrelated because their respective styles of deformation represent very different pressure-temperature conditions and because the two structures dip in opposite directions and project into each other at a high angle (Figure 1). In contrast, Davis (1980), Rehrig and Reynolds (1980), Davis and Hardy (1981), Spencer (1984), and Naruk (1986a, 1987) interpret the two structures as one continuous brittle-ductile shear zone because the senses and magnitudes of transport are approximately the same.

The Galiuro Mountains to the west of Eagle Pass are composed of nearly flat-lying, undeformed, mid-Tertiary andesites, rhyolites, and volcaniclastics (Figure 1; Creasey and others, 1961; Creasey and Krieger, 1978; Creasey and others, 1981). The northeastern range front is apparently not bounded by high-angle normal faults and has been interpreted as the footwall, or breakaway, of the Eagle Pass detachment fault (Spencer, 1984). Similarly, the southwestern range front is not bounded by a high-angle fault and has been interpreted as the breakaway of the Santa

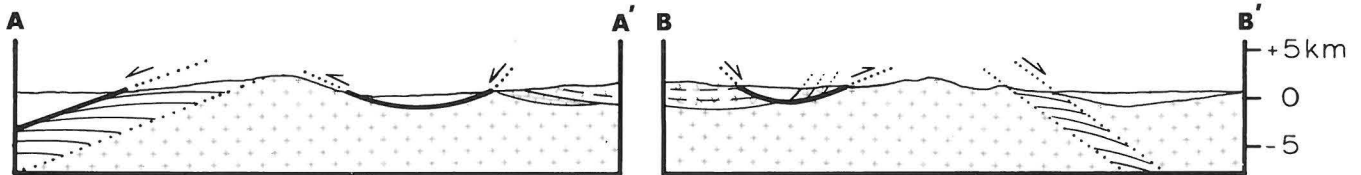
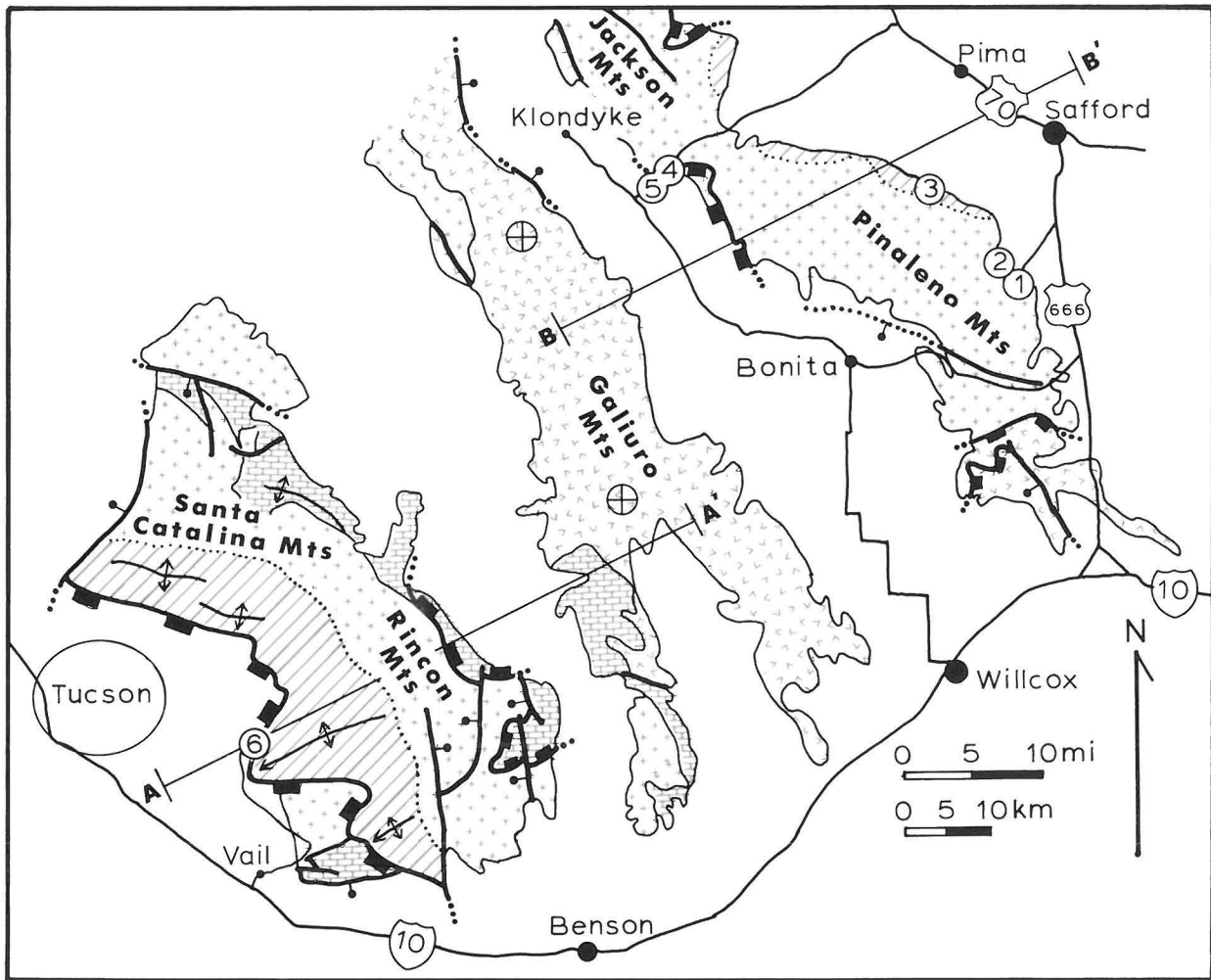


Figure 1. Generalized geologic map and cross sections of the Pinaleno, Galiuro, and Rincon Mountains, showing field-trip route and stops. Cross pattern represents undifferentiated Proterozoic gneisses and younger intrusives. Brick pattern represents Paleozoic and Mesozoic sedimentary rocks. V pattern represents mid-Tertiary volcanics. Diagonally ruled pattern represents core-complex mylonites. Light dotted lines represent mylonite zone boundaries. Heavy lines with rectangles represent detachment faults (rectangles on upper plate).

Catalina detachment fault (Dickinson and others, 1986).

The Rincon and Santa Catalina Mountains form the next range to the southwest of the Galiuro Mountains (Figure 1). On the northeast side, the Rincon Mountains are bounded by an 80° east-dipping normal fault system (Drewes, 1977). On the west side, the mountains are bounded by the curvilinear, 20° - 30° southwest-plunging Santa Catalina detachment fault (Drewes, 1977; Davis, 1980). Within the range, a carapace of Paleozoic and Mesozoic sedimentary and metamorphic rocks structurally overlies mylonitic gneisses derived from a variety of Proterozoic, Cretaceous, and Eocene intrusives (Drewes, 1976, 1977; Davis, 1980; Keith and others, 1980; Drewes and Thorman, 1981; Thorman and

others, 1981). The carapace rocks have experienced one or more episodes of pre-Eocene compressional deformation, as well as an episode of post-Eocene extensional deformation (Drewes, 1977; Keith and others, 1980; Thorman and others, 1981; Bykerk-Kauffman and Janecke, 1987). The mylonitic foliation surfaces below the carapace rocks define antiforms and synforms that plunge gently $S60^\circ$ - $70^\circ W$. Throughout most of the range, pervasive mineral lineations in the mylonites also trend $S60^\circ$ - $70^\circ W$ or $N60^\circ$ - $70^\circ E$. On the northern flank of the range, however, intersection and mineral lineations trend north-northeast to north-northwest.

Throughout most of the range, microstructures within the mylonites indicate a top-to-the-southwest

sense of shear. In the carapace rocks, the vergence of folds is variable and was interpreted by Davis (1975) as indicating radial movement and later reinterpreted by him as indicating southwest movement (Davis, 1983). Drewes (1976, 1978, 1981) interprets tectonic duplication of Paleozoic and Mesozoic rocks as indicating northeast tectonic transport of at least 32 km during the Cretaceous. However, the mylonitic microstructures suggest that the Rincon mylonites are correlative with southwest-vergent mylonitic domains in the Santa Catalina Mountains, which represent more than 40 km of post-Eocene, southwest, tectonic transport (Naruk, 1986b).

The mylonites in the Rincon Mountains are structurally overlain by propylitically and argillically altered (chloritized) microbreccias. These are derived from the mylonites, although the contact between the two is a distinct fault (Davis and others, 1981). Within the breccias, the orientations of remnant mylonitic fabrics demonstrate that significant rotations accompanied faulting and cataclasis. The actual detachment fault is marked by a gently dipping, several-meter-thick ledge of ultracataclasite.

The hanging wall of the Santa Catalina detachment fault is composed of Proterozoic granite and schist, Paleozoic and Mesozoic metamorphic and sedimentary rocks, and Tertiary sedimentary rocks. The granitic rocks are intensely fractured and the sedimentary rocks are complexly folded. The pre-Tertiary rocks contain both compressional and extensional features, including mylonites. In contrast, the Tertiary rocks show only extensional features and no evidence of metamorphism or mylonitization.

Thorman (1977) and Drewes (1976, 1977, 1981) propose that the Rincon mylonites formed by Late Cretaceous, large-scale northeast thrusting, and that the Santa Catalina detachment resulted from southwest-directed gravitational sliding associated with uplift of the complex in the middle Tertiary. In contrast, Davis (1980, 1983, 1987a) interprets both the mylonites and the detachment as the products of early to middle-Tertiary extensional deformation.

Summary of Trip Itinerary

At stop 1 we will examine the nonmylonitic gneiss of Johns Dam, one of the Proterozoic, porphyritic orthogneisses of the core of the Pinaleno Mountains. Stop 2 provides an overview of the Pinaleno mylonite zone and Gila Valley geology. Following stop 2, an optional stop may be included to see the mylonitic gneiss of Johns Dam. At stop 3 we will traverse across the lower boundary of the Pinaleno mylonite zone, from SC-mylonites into their essentially undeformed granite equivalent. At stops 4 and 5 we will examine structures associated with the Eagle Pass detachment fault. At stop 4 we will see both undeformed and brecciated footwall granodiorite and the actual detachment-fault surface. At stop 5 we will see the hanging-wall structures that indicate the sense of displacement. Lastly, at stop 6 in the Rincon Mountains, we will traverse structurally upwards, through mylonites derived from Proterozoic and Eocene(?) protoliths, into breccias derived from the mylonites, and across the Santa Catalina detachment fault into extraordinarily folded Paleozoic rocks and structurally overlying Proterozoic Pinal Schist.

GEOLOGIC HIGHLIGHTS EN ROUTE TO STOPS 1 AND 2

Proceed 7 miles south of Safford on US 666 to AZ 366 at Swift Trail Junction and turn right (southwest) towards the Pinaleno Mountains (Figure 2).

As we proceed southward from Safford on US 666, the most conspicuous geology is the spectacular, dissected pediment surfaces that bound the northern flank of the range. These surfaces are cut on Precambrian crystalline rocks as well as Pliocene valley fill and are capped by weathered gravels 1-5 m thick. To the south of Swift Trail Junction, these surfaces are just beginning to be dissected. Headward erosion by the Gila River tributaries has not progressed much beyond this point since the last major change in base level of the Gila River. The drive up AZ 366 crosses multiply dissected pediment surfaces that extend into the range to elevations of several thousands of feet above the valley floor. The shiny surfaces that extend from low in the range to several thousand feet above the valley floor are reflections from parting planes in the gneisses. Those that are lower down and to the west are in mylonitic rocks.

STOP 1

Take the left turn onto the dirt road at the first right-hand bend in AZ 366 at the mountain front (Figure 2). Park and walk up Jacobson Canyon to Johns Dam, the type locality for the gneiss of Johns Dam (JD gneiss), a unit to be formally named Johns Dam Gneiss by Thorman.

This stop provides an introduction to the Precambrian geology of the Pinaleno Mountains, as well as an introduction to the major lithologic units that are the protoliths to the mylonites along the range front to the west. The JD gneiss comprises two rock types that are interlayered on a mesoscopic to macroscopic scale: a porphyritic granodiorite unit intruded lit-par-lit on a grand scale into quartzofeldspathic gneisses. Individual layers of the granodiorite range from a few centimeters up to more than 30 m in thickness. The quartzofeldspathic gneisses, where not intruded by the porphyritic granodiorite, compose the gneiss of Pinaleno Mountains, which underlies most of the range and is the oldest unit observed.

The granodiorite is a medium-grained, biotite-rich rock with porphyroblasts of K-spar up to several centimeters in size. The typical rocks contain 62-65% SiO₂, with quartz, microcline, oligoclase-andesine plagioclase, biotite, epidote, and sphene. A prominent foliation and weak lineation were developed during intrusion and subsequent regional metamorphism, as can be seen at this locality where the rock has not been involved in subsequent deformation. This observation is important because where this lithology was caught in the mylonite zone, the strong foliation and lineation are commonly attributed solely to the mylonitic event without considering the previous state of the rock.

The gneiss of the Pinaleno Mountains includes a wide variety of lithologies, but the most common are quartz-two-feldspar-biotite, quartz-plagioclase-biotite, quartz-plagioclase-microcline-muscovite, quartz-two-mica-feldspar, and muscovite-bearing quartzite rocks. Compositional banding or layering of these rocks is on a scale of a few centimeters to a meter or more.

STOP 2

Proceed up the canyon on AZ 366 1.8 miles and take the dirt road to the right (Figure 2). Park at the sharp bend in the road at the rock wall.

At this stop the JD gneiss is weakly deformed. The rocks have been locally strongly folded and sheared, but the deformation is highly variable and not uniformly distributed. The mylonite-zone lower boundary, or "mylonitic front," can be seen at the

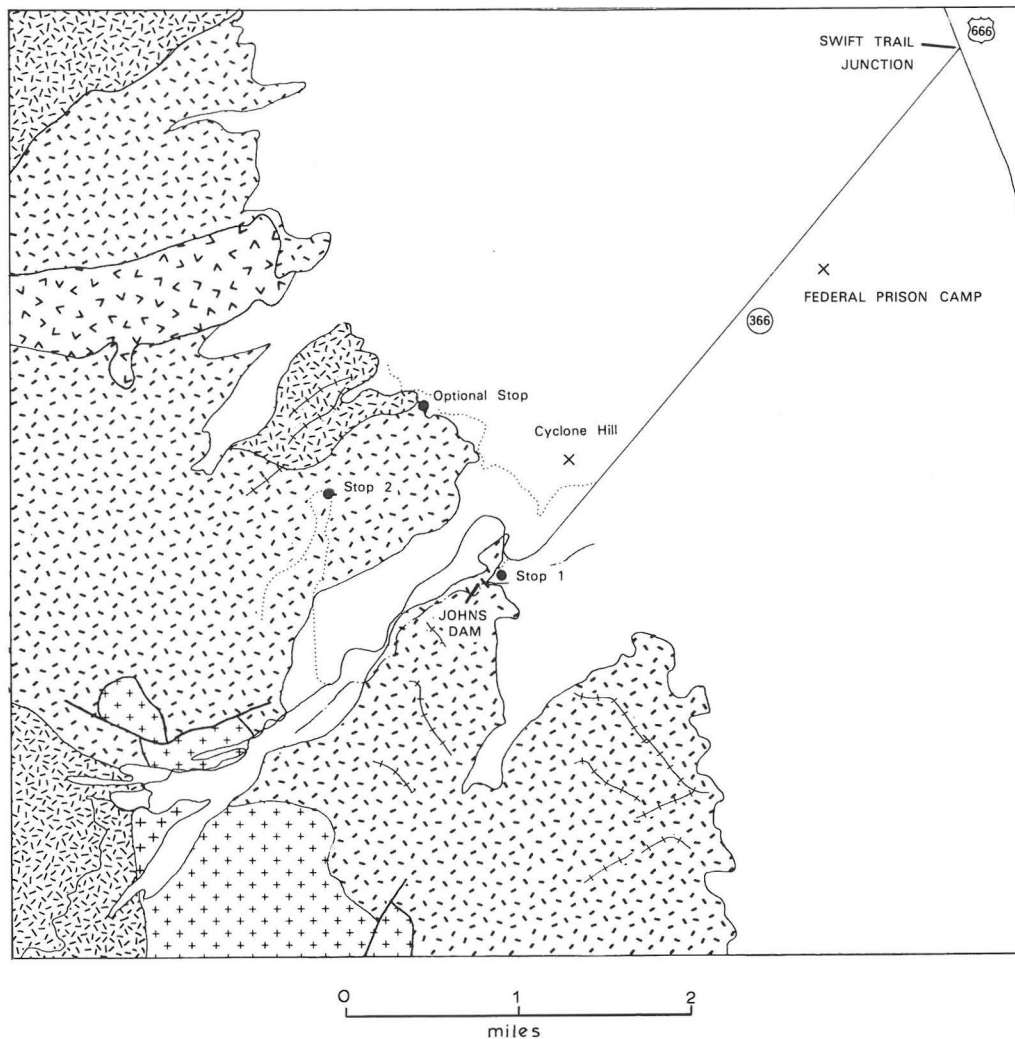


Figure 2. Generalized geologic map of the northeastern Pinaleno Mountains showing the field-trip route, stops 1 and 2, and the optional stop. The map units are Gneiss of the Pinaleno Mountains (heavy, dense chicken-track pattern); Gneiss of Johns Dam (light, less dense chicken-track pattern); Granite of Veach Ridge (+ pattern); Granite of Slick Rock (v pattern); and metarhyolite dikes (solid line with cross bars). All units are Proterozoic in age.

foot of this ridge to the northeast (about 3/4 mile), located near several small concrete buildings. The "front" dips to the northeast about 15°-25° and strikes northwesterly, projecting directly over us at this point. Only a few small patches of mylonitic rock have been observed on a couple of hills east of here.

In the prominent ridge approximately 3 miles to the northwest of here, the "front" is very well exposed on the eastern flank of Deadman Peak, the northernmost peak of the ridge. On the low northern side of the peak, pervasive mylonitic foliation in JD gneiss dips 20° northeast. The foliation terminates up-dip to the southwest, defining a 35°-northeast-dipping, gradational boundary with nonmylonitic JD gneiss like that at our feet.

OPTIONAL STOP

Return down the canyon towards Swift Trail Junction. Take the dirt road about 1.1 miles down the road (0.7 mile northeast of stop 1) and head west

around Cyclone Hill (Figure 2). About 1.5 miles from the pavement is a cement building behind a fence on the left side. Park outside the fence and walk southeast to a knob of JD gneiss.

Two things to be noted at this exposure are (1) the low knob of northeast-dipping, moderately to strongly mylonitic JD gneiss, and (2) the essentially undeformed JD gneiss that underlies the range and is strongly discordant to the mylonitic rocks. The small saddle separating the two outcrops marks the "mylonitic front." Unfortunately, the actual transition from nonmylonitic rocks to mylonite is not exposed. However, it is clear that the structural trend in the undeformed JD gneiss is obliterated by the mylonitic event.

GEOLOGIC HIGHLIGHTS EN ROUTE TO STOP 3

The Pinaleno mylonite-zone lower boundary is spectacularly exposed as a northeast-dipping, "Ramsay-and-Graham-type" simple-shear-zone boundary in Ash Creek Canyon near the end of the Ash Creek Canyon jeep

road (SE 1/4 sec. 3, T. 8 S., R. 24 E.; Figure 3). Four-wheel drive is required for at least the last 1/2 mile.

Follow US 70 from Safford to the town of Pima. Turn south on Main Street (mile 0). Make a right turn at 1.5 miles and a left turn at 2.0 miles onto National Forest Route 307. Proceed south to the Arizona Game and Fish Department Cluff Reservoirs at 6.0 miles. At 6.3 miles, take the left fork, passing Cluff Reservoir No. 1 on your right. At 7.4 miles, make a 90° left turn and proceed south, crossing Ash Creek at 8.7 miles. Continue south to National Forest foot trail 307 and the end of the jeep road at 10.0 miles.

STOP 3

The outcrops at stop 3 consist of mylonitic and nonmylonitic granite of White Streaks Canyon. The granite shows a remarkable range in composition that reflects its chemical evolution. The rock contains

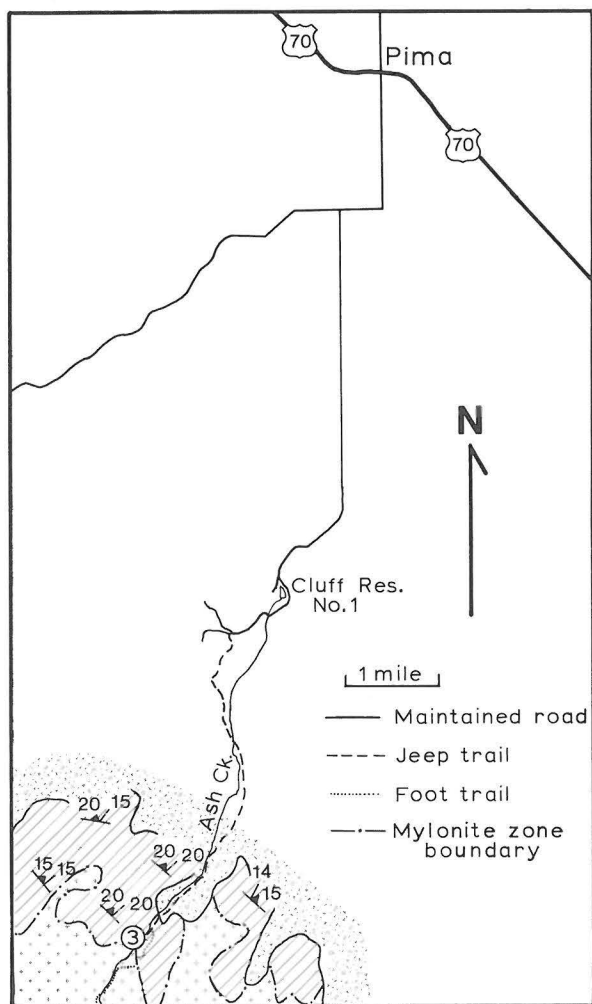


Figure 3. Generalized geologic map of Ash Creek Canyon, showing field-trip route and location of stop 3. Cross pattern represents nonmylonitic granite, granodiorite, and gneiss. Diagonally ruled pattern represents mylonites. Gravel pattern represents Quaternary-Tertiary gravels. Strike and dip symbols represent strike and dip of foliation (S-surfaces), and trend and plunge of lineation.

hornblende, biotite, and epidote in nearly all phases and ranges from 50-75% SiO₂ with the bulk of the unit having 65-75%. A systematic change in composition occurs in more than 15 elements and is reflected in the modal mineralogy of more than 25 samples.

Mylonitic fabrics are very well exposed in outcrops along the east side of the jeep road, in the creek itself, and on the slopes above the west bank of the creek (Figure 3). Pervasive foliation surfaces (S-surfaces) are defined by planar alignments of quartz ribbons, feldspar ribbons, and the long dimensions of feldspar porphyroclasts. Spaced shear surfaces (C-surfaces) are defined by the alignment of the asymmetric tails of the ribbons and porphyroclasts. A very well developed lineation is defined by extreme down-dip elongation of ribbons and porphyroclasts. The mylonite-zone lower boundary, or "mylonitic front," here strikes N60°W and dips 33°NE. In contrast, the S-surfaces here have a mean orientation of N55°W, 20°NE, and the lineations have an orientation of 19°, N50°E. The C-surfaces have a mean orientation of N56°W, 38° northeast.

The transition from mylonitic to nonmylonitic granite, the shear-zone lower boundary, is located approximately 200 m south of the end of the jeep road. Immediately south of the boundary, the granite is relatively undeformed. Macroscopically, the granite is cut by northeast-dipping, normal-slip, minor shear zones that parallel the mylonite-zone boundary. These zones are spaced on the order of a meter apart and have displacements on the order of a few centimeters. Although the granite contains a weak primary fabric (biotite-enriched bands) and a very weak, secondary, subhorizontal flattening fabric, it essentially retains a primary-igneous, xenomorphic-granular texture, in sharp contrast to the granite to the north. Quartz in this nonmylonitic granite exhibits undulose extension and no significant subgrain development. Ribbons, core-and-mantle structures, and mortar textures are not present. There is no kinking, fracturing, or preferential alignment of phyllosilicates or feldspars.

A clear overview of the shear-zone lower boundary can be obtained from the east side of Ash Creek Canyon. The boundary is apparent in the west wall of the canyon as a gradational contact between foliated granite to the north, and massive, unfoliated granite to the south. The contact clearly dips northeast. Furthermore, it clearly dips more steeply northeast than the foliation. Naruk (1986a) shows that this difference in attitude is a direct function of the simple-shear strain within the mylonite zone and that the shear strain can be calculated from this angle using the equations of Ramsay and Graham (1970).

GEOLOGIC HIGHLIGHTS EN ROUTE TO STOPS 4 AND 5

Upon returning to Highway 70 in Pima, head northwest to Glenbar. Approximately 3.5 miles west of Glenbar, turn left onto the road to Klondyke (Figure 1). As we drive southwest along this well-maintained secondary road, the Pinaleno Mountains mark the skyline to the left of the road and the Santa Teresa Mountains define the skyline topography to the right of the road. The pass between these two mountains is Eagle Pass.

Whereas the Pinaleno Mountains are composed of Precambrian crystalline rocks, the Santa Teresa Mountains contain mid-Tertiary quartz monzonitic plutonic rocks in addition to Proterozoic quartz monzonite and Pinal Schist. Pinal Schist in the Santa Teresa Mountains contains thick sequences of quartzite, which expresses itself in some of the skyline topography. The northeasternmost projection of the Santa Teresa

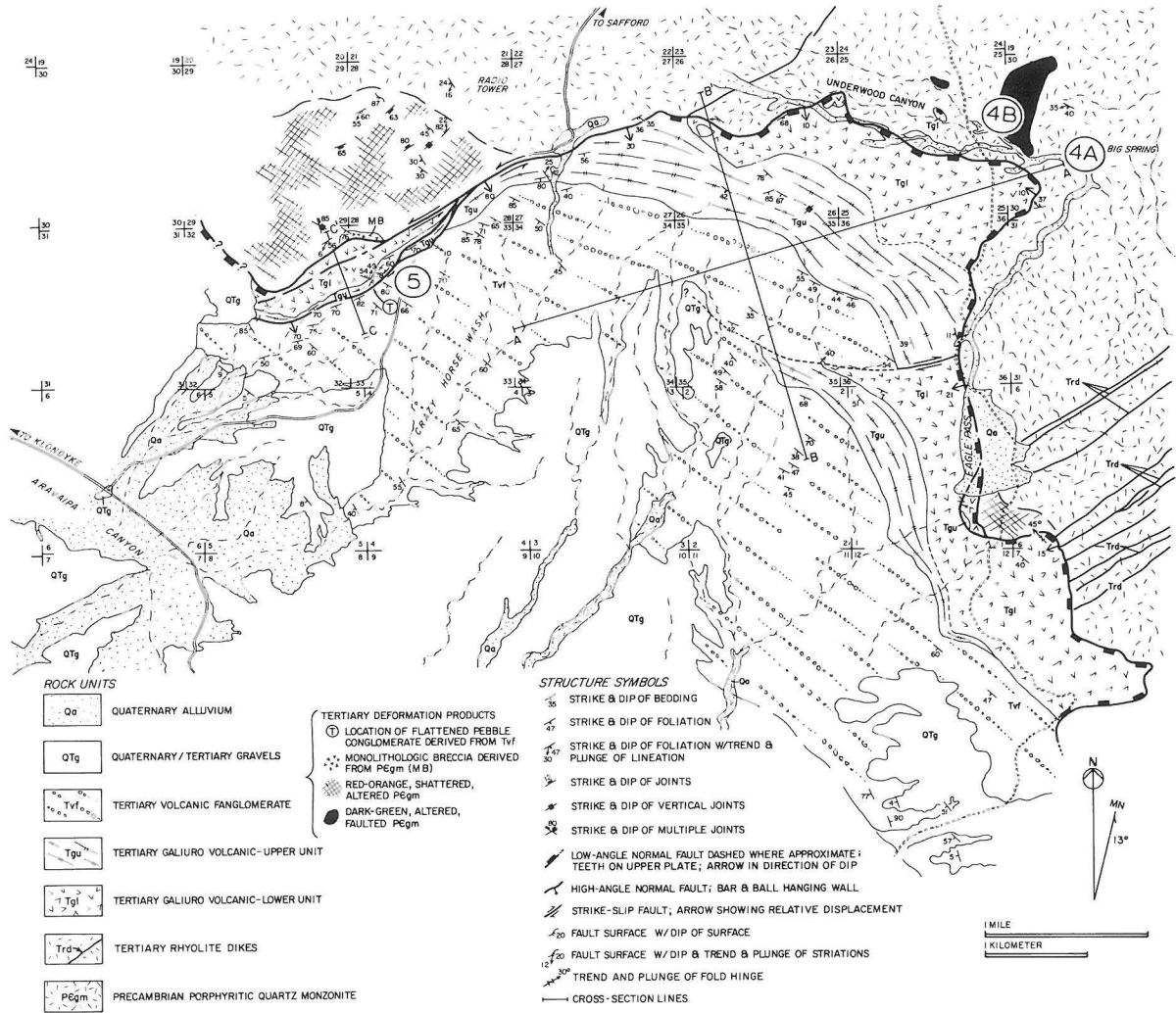


Figure 4. Geologic map of the Eagle Pass area (from Davis and Hardy, 1981), showing the locations of stops 4A, 4B, and 5.

Mountains is Jackson Mountain, a N40°E half-arch of strongly lineated mylonitic rocks that dip gently to moderately southeast. Indeed, this is a clear expression of the northern continuation of the Pinaleno Mountains shear zone. Quartzites of the Pinal Schist are transformed to a carapace containing splendid fold structures.

Climbing in elevation and nearing Eagle Pass, Proterozoic porphyritic quartz monzonite is well exposed in roadcuts and arroyo cuts. These outcrops lie beneath the shear-zone lower boundary. The rocks represent just one of the protoliths from which the mylonites were derived. In Eagle Pass proper, the presence of the quartz monzonite bedrock is expressed in ubiquitous grus and in the scattered occurrences of weathered bedrock in the form of great rounded "boulders of granite."

Within the broad expanse of Eagle Pass, it will become apparent that the western edge of the saddle is marked by a low ridge, one that is actually semicircular in its plan expression. This ridge contains Miocene volcanics and sedimentary rocks that compose the upper plate of the Eagle Pass detachment fault.

The tilted Miocene rocks rest in very low-angle fault contact on the Proterozoic quartz monzonite.

In order to see the Eagle Pass fault and the underlying footwall rocks of Proterozoic quartz monzonite, we will turn left from the Klondyke Road at the turnoff marked Camp Thomas Road. This turnoff is located approximately 17.2 miles from Highway 70. We will follow this National Forest service access road approximately 3.1 miles and then turn left down a broad sand wash lined with great oak trees (part of Underwood Canyon drainage).

STOP 4

Our structural location is in the immediate footwall of the Eagle Pass detachment fault (see Figure 4, sites 4A and 4B).

As is evident in Figure 4, the trace of the Eagle Pass detachment fault is quite sinuous. The form of the fault is that of a southwest-plunging irregular trough marked by millionlike asperities whose orientations are consistent with a NE/SW line of movement (Blacet and Miller, 1978; Davis and Hardy, 1981).

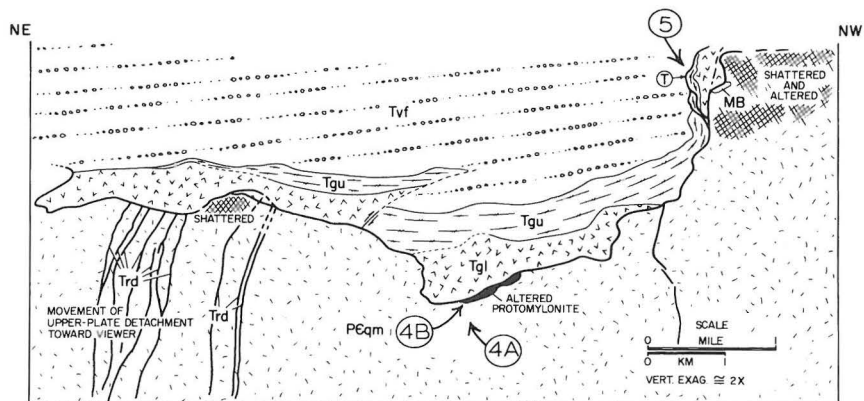


Figure 5. Down-plunge projection of Eagle Pass fault (from Davis and Hardy, 1981), showing locations of stops 4A, 4B, and 5.

Figure 5 describes the form of the fault in down-structure view, and portrays the locations of the stop 4 sites as points 4A and 4B. Clearly we are sitting in an unusual structural location!: in footwall quartz monzonite beneath the keel of an allochthonous "ship," many hundreds of kilometers thick, that moved 6–9 km northeast to its present location.

Stop 4A, near Big Springs and no more than 30 m beneath the detachment fault, features excellent exposures of Proterozoic porphyritic quartz monzonite. The quartz monzonite is not anomalously fractured, nor has it been microbrecciated or altered.

Stop 4B, on the other hand, is a clear expression of the structural transformation of the quartz monzonite directly beneath the keel of the detached upper-plate body. The porphyritic quartz monzonite is converted into a quasi-tabular, nearly horizontal zone of microbreccia, approximately 10 m thick. The quartz monzonite shows no signs of mylonitization. Instead, the mechanical response appears to have been exclusively brittle in nature and marked by extreme fracturing, microbrecciation, cataclasis, and ultracataclasis. Hydrothermal alteration of the shattered broken rock is extensive. Planar fracture surfaces, with or without striations, are commonly metallic gray or black in color and bound rocks that are themselves chloritically altered in hues of greenish-blue, ferruginous in hues of brown and orange, or heavily coated in black manganese stains. In comparison with other segments of the Eagle Pass detachment fault, this segment suggests that mechanical deformation of the quartz monzonite was unusually highly concentrated beneath the keel of the overriding upper-plate rocks and that unusually large volumes of hydrothermal fluids moved within the structural trough of the fault.

Whereas mineral lineations in the Pinaleno mylonites display a strongly preferred orientation (N40°E), the same cannot be said of the orientations of striae within the microbrecciated quartz monzonite. There is significant scatter in striae orientations, reflecting a complex internal movement plan. In contrast, mullionlike ridges and grooves in the microbrecciated quartz monzonite show a strongly preferred orientation of N40°E/S40°W, i.e., parallel to the mineral lineation in the nearby Pinaleno shear zone.

GEOLOGIC HIGHLIGHTS BETWEEN STOPS 4 AND 5

We now return to the Klondyke Road and continue driving southwest. Our route takes us into the hanging wall of the Eagle Pass detachment at a structural location that is both unusual and illuminating. Our route to stop 5 takes us into a northeast-striking, steeply dipping lateral ramp, the northwestern flank of the troughlike structure that characterizes the form of the Eagle Pass detachment (Figure 5).

Along this stretch of the fault the hanging-wall strata are dragged and sheared into parallelism with the lateral ramp. As a result, strata are northeast striking and nearly vertical, in dramatic contrast to the typical N50°W strike and moderate to steep SW dip of the hanging-wall stratigraphy (see Figure 5).

The normal stratigraphy consists of three major upper-plate units (Blacet and Miller, 1978; Davis and Hardy, 1981): from oldest to youngest, these are andesite, rhyolite, and fanglomerate. The andesite and rhyolitic rocks, taken together, are a part of the Galiuro Volcanics, approximately 28 to 22 Ma in age. These volcanic rocks in the Eagle Pass area are approximately 1500 m thick. The overlying fanglomerate composes a sequence in the hanging wall that is approximately 4500 m thick. It is composed of lahar deposits and mudflow breccias that are rich in boulders and cobbles of angular to subrounded andesite and rhyolite. The mid-Tertiary timing of the detachment faulting is obvious, given the Miocene age of hanging-wall strata and given the fault truncation of 25-m.y. dikes in the footwall (Rehrig and Reynolds, 1980).

Several observations are worth noting along the short drive to stop 5 (Figure 4). Where the road intercepts Crazy Horse Wash, cliff exposures on the left reveal a set of normal faults that have accommodated extension of marker units within the rhyolite. The effect is that of lozenge boudinage at a site approximately 20 m above the fault itself. Further toward stop 5, it becomes obvious that footwall quartz monzonite, exposed over a great expanse to the north of the road, is strongly altered to red and orange hues. The rock in which this alteration is so strong-

ly developed is very highly fractured and locally microbrecciated. These characteristics are yet additional expressions of the mechanical response of the quartz monzonite footwall to faulting and to the enormous infusion of hydrothermal solutions within the fractured rocks. Finally, as we move closer and closer to stop 5, we will see white resistant units within the rhyolite sequence progressively rotated to vertical. Polished fault surfaces, subparallel to the lateral ramp, are common within the rhyolitic rocks along this segment of the Eagle Pass fault.

STOP 5

To fully appreciate the expanse of hanging-wall rock in the Eagle Pass fault, and thus to more fully appreciate the Eagle Pass fault itself, we will first peer into Crazy Horse Wash to the southeast of the road. Exposed on the hillslopes and canyon walls are hundreds of meters of fanglomerate, dipping consistently at about 60°SW. These upper-plate strata dip in a direction opposite to the direction of tectonic transport. Far to the west on the skyline are the Galiuro Mountains, the structural provenance of the allochthonous rocks that now occupy Eagle Pass.

The strike of the fanglomerate units is N50°W, and it will be instructive to hike along strike to the northwest toward the vertical walls of rhyolite that loom to the northwest of the road. Exposures are near-perfect, and thus it is possible to examine the structural and petrological character of the fanglomerate as we hike. Within 20 m of the walls of rhyolite, strike-slip faulting is conspicuously displayed by horizontal striae on polished fault, fracture, and bedding surfaces in the rhyolite. Conjugate strike-slip faults offset lithologic layering in the rhyolite in such a way as to flatten the rock perpendicular to the northeast line of strike. The fanglomerate maintains its N50°W strike to within just a few tens of meters of the wall of rhyolite, at which point its bedding is dragged abruptly into parallelism with the lateral ramp. Within the zone of drag the fanglomerate is cut by abundant strike-slip shear zones. Pumice fragments within the fanglomerate are locally flattened and/or offset within the sheared rocks. Locally there is developed a true flattened pebble tectonite — in rock only 20 m.y. old!

Pressing further to the northwest beyond the walls of rhyolite, the lowest stratigraphic unit within the hanging-wall strata is exposed — namely the andesite, which at this location has been strongly deformed by the strike-slip movement. Beyond the andesite along "Drugstore Wash" to the northwest is the Eagle Pass fault contact with highly fractured and altered quartz monzonite footwall rock.

GEOLOGIC HIGHLIGHTS EN ROUTE TO WILLCOX FROM STOP 5

From stop 5 continue west on the Klondyke road approximately 3 miles to Aravaipa Road (mile 0). Turn left on Aravaipa Road and proceed southeast to Bonita at mile 22.8.

As discussed in the introduction, the mountains to the west of Aravaipa Road are the Galiuro Mountains, composed of flat-lying, 22- to 28-m.y.-old volcanics. The Galiuro range front is interpreted as the "breakaway" of the Eagle Pass detachment fault. The mountains to the east of the road are the Pinaleno Mountains. Gravity, magnetic, and well data indicate that the western front of the Pinaleno range, southeast of approximately mile 15, is a young high-angle fault (Drewes and others, 1985). Gravity and well data indicate that this northwestern part of the

Sulphur Springs Valley contains approximately 2000 feet of Cenozoic, coarse-grained alluvium and fanglomerate (Oppenheimer and Sumner, 1980; Drewes and others, 1985).

In Bonita, turn right on Fort Grant Road at mile 22.8 and take the left fork at mile 23.1. At 28.1 miles, make a 90° right turn, and at 28.4 miles make a 90° left turn. Proceed south to 34.4 miles. At 34.4 miles, make a 90° left turn and then make a 90° right turn at 34.5 miles. Continue tacking into Willcox, making a left turn at 37.4 miles, a right turn at 39.4, a left turn at 43.4, a right turn at 46.4, and a left turn at 51.4 miles.

GEOLOGIC HIGHLIGHTS BETWEEN WILLCOX AND STOP 6

Several notable geologic features will be evident during the course of our trip between Willcox and Tucson (Figure 1). During the first 10 miles out of Willcox, we will be driving along the northern edge of the Willcox Playa, the vestige of what once was Plio-Pleistocene Lake Cochise.

To the south-southwest of Willcox Playa lie the Dragoon Mountains. A mid-Tertiary granite pluton is very well exposed in the core of the range, where it intrudes Paleozoic and Mesozoic strata. The bold physiographic expression of the granite can be seen even from a great distance. The granite body is known as the Stronghold Granite (24 Ma), aptly named for Cochise's Stronghold, the box canyon hideaway for Apache Chief Cochise and his people.

Another spectacular granite body, the Texas Canyon stock (approximately 50 Ma), is exposed in the Dragoon Mountains near Johnson Camp and Dragoon. Interstate 10 passes right through it. Weathering and erosion of the corners of joint-bounded blocks of granite have created a landscape of "boulders" of granite and balanced rocks. Many scenes from the Lone Ranger adventure series were filmed in Texas Canyon.

West of Texas Canyon we will descend into the San Pedro Valley, observing as we travel the badlands topography created by erosion of Plio-Pleistocene sediments. Next we will pass just north of the Whetstone Mountains, which contain one of the structurally simplest sequences of Paleozoic strata in all of southern Arizona. To the north of the highway lie the southeasternmost Rincon Mountains.

We will exit Interstate 10 at Vail and cross the Rincon Valley, skirting the edge of the mountain and observing the gross geologic characteristics of the Rincons along the way. Upon entering Saguaro National Monument, we will stop briefly at the Visitors' Center before heading to our geologic stops.

The site that we will examine at Saguaro National Monument (Figure 6) is featured in the Centennial Field Guide to the 100 best field localities in the West (Davis, 1987b). The locality was featured during the Geological Society of America 1977 Penrose Conference on Cordilleran Metamorphic Core Complexes (Crittenden and others, 1980) and has served as the basis for distinguishing and classifying the structural characteristics of metamorphic core complexes (Davis, 1977, 1980; Davis and Coney, 1979). The geologic map of the Rincon Valley quadrangle (Drewes, 1977), which includes this site, is available for purchase at the Visitors' Center.

The purpose of this stop is to gain a clear picture of the fundamental components of metamorphic core complexes. The components here consist of mylonite and ultramylonite derived from Precambrian quartz monzonite; chloritically altered microbreccias derived from the mylonite and ultramylonite; fine-grained microbreccias (cataclasites and ultracataclasites) derived from the chloritically altered breccias; the

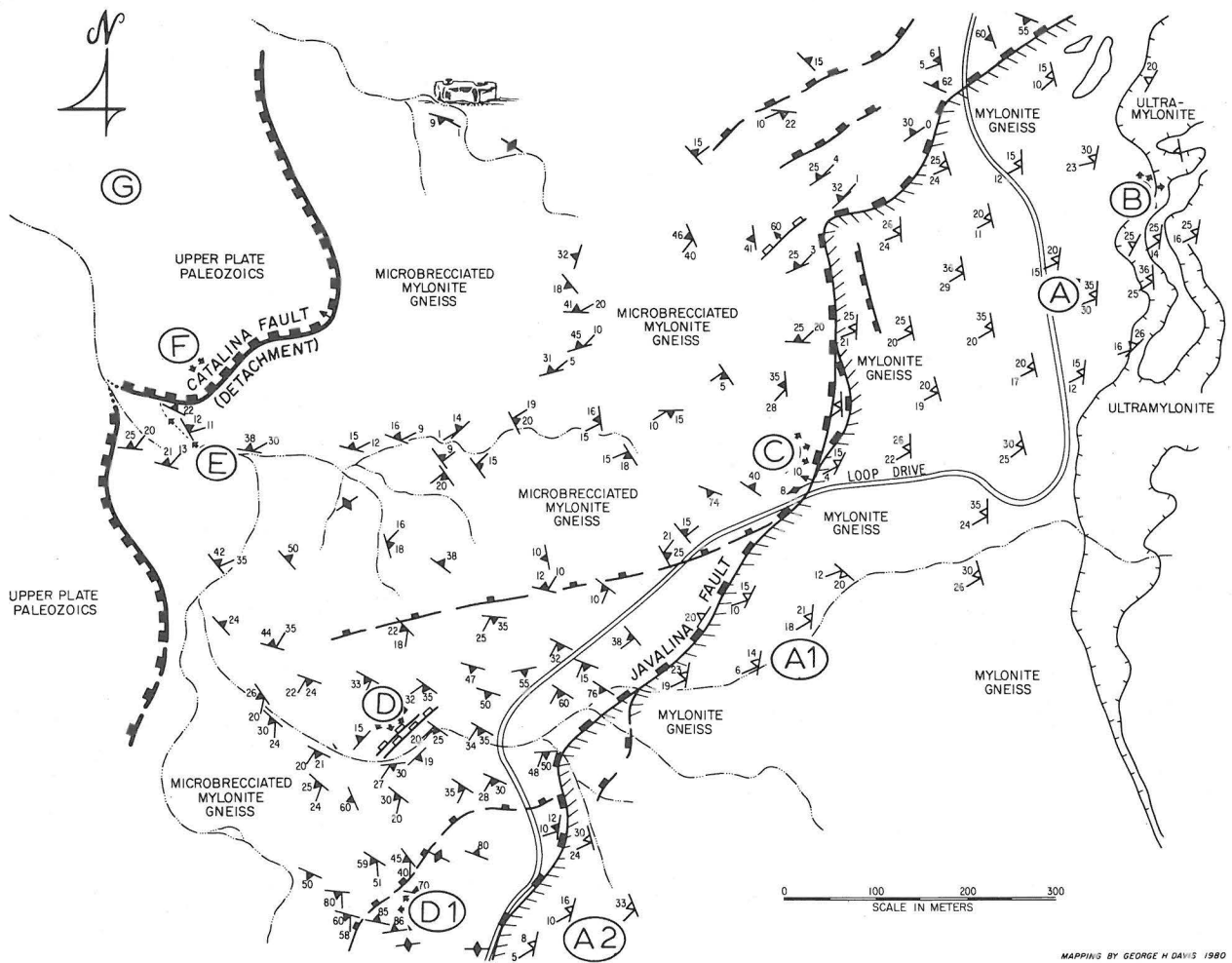


Figure 6. Structural geologic map of part of Saguaro Monument (from Davis, 1987b), showing the locations of stops A-C.

detachment fault (or décollement) separating cataclastic and mylonitic rocks below from nonmylonitic, non-cataclastic cover rocks above; and folded Paleozoic cover rocks.

According to Davis (1987a), the mylonites of the Rincon Mountains represent a mountain-size geologic exposure of the deep reaches of a ductile-brittle shear zone. Normal-slip simple-shear resulted in many kilometers of translation. Mylonites formed within the shear zone at a depth level of 10 km and more. The denudation that accompanied progressive simple-shear raised early-formed, deep-level mylonites through higher and higher structural levels. The mylonites thus experienced a progressive deformation (mylonitization through cataclasis to faulting along discrete surfaces), carried out under conditions of steadily decreasing temperature and confining pressure. The record of fault rocks and fabrics displays this history strikingly: mylonite gneiss composing the interior of the shear zone is transformed upward in microbrecciated mylonite gneiss, which in turn is converted to cataclasite (and even ultracataclasite) derived from microbrecciated mylonite gneiss. All of

this action was "simply" one form of accommodation to profound regional extension of the continental crust (Davis, 1987a).

STOP 6A

Stop 6A is located 4.8 miles from the start of the 9-mile, one-way Loop Drive.

Exposed here is coarse-grained mylonite gneiss with abundant augen of feldspar porphyroclasts. Protolith for the mylonite is Proterozoic quartz monzonite. Ribbon-quartz layers and laminae wrap around the feldspars in a gently undulating habit. Alignment of nonequidimensional feldspar porphyroclasts also contributes to the expression of the foliation. The strike of the foliation at this stop is north-south. The foliation dips gently, typically less than 30°, to the west. Mineral lineation is penetratively developed, trending N60°E. The relative orientations of foliation surfaces (S-surfaces) and C-surfaces indicate a top-to-the-southwest sense of shear.

STOP 6B

At this stop we will examine steel-gray to black ultramylonite, which composes a 5- 10-m-thick shear zone separating the coarse-grained mylonite gneisses derived from Precambrian quartz monzonite, and finer grained mylonite gneisses derived from Tertiary(?) garnet-mica quartz monzonite. Sense of shear in the ultramylonitic shear zone can be deduced in hand specimens on the basis of the orientations of mica fish, which are systematically inclined with respect to penetrative ultramylonitic foliation (fish-flash technique!). This ultramylonite shear zone can be traced as a discrete unit for many kilometers within the Rincon and Tanque Verde Mountains.

STOP 6C (5.1 mi along Loop Drive)

This stop highlights the Javalina fault, which separates mylonite and ultramylonite on the footwall (to the east) from chloritically altered brecciated mylonites on the hanging wall. The fault has the form of a gently dipping surface underlain by relatively highly fractured, hematite-stained mylonitic gneiss. To the east of the fault, the rocks are normal mylonite gneiss. To the west of the fault trace are brecciated, microbrecciated, and altered mylonitic gneisses. Alteration assemblages of chlorite, epidote, hematite, and manganese transform the fresh, light-colored, mylonite gneiss to the blue-green, fractured/brecciated counterparts.

STOP 6D

Some of the most graphic outcrop expressions of the brecciated and microbrecciated mylonitic gneisses are exposed at this stop. Where microbrecciation has been most intense, the average size of feldspar chips is only about 0.1 mm. Mapping the internal structural fabric of the brecciated and microbrecciated mylonitic rocks has revealed the presence of discrete, acre-size, fault-bounded blocks that have rotated with respect to one another. Overall, the relict foliation in the zone of breccia averages northwest, radically different from the north-northeast lines of strike that characterize the normal, nonmicrobrecciated mylonites nearby. The typical east-northeast lineation which characterizes nonbrecciated mylonites shifts to other orientations, notably more southerly. Locally relict foliation dips vertically, in stark contrast to the normal gentle dips of the nonbrecciated mylonites.

The zone of microbrecciation appears to have been produced by prolonged superposed faulting and fracturing under conditions of elevated fluid pressure (Davis and Coney, 1979). Although the microbrecciation, fracturing, and rotation of fabrics obviously post-dated the formation of the original mylonites, the structural movements that produced microbrecciation and rotational faulting seem to have been coordinated with the geometry of shearing that fashioned the mylonites. This is shown in part by the tendency of the strike of rotated relict foliation in the microbreccias to be aligned roughly at right angles to the trend of lineation in the footwall mylonites.

STOP 6E

Here we will examine the ledge of the cataclasite and ultracataclasite, which marks the very top of the zone of microbrecciated mylonite gneiss. The top surface of the ledge of cataclasite is the Santa Catalina fault, the major detachment fault of the Catalina-Rincon metamorphic core complex. The cata-

clasite has no directional fabric whatsoever, and the entire gently dipping, 4-m-thick tabular ledge is discordant to the moderately steeply dipping relict foliation in underlying microbrecciated mylonitic gneiss. The cataclasite formed at the expense of microbreccia in the late stages of the ductile-brittle shear.

STOP 6F

The Santa Catalina detachment fault marks the top of the cataclasite ledge. This outcrop of the fault is just a small part of the 70-km trace length of the fault, which follows the front of the Santa Catalina, Tanque Verde, and Rincon Mountains (Figure 1). Its form overall is that of a cylindrically folded surface plunging 15° to 30° west-southwest, parallel to the dominant direction of mineral lineation in the mylonite gneiss. Tectonic transport is hanging-wall to the west-southwest. The fault appears to be a low-angle normal-slip fault that helped accommodate crustal extension in mid-Tertiary time. Its hanging-wall contains faulted strata as young as 20 Ma. Cover rocks exposed above the fault were derived from sources more than 10 km to the northeast.

STOP 6G

This stop displays spectacularly folded Paleozoic strata, constituting some of the cover rocks that rest atop the Santa Catalina detachment fault. To the west, these Paleozoic strata are structurally overlain by Precambrian Pinal Schist.

REFERENCES CITED

- Blacet, P.M., and Miller, S.T., 1978, Reconnaissance geologic map of the Jackson Mountain quadrangle, Graham County, Arizona: U.S. Geological Survey Miscellaneous Field Studies Map MF-939, scale 1:62,500.
- Bykerk-Kauffman, A., and Janecke, S., 1987, Late Cretaceous to early Tertiary ductile deformation, Catalina-Rincon metamorphic core complex, southeastern Arizona: *Geology*, v. 15, p. 462-465.
- Coney, P.J., 1980, Cordilleran metamorphic core complexes; an overview, in Crittenden, M.D., Jr., and others, eds., *Cordilleran metamorphic core complexes*: Geological Society of America Memoir 153, p. 7-31.
- Creasey, S.C., Jackson, E.D., and Gulbrandsen, R.A., 1961, Reconnaissance geologic map of parts of the San Pedro and Aravaipa Valleys, south-central Arizona: U.S. Geological Survey Mineral Investigations Field Studies Map MF-238, scale 1:125,000.
- Creasey, S.C., Jinks, J.E., Williams, F.E., and Meeves, H.C., 1981, Mineral resources of the Galiuro Wilderness and contiguous further planning areas, Arizona: U.S. Geological Survey Bulletin 1490, 94 p.
- Creasey, S.C., and Krieger, M.H., 1978, Galiuro Volcanics, Pinal, Graham, and Cochise Counties, Arizona: U.S. Geological Survey Journal of Research, v. 6, p. 115-121.
- Crittenden, M.D., Jr., Coney, P.J., and Davis, G.H., 1980, Cordilleran metamorphic core complexes: Geological Society of America Memoir 153, 490 p.
- Davis, G.H., 1975, Gravity-induced folding off a gneiss dome complex, Rincon Mountains, Arizona: Geological Society of America Bulletin, v. 86, p. 979-990.
- _____, 1977, Characteristics of metamorphic core complexes, southern Arizona: Geological Society of America Abstracts with Programs, v. 13, p. 66.

- 1980, Structural characteristics of metamorphic core complexes, southern Arizona, *in* Crittenden, M.D., Jr., and others, eds., Cordilleran metamorphic core complexes: Geological Society of America Memoir 153, p. 35-77.
- 1983, Shear zone model for the origin of metamorphic core complexes: *Geology*, v. 11, p. 342-347.
- 1987a, A shear zone model for the structural evolution of metamorphic core complexes in southeastern Arizona: Geological Society of London Memoir on Continental Crustal Extension (in press).
- 1987b, Saguaro National Monument and its outstanding display of structural characteristics of metamorphic core complexes: Geological Society of America Centennial Field Guide (in press).
- Davis, G.H., and Coney, P.J., 1979, Geologic development of the Cordilleran metamorphic core complexes: *Geology*, v. 7, p. 120-124.
- Davis, G.H., Gardulski, A.F., and Anderson, T.H., 1981, Structural and structural-petrological characteristics of some metamorphic core complex terranes in southern Arizona and northern Sonora, *in* Ortleib, L., and Roldan, J.Q., eds., *Geology of northwestern Mexico and southern Arizona*: Instituto de Geologia, U.N.A.M., Hermosillo, Sonora, p. 323-365.
- Davis, G.H., and Hardy, J.J., Jr., 1981, The Eagle Pass detachment, southeastern Arizona; product of mid-Miocene listric(?) normal faulting in the southern Basin and Range: Geological Society of America Bulletin, v. 92, p. 749-762.
- Dickinson, W.R., Goodlin, T.C., and Mark, R.A., 1986, Low-angle normal-fault system along southwest flank of Galiuro Mountains in southeast Arizona: Geological Society of America Abstracts with Programs, v. 18, p. 101.
- Drewes, H., 1976, Laramide tectonics from Paradise to the Gates of Hell, *in* Wilt, J.C., and Jenney, J.P., eds., *Tectonic digest: Arizona Geological Society Digest*, v. 10, p. 151-168.
- 1977, Geologic map and sections of the Rincon Valley quadrangle, Pima County, Arizona: U.S. Geological Survey Miscellaneous Field Studies Map I-997, scale 1:48,000.
- 1978, The Cordilleran orogenic belt between Nevada and Chihuahua: Geological Society of America Bulletin, v. 89, p. 641-657.
- 1981, Tectonics of southeastern Arizona: U.S. Geological Survey Professional Paper 1144, 96 p.
- Drewes, H., Houser, B.B., Hedlund, D.C., Richter, D.H., Thorman, C.H., and Finnel, T.L., 1985, Geologic map of the Silver City 1° x 2° quadrangle, New Mexico and Arizona: U.S. Geological Survey Miscellaneous Investigations Series Map I-1310-C, scale 1:250,000.
- Drewes, H., and Thorman, C.H., 1981, Regional thrust faulting and the Rincon Mountains gneiss cored domes: Geological Society of America, Cordilleran Section Meeting, Road Log, p. 157-166.
- Keith, S.B., Reynolds, S.J., Damon, P.E., Shafiqullah, M., Livingston, D., and Pushkar, P.D., 1980, Evidence for multiple intrusion and deformation within the Santa Catalina-Rincon-Tortolita crystalline complex, southeastern Arizona, *in* Crittenden, M.D., Jr., and others, eds., *Cordilleran metamorphic core complexes: Geological Society of America Memoir 153*, p. 217-267.
- Miller, E.L., Gans, P.B., and Garing, J., 1983, The Snake Range Décollement; an exhumed mid-Tertiary ductile-brittle transition: *Tectonics*, v. 2, p. 239-263.
- Naruk, S.J., 1986a, Strain and displacement across the Pinaleno Mountains shear zone, Arizona, USA: *Journal of Structural Geology*, v. 8, p. 35-46.
- 1986b, Finite strains and mylonitic fabrics in the Santa Catalina metamorphic core complex, southeastern Arizona: Geological Society of America Abstracts with Programs, v. 18, p. 163.
- 1987, Displacement calculations across a metamorphic core complex mylonite zone; Pinaleno Mountains, southeastern Arizona: *Geology*, v. 15 (in press).
- Oppenheimer, J.M., and Sumner, J.S., 1980, Depth-to-bedrock map, Basin and Range Province, Arizona: University of Arizona, Laboratory of Geophysics, scale 1:1,000,000.
- Ramsay, J.G., and Graham, R.H., 1970, Strain variation in shear belts: *Canadian Journal of Earth Sciences*, v. 7, p. 786-813.
- Rehrig, W.A., and Reynolds, S.J., 1980, Geologic and geochronologic reconnaissance of a northwest-trending zone of metamorphic core complexes in southern and western Arizona, *in* Crittenden, M.D., Jr., and others, eds., *Cordilleran metamorphic core complexes: Geological Society of America Memoir 153*, p. 131-157.
- Simons, F.S., 1987, Geologic map of the Black Rock Wilderness Study Area, Graham County, Arizona: U.S. Geological Survey Miscellaneous Field Studies Map MF-XXX, scale 1:24,000 (in press).
- Simons, F.S., Theobald, P.K., Tidball, R.R., Erdman, J.A., Harms, T.F., Griscom, A., and Ryan, G.S., 1987, Mineral resources of the Black Rock Wilderness Study Area, Graham County, Arizona, *in* Mineral resources of wilderness study areas -- southeastern Arizona: U.S. Geological Survey Bulletin 1703-C (in press).
- Spencer, J.E., 1984, Role of tectonic denudation in warping and uplift of low-angle normal faults: *Geology*, v. 12, p. 95-98.
- Thorman, C.H., 1977, Discussion of 'Gravity-induced folding off a gneiss dome complex, Rincon Mountains, Arizona': Geological Society of America Bulletin, v. 88, p. 1211-1212.
- 1981a, Road log and trip guide to the geology of the northern flank of the Pinaleno Mountains, southeastern Arizona: Arizona Geological Society, Field Trip 3, 21 p.
- 1981b, Geology of the Pinaleno Mountains, Arizona; a preliminary report: Arizona Geological Society Digest, v. 13, p. 5-12.
- Thorman, C.H., Drewes, H., and Lane, M., 1981, Mineral resources of the Rincon Wilderness Study Area, Pima County, Arizona: U.S. Geological Survey Bulletin 1500, 62 p.
- Wernicke, B., 1985, Uniform-sense simple shear of the continental lithosphere: *Canadian Journal of Earth Science*, v. 22, p. 108-125.



Pinto Valley Copper Deposit

Richard A. Breitrick and Gary W. Lenzi
 Pinto Valley Division, Magma Copper Company
 P.O. Box 100
 Miami, Arizona 85532

PURPOSE

This tour will show the principal features of the Pinto Valley porphyry copper deposit (Figures 1 and 2), and emphasis will be placed on the effects of hydrothermal alteration and accompanied sulfide mineralization. Examples of vein-controlled and pervasive alteration will be seen. The deposit shows the effects of Laramide intrusion and alteration on Precambrian quartz monzonite host rocks.

GEOLOGIC SUMMARY OF THE PINTO VALLEY PORPHYRY

Copper Deposit

Host rock for the Pinto Valley porphyry copper deposit is the Precambrian Lost Gulch Quartz Monzonite,

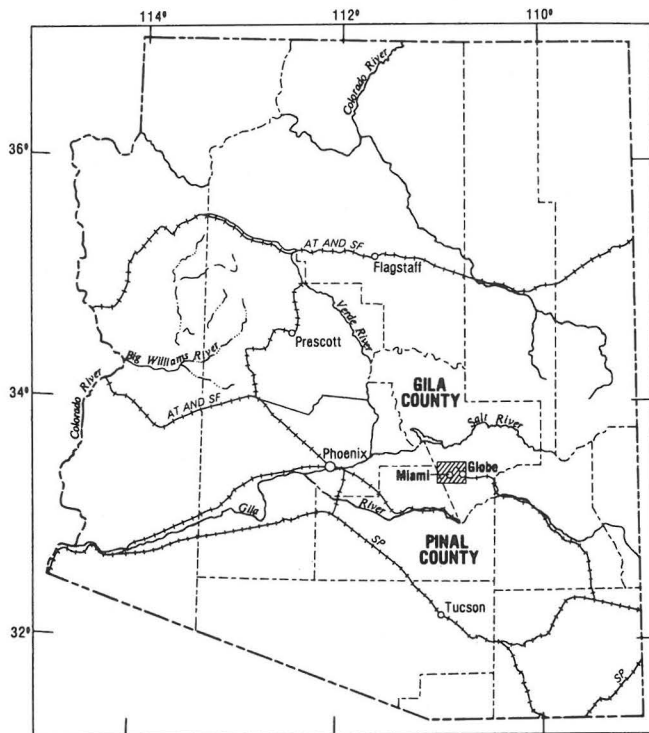


Figure 1. Location of the Globe-Miami district, Arizona (Creasey, 1980).

which is equivalent to the Ruin Granite. Formation of the deposit was associated with the intrusion of small bodies and dikes of granite porphyry and granodiorite, whose ages are about 61.2 Ma. Copper mineralization has been dated at 59.1 Ma. (Creasey, 1980). There is evidence to suggest that the original configuration of the copper zone was that of a distorted inverted bowl with its long axis striking approximately N.80°E., and with the ore shell surrounding a low-grade core. As presently defined, the deposit is bounded by post-mineral faults. On the south is the South Hill fault,

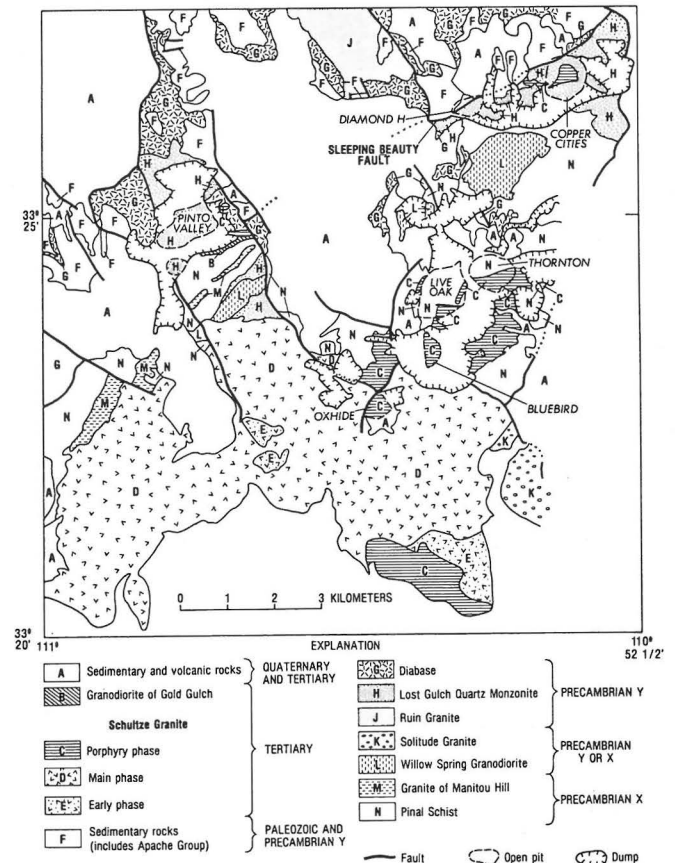


Figure 2. Generalized geology of the western part of the Globe-Miami district, Arizona (Creasey, 1980).

on the east is the Jewel Hill fault, and on the west is the Gold Gulch fault (Figure 3). Minor postmineral normal displacement has taken place on the Dome fault, a premineral structure that strikes northeasterly across the north limb of the deposit.

Primary sulfide mineralization consists of pyrite, chalcopyrite, and minor molybdenite that occur in veins and microfractures, and less abundantly as disseminated grains predominantly at biotite sites. The ore zone grades outward into a pyritic zone with higher total sulfide content and grades inward toward the low-grade core having lower total sulfides. Molybdenum distribution generally reflects copper distribution, with higher molybdenum values usually found in the high-grade copper zones.

The Pinto Valley deposit has all of the major alteration features associated with most porphyry copper systems hosted by a monzonitic intrusion. The most prominent is a selectively pervasive argillic hydrothermal alteration that permeated the mineral deposit and is characterized by the alteration of plagioclase to montmorillonite. Phyllic alteration is vein controlled, occurring as sericitic selvages along quartz-sulfide veins, and is most strongly developed in the pyritic halo outside and above the ore zone. Potassic alteration grades from early, narrow zones of texture-destructive alteration into a broader zone of hydrothermal biotite. Narrow zones of early texture-destructive sodic-potassic alteration, characterized by the replacement of both original orthoclase and oligoclase by fine granular K-feldspar and albite, are restricted to the low-grade core. This earliest alteration type evolved into widespread potassic hydrothermal biotite alteration characterized by the introduction of biotite along joints and microfractures and the recrystallization of original biotite to fine-grained "felty" biotite (the aggregate biotite of Peterson and others, 1951).

The Pinto Valley deposit is a hypogene orebody with chalcopyrite, pyrite, and minor molybdenite as the only significant primary sulfide minerals. A chalcocite-enriched zone was mined from 1943 through 1953 (Castle Dome mine) and produced 41 million tons of ore having an average grade of 0.62% copper. Pinto Valley ore reserves as of March 1986 were 354 million tons averaging 0.40% copper (Newmont Mining Corp., 1986). Total ore mined from the beginning of production in July 1974 through October 1986 was 172 million tons. The average molybdenum content of the ore for the 7-year period from 1975 through 1981 was 0.01% Mo.

STOP 1

This outcrop of Precambrian Lost Gulch Quartz Monzonite is on the outer edge of the propylitic zone. Porphyritic quartz monzonite occurs north of the saddle, and quartz monzonite porphyry lies to the south. Both are intruded by Precambrian aplite. This exposure is about 1300 feet northwest of exposures of good vein-controlled phyllic alteration and is about 1600 feet north of the northern limit of 0.3% copper mineralization.

Propylitic alteration is fracture controlled and has produced an array of associated veins and microveins that differ mineralogically with respect to both vein filling and alteration selvage mineralogy. Prominent among the minerals produced during propylitic alteration as vein fillings and alteration products are clinozoisite, epidote, quartz, adularia, pennite, and primary chlorite. Anhydrite, pyrite, and chalcopyrite occur in trace amounts. Propylitic veins that carry trace amounts of sulfides were accompanied by weak sericitic alteration in the adjacent oligoclase phenocrysts. Propylitic alteration was most strongly

developed as an outer halo to the deposit; however, propylitic microveins also extend sparingly into the copper zone.

Chlorite-altered hydrothermal biotite microveins are present in the 6-foot by 10-foot vertical face on the west edge of the outcrop. This is the only occurrence of hydrothermal biotite alteration in the outcrop and is the furthest known occurrence of hydrothermal biotite north of the mine. No biotite has been found in any of the propylitic veins or any of their alteration selvages. However, sparse microveins containing both biotite and epidote have been found in a single drill hole located closer to the mine, providing evidence that potassic (biotite) alteration and propylitic alteration were at least partially synchronous.

Note that the microvein density is very low. Epidote and K-feldspar + quartz + chlorite microveins are common and locally abundant. Note the pale pink planar faces on many of the boulders and in the outcrop, which exposes one of the more common propylitic veins. They are open fractures coated with pink to white euhedral adularia, quartz, chlorite, and sparse oxidized pyrite cubes. Some also contain minor epidote and(or) clinozoisite.

Weak to incipient pervasive argillic alteration of the plagioclase is also present. Most of the plagioclase phenocrysts are a cloudy white to buff color, but unaltered glassy, clear phenocrysts are present, usually in clusters.

GEOLOGIC HIGHLIGHTS EN ROUTE TO STOP 2

The route will proceed south within the pyrite-rich upper levels of the mineral deposit. The prominent vein set is composed of phyllic veins. These pyrite-rich veins have strong sericitic selvages, which replace the main minerals except quartz. They form a set that strikes east-northeast and dips to the southeast. Integrated fracture density on upper levels is less than 0.13 cm⁻¹. Isolated areas of chalcocite enrichment can be seen.

The Paleozoic limestone cliffs to the east form Jewel Hill. At the base of the hill, the West Jewel Hill fault has displaced the east end of the orebody. The limestones have only a few thin replacement beds of garnet skarn and an oxidized "magnetite" skarn. Copper mineralization did not extend into the limestone.

Precambrian diabase is the dark-gray rock exposed south of the Dome fault. It has been intruded by a small stock of granite porphyry. Both rock types contain pyrite and very little chalcopyrite.

STOP 2

This stop is a walk-through along the east side of the road. The exposures are within the weathered and oxidized pyrite halo and about 300' above the top of the primary orebody (see cross section C-C', Figure 4). Chalcocite enrichment is preserved within the gray exposures near the bottom of the face. The reddish-brown limonite surrounding it is characteristic of oxidized chalcocite, which has been a diagnostic tool used in exploration for porphyry copper deposits. Alteration present is pervasive argillic and vein-controlled phyllic. From south to north the rock types are granite porphyry, quartz monzonite porphyry, rhyolite intruding quartz monzonite porphyry, quartz monzonite, small dikes of aplite, alaskite porphyry, and diabase. The quartz monzonite, quartz monzonite porphyry, aplite, and alaskite porphyry are all phases of the Lost Gulch Quartz Monzonite and are dated at 1415 Ma. (Creasey, 1980). The diabase has an

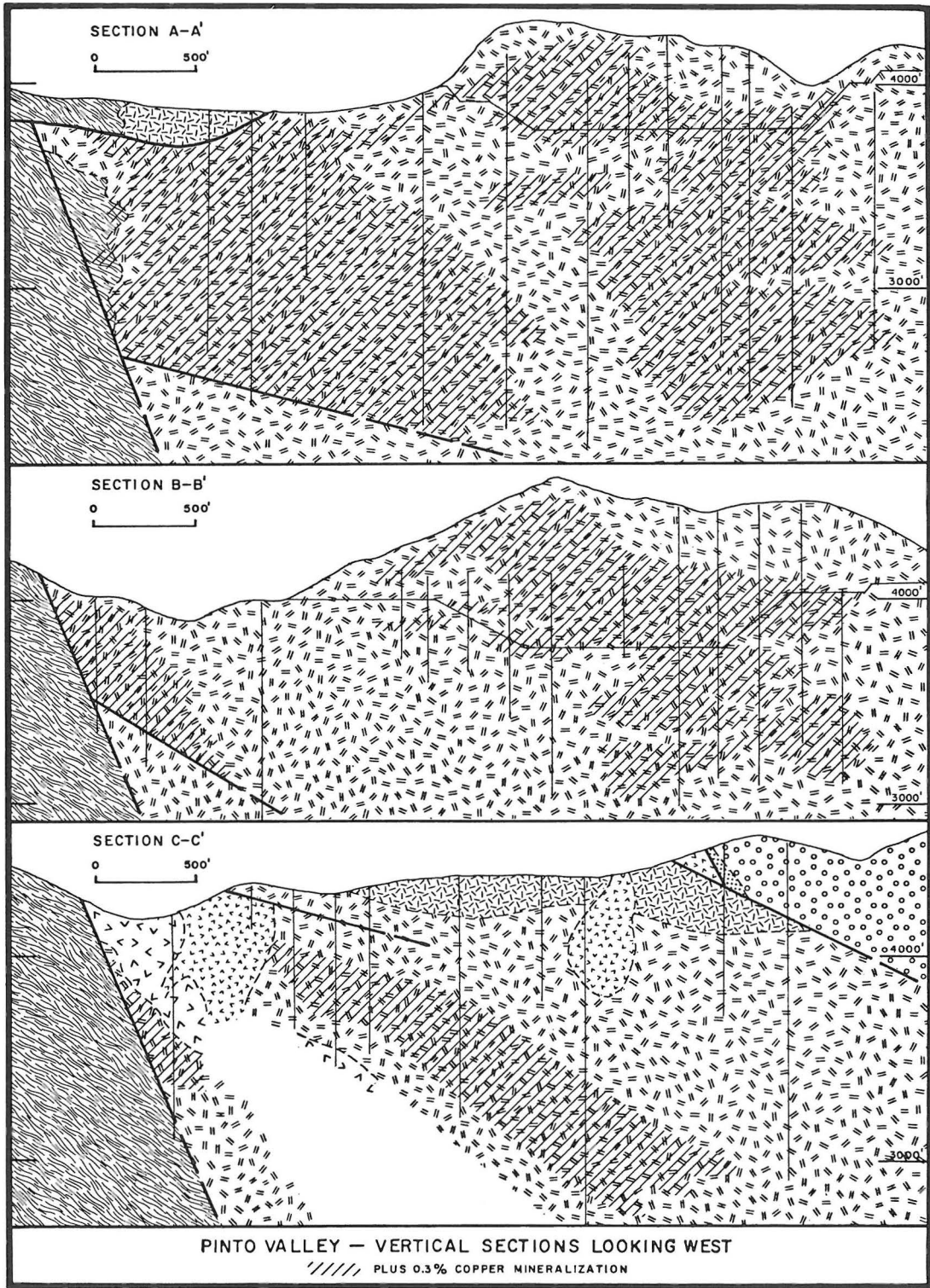


Figure 4. Pinto Valley vertical cross sections looking west.

age of 1079 Ma. Rhyolite is related to granite porphyry.

Granite porphyry is a phase of the Schultze Granite. It is distinguished by its clear, euhedral quartz eyes, altered plagioclase, pink orthoclase phenocrysts, and fine-grained biotite in a microcrystalline groundmass. The phenocrysts of biotite and pink orthoclase are fewer than those of plagioclase and quartz. Orthoclase phenocrysts are generally much larger than the others. Its contact with quartz monzonite porphyry is sharp and several veins can be seen cutting the contact. Granite porphyry is associated with economic mineralization at Pinto Valley, Copper Cities, and Old Dominion vein area, and the Cactus breccia. It has a lower sulfide content than the quartz monzonite porphyry. In several drill holes, the ore boundary is found at granite porphyry-quartz monzonite porphyry contacts with ore in the quartz monzonite porphyry. Beginning 300 feet below the surface the quartz monzonite porphyry averages 0.453% copper, whereas the adjacent granite porphyry only averages 0.128%.

The quartz monzonite porphyry contains altered phenocrysts of oligoclase, quartz, and biotite that are much larger than phenocrysts in the granite porphyry. It also contains pink to reddish-brown orthoclase phenocrysts that range from 1 to 3 inches in size. The finer grained groundmass is composed of quartz and orthoclase in varying amounts and crystal sizes.

Near the top of the road cut, a one-foot thick aphanitic diabase dike intruded the quartz monzonite porphyry.

Rhyolite is the white aphanitic rock with rare, small quartz phenocrysts. It has both normal and faulted contacts. Other exposures of rhyolite show that it is an aphanitic phase of granite porphyry.

The contact between quartz monzonite porphyry and quartz monzonite is occupied by a thin aplite dike. Quartz monzonite looks like quartz monzonite porphyry except that groundmass is absent. Plagioclase, quartz, and biotite occur in a nearly equigranular texture with larger orthoclase phenocrysts.

Within the quartz monzonite is a small dike of alaskite porphyry. It has the same mineral composition as aplite with a few phenocrysts of quartz, oligoclase, biotite, and rare orthoclase.

GEOLOGIC HIGHLIGHTS EN ROUTE TO STOP 3

On the way to stop 3, we pass outcrops of granodiorite, which is believed to be cogenetic but slightly older than granite porphyry. This area is within the central low-grade core of the deposit. The hill to the south is composed of unmineralized Precambrian Pinal Schist. The South Hill fault separates mineralized granodiorite and quartz monzonite from unmineralized schist, and has removed about one-third of the original deposit (>0.3% copper). A low-angle fault has displaced schist to the north at the nose near the road. This fault block overrode the South Hill fault and can be seen in dozer cuts where gray schist overlies tan granodiorite and quartz monzonite.

STOP 3

At this stop we can see some wall-rock control of mineralization in an area of typical ore. The average grade of quartz monzonite porphyry is about 0.4% Cu. Mineralization occurs mainly as narrow veinlets of quartz, chalcopryite, and pyrite, but sulfides are also disseminated in biotite sites. An aplite dike intruding the quartz monzonite porphyry averages 0.2% copper forming a zone of internal waste. Veining can be seen in the aplite at about the same density as in

quartz monzonite porphyry (0.2-0.3 cm-1). The lower copper grade in the aplite is probably due to the lack of biotite, which some observers suggest provides iron for the precipitation of copper.

The principal alteration within the orebody is argillic, or as Peterson and others (1951) described it, clay alteration. The main feature of this alteration is the replacement of oligoclase phenocrysts by a slightly yellowish to greenish clay that Peterson and others identified as beidellite. It is due to hydrothermal alteration and is not simply a supergene effect as has been suggested by some to account for the type of alteration at other porphyry copper deposits.

Some of the sulfide veins, particularly the more pyrite-rich veins, have sericite selvages. These phyllic veins are less abundant here than they were on the upper levels. Peterson and others (1951) give evidence that at least some of the sericite may be older than the clay alteration. Because clay alteration is selectively pervasive and not vein controlled, crosscutting relationships between the argillic alteration and phyllic veins cannot be established.

Attempts were made to establish the age of copper versus molybdenum mineralization. Both metallic phases precipitated in veins that cut one another. Generally there are more chalcopryite-bearing veins cut by molybdenite-bearing veins than vice versa. Mineralization may have formed from repeated pulses of fluids that began as copper precipitating and evolved into molybdenum precipitating.

Attitudes of veins were also taken. Figure 5 is a histogram showing the distribution of 1214 veins

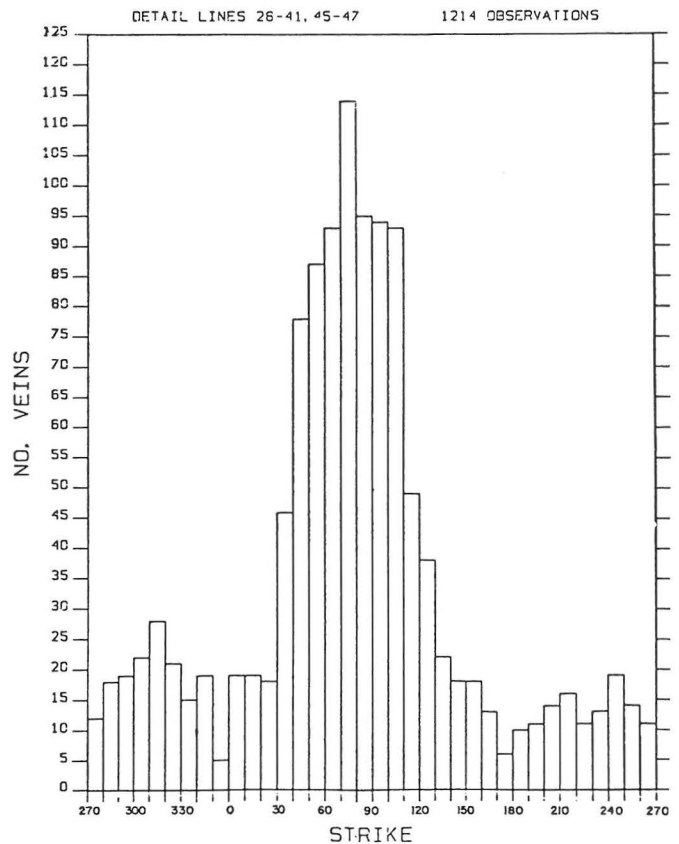


Figure 5. Histogram of number of veins versus strike direction at Pinto Valley.

according to strike direction. All veins were measured with dip to the right of the strike direction. The diagram shows a strong, nearly easterly striking, vein set and minor sets at 325° and 240°. These sets were also reported by Peterson and others (1951).

STOP 4

Several alteration types and rock types will be seen here. Argillic alteration is seen at the top of the ramp in quartz monzonite. At the quartz monzonite/quartz monzonite porphyry contact, texture-destructive sodic-potassic alteration is exposed and is cut by biotite veining to the west.

Formation of the deposit began with sodic-potassic alteration starting with the introduction of K-feldspar and albite, which evolved into hydrothermal biotite alteration. The transition from the early phase to the later phase was gradational. In the early phase orthoclase phenocrysts were replaced by granular K-feldspar and minor albite, and oligoclase phenocrysts were altered to albite and partially replaced by granular K-feldspar. During the hydrothermal biotite phase, orthoclase was stable, igneous biotite was recrystallized to clots of fine-grained "felty" biotite, and hydrothermal biotite was introduced along joints and microfractures. Locally hydrothermal biotite was also finely disseminated in the oligoclase phenocrysts, which continued to be altered to albite during the early stage of hydrothermal biotite alteration. The early sodic-potassic altera-

tion was restricted to the low-grade core, and its occurrence at present levels of exposure and in the drill-hole intercepts is limited to relative narrow linear zones. Hydrothermal biotite alteration was much more extensive and was described by Peterson and others (1951) in the Castle Dome deposit.

Following potassic alteration, granodiorite was intruded at about the same time that barren quartz veins were formed in the host rock. Granite porphyry was then emplaced with accompanying igneous intrusive breccias during early stages of granite porphyry emplacement. Various sulfide-bearing veins followed the intrusions of granodiorite, granite porphyry, and igneous breccias.

A narrow dike of porphyritic monzonite without quartz phenocrysts can be seen, which is highly altered by hydrothermal biotite. Intense zones of hydrothermal biotite veining form biotite breccias, which are common for several hundred feet to the west in quartz monzonite porphyry.

REFERENCES

- Creasey, S.C., 1980, Chronology of intrusion and deposition of porphyry copper ores, Globe-Miami district, Arizona: *Economic Geology*, v. 75, p. 830-844.
- Newmont Mining Corp., 1986, Company report.
- Peterson, N.P., Gilbert, C.M., and Quick, G.L., 1951, Geology and ore deposits of the Castle Dome area, Gila County, Arizona: U.S. Geological Survey Bulletin 971, 134 p.

Tectonic Setting and Sedimentological Features of Upper Mesozoic Strata in Southeastern Arizona

William R. Dickinson and Margaret A. Klute
Department of Geosciences
University of Arizona
Tucson, Arizona 85721

William L. Bilodeau
Department of Geology
University of Colorado at Denver
1100 14th Street, Denver, Colorado 80202

INTRODUCTION

Late Mesozoic geologic relations in southern Arizona forged a tectonic linkage between the Cordilleran orogenic belt along the Pacific fringe of the continent and the rift system of the Gulf of Mexico in the Caribbean region. Upper Mesozoic lithotectonic assemblages have affinities both with magmatic arcs of the circum-Pacific and with the Atlantic-related sedimentary prism of the Gulf Coast. The fundamental purpose of this trip is to examine aspects of the Cordilleran-Caribbean connection.

The field trip will focus on the geotectonic setting and sedimentological features of the Bisbee Group and its local correlatives as exposed in seven mountain ranges of southeastern Arizona, but will also visit exposures of key underlying and overlying units (Figures 1 and 2). Lower Cretaceous correlatives of the Bisbee Group extend laterally to the Gulf Coast, whereas underlying and overlying volcanogenic units reflect magmatism related to subduction of oceanic lithosphere along the Pacific margin.

TECTONIC HISTORY

Overall geologic relations in southeastern Arizona have been discussed by Drewes (1980, 1981) and references he cites. We here interpret the Mesozoic geologic history of the region in terms of five successive tectonostratigraphic phases as follows:

(1) Dominantly Early Jurassic (but perhaps also Late Triassic and Middle Jurassic) arc volcanism and associated plutonism; local intercalations of wind-blown quartzose sand were derived from an extensive mid-Mesozoic erg lying farther north in the region of the present Colorado Plateau.

(2) Middle to Late Jurassic eruption of widespread silicic ignimbrites and local emplacement of associated granitic plutons along an intra-arc to back-arc rift belt, which was connected spatially through the Chihuahua trough with new ocean floor generated by seafloor spreading in the Gulf of Mexico.

(3) Late Jurassic to Early Cretaceous syntectonic sedimentation of the basal conglomeratic phase of the Bisbee Group in grabens or half-grabens, and calderas or other volcano-tectonic depressions; locally intercalated lavas and ignimbrites represent waning phases of rift-related magmatism.

(4) Early to mid-Cretaceous sedimentation of fluvial, lacustrine, strandline, and marine facies of the Bisbee Group during passive thermotectonic subsidence of stretched crust beneath the extensional

Bisbee basin, which was a distal rift arm of the Gulf of Mexico structural depression far to the southeast; Aptian-Albian marine transgression connected the Bisbee basin to the marine Gulf of Mexico.

(5) Late Cretaceous contractional deformation, continuing into Paleogene time and accompanied by gradual renewal of arc magmatism, produced Laramide successions of dominantly conglomeratic nonmarine sediments, which were deposited in local basins and are associated with or overlain by widespread volcanogenic sequences.

BISBEE GROUP AND BISBEE BASIN

The geotectonic setting and facies framework of the Bisbee Group have been reviewed by Hayes (1970b), Bilodeau and Lindberg (1983), Mack and others (1986), and Dickinson and others (1986, 1987). The Bisbee basin was a structural depression at the northwest extremity of the Chihuahua trough, a rift arm of the Gulf of Mexico. Marine faunas in the medial Bisbee Group have clear affinities with those in correlative strata of the Texas Gulf Coast.

Exposures of the Bisbee Group in Arizona can be divided into northwestern and southeastern facies, for which different formational names are used for strata above the basal Glance Conglomerate (Figure 3). Aptian-Albian marine faunas in the Mural Limestone and associated strata of the southeastern facies provide the only firm biostratigraphic control for the age of the sequence in Arizona and date the time of maximum marine transgression within the Bisbee basin. Strata of the northwestern facies are entirely nonmarine except for one oyster-bearing horizon apparently correlative with the Mural Limestone (Archibald, 1982).

Sandstone petrofacies within the Bisbee Group include three distinctive types as well as a transitional petrofacies (Figure 4): (a) quartzose petrofacies derived from the craton to the northeast or recycled from cratonal Paleozoic strata is present throughout the southeastern facies (both Morita and Cintura Formations) and in the upper northwestern facies (Turney Ranch Formation); (b) arkosic petrofacies derived from uplifted basement exposed in local fault blocks or in the Mogollon highlands of central Arizona characterizes the lower northwestern facies (Willow Canyon and Apache Canyon Formations); (c) volcanoclastic petrofacies derived from erosion of Jurassic volcanogenic sequences or from an active magmatic arc lying to the southwest occurs randomly interbedded in the southeastern facies in the Huachuca

Mountains; and (d) transitional, mixed-provenance petrofacies documents up-section evolution in the source area for the medial northwestern facies from basement-uplift sources to arc and cratonic sources (Shellenberger Canyon Formation).

STOP 1: AMOLE ARKOSE

Lying unconformably beneath the Cat Mountain Rhyolite, the complexly deformed Amole Arkose, studied recently by Risley (1987), includes about 1000 m of nonmarine alluvial and lacustrine strata that are apparently correlative with the Bisbee Group. Local facies exposed in several isolated structural blocks within the Tucson Mtns include (a) massive subangular fanglomerate with minor interbedded sandstone; (b) interbedded conglomeratic sandstone and siltstone containing paleocaliche horizons and interpreted as braided floodplain deposits; (c) intercalated playa lacustrine deposits of laminated black mudstone, limestone, and thin-bedded cross-laminated sandstone, and floodplain fluvial deposits of cross-bedded sandstone occurring in locally lenticular fining-upward cycles; and (d) coarsening-upward lacustrine delta successions whose thicknesses of 25-75 m may be a rough measure of maximum lake depths. Basal Amole strata rest unconformably on both Paleozoic carbonate rocks and mid-Mesozoic volcanoclastic rebeds. Intertonguing relationships and arkosic compositions indi-

OVER GATES PASS TO STOP 1

Heading west from Interstate 10 on St Mary's Rd in Tucson, "A" Mountain and Tumamoc Hill on the left are composed of dark-colored mid-Tertiary volcanics (24-28 Ma, K-Ar). From Silverbell Rd, the Santa Catalina Mtns lie to the right across Tucson. On Speedway Blvd, the Tucson Mtns lie straight ahead. Their crest and near flanks expose thick (300-400 m) Laramide ignimbrite of the Cat Mountain Rhyolite (72 Ma, K-Ar), dipping gently northeast. A basal chaotic unit, exposed locally in roadcuts beyond Gates Pass, is composed of large (10-100 m) blocks of sedimentary and volcanic rocks set in a pyroclastic matrix. The block-rich unit is interpreted as intracaldera collapse breccia, and the overlying ignimbrite pile as tilted caldera fill (Lipman and Sawyer, 1985).

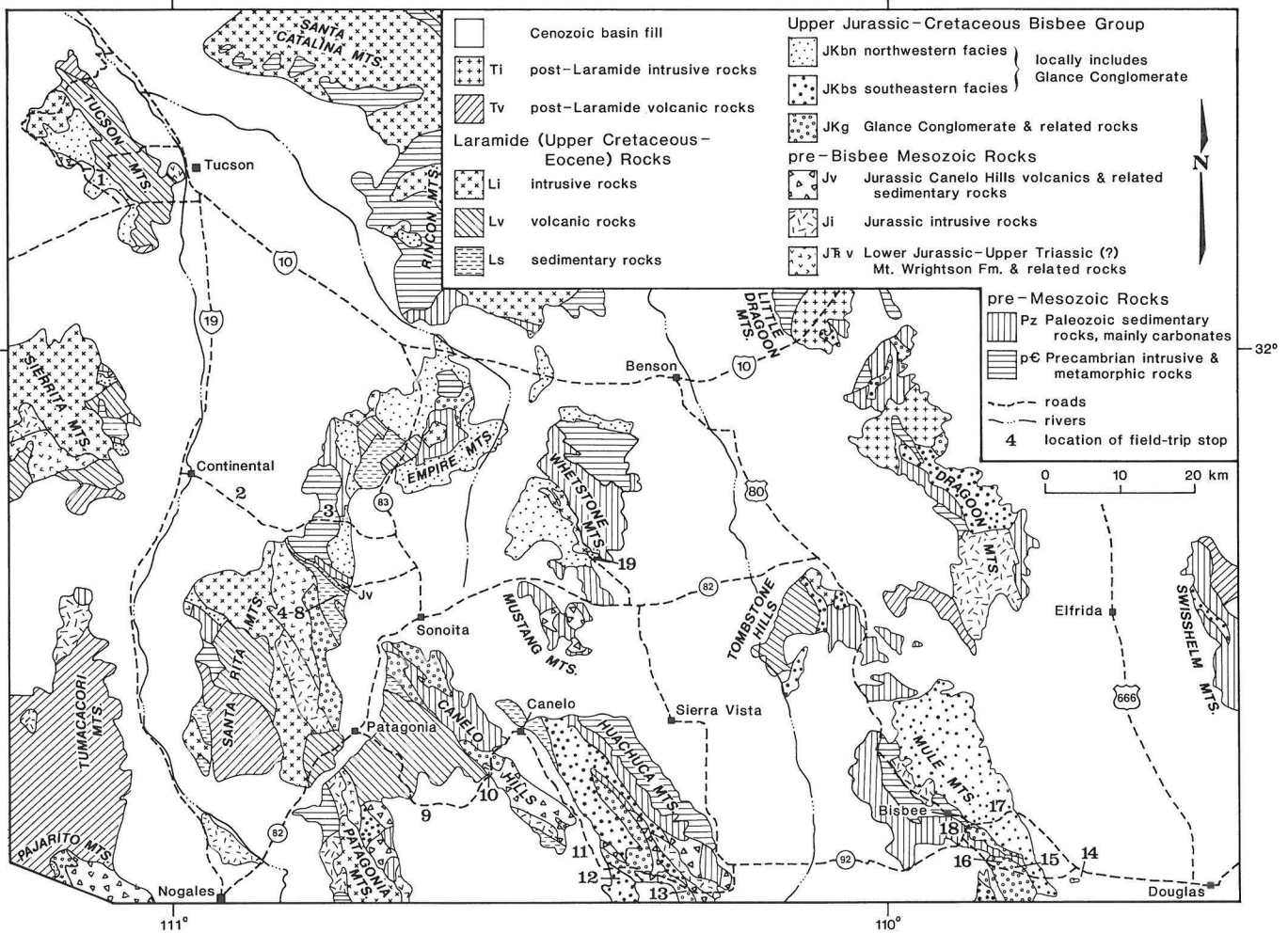


Figure 1. Generalized geologic map of southeastern Arizona showing field-trip route and stops (after Wilson and others, 1969; Drewes, 1980; Kluth, 1982; Vedder, 1984); Laramide volcanics and intrusives are latest Cretaceous to Paleocene in age, whereas post-Laramide volcanics and intrusives are Oligocene to Miocene.

cate that the strata accumulated within a structurally defined lake basin with clastic detritus derived from nearby uplands. Regional relations imply that the lake occupied part of the landward end of a structural trough open on the southeast to marine environments of the Gulf of Mexico. Fluvial paleocurrent indicators in the Amole Arkose define net streamflow toward the southeast.

The lacustrine delta succession exposed at Stop 1 on the west slope of Bren Mountain includes the following constituent facies from bottom to top (Figure 5): (a) foredelta facies of dark anoxic mudstone intercalated with sharply bounded and weakly graded sandstone beds, which contain traction structures and are interpreted as turbid-underflow deposits; (b) delta-front facies of interbedded mudstone and laminated to cross-laminated lenticular sandstone passing gradationally upward into cross-bedded sandstone bodies, which display internal scour surfaces and are interpreted as sandy mouthbar deposits of middle-ground shoals on a braided delta fringe; (c) distributary-channel facies of amalgamated sandstone beds (1-5 m thick) displaying horizontal lamination and trough cross-beds, and containing pebbly lag deposits above basal scour surfaces; and (d) lakeshore facies of laminated or bioturbated sandstone and siltstone with interbedded stromatolitic limestone beds (0.1-1.0 m thick) displaying crenulated cryptal-

gal laminae with fenestral microscopic fabric. Fresh-water bivalve fossils occur locally in black coquinoïd limestone within the lakeshore facies.

TUCSON MOUNTAINS TO STOP 2

Leaving Gates Pass, we can see probable correlatives of the Cat Mountain Rhyolite widely exposed across Avra Valley in the low-lying Roskrige Mtns, where strata lithologically similar to Amole Arkose contain intercalated Lower Cretaceous lava (110 Ma, K-Ar). As we turn south on Kinney Rd, the Sierrita Mtns ahead expose sections of Angelica Arkose similar to the Amole Arkose. From Ajo Rd, the Rincon Mtns lie east beyond Tucson. From Interstate 19, as we travel south up the Santa Cruz River, open-pit porphyry copper mines are prominent on pediments of the Sierrita Mtns to the right near Green Valley.

STOP 2: SANTA RITA MOUNTAINS OVERVIEW

The central highlands of the Santa Rita Mtns are composed of structurally complex Mesozoic volcanic and plutonic rocks (Drewes, 1971a, 1971b, 1971c, 1972b, 1976) and similar units are exposed in the Sierrita Mtns across the Santa Cruz Valley (Cooper, 1971). The oldest Mesozoic unit is the volcanogenic Mount Wrightson Formation, for which as yet unpublished Rb-Sr and

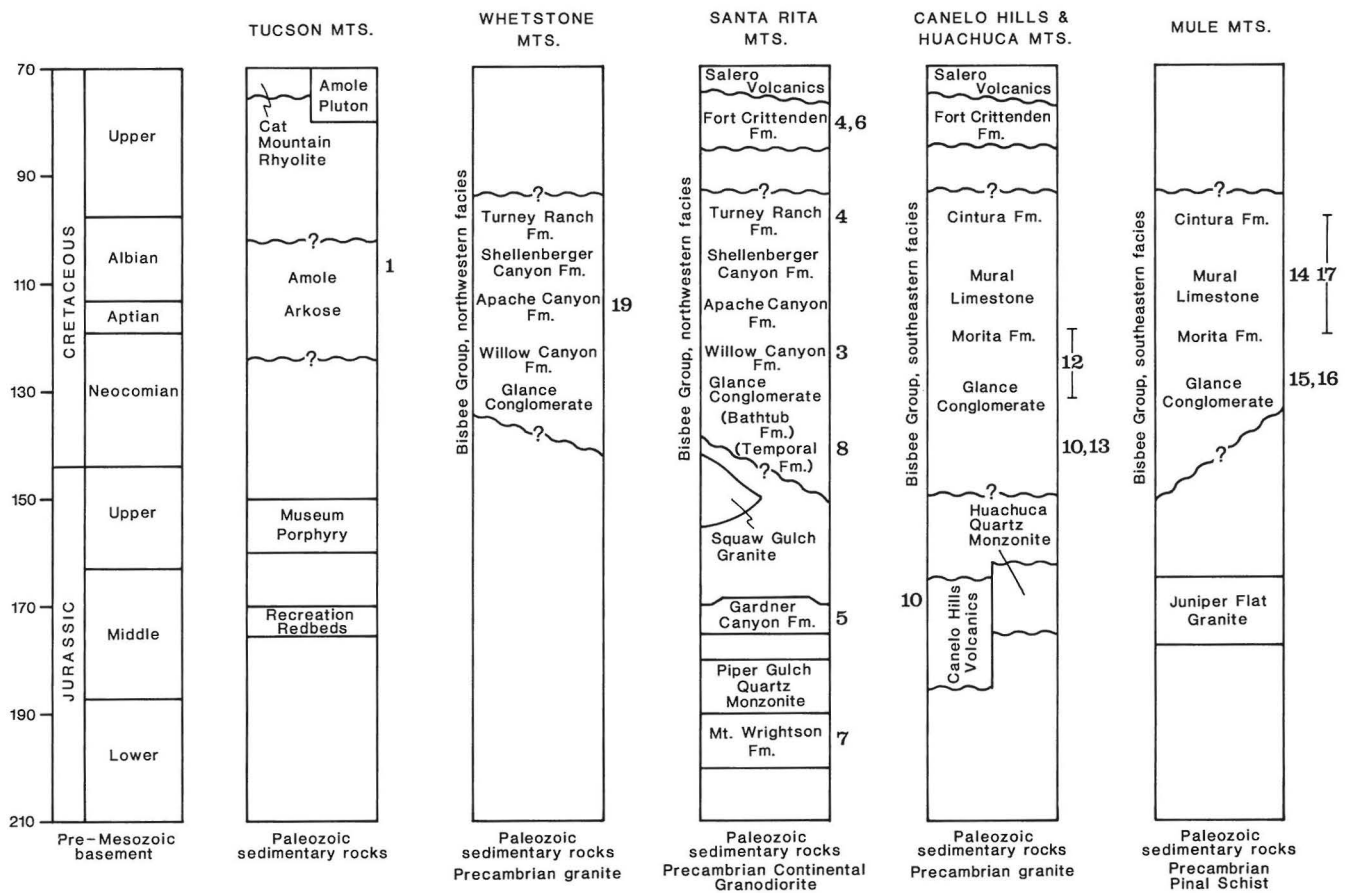


Figure 2. Stratigraphic nomenclature of Mesozoic rocks of the field-trip area. Bold numbers adjacent to columns refer to field-trip stops.

U-Pb systematics suggest an age near the Triassic-Jurassic time boundary. Lower to Middle Jurassic (170-190 Ma) volcanoclastic sequences are widespread farther west in Papagueria, where they are intruded by Middle Jurassic (c. 160-165 Ma) granitoids (Tosdal and others, 1987). Upper Jurassic plutons (c. 150-155 Ma, K-Ar) occur in both ranges, as do a variety of Laramide igneous rocks (c. 55-75 Ma, K-Ar). The mid-Mesozoic and Laramide volcano-plutonic assemblages are widely thought to represent arc magmatism related to circum-Pacific subduction both preceding and following sedimentation in the Bisbee basin.

STOP 3: BOX CANYON

The bedrock exposed in lower Box Canyon is megacrystic granitic rock, mapped locally as Continental Granodiorite (Drewes, 1971b) and lithologically similar to Middle Proterozoic granitoids of the Oracle-Ruin suite dated elsewhere in southern Arizona near 1440 Ma (U-Pb). At Stop 3, the nature of the steep contact between Precambrian granite and Glance

Conglomerate of the Bisbee Group is controversial. It was mapped by Drewes (1971b) as a fault juxtaposing supposedly allochthonous Bisbee strata in the Cochise thrust with autochthonous Precambrian basement (Drewes, 1981). The Cochise thrust is inferred by him to be subhorizontal regionally and provisionally to have accommodated as much as 100 km of lateral tectonic transport. Although local Laramide thrusts are clearly present in many mountain ranges of southeastern Arizona, we contend that the coherent regional distribution of Bisbee facies precludes offsets of such magnitude and doubt that continuous regional thrusts of the sort he envisions are actually present.

In our view, the contact in Box Canyon is a depositional unconformity, along which minor movement may have occurred during intense Laramide deformation. In the roadcut outcrop, megacrystic Precambrian granite passes gradationally through a zone of weathered reddish grus into reworked granitic detritus forming the massive basal bed of the overlying Glance Conglomerate. Rounding, sorting, and heterogeneity of clasts increase gradually up-section into granite-

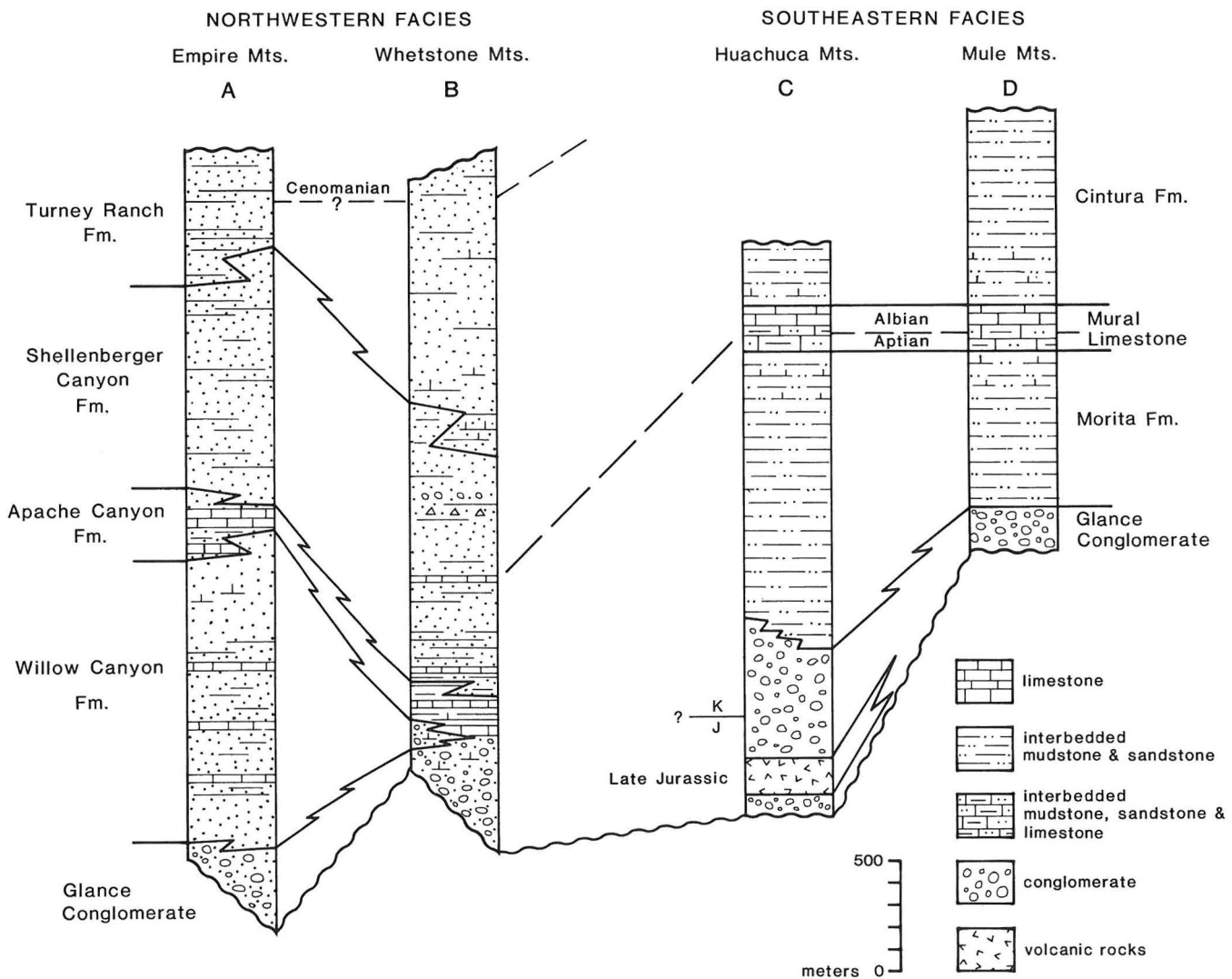


Figure 3. Generalized stratigraphic columns of northwestern and southeastern facies of the Bisbee Group. Note drastic thinning of Willow Canyon Formation from northwest to southeast (after Dickinson and others, 1986, 1987).

clast fanglomerate. Local stratigraphic relations are complicated, however, by the presence of a lenticular body of Cambrian Bolsa Quartzite in the canyon below the roadcut. Drewes (1971b) interpreted the Bolsa exposure as a fault sliver, whereas we view it as bracketed by unconformities in a structural position produced by onlap of the Precambrian basement by Glance Conglomerate, which rests on Paleozoic strata to the north and on Precambrian granite to the south.

Outcrops along the canyon floor display the conformable contact between the Glance Conglomerate and the overlying Willow Canyon Formation, composed dominantly of sandy braided-stream facies with locally developed fining-upward cycles of channel and overbank deposits (Figure 6). Horizontal laminations and trough cross-bedding are both prominent in the sandy channel deposits, which are part of the northwestern arkosic petrofacies of the Bisbee Group (Figure 4).

BOX CANYON TO GARDNER CANYON

As we continue eastward up Box Canyon to the Neogene basin fill of Sonoita Valley, the Whetstone Mtns lie straight ahead. As we turn south toward Sonoita, the craggy Mustang Mtns are in view on the left and beyond them are the bulky Huachuca Mtns, with the low-lying Canelo Hills straight ahead. Our route leads us up Gardner Canyon into the Santa Rita Mtns to examine a number of Mesozoic units at closely spaced stops (4 through 8) before we continue to Sonoita and Nogales (Figure 7).

STOP 4: FORT CRITTENDEN AND TURNERY RANCH FORMATIONS

A traverse along Gardner Canyon displays conglomeratic strata of the Upper Cretaceous Fort Crittenden Formation, which is younger than the Bisbee Group, in fault contact with strata of the Turney Ranch Formation, the uppermost unit in the northwestern facies of the Bisbee Group. The fault is a strand of the complex Sawmill Canyon fault zone, whose movement history is not well understood. Major stratigraphic contrasts across the fault system and structures with a geometry suggestive of wrench folds within it both suggest the possibility of significant strike slip during Laramide deformation. However, no one has yet identified specific lateral offsets that preclude alternate hypotheses of multiple dip slip instead.

The Fort Crittenden Formation, studied recently by Hayes (1987), is composed dominantly of pebble to cobble conglomerate and conglomeratic sandstone with subordinate interbedded sandstone and mudstone. The local depositional setting was a broad alluvial fan or braidplain. Gravel occurs randomly dispersed in sandy matrix, as clast-supported lenses, and in stringers that accentuate bedding. Varied clast types include (a) volcanic rocks derived mainly from mid-Mesozoic sources but partly from coeval Laramide complexes; (b) granitic rocks derived mainly from Precambrian basement but partly from Jurassic plutons; and (c) sedimentary rocks derived mainly from the Bisbee Group but partly from Paleozoic sources. Sandstones are lithic arkose. Paleocurrent indicators in the

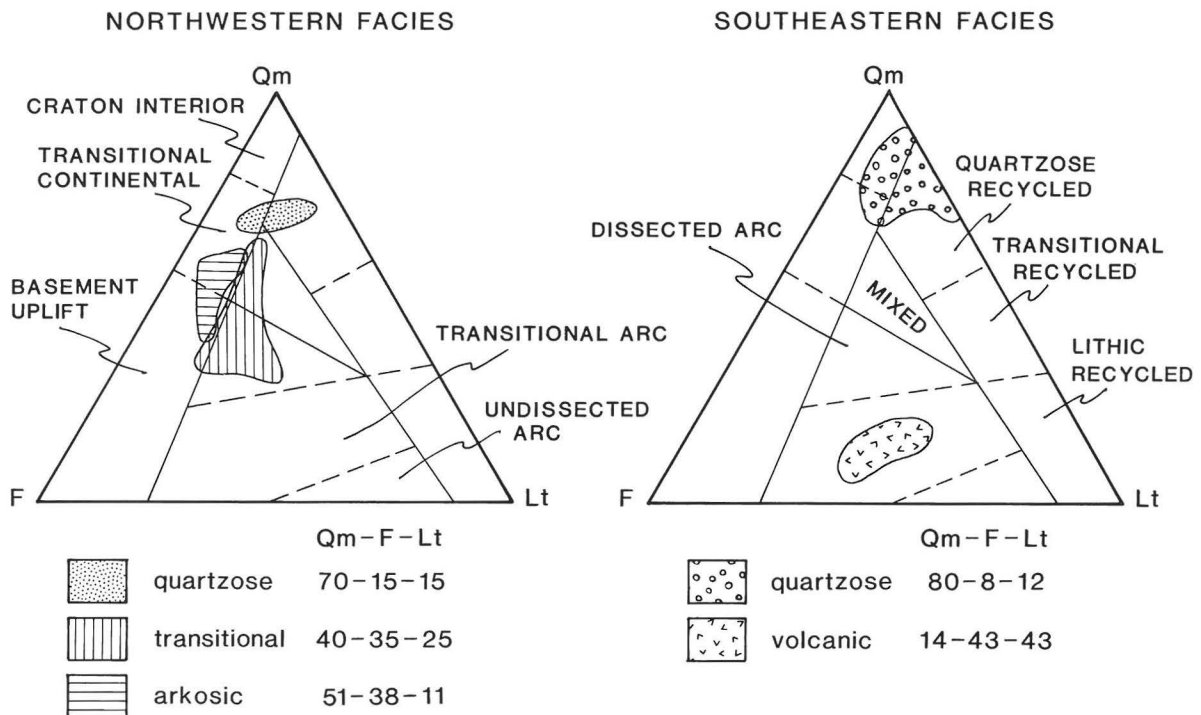


Figure 4. Ternary plots showing preliminary classification of Bisbee Group petrofacies. Pole abbreviations: Qm = monocrystalline quartz grains; F = plagioclase + potassium feldspar; Lt = total polycrystalline lithic grains, including volcanic and sedimentary lithic fragments, polycrystalline quartz, and chert. Tectonic provenance categories from Dickinson and Suczek (1979) and Dickinson and others (1983).

FACIES

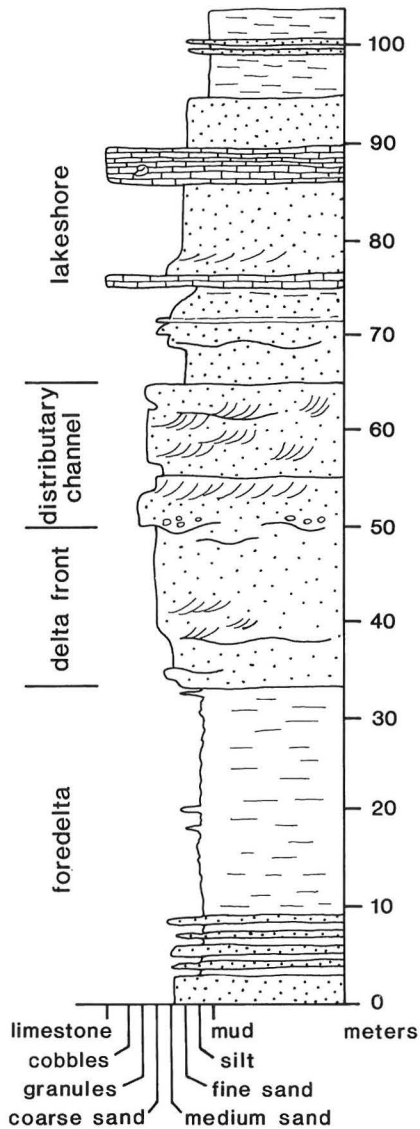


Figure 5. Generalized stratigraphic column of lacustrine delta succession in the Amole Arkose, Bren Mtn area, Tucson Mtns (after Risley, 1987). Grain-size scale across bottom.

Santa Rita Mtns reflect streamflow dominantly toward the northwest, but locally toward the southwest in beds especially rich in reworked Bisbee clasts near the erosional top of the formation. Thin rhyolitic tuffs occur in the upper part of the formation. On the western flank of the Santa Rita Mtns, isolated exposures mapped as Fort Crittenden Formation are overlain conformably by Laramide ignimbrite (74 Ma, K-Ar). At Corral Canyon in the Canelo Hills, however, the lowest exposed horizons of the Fort Crittenden Formation appear to be interbedded with volcanics of similar age (75 Ma, K-Ar).

The Turney Ranch Formation is composed of interbedded gray quartzose sandstone and red mudstone that contains pedogenic carbonate nodules. Sandstones are both horizontally laminated and cross-bedded at different horizons within the same beds. Fining-upward

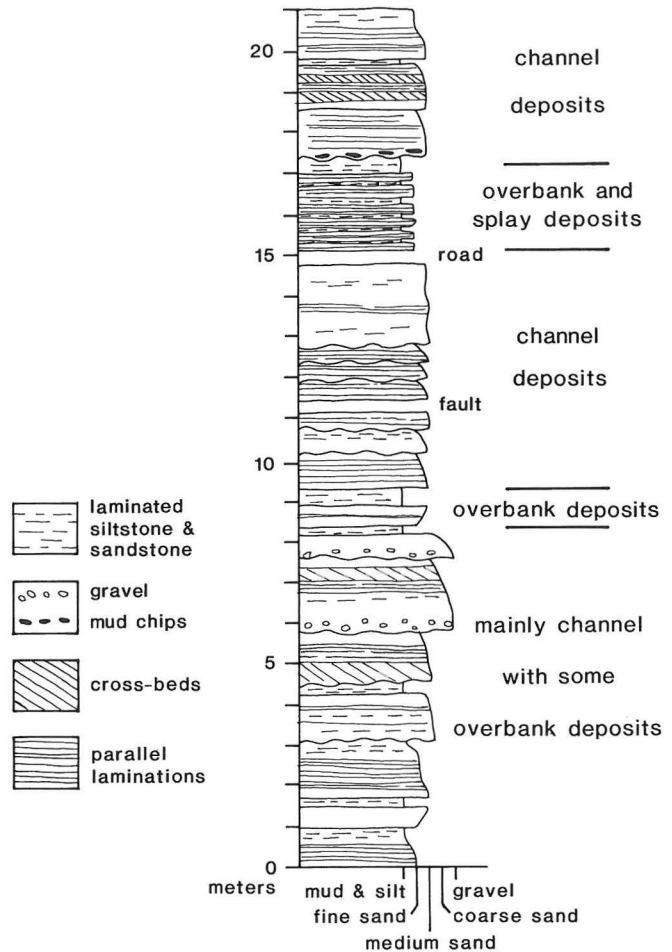


Figure 6. Generalized stratigraphic column of part of the Willow Canyon Formation, Box Canyon, Santa Rita Mtns (after Knepp, 1980). Grain-size scale across bottom.

cycles of fluvial aspect are common. The depositional environment is interpreted as a coastal plain traversed by stream channels of high sinuosity and influenced at intervals by tidal currents in shallow estuarine settings (Archibald, 1982). At Adobe Canyon farther south, strandline sandstone bodies of shoreface and beach deposits rest on erosional ravinements and reflect a local marine transgression of probable Cenomanian age (Inman, 1987).

At Adobe Canyon, the contact between the Turney Ranch and Fort Crittenden Formations is structurally concordant but disconformable (Inman, 1987). The lower part of the Fort Crittenden Formation in that locality is composed of floodplain and lacustrine mudstones, overlain by progradational fan-delta deposits that are transitional up-section into the alluvial-fan deposits that form the bulk of the formation. Available isotopic dates (see above) suggest that the alluvial-fan sediments were deposited near the Campanian-Maastrichtian time boundary, but the underlying lacustrine sequence may include considerably older strata. In the Huachuca Mtns, the Fort Crittenden Formation rests unconformably on the Cintura Formation of the southeastern facies of the Bisbee Group.

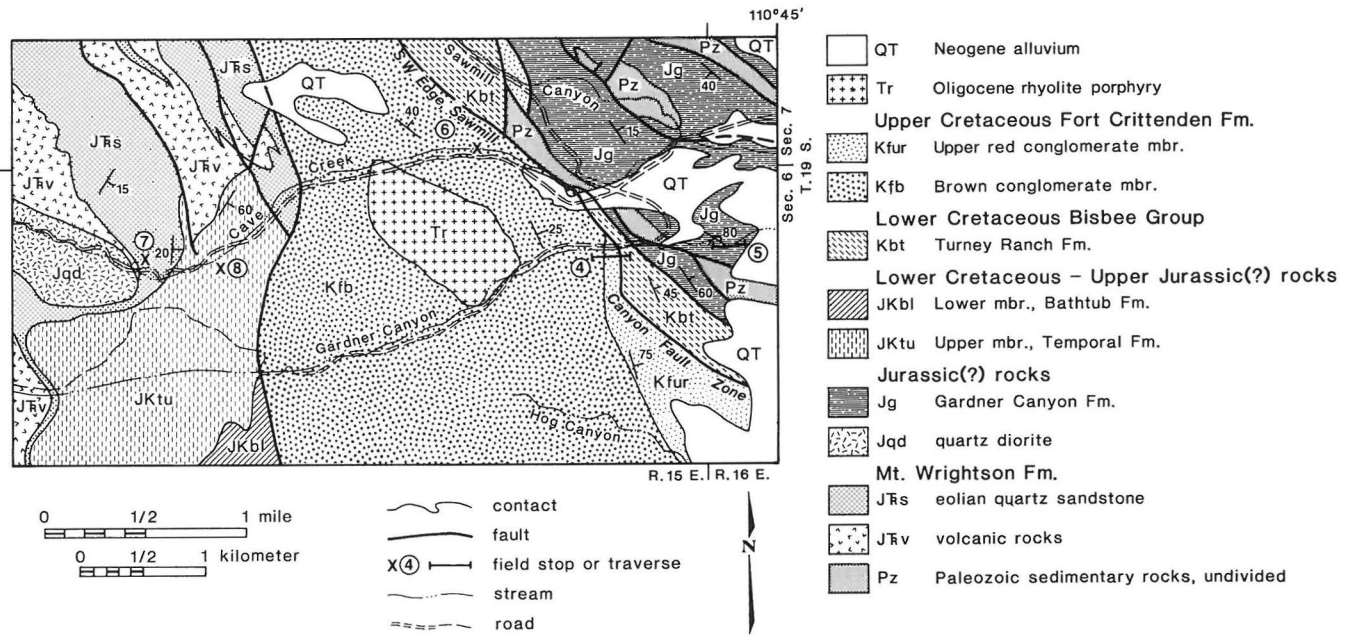


Figure 7. Geologic sketch map of the Gardner Canyon area, Santa Rita Mtns (after Drewes, 1971c).

STOP 5: GARDNER CANYON FORMATION

The poorly dated Gardner Canyon Formation is composed of mid-Jurassic volcanoclastic redbeds (Beatty, 1987). Massive red mudstone with pale thin tuff beds, volcanoclastic sandstone, and volcanic conglomerate are all exposed in steep gorge walls along Gardner Canyon. From recent work in the Canelo Hills, we conclude that these strata lie concordantly beneath the Canelo Hills Volcanics of Middle Jurassic age (c. 170–175 Ma, K–Ar). Similar mid-Jurassic volcanics and redbeds occur locally in many nearby ranges. We infer that these pre-Bisbee volcanogenic sequences formed during incipient intra-arc rifting that initiated the crustal stretching that eventually produced subsidence of the Bisbee basin.

STOP 6: FORT CRITTENDEN DEBRIS-FLOW FACIES

In outcrops along Cave Creek, fine-grained sheet-flood debris-flow deposits form distinctive sedimentational units within the Fort Crittenden Formation. Resistant conglomerate and sandstone beds, locally lenticular, represent streamflow and streamflow channel deposits. Less resistant sandy and pebbly mudflow layers represent overbank debris-flow deposition. Analogous Holocene low-energy debris-flow sheets are spread at intervals over the narrow floodplains of small ephemeral streams and braided desert washes in the modern climatic regime of the greater Southwest.

STOP 7: MOUNT WRIGHTSON EOLIAN SANDSTONES

Lenses of quartzose eolian sandstone are interbedded with volcanoclastic strata of the Mount Wrightson Formation on wooded slopes above Cave Creek (Drewes, 1971a). Analogues of these beds are intercalated within Lower Jurassic volcanogenic units in many ranges of southern Arizona and the Mojave Desert (Bilodeau and Keith, 1986). The source of the wind-

blown sand is inferred to have been the vast Aztec-Navajo erg of the Colorado Plateau region, from which the sand was blown into the inland fringe of the magmatic arc that lay subparallel to the continental margin. The presence in southern Arizona of quartzose sand that was transported by winds from a northern source implies that the Mogollon highlands in central Arizona did not exist as a prominent positive feature until later in Mesozoic time (Bilodeau, 1986). We conclude that the Mogollon highlands represented the uplifted rift shoulder of the extensional Late Jurassic to Early Cretaceous Bisbee basin, and hence did not begin to develop until after mid-Jurassic time. The paleowind direction inferred from cross-bed inclinations at this locality is S15W, at right angles to the trend of the Mogollon highlands.

STOP 8: TEMPORAL FORMATION

We refer conglomeratic strata, mapped locally by Drewes (1971a,c) as Temporal and Bathtub Formations, to the basal conglomeratic phase of the Bisbee Group, termed Gance Conglomerate regionally (Bilodeau, 1979). Lavas and ignimbrites intercalated within the Temporal and Bathtub Formations have counterparts in the Gance Conglomerate of the Huachuca Mtns and Canelo Hills. We infer that the interbedded volcanics represent waning phases of mid-Jurassic rift magmatism. Subangular Temporal conglomerates along Cave Creek contain dominant volcanic clasts, common granitic clasts, and subordinate sedimentary clasts. As Gance clast populations generally reflect nearby or subjacent sources, the lithology of the unit varies widely throughout the region (Bilodeau, 1979). Paleocurrent indicators, mostly clast imbrications in conglomerate, document local streamflow to virtually every point of the compass and suggest that complexly broken topography, developed by syndepositional block faulting, extended over essentially the whole region of Gance deposition (Bilodeau, 1982).

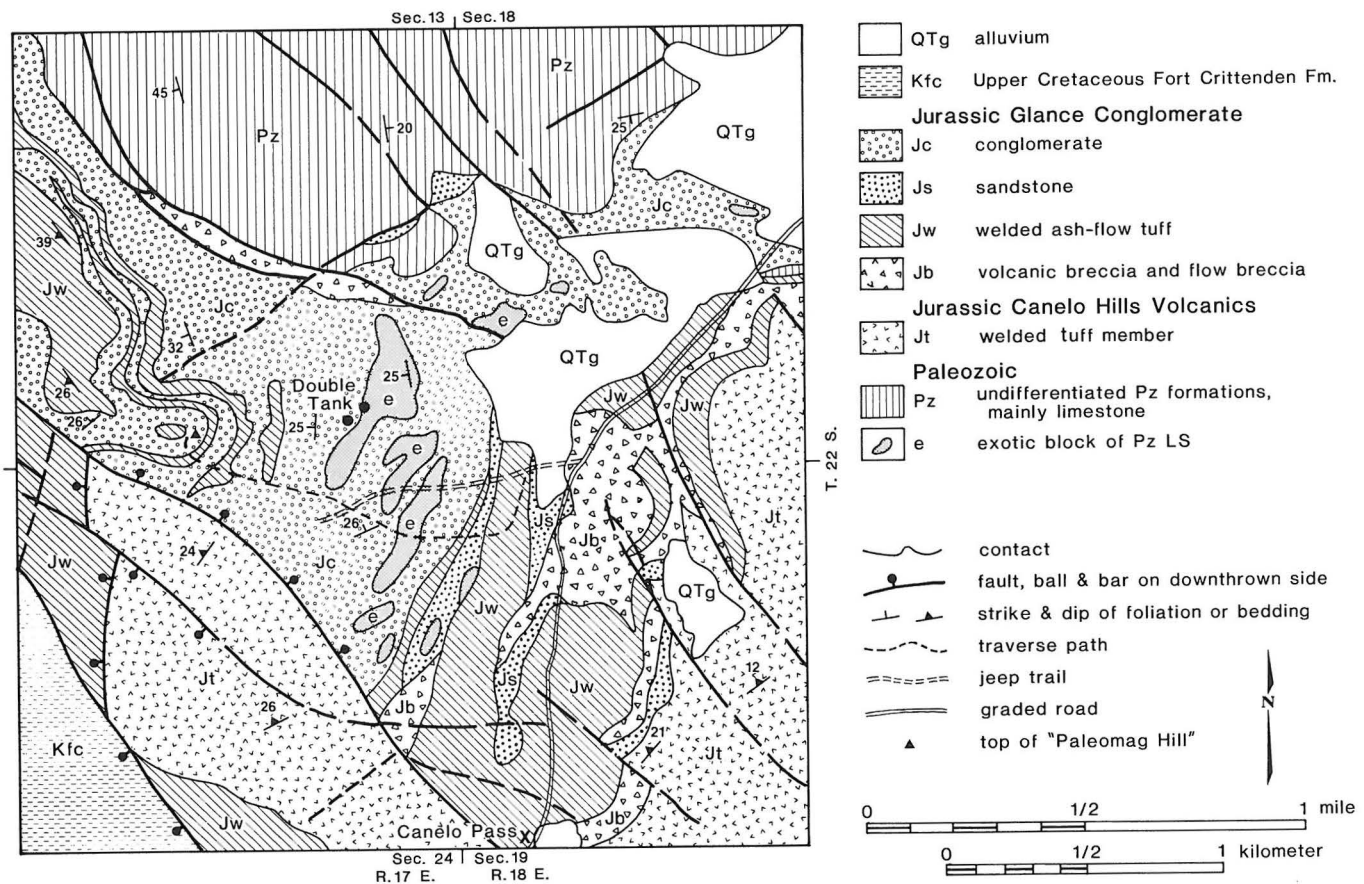


Figure 8. Geologic sketch map of the Canelo Pass area, Canelo Hills (after Kluth, 1982).

NOGALES TO STOP 9 VIA PATAGONIA

The low hills around Nogales are underlain by tilted mid-Tertiary conglomeratic strata of the Nogales Formation. As we leave Nogales, the Patagonia Mtns lie ahead to the east, with the Santa Rita Mtns to the north. From broad terraces traversed after we cross the Santa Cruz River, we can see isolated San Cayetano Peak on the left. Bold outcrops along Patagonia Creek are Laramide igneous rocks, and the narrowest part of the canyon is cut into Paleocene Gringo Gulch Volcanics (62 Ma, K-Ar). Beyond Patagonia, surrounding wooded hills are underlain by varied Laramide igneous rocks. The Patagonia Mtns to the south include exposures of pre-Laramide units similar to those of the Santa Rita Mtns (Simons, 1972). Dissected Neogene basin fill of the San Rafael Valley is exposed along the gulch leading upward to the sedimented valley surface.

STOP 9: SAN RAFAEL VALLEY OVERVIEW

San Rafael Valley at the headwaters of the Santa Cruz River affords a view of the Huachuca Mountains ahead to the east and of the Canelo Hills north of the valley. Laramide volcanics underlie the rocky hills due north of the stop. After we cross the valley, however, the first bedrock outcrops along the grade to Canelo Pass are rhyolitic Middle Jurassic ignimbrites and minor lavas of the Canelo Hills Volcanics (165-185 Ma, K-Ar), erupted during rift magmatism

associated in time with the opening of the Gulf of Mexico.

STOP 10: CANELO PASS

At Canelo Pass (Figure 8), strata of the basal conglomeratic phase of the Bisbee Group rest positionally on the Canelo Hills Volcanics along a disconformable but generally concordant contact representing a hiatus of uncertain duration. The conglomeratic sequence, once inferred to lie stratigraphically beneath the Canelo Hills Volcanics (Hayes and others, 1965), was shown to overlie the Canelo Hills Volcanics by Kluth (1982, 1983). He termed the strata "rocks of Mount Hughes," but noted their lithologic similarity to the Glance Conglomerate and regarded the two units as parts of the same lithotectonic assemblage. Vedder (1984) later showed that the succession above the Canelo Hills Volcanics at Canelo Pass is lithologically and stratigraphically indistinguishable from the Glance Conglomerate of the Huachuca Mountains, with which she thus correlated the "rocks of Mount Hughes." We follow her usage here.

From the road, we traverse up-section on foot to a hilltop on the crest of the Canelo Hills. The traverse begins within a unit of rhyolitic ignimbrites and breccias about 75 m thick. This unit has been included in the Glance Conglomerate because thin sandstones and conglomerates are present locally at its base (Vedder, 1984). However, lithologic and geochemical similarity of these rhyolitic rocks to

concordantly underlying welded tuffs of the Canelo Hills Volcanics (Krebs, 1987) suggests that the base of the Glance Conglomerate is better placed at the top of the volcanogenic strata where conglomerate becomes the dominant lithology. The interbedded nature of the contact exposed here at Canelo Pass is evidence for a gradual transition between accumulation of rift-related ignimbrites and subsequent deposition of syntectonic fanglomerates.

Above the rhyolitic strata, the following outcrops are encountered within the Glance Conglomerate: (a) mixed-clast conglomerate containing rhyolite and limestone clasts; (b) sedimentary megabreccias and slide blocks of exotic Paleozoic carbonate rock, displaying characteristic crackle-breccia fabric and shattered chert nodules; (c) limestone-clast conglomerate (with minor volcanic clasts), classically typical Glance lithology (exposed on the slope leading to the first divide); (d) dark alkalic lava and flow-breccia (exposed in the roadbed on the divide), similar to Glance strata described previously as "andesitic" in the Huachuca Mtns (Hayes and Raup, 1968); (e) red mudstone, flow-breccia, and mixed-clast conglomerate (exposed in the adjacent ravine); (f) gray and red ignimbrites intercalated within the Glance Conglomerate (on the lower slopes of the hill); (g) conglomerates containing both rhyolite and limestone clasts; (h) more gray ignimbrite (exposed along the crest line); and (i) more conglomerate overlain by pink ignimbrite at the hilltop, from which there are fine panoramic views. The near ridge to the north is underlain by gray Paleozoic carbonate units.

Samples from ignimbrites exposed on the hillslope were used by Kluth and others (1982) to define a Late Jurassic Rb-Sr isochron (151 Ma). The geochemical data of Krebs (1987) indicate that the ignimbrites intercalated within the Glance Conglomerate are closely comparable petrochemically to ignimbrites in the underlying Canelo Hills Volcanics. Although valid age relationships are difficult to document because of widespread post-eruptive alteration in both units, we infer that rhyolitic magmatism immediately preceding and accompanying deposition of the basal conglomeratic phase of the Bisbee Group reflected initiation of the extensional tectonism that produced the Bisbee basin. This inference raises the possibility that some of the rugged relief that existed during deposition of the Glance Conglomerate may have been inherited from the formation of local calderas and associated volcano-tectonic depressions, rather than flanking simple grabens and half-grabens alone.

CANELO PASS TO STOP 11

As we leave Canelo Pass, the Huachuca Mtns lie to the east. South of the townsite of Canelo, exposures of the Bisbee Group and Fort Crittenden Formation underlie grassy and wooded slopes of the northwestern Huachuca Mtns across Lyle Canyon on the east. Roadcuts in the Canelo Hills expose Neogene gravel deposits, followed by exposures of underlying Canelo Hills Volcanics (near the turnoff to the lunch stop). Thick ignimbrite successions near Parker Canyon Lake contain large exotic blocks of Paleozoic carbonate rocks and are interpreted as caldera-fill sequences by Lipman and Sawyer (1985).

STOP 11: LONE MOUNTAIN OVERVIEW

From Parker Canyon Lake, the route traverses poorly exposed Bisbee Group partly masked by Neogene basin fill along the flank of San Rafael Valley. The crest of Lone Mountain (the near ridge at the foot of the Huachuca Mtns) is underlain by the Canelo Hills

Volcanics. The depositional contact with the overlying Glance Conglomerate is well exposed in small ravines along the flank of Lone Mountain (Vedder, 1984). Several ignimbrite sheets and a dark lava occur within the Glance Conglomerate at Lone Mountain, and its upper contact with the Morita Formation is marked by a zone of paleocaliche layers indicative of a condensed section. The Glance section at Lone Mountain is similar to the Glance section just traversed at Canelo Pass and can be traced laterally along homoclinal strike into the Glance exposures at Bear Creek.

Beyond Lone Mountain, a full Bisbee succession topped by Fort Crittenden Formation dips steeply off the flank of the Huachuca Mtns, near whose crest the Glance Conglomerate rests unconformably on both mid-Mesozoic volcanics and Paleozoic carbonates, into which pre-Bisbee erosion cut deep paleovalleys now filled with Glance Conglomerate. At least two thick "andesitic" lavas (probably actually altered alkalic basalt) are interbedded with the conglomerates and overlie typical limestone-clast Glance beds exposed near the skyline.

STOP 12: BEAR CREEK

Outcrops in Bear Creek at the southern end of Lone Mountain expose a complete section through the southeastern facies of the Bisbee Group (Figure 3C), including depositional contacts with underlying Canelo Hills Volcanics and overlying Fort Crittenden Formation. A traverse here across the Glance-Morita contact will focus on (1) clast compositions in the Glance Conglomerate; (2) a lava near the top of the Glance Conglomerate; (3) paleocaliche deposits in the Glance-Morita transition zone; and (4) interbedded quartzose and volcanoclastic sandstone petrofacies in the Morita Formation.

The Glance Conglomerate is 315 m thick in Bear Creek. Volcanic clasts derived from the underlying Canelo Hills Volcanics dominate the lower part of the section. Sedimentary clasts, mostly Paleozoic carbonates, become more abundant up-section. The traverse lies through the upper part of the section, where the conglomerate is composed of approximately 60 percent volcanic clasts, 40 percent Paleozoic limestone clasts, and rare chert and quartzite clasts (Vedder, 1984). Lenses of pale-red volcanic litharenite sandstone with shallow trough cross-beds are interbedded with the conglomerate.

South of the bridge, a gorge cut through Glance Conglomerate ends at exposures of a dark aphanitic lava that is about 30 m thick. Vedder (1984) interpreted the rock as a subaerial flow based on the presence of flow banding near its base and vesicular textures at its top. The lava and an overlying sandy pebble conglomerate both thin and pinch out to the northwest. Vedder (1984) attributed the thinning to the presence of a local paleohigh to the northwest that was created by syndepositional faulting during Glance deposition. However, the absence of an overlying coarse conglomerate on the east side of Bear Creek suggests that relations may be more complex. Alternative explanations include truncation by a paleochannel or reinterpretation of the volcanic body as a sill rather than a flow.

A zone of paleocaliche at the contact between Glance Conglomerate and Morita Formation has three distinct lithofacies (Vedder, 1984): (1) calcareous maroon mudstone containing nodules and stringers of pale-gray pedogenic limestone; (2) sandy, unfossiliferous limestone caliche beds with intercalated red, green, or black chert; and (3) well-sorted sandy pebble conglomerate composed mainly of reworked soil

caliche pebbles. Both limestone and chert are apparently of replacement origin. The paleocaliche transition zone is a condensed stratigraphic sequence inferred to represent a lengthy interval of soil formation.

Nearly 2000 m of transgressive-regressive deposits of the upper part of the Bisbee Group overlie the Glance Conglomerate in Bear Creek (Hayes, 1970a). The Morita Formation (1300 m) is fluvial in its lower part, but grades into coastal-plain and marginal-marine deposits near its top. Bioclastic oyster- and *Orbitolina*-bearing limestone and interbedded calcareous mudstone and sandstone in the Mural Limestone (250 m) have been interpreted as tidal and lagoonal deposits (Sindlinger, 1981). Patch-reef deposits like those seen later in the Mule Mtns do not occur in this section. Interbedded mudstone and limestone of the overlying Cintura Formation (400 m) record marine regression, grading up-section from marginal-marine to nonmarine facies. Only the lower Morita Formation will be examined in our traverse.

Steeply dipping resistant ledges of Morita Formation sandstone form prominent outcrops in Bear Creek. Interbedded red and gray mudstone and siltstone are poorly exposed. Sandstones consist of horizontally laminated and cross-bedded fining-upward packages with basal scour surfaces and mud-chip lenses and are interpreted as channel and bar complexes in a high-sinuosity fluvial system. Finer grained intervals include massive to laminated mudstone, ripple-laminated siltstone, and pedogenic caliche nodules and beds that formed as floodplain overbank deposits.

The stratigraphically lowest light-gray sandstone beds encountered in the stream banks are representative of the southeastern quartzose petrofacies, with average Qm-F-Lt mode of 80-8-12 (Figure 4). Dark-gray volcanoclastic sandstone beds that occur farther up-section contain abundant volcanic lithic fragments and plagioclase feldspar, with average Qm-F-Lt mode of 14-43-43. Quartzose sandstones are more abundant than volcanoclastic sandstones, but the two petrofacies are randomly interbedded throughout the Morita and Cintura Formations in the Bear Creek section. This relationship suggests influx of pulses of sediment from two different sources to the drainage basin. Eroding Jurassic arc volcanics to the west and cratonic quartzose rocks to the northeast are the most likely sources for the two petrofacies.

STOP 13: MONTEZUMA PASS

From Bear Creek to Montezuma Pass, most of the route lies along strike within Glance Conglomerate, which forms rugged outcrops around Coronado Peak. On the south flank of Montezuma Canyon east of the pass, Glance Conglomerate rests upon ignimbrites of the Canelo Hills Volcanics. On the north side of the canyon, steep slopes leading up to Montezuma Peak are underlain by a Middle Jurassic pluton of Huachuca Quartz Monzonite (165-170 Ma, K-Ar). The pluton is intruded into mid-Jurassic ignimbrites rich in exotic blocks and may occupy a subsequently deformed resurgent cauldron. To the east across the San Pedro River lie the Mule Mtns near Bisbee and San Jose Peak south of the border.

MONTEZUMA PASS TO DOUGLAS

As we approach the Mule Mtns (Figure 9), we can see spurs on the left underlain by complexly deformed Paleozoic strata. As we cross a low saddle into Mule Gulch, the gray cuesta visible straight ahead is upper

Mural Limestone of the medial Bisbee Group in the type area. The narrow roadcut along Mule Gulch exposes lower Mural Limestone and the upper part of the underlying Morita Formation. The overlying Cintura Formation is exposed on low spurs beyond the roadcut. Sulphur Springs Valley, where Douglas lies, is the largest structural depression in southeastern Arizona.

STOP 14: MURAL PATCH REEF

From this spot on the flank of Sulphur Springs Valley (Figure 9), the morphology of a small patch reef in the Mural Limestone is displayed by a bold outcrop on a small knob rising from the desert flats near Paul Spur (Scott, 1979). The reef core of coralgall-rudistid boundstone is flanked by encrusted coral-rudist packstone and rudstone with foreset stratification. Reef-flank deposits grade laterally into wackestone and packstone that accumulated on the surrounding seafloor. The original bathymetric relief of the patch reef is well shown by the present outcrop relief. Patch reefs in the Mural Limestone occupy a belt trending east-northeast as a local facies of more widespread carbonate deposition in shallow shelf environments during the time of maximum marine transgression in the Bisbee basin. Correlative mid-Cretaceous patch reefs occur throughout the Gulf Coast region (Scott, 1979; Warzeski, 1983).

THROUGH GLANCE NARROWS TO STOPS 15 AND 16

In the narrows of Glance Creek, the route crosses the Gold Hill fault zone, a Laramide thrust that developed along the trend of a syn-Glance normal-fault system (Figure 9). Similar Laramide reactivation of older rift structures, with reversal of the sense of displacement, has been noted within a number of mountain ranges (Bilodeau, 1979). Bold outcrops of gray Paleozoic carbonate rocks in the hanging wall on the northwest side of the narrows were thrust above Bisbee Group exposed to the northeast. Earlier normal slip carried the hanging wall downward to foster the accumulation of an unusually thick section (2000 m) of Glance Conglomerate on the block to the southwest. This Glance succession displays inverted clast stratigraphy that reflects progressive unroofing of ground north of the fault zone during Glance deposition. In multiple drill holes sunk for copper exploration, limestone-clast conglomerates (Stop 15) derived from the stripping of Paleozoic cover consistently underlie schist-clast conglomerates (Stop 16) derived from subsequently exposed basement. In several other ranges, systematic internal distributions of clast types in Glance Conglomerate document analogous inverted clast stratigraphy, developed in each case adjacent to paleofault scarps that flanked local Glance depocenters (Bilodeau, 1979, 1982).

THROUGH BLACK GAP TO STOP 17

Passing through Black Gap to Mule Gulch (Figure 9), the route crosses two syn-Glance normal faults hidden in the subsurface. Predominantly schist-clast conglomerates, exposed in low roadcuts opposite the tailings pile just outside Warren, form the Glance section between the faults; this Glance section rests unconformably on Paleozoic carbonate units tilted during pre-Glance and/or syn-Glance fault movements and reaches a thickness of about 200 m. In contrast, the Glance sequence on the highest standing paleoblock north of both faults is a thin overlapping sheet only 10-25 m thick.

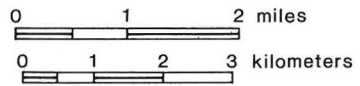
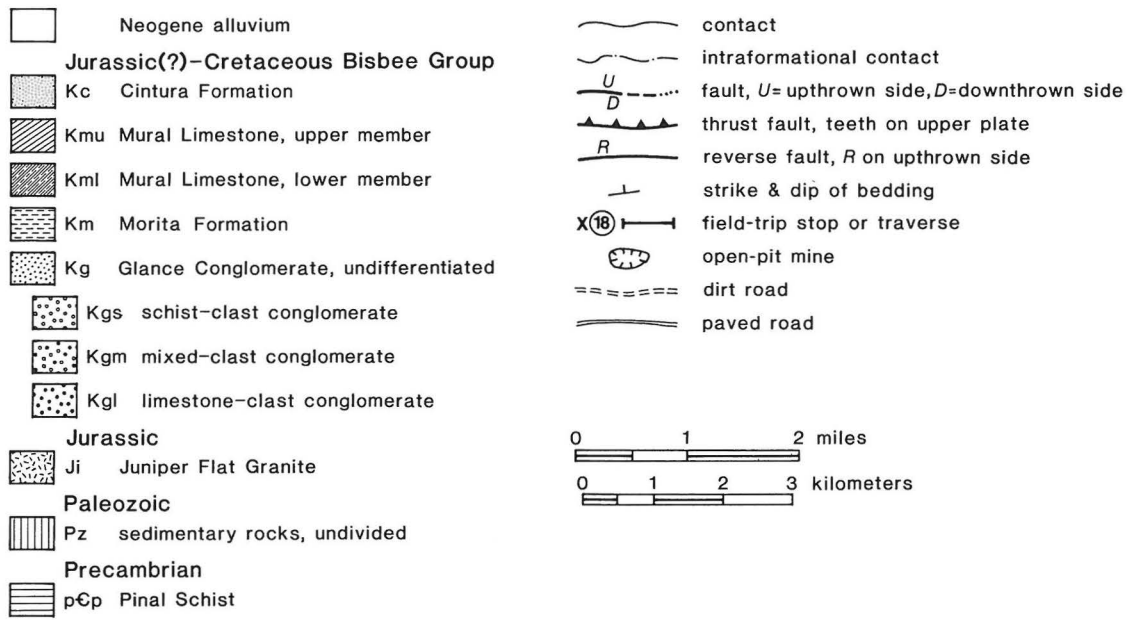
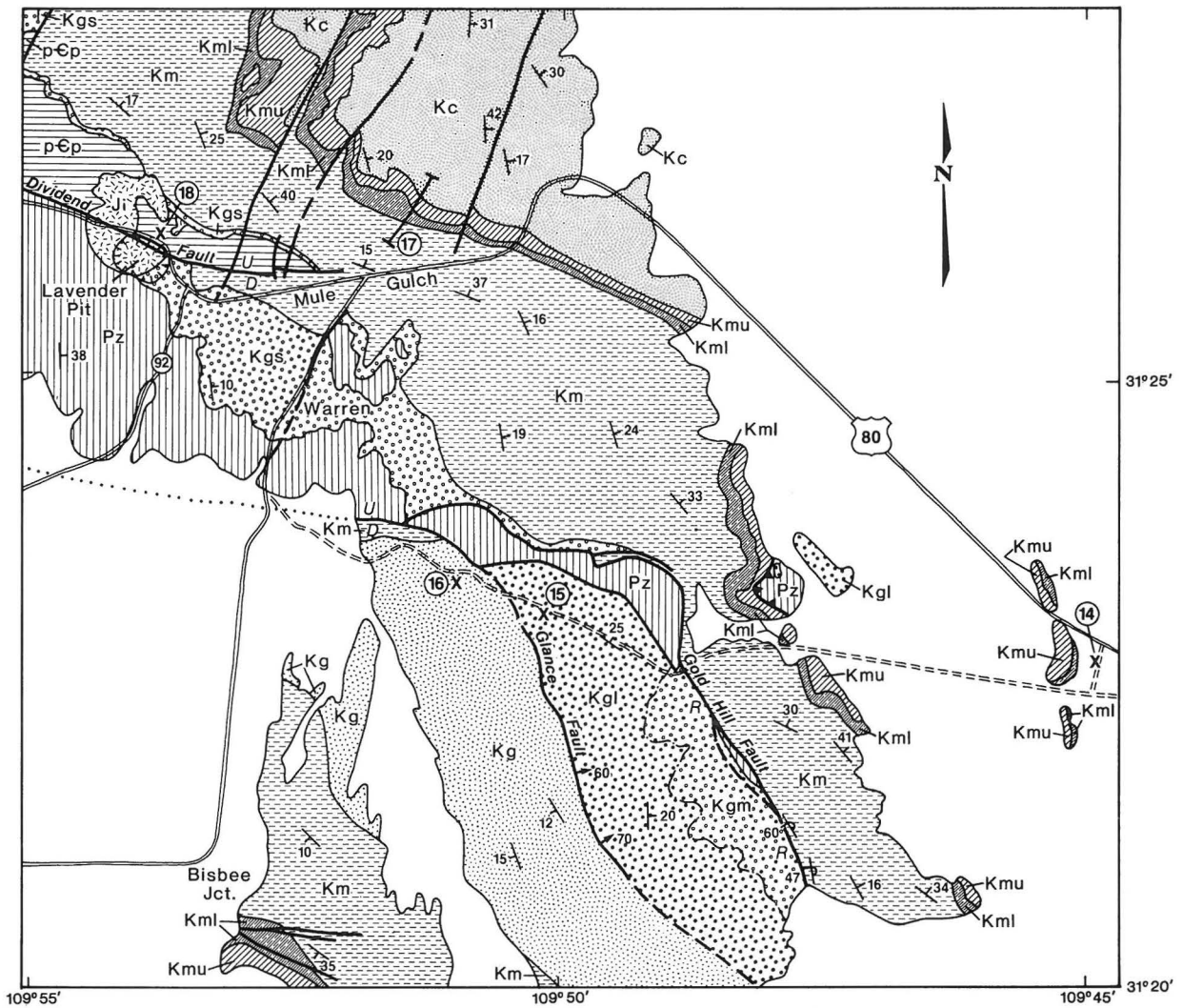


Figure 9. Geologic sketch map of the southern Mule Mtns (after Bilodeau, 1979).

Climbing the slopes of ridges north of Mule Gulch allows us close examination of the main transgressive-regressive cycle (Hayes, 1970a) in the type Bisbee Group, as represented by the transition up-section from nonmarine Morita Formation into marine Mural Limestone and back to nonmarine Cintura Formation (Figures 3D and 9).

At the base of the section, 15 m of schist-clast Glance Conglomerate rest unconformably on Precambrian Pinal Schist. The overlying Morita Formation is 850 m thick. The traverse begins on a prominent strike-ridge underlain by resistant sandstones of the upper Morita Formation. Pale-gray, horizontally laminated, and trough cross-bedded sandstone interbedded with red and gray mudstone and siltstone are fluvial and coastal-plain channel and overbank deposits.

A gradational contact between the Morita Formation and lower Mural Limestone underlies the adjacent saddle. The contact is placed where thin beds of fine-grained calcareous sandstone, calcareous siltstone, and impure oyster-bearing limestone become more abundant than thick, resistant sandstone beds. The contact represents a gradual shift to marginal-marine environments as the northward-transgressing sea inundated the subsiding coastal plain. Calcareous and coquinoid ledges become more prominent toward the top of the lower Mural Limestone.

The thick, resistant cliff that caps the next ridge is the upper Mural Limestone. Prominent lithofacies in the cliff include coral-algal-rudist boundstone; pelletoid-, *Orbitolina*-, mollusk-, milliolid- and echinoid-bearing packstone and wackestone; and ooid grainstone. According to detailed facies analyses by Warzeski (1983), carbonate shoals and patch reefs that formed on a paleohigh in this area separated a broad, shallow carbonate lagoon to the north from the open marine shelf to the south. The total thickness of Mural Limestone here is 200 m.

The Cintura Formation (550 m thick) underlies the next ridge, with the lower contact placed at the top of the uppermost prominent limestone ledge. Interbedded fossiliferous marine limestone, sandstone, and mudstone in the lower Cintura Formation were deposited during marine regression. Limestone decreases in abundance up-section, and marginal-marine to lagoonal facies give way to red delta-plain mudstone and quartzose channel sandstone.

Bisbee sandstones in the Mule Mtns are consistently quartzose, but are slightly more feldspathic than sandstones in the quartzose petrofacies in the Huachuca Mtns (Figure 4). Both plagioclase and K-feldspar are present, with modal Qm-F-Lt=77-12-11. Jamison (1983) identified one interval in the lower Morita Formation containing volcaniclastic sandstone, implying that west-derived arc debris was occasionally transported as far east as the Mule Mtns.

STOP 18: LAVENDER PIT

Up Mule Gulch lies the old mining camp of Bisbee, the only major porphyry copper deposit of Jurassic age in southern Arizona. The walls of Lavender Pit expose Glance Conglomerate, Paleozoic limestones of the Naco Group, and Jurassic intrusives of the Sacramento stock, which was intruded along the Dividend fault trend, first active during Jurassic magmatism but later reactivated as a syndepositional normal fault during Glance sedimentation (Bilodeau, 1979, 1982).

After passing outcrops of Paleozoic rocks near Bisbee, the Mule Pass road crosses into Precambrian Pinal Schist. At the tunnel entrance are exposures of Middle Jurassic Juniper Flat Granite (175 Ma, K-Ar). In Banning Canyon beyond the tunnel, the road follows roughly along the contact between schist on wooded ridges to the left and granite in bold outcrops on the right. The contact is exposed as a sheared and locally faulted zone in one of the roadcuts. In lower Banning Creek, gray outcrops on surrounding ridges are Paleozoic carbonate units and the Whetstone Mtns are visible to the northwest beyond the San Pedro River. On the way to Tombstone, we pass several low ridges displaying banded outcrops of the upper Paleozoic Naco Group. In the Tombstone Hills, complex geologic features include varied Laramide structures, intrusions, and volcanic rocks. Northeast of Tombstone, craggy outcrops of mid-Tertiary Stronghold Granite (c. 25 Ma, K-Ar) are prominent on the skyline in the Dragon Mtns, where the Middle Jurassic Gleeson Quartz Monzonite (c. 180-185 Ma, K-Ar) and strata of the Bisbee Group are also exposed. The route from Tombstone to Mustang Corners crosses a broad expanse of Neogene basin fill along the San Pedro River.

STOP 19: APACHE CANYON FORMATION

An incomplete section, 300 m thick, of Apache Canyon Formation is exposed in hillside outcrops along Mine Canyon. The exposures illustrate the range of lacustrine lithologies described by Archibald (1982) in the northwestern facies of the Bisbee Group.

Deep lacustrine lithofacies include laterally continuous, laminated to thinly laminated, micritic limestone and dark shale. Shallow lacustrine facies include algal-laminated limestone, and thin- to thick-bedded gray micrite, biomicrite, and biomicrudite. Fresh to brackish water gastropods, pelecypods, and charophyte stems are locally abundant in the shallow lacustrine facies. Biosparudite beds containing broken fossils and angular to subangular granules and pebbles of granite, feldspar, and quartz represent storm deposits. In the northern Whetstone Mtns, the upper Apache Canyon Formation contains abundant clastic lithologies, including sandstone, shale, siltstone, and argillaceous micrite. These lithologies represent marginal-lacustrine, deltaic, and fluvial facies that prograded over the open-lacustrine deposits of the lower part of the formation.

The Apache Canyon Formation lake probably formed in a closed basin adjacent to local block-faulted uplifts that exposed Paleozoic carbonates and Precambrian basement rocks. Marginal alluvial fan conglomerates (Glance Conglomerate) and braided-stream deposits (Willow Canyon Formation) interfinger vertically and laterally with the Apache Canyon Formation, indicating synchronicity of these environments (Figure 3B). Arkosic petrofacies of Willow Canyon and Apache Canyon Formation sandstones can be attributed to sources in local basement uplifts.

The overlying Shellenberger Canyon Formation (about 1000 m thick) consists of deltaic, fluvial, and marginal-marine facies (Figure 3B). Sandstones of the Shellenberger Canyon Formation are a transitional petrofacies that ranges in composition from lithic arkose to subarkose (Figure 4). The transitional petrofacies records a mixed provenance of basement uplift, transitional arc, and recycled quartzose sources. Volcanic detritus was probably derived from the arc terrane to the west. Quartzose debris from

the Mogollon highlands to the north and the craton to the northeast became dominant as local basement-uplift sources for arkosic debris were worn down. Marine deposits in the middle of the Shellenberger Canyon Formation are probably correlative with the Mural Limestone and suggest that the drainage divide between the northwestern and southeastern parts of the basin had foundered by mid-Cretaceous time. Northwestern and southeastern parts of the basin were joined when marine deposits topped the divide. By the time of deposition of coastal-plain and estuarine deposits of the Turney Ranch Formation, cratonic and recycled quartzose source terranes to the northeast were supplying sediment to the entire Bisbee basin.

ACKNOWLEDGMENTS

Special thanks go to Arizona students whose recent thesis research has helped us understand key Mesozoic relations in southern Arizona: Larry Archibald, Barb Beatty, Skip Buffum, Ann Bykerk-Kauffman, Bob Ferguson, Tom Goodlin, Dwight Hall, Lucy Harding, Mike Hayes, Kerry Inman, Kermit Jamison, Susanne Janecke, Chuck Kluth, Candy Krebs, Rick Leveque, Alan Lindberg, Roger Mark, Steve May, Rogelio Monreal, Steve Richard, Nancy Riggs, Rob Risley, Susan Sindlinger, Debbie Stoneman, Larry Sumpter, Peter Swift, Laurel Vedder, and Ken Yeats. Our own recent research was supported by National Science Foundation Grant EAR-8417016.

REFERENCES

- Archibald, L. E., 1982, Stratigraphy and sedimentology of the Bisbee Group in the Whetstone Mountains, Pima and Cochise Counties, southeastern Arizona [M.S. thesis]: Tucson, University of Arizona, 195 p.
- Beatty, Barbara, 1987, Correlation of some Mesozoic rebeds in southeastern Arizona [M.S. thesis]: Tucson, University of Arizona, in preparation.
- Bilodeau, W. L., 1979, Early Cretaceous tectonics and deposition of the Gance Conglomerate, southeastern Arizona [Ph.D. thesis]: Stanford, Stanford University, 145 p.
- _____, 1982, Tectonic models for Early Cretaceous rifting in southeastern Arizona: *Geology*, v. 10, p. 466-470.
- _____, 1986, The Mesozoic Mogollon highlands, Arizona; an Early Cretaceous rift shoulder: *Journal of Geology*, v. 94, p. 724-735.
- Bilodeau, W. L., and Keith, S. B., 1986, Lower Jurassic Navajo-Aztec-equivalent sandstones in southern Arizona and their paleogeographic significance: *American Association of Petroleum Geologists Bulletin*, v. 70, p. 690-701.
- Bilodeau, W. L., and Lindberg, F. A., 1983, Early Cretaceous tectonics and sedimentation in southern Arizona, southwestern New Mexico, and northern Sonora, Mexico, in Reynolds, M. W., and Dolly, E. D., eds., *Mesozoic paleogeography of the west-central United States*: Society of Economic Paleontologists and Mineralogists, Rocky Mountain Section, Rocky Mountain Paleogeography Symposium 2, p. 173-188.
- Cooper, J. R., 1971, Mesozoic stratigraphy of the Sierrita Mountains, Pima County, Arizona: U.S. Geological Survey Professional Paper 658-D, 42 p.
- Dickinson, W. R., Beard, L. S., Brakenridge, G. R., Erjavec, J. L., Ferguson, R. C., Inman, K. F., Knapp, R. A., Lindberg, F. A., and Ryberg, P. T., 1983, Provenance of North American Phanerozoic sandstones in relation to tectonic setting: *Geological Society of America Bulletin*, v. 94, p. 222-235.
- Dickinson, W. R., Fiorillo, A. R., Hall, D. L., Monreal, R., Potochnik, A. R., and Swift, P. N., 1987, Cretaceous strata of southern Arizona, in Jenney, J. P., and Reynolds, S. J., eds., *Geology of Arizona*: Arizona Geological Society Digest, v. 17 (in press).
- Dickinson, W. R., Klute, M. A., and Swift, P. N., 1986, The Bisbee basin and its bearing on late Mesozoic paleogeographic and paleotectonic relations between the Cordilleran and Caribbean regions, in Abbott, P. L., ed., *Cretaceous stratigraphy of western North America*: Society of Economic Paleontologists and Mineralogists, Pacific Section, Book 46, p. 51-62.
- Dickinson, W. R., and Suczek, C. A., 1979, Plate tectonics and sandstone compositions: *American Association of Petroleum Geologists Bulletin*, v. 63, p. 2164-2182.
- Drewes, H. D., 1971a, Mesozoic stratigraphy of the Santa Rita Mountains, southeast of Tucson, Arizona: U. S. Geological Survey Professional Paper 658-C, 81 p.
- _____, 1971b, Geologic map of the Sahuarita quadrangle, southeast of Tucson, Pima County, Arizona: U. S. Geological Survey Miscellaneous Geologic Investigations Map I-613, scale 1:48,000.
- _____, 1971c, Geologic map of the Mount Wrightson quadrangle, southeast of Tucson, Santa Cruz and Pima Counties, Arizona: U. S. Geological Survey Miscellaneous Geologic Investigations Map I-614, scale 1:48,000.
- _____, 1972a, Cenozoic rocks of the Santa Rita Mountains, southeast of Tucson, Arizona: U. S. Geological Survey Professional Paper 746, 66 p.
- _____, 1972b, Structural geology of the Santa Rita Mountains, southeast of Tucson, Arizona: U. S. Geological Survey Professional Paper 748, 35 p.
- _____, 1976, Plutonic rocks of the Santa Rita Mountains, southeast of Tucson, Arizona: U. S. Geological Survey Professional Paper 915, 75 p.
- _____, 1980, Tectonic map of southeast Arizona: U. S. Geological Survey Miscellaneous Investigations Series Map I-1109, scale 1:125,000.
- _____, 1981, Tectonics of southeastern Arizona: U. S. Geological Survey Professional Paper 1144, 96 p.
- Hayes, M. J., 1987, Sedimentology, stratigraphy, and paleogeography of the Upper Cretaceous Fort Crittenden Formation in southeastern Arizona, in Dickinson, W. R., and Klute, M. A., eds., *Mesozoic geology of southern Arizona and adjacent areas*: Arizona Geological Society Digest, v. 18 (in press).
- Hayes, P. T., 1970a, Mesozoic stratigraphy of the Mule and Huachuca Mountains, Arizona: U. S. Geological Survey Professional Paper 658-A, 28 p.
- _____, 1970b, Cretaceous paleogeography of southeastern Arizona and adjacent areas: U. S. Geological Survey Professional Paper 658-B, 42 p.
- Hayes, P. T., and Landis, E. R., 1964, Geologic map of part of the Mule Mountains, Cochise County, Arizona: U. S. Geological Survey Miscellaneous Geologic Investigations Map I-418, scale 1:48,000.
- Hayes, P. T., and Raup, R. B., 1968, Geologic map of the Huachuca and Mustang Mountains, southeastern Arizona: U. S. Geological Survey Miscellaneous Geologic Investigations Map I-509, scale 1:48,000.
- Hayes, P. T., Simons, F. S., and Raup, R. B., 1965, Lower Mesozoic extrusive rocks in southeastern

- Arizona -- the Canelo Hills Volcanics: U. S. Geological Survey Bulletin 1194-M, 9 p.
- Inman, K. F., 1987, Depositional environments and sandstone petrography of Upper Cretaceous sedimentary rocks, Adobe Canyon, Santa Rita Mountains, southeast Arizona, *in* Dickinson, W. R., and Klute, M. A., eds., Mesozoic geology of southern Arizona and adjacent areas: Arizona Geological Society Digest, v. 18 (in press).
- Jamison, K., 1983, The depositional environment and petrographic analysis of the Lower Cretaceous Morita Formation, Bisbee Group, southeastern Arizona and northern Sonora, Mexico [M.S. thesis]: Tucson, University of Arizona, 157 p.
- Kluth, C. F., 1982, Geology and mid-Mesozoic tectonics of the northern Canelo Hills, Santa Cruz County, Arizona [Ph.D. thesis]: Tucson, University of Arizona, 245 p.
- _____, 1983, Geology of the northern Canelo Hills and implications for the Mesozoic tectonics of southeastern Arizona, *in* Reynolds, M. W., and Dolly, E. D., eds., Mesozoic paleogeography of the west-central United States: Society of Economic Paleontologists and Mineralogists, Rocky Mountain Section, Rocky Mountain Paleogeography Symposium 2, p. 159-171.
- Kluth, C. F., Butler, R. F., Harding, L. E., Shafiqullah, M., and Damon, P. E., 1982, Paleomagnetism of Late Jurassic rocks in the northern Canelo Hills, southeastern Arizona: *Journal of Geophysical Research*, v. 87, p. 7079-7086.
- Knepp, R. R., 1980, Columnar stratigraphic section of a part of the Willow Canyon Formation of the Cretaceous Bisbee Group, Santa Rita Mountains, Pima County, Arizona: Tucson, University of Arizona, Department of Geosciences, unpublished course report.
- Krebs, C. K., 1987, Geochemistry of the Canelo Hills Volcanics and implications for the Jurassic tectonic setting of southeastern Arizona, *in* Dickinson, W. R., and Klute, M. A., eds., Mesozoic geology of southern Arizona and adjacent areas: Arizona Geological Society Digest, v. 18 (in press).
- Lipman, P. W., and Sawyer, D. A., 1985, Mesozoic ash-flow caldera fragments in southeastern Arizona and their relation to porphyry copper deposits: *Geology*, v. 13, p. 652-656.
- Mack, G. H., Kolins, W. B., and Galemore, J. A., 1986, Lower Cretaceous stratigraphy, depositional environments, and sediment dispersal in southwestern New Mexico: *American Journal of Science*, v. 286, p. 309-331.
- Risley, R., 1987, Sedimentation and stratigraphy of the Lower Cretaceous Amole Arkose, Tucson Mountains, Arizona, *in* Dickinson, W. R., and Klute, M. A., eds., Mesozoic geology of southern Arizona and adjacent areas: Arizona Geological Society Digest, v. 18 (in press).
- Scott, R.W., 1979, Depositional model of Early Cretaceous coral-algal-rudist reefs, Arizona: *American Association of Petroleum Geologists Bulletin*, v. 63, p. 1108-1127.
- Simons, F. S., 1972, Mesozoic stratigraphy of the Patagonia Mountains and adjoining areas, Santa Cruz County, Arizona: U. S. Geological Survey Professional Paper 658-E, 23 p.
- Sindlinger, S., 1981, Facies variations in the lower Mural Limestone, southeastern Arizona [M.S. thesis]: Tucson, University of Arizona, 75 p.
- Tosdal, R. M., Haxel, G. B., and Wright, J. E., 1987, Jurassic geology of the Sonoran Desert region, southern Arizona, southeast California, and northernmost Sonora; construction of a continental-margin magmatic arc, *in* Jenney, J. P., and Reynolds, S. J., eds., *Geology of Arizona: Arizona Geological Society Digest*, v. 17 (in press).
- Vedder, L. K., 1984, Stratigraphic relationships between the Jurassic Canelo Hills Volcanics and the Glance Conglomerate, southeastern Arizona [M.S. thesis]: Tucson, University of Arizona, 129 p.
- Warzeski, E. R., 1983, Facies patterns and diagenesis of a Lower Cretaceous carbonate shelf; northeastern Sonora and southeastern Arizona [Ph.D. thesis]: Binghamton, State University of New York, 401 p.
- Wilson, E. D., Moore, R. T., and Cooper, J. R., 1969, Geologic map of Arizona: Arizona Bureau of Mines and U. S. Geological Survey, scale 1:500,000.

Lower Cretaceous Coral-Algal-Rudist Patch Reefs in Southeastern Arizona¹

Joseph F. Schreiber, Jr.
Department of Geosciences
University of Arizona
Tucson, Arizona 85721

Robert W. Scott
Amoco Production Company
Post Office Box 3385
Tulsa, Oklahoma 74102

INTRODUCTION

Patch reefs constructed primarily of corals and encrusting algae developed extensively across a shallow shelf at the northern end of the Chihuahua Trough in Mexico and Arizona during the Early Cretaceous. These reefs and associated environments comprise facies of the lower Albian Mural Limestone (Hayes, 1970b). The reefs are located in the Bisbee Basin of several authors (Bilodeau and Lindberg, 1983; Dickinson and others, 1987). Although the Bisbee Basin contains marine, marginal marine, and abundant nonmarine strata, the patch reefs are concentrated in the southern third of Cochise County (Figure 1). They are up to 25 m thick and about 1.5 km long and thus small in extent and probably oval to ellipsoidal in shape. These reefs are good examples of the Caribbean Cretaceous patch reefs described by Kauffman and Sohl (1974, p. 443).

The regional setting was a carbonate shelf sloping gently southward into Mexico (Warzeski, 1979). Mural Limestone strata were deposited during the major marine transgression into the Bisbee Basin from the southeast-trending Chihuahua Trough. Morita Formation nonmarine and marginal-marine rocks underlie the Mural (Figure 2). The Cintura Formation overlies the Mural with strata that are very similar to those of the Morita. The Morita-Mural-Cintura sequence attains a combined maximum thickness of 2050 m in the Mule Mountains (see Figure 1 for location), but the Mural Limestone is only 150-250 m of this thickness.

The same sandwiching of the Mural Limestone between dominantly nonmarine formations occurs in a swath 125 km in length across southeastern Arizona. A similar arrangement 60 km to the east in southwest New Mexico is seen in the Hell-to-Finish - U-Bar (Mural Limestone equivalent) - Mojado Formations sequence of the Big Hatchet Mountains.

Current studies place the Bisbee Basin between an active magmatic arc to the southwest and the Mogollon Highland of central Arizona and west-central New

Mexico to the north-northeast (Dickinson and others, 1986).

The reefs exhibit a biotic succession from the pioneer *Actinastrea* community to the reef framework *Microsolena-stromatolite* community, which is succeeded by the final reef flat *Coalcomana-Petalodontia* community (Scott and Brenckle, 1977). Several important reef niches were occupied by encrusting corals; blue-green, red, and green algae; boring algae, sponges and bivalves; and sediment-trapping corals, caprinid, and thick-walled monopleurid rudists. Various growth forms of corals and algae and the interactions among the reefal organisms indicate that these reefs were complex and diverse ecosystems. This complexity implied a relatively stable, predictable environment.

These patch reefs developed upon a shallow shelf substrate of mollusk-miliolid-orbitolinid muds, now wackestone and packstone (Scott, 1979). In the reef core facies, corals comprise 10-60% of massive beds that are 3-28 m thick, and rudists comprise 10-15% and rarely up to 48% of the same units. The reefs grade laterally into flank facies of coral-rudist fragment sands, which grade up slope (northwestward) into peloid-oid sands (grainstone). Landward (north and west) of this shoal-bank complex was a shallow lagoon represented by mollusk-miliolid-orbitolinid packstone that grades landward into the ostracod-mollusk-skeletal algal wackestone and sandstone-mudstone of the restricted lagoon.

Bisbee Group Stratigraphy

The Morita Formation, Mural Limestone, and Cintura Formation, together with the Glance Conglomerate, which underlies the Morita, comprise a single, major transgressive-regressive cycle of deposition at the northwestern end of the Chihuahua Trough. These four units make up the Bisbee Group (Hayes, 1970a). Although its upper and basal parts are unfossiliferous, this group probably ranges in age from Neocomian to Albian (Hayes, 1970b). The lateral relations of these units have been discussed by Hayes (1970b).

The Mural Limestone (Ransome, 1904), 150 to 250 m thick, is predominantly limestone, with subordinate amounts of shale and sandstone (Figure 2). At the type locality on Mural Hill near Bisbee (Hayes, 1970a), the Mural is divided into two members. The lower member is from 91 to 160 m thick (Hayes, 1970a) and consists of thin interbeds of shale, mudstone, siltstone, sandstone, and fossiliferous limestone. The base is placed at the top of the uppermost prominent sandstone bed of the Morita Formation. This

¹Portions of this field-trip guide are taken from journal articles by R.W. Scott (1979, 1981) and reprinted here with minor revisions with the permission of the American Association of Petroleum Geologists and the editor of the Journal of Paleontology, respectively.

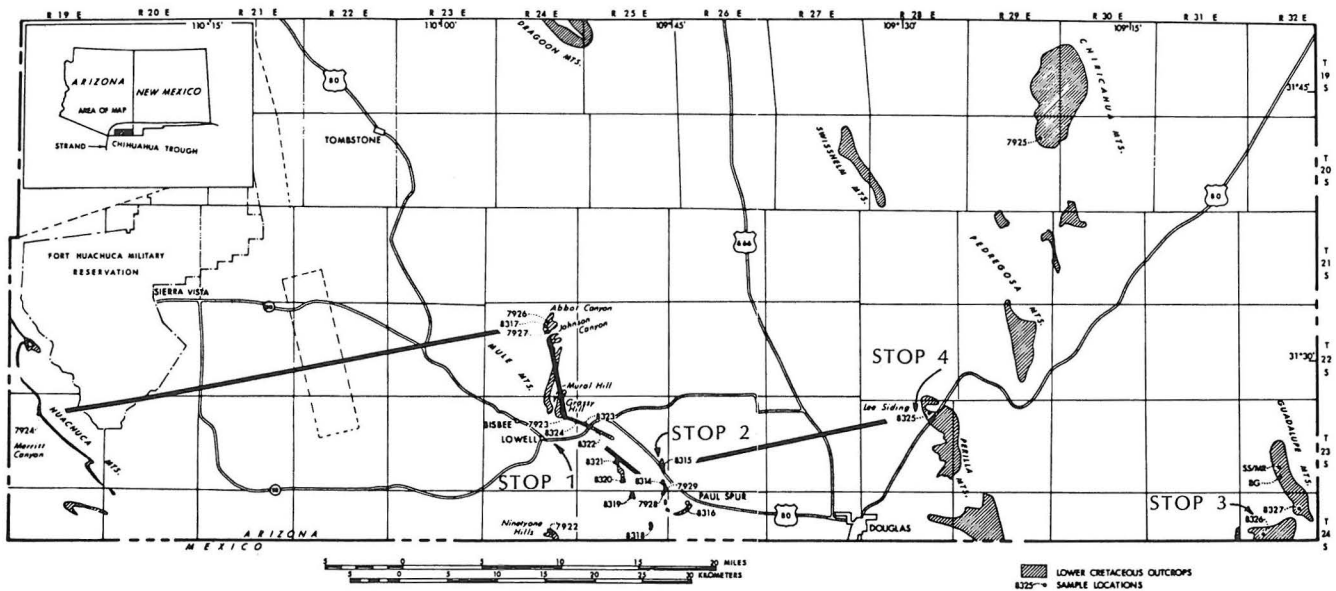


Figure 1. Index map showing outcrops of Mural Limestone in southern Cochise County. Scott's (1979, p. 1127) sample localities are designated by numbers; SS/MR and BG are localities from Grocock (1975). Heavy lines indicate section in Figure 5. (Adapted from Scott, 1979).

contact is conformable and probably is intertongued over several kilometers. The upper member is massive to thin-bedded, cliff-forming limestone 50 to 75 m thick. At many places, lenticular massive limestone buildups occupy the lower part of the upper Mural. In the central part of the Mule Mountains, the massive-bedded limestone is tabular and gradually thins northward. Most of the lenticular buildups are southeast of this tabular mass. The basal contact of the upper Mural is picked at the base of the massive to thick-bedded, resistant limestone above the green-gray shale and sandstone of the lower Mural. The conformable contact is sharp, but it is intertongued along the scarp just north of U.S. Highway 80 and 3.3 miles (5.3 km) east of Bisbee. In places, the basal beds are orbitolinid-rich limestone interbedded with thin shale. Commonly this contact is covered by talus.

The underlying Morita Formation is 780 to 1260 m thick (Hayes, 1970a) and consists of brown sandstone, conglomerate, maroon mudstone and siltstone, greenish-gray shale, and thin limestone beds. The Morita was deposited on a coastal plain in alluvial-channel, overbank, lacustrine, deltaic, and tidal-flat environments (Hayes, 1970a).

The overlying Cintura Formation is up to 540 m thick (Hayes, 1970a) and consists mainly of shale, mudstone, and sandstone. Thin sandy limestone beds are intercalated in the basal part. Sandstone channel fills and maroon shales are common in the upper part. The base of the Cintura is placed at the top of the thick, continuous limestone sequence of the upper Mural. The contact is sharp but conformable. The Cintura was deposited in nearshore, deltaic, and alluvial-plain environments (Hayes, 1970a).

The Glance Conglomerate is the basal formation of the Bisbee Group. In the Mule Mountains it consists of poorly sorted cobbles and pebbles in a reddish-brown sandy mudstone matrix. At all locations the detrital clasts reflect the composition of the underlying bedrock, which may include Precambrian schist,

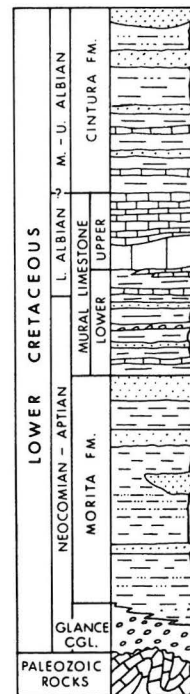


Figure 2. General stratigraphic section of Lower Cretaceous rocks in the Mule Mountains-Douglas area of southeastern Arizona (from Scott, 1979).

Paleozoic sedimentary rocks, and a Jurassic-age granite (Hayes and Landis, 1964; Hayes, 1970a). Because the bedrock surface is so highly irregular, thickness is also highly variable -- zero to several hundred feet in the Mule Mountains, but greater in other mountain ranges (Hayes, 1970a). The Glance Conglomerate grades upward into the Morita Formation.

Mural Limestone and Related Studies: Building Blocks for a Field Trip

Studies of Lower Cretaceous rocks in the southeasternmost corner of Arizona and adjacent Sonora during the past 10 years have emphasized the Mural Limestone. The first definitive study was by Scott and Brenckle (1977) on the biotic zonation of Mural patch reefs. It was followed closely by Scott's (1979, 1981) two detailed studies, which proposed a depositional model for these complex reefs and further described the biotic relations, respectively.

The first University of Arizona contribution was Gretchen H. Roybal's 1979 M.S. thesis on the facies relationships displayed on erosional surfaces in a patch reef located on U.S. 80 just west of Paul Spur. Three other M.S. theses followed. Robert C. Ferguson (1983) worked with the Mural Limestone and the underlying Morita Formation in the Guadalupe Canyon area, which is located in the extreme southeast corner of Arizona and immediately adjacent to the U.S.-Mexico border.

Rogelio Monreal (1985), building on Scott's (1979) earlier work, mapped in detail the patch reef most splendidly exposed in the abandoned lime quarry located near Lee Siding northeast of Douglas. William E. Malvey (M.S. thesis in progress) is investigating the lower member of the Mural across the southern end of Cochise County in order to better define the transition from lower to upper Mural deposition. These last three theses also explore the diagenesis of the carbonate and terrigenous rocks.

E. Robert Warzeski (1983) studied the upper Mural Limestone in southeastern Arizona and northeastern Sonora. He recognized a significant lithologic change as he followed the informal upper member southward into Mexico, and based upon these findings he established five new formal members in Sonora. These members form two sequential barrier-reef banks at the southernmost exposed Mural platform margin just 15-30 km south of Douglas, Arizona.

Several authors have reviewed the stratigraphy of the Lower Cretaceous Bisbee Group, which includes the Mural Limestone. The papers by Bilodeau and Lindberg (1983) and Dickinson and others (1987) are particularly recommended. Dickinson and others (1986) most recently focused on the tectonic setting of the Bisbee Basin; this paper is also highly recommended.

This trip will build upon the work of the authors cited above. The purpose of the trip is to study firsthand on the outcrop the coral-algal-rudist patch reefs and to tie the reefs into the other lithofacies of the Mural. We, the trip leaders, expect the participants to recognize in particular an alternate paleoecologic model to the rudist-dominated reefs of other regions, and in general to gain useful knowledge of Cretaceous patch reefs that may be applied on the surface and in the subsurface elsewhere in the world.

The four stops are located in a band that covers approximately 360 sq km in southern Cochise County (Figure 1). After a brief introduction the Mural Limestone is easily recognized by its bold outcrops in low hills and on the flanks of several mountain ranges. In the semiarid climate the rock faces are etched so that much fine and coarse textural detail is visible on the outcrop. This feature makes color

photography very easy and rewarding. Ample time will be allowed at each stop for discussion, questions, collecting, and photography.

This guidebook is by necessity short. Since the trip leaders recognize the importance of bringing together some of the pertinent literature on the Mural Limestone patch reefs and related rocks, a supplement to this guidebook will be distributed to participants. The supplement will contain R.W. Scott's 1979 and 1981 journal articles; G.H. Roybal's 1981 paper from *The Mountain Geologist*; abstracts or extended abstracts by E.R. Warzeski (1986), R.W. Ferguson (1986), R. Monreal (1986), and W.E. Malvey (1986); and newer contributions from R.C. Ferguson, R.W. Scott, and E.R. Warzeski.

Itinerary

Friday, October 23, 1987

- 07:30 Depart Tucson and proceed via Interstate 10 (I-10), State 90, and U.S. 80 to Bisbee (brief rest stop at the Lavender Pit); continue eastward on U.S. 80 to stop 1. See Figure 3.
- 10:00 Stop 1: Mural facies at Grassy Hill in Mule Gulch.
- 12:00 Stop 2 and lunch stop: Paul Spur patch reefs.
- 16:30 Depart stop 2 for Douglas; accommodations for October 23 and 24 will be at the Gadsden Hotel; assemble after supper at 19:30 for brief talks and a slide show.

Saturday, October 24, 1987

- 08:00 Depart Douglas and proceed via 15th Street, the Geronimo Trail, and ranch roads to Guadalupe Canyon.
- 09:30 Stop 3: Mexican Saddlehorn locality for a lower and upper Mural Limestone section; lunch in the field.
- 16:30 Ranch-style cookout in Guadalupe Canyon.
- 18:30 Depart Guadalupe Canyon Ranch for Douglas.

Sunday, October 25, 1987

- 08:00 Depart Douglas via U.S. 80 and proceed northeast to stop 4.
- 08:30 Stop 4: Abandoned lime quarry at Lee Siding.
- 10:30 Return to Tucson via U.S. 80, Tombstone, and I-10; lunch en route.
- 14:00 Arrive in Tucson and transfer to other vehicles for the trip to Phoenix; arrive in Phoenix at approximately 16:30.

GEOLOGIC HIGHLIGHTS — TUCSON TO BISBEE

Because the purpose of this trip is to spend as much time as possible on Mural Limestone outcrops, stops will not be made between Tucson and Bisbee. However, we are passing through Basin and Range country, which contains not only some classic geology but also its own unique scenery. The geologic highlights and prominent geographic features will be pointed out by vehicle drivers while en route to Bisbee. Also see Figure 3. Several geologic highlights are also described in later paragraphs. It seems appropriate to describe first the Basin and Range general topographic and geologic setting. Much of this description is taken from the recent and excellent book chapter by Damon and others (1984).

The trip route from Tucson to Bisbee lies in the Southern Basin and Range Province and almost entirely in the Eastern Mountain subprovince of southeastern Arizona. Only Tucson is in the Sonoran Desert sub-

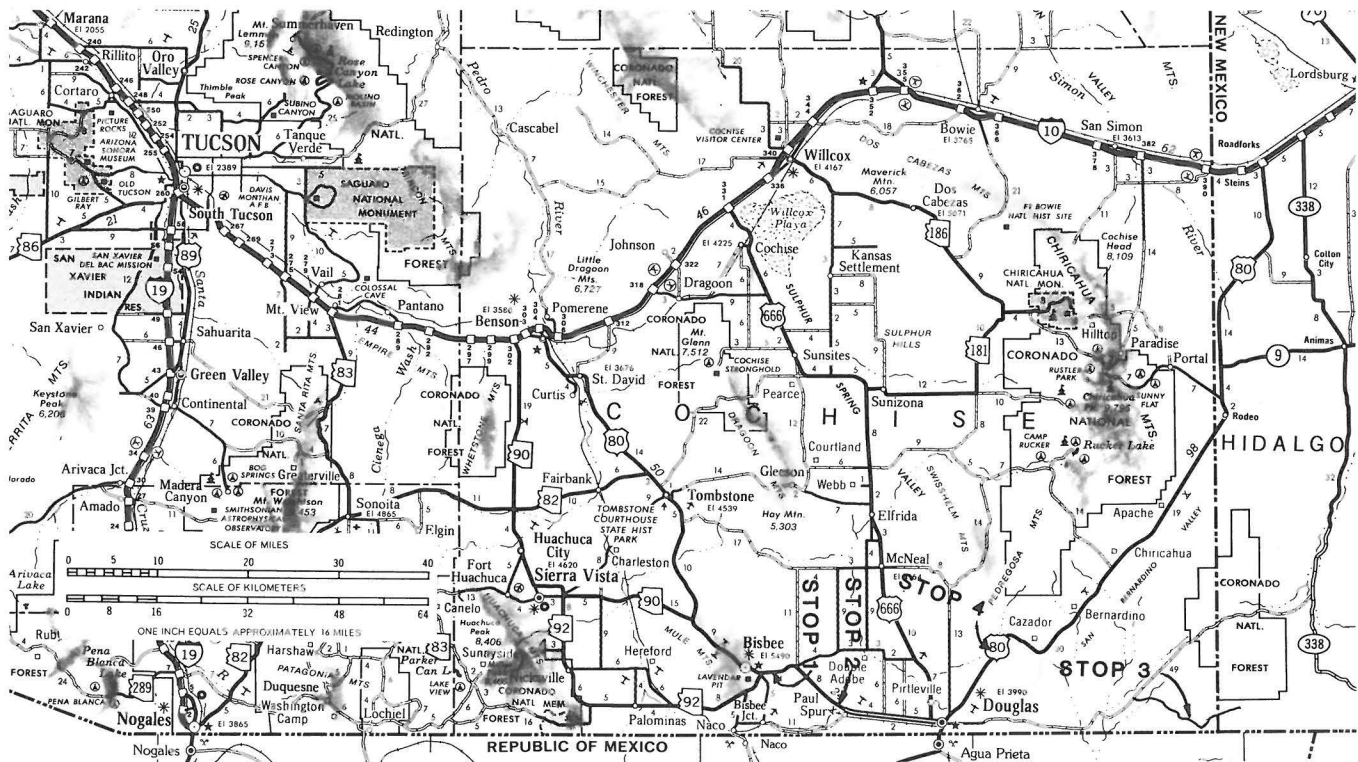


Figure 3. Location map and stops 1-4 -- Tucson to the Douglas area (courtesy of the Arizona Highways Magazine).

province. The Eastern Mountain region is characterized by valleys that are much narrower than the adjacent mountain ranges and valley-floor elevations of more than 800 meters (Damon and others, 1984). Indeed the mountains seem to rise abruptly from the desert basins. The earliest attempts to explain this physical feature relied upon "basin subsidence along faults to form series of horsts and grabens" (Damon and others, 1984, p. 179). Today the basin and mountain topography is explained by listric normal faults that "have steep dips at the surface but flatten out at depth" (Damon and others, 1984, p. 180). R.E. Anderson (1971) first recognized the role of these shallow dipping and curved faults, which he termed "listric normal faults." The steep dips seen in some mountain ranges may be explained by having originally horizontal strata rotate to steeper dips by movement along the curved fault planes (Anderson, 1971; Proffitt, 1977). This model has been applied very successfully to southeastern Arizona geology.

The modern landscape is chiefly the product of vertical movements without much rotation and basin filling in the past 12 to 15 m.y. (Damon and others, 1984, p. 182-190). These authors also recognized an earlier mid-Tertiary orogeny that developed a rugged landscape, led to thick, rapidly deposited basin fills, and even produced rotation of some of the basin-fill sediments. In order to arrive at the 12- to 15-m.y. date they used the ages of the youngest tilted volcanic flows and the oldest flat-lying volcanic flows in various places to establish the close of rotational tectonics.

We will be heading southeast when we enter I-10 at the Kolb Road exit. The Santa Rita Mountains are to the southeast and to the north and east-northeast are the Santa Catalina and Rincon Mountains, respectively. About 20 miles east of Tucson and beginning at Milepost 284, or just before the bridge over Davidson Canyon, the roadcuts expose chiefly the

eastward-dipping beds of the Pantano Formation. The Pantano outcrops continue for several miles and expose alluvial-fan deposits, lake beds, and volcanic rocks. An andesite flow separates the alluvial fan and lake beds at several locations. Plagioclase from the andesite has been dated at 24.93 m.y. A rhyolite tuff with a radiometric date of 36.7±1.1 m.y. disconformably underlies the Pantano. These dates indicate that deposition occurred during Oligocene to early Miocene time (Balcer, 1984). The total thickness of the Pantano Formation is 1250 m, but the thickness exposed along I-10 is much greater because parts of the section are repeated by faulting.

The trip route takes a right turn (south) at Exit 302 on Arizona 90, which follows the west side of the San Pedro Valley and parallels the Whetstone Mountains for the next 15 miles (24 km). Arizona 90 leads to Fort Huachuca and Sierra Vista before trending south-eastward toward Bisbee. Numerous roadcuts for the next 4 miles are in a late Pleistocene coarse alluvium. Gray (1967) called this alluvium "granite wash" since it consists chiefly of coarse granitic debris derived from the Precambrian rocks located at the north end of the Whetstone Mountains; Cambrian quartzite clasts are also abundant.

The St. David Formation underlies this alluvium and crops out in badland topography on both sides of the San Pedro River in the valley to the east. Fine-grained fluvial sediments and smaller quantities of sand, gravel, pyroclastic units, and paleosols make up most of the formation (Gray, 1967). A few freshwater limestones and clays contain algae, ostracods, and mollusks and suggest deposition in small lakes and ponds. Sediments exposed on the surface total 183 m, but deep water wells in the valley suggest a total thickness of more than 490 m. The age of the St. David Formation is late Pliocene-middle Pleistocene based upon a well-studied vertebrate fauna (Lindsay and Tessman, 1974; Lindsay, 1978); recognition of

magnetic polarity zones (Johnson and others, 1975); and dates on ash beds of 2.01 m.y. (mean of several K-Ar ages) and 3.1±0.7 m.y. (fission track-zircon) at the Post Ranch and California Wash localities, respectively (Izett, 1981).

The Whetstone Mountains contain some of the most complete sections of relatively undisturbed Paleozoic rocks in southern Arizona. French Joe Canyon road, located 9.4 miles (15 km) south of I-10, provides access to a well-exposed lower Paleozoic section. The large butte on the north side of the canyon is capped by the Bolsa Quartzite (Cambrian). Other formations, including the Abrigo Formation (Cambrian) and the Martin Limestone (Devonian), are difficult to see from Arizona 90, but are well exposed in the lower slopes behind the butte. The higher cliffs are chiefly limestones of Mississippian and Pennsylvanian age. The Mississippian Escabrosa Limestone, Black Prince Limestone (Morrowan), and the Pennsylvanian-Permian Naco Group rocks are more accessible in Dry Canyon, which is the next large canyon about 2 miles (3.2 km) to the south. Included in the Naco Group are the Horquilla Limestone (Pennsylvanian), Earp Formation (Pennsylvanian-Permian), Colina Limestone (Wolfcampian-early Leonardian), Epitaph Formation, Scherrer Formation, Concha Limestone (Leonardian-early Guadalupian), and the Rainvalley Formation.

The Mustang Mountains, located immediately south of the Whetstones, contain similar sections of the Naco Group. In addition, the higher peaks to the south of Arizona 82 are capped by Triassic and Jurassic volcanics and sedimentary rocks (Hayes and Raup, 1968).

The trip route continues south and crosses Arizona 82 at Whetstone Junction. Straight ahead in the distance are the Huachuca Mountains. To the east or left are Tombstone and the Tombstone Hills. Our route turns east at Sierra Vista and crosses the San Pedro Valley before joining U.S. 80 13.2 miles (21.2 km) northwest of downtown Bisbee.

U.S. 80 passes through numerous road cuts of Bolsa Quartzite and Abrigo Formation (both Cambrian) quartzites, fine-grained clastics, and limestones; Pinal Schist (Precambrian); and Juniper Flat Granite (Jurassic). Our vehicle caravan will slow down as we approach Bisbee so that you may appreciate this town's unusual location. A brief rest stop will be taken at the Lavender Pit overview of the Phelps Dodge Corporation. The brightly colored oxidized outcrops seen on the left side of the highway as we approach the Lavender Pit are alteration zones related to porphyry copper mineralization in alkali granite of the Jurassic Sacramento stock. Jan C. Wilt prepared the following summary of the geology of the Lavender Pit:

The upper benches of the southeast pit wall are in maroon outcrops of the Gance Conglomerate (Lower Cretaceous). The Gance rests depositionally on the Jurassic Sacramento stock in the greenish brown outcrops of the lower benches. The southwest pit wall is contact-altered Horquilla Limestone, Earp Formation and Colina Limestone (upper benches), which are overlain by Gance Conglomerate. The entire south wall of Lavender Pit has been downfaulted along the west-northwest-striking Dividend fault which traces through the center of the pit. The north wall of the pit is in upthrown Pinal Schist and is intruded by the Sacramento stock of Jurassic age. The operation closed in 1975, although leaching of the tailings and workings continued.

UPPER MURAL LIMESTONE FACIES AND ENVIRONMENTS

Rocks of the upper Mural have been divided into mappable facies and microfacies (Figure 4) by Scott (1979). The mappable facies are sequences of beds, each characterized by a predominant lithology and set of carbonate microfacies. The sequences are named on the basis of the textural classes of Dunham (1962) modified by the two or three most abundant allochems. Regional relations of the facies are shown in Figure 5. Five depositional environments also have been interpreted by analysis of facies and stratigraphic relations.

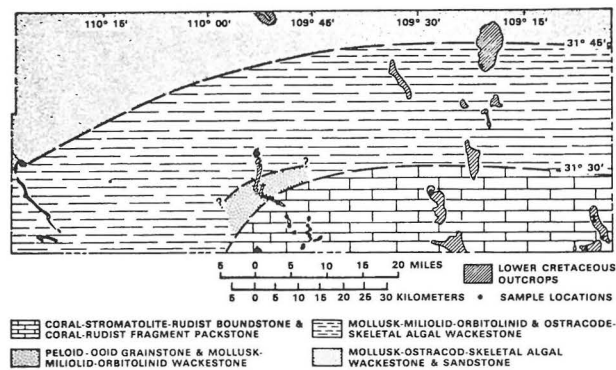


Figure 4. General facies distribution map of upper Mural Limestone (from Scott, 1979). The Mule Mountains-Paul Spur outcrops are located just west of longitude 109°45' west.

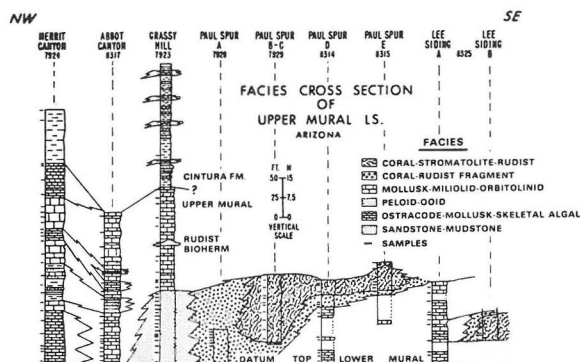


Figure 5. Northwest-southeast facies cross section of upper Mural Limestone (from Scott, 1979). See Figure 1 for line of section.

Scott's (1979) detailed descriptions of the facies and environments may be read in the supplement to this field guide. The section dealing with a depositional model for Mural reefs is also highly recommended.

STOP 1. MURAL FACIES AT GRASSY HILL

Stop 1 is about 2-1/4 miles (3.6 km) from the Lavender Pit. Leave the Lavender Pit overlook headed south or downhill on U.S. 80; mileage begins at the underpass on U.S. 80. Follow traffic circle around to exit east to Douglas on U.S. 80. Watch for Gance

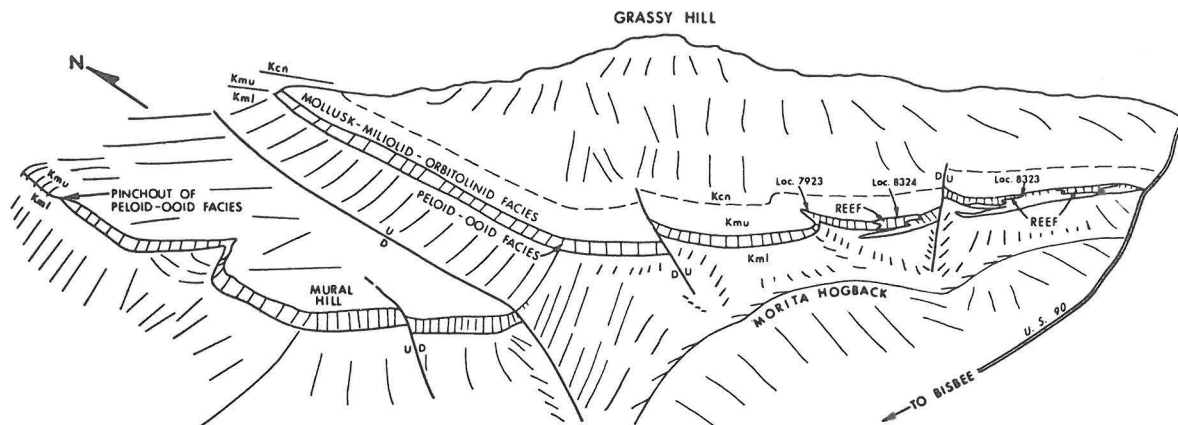


Figure 6. Geometry of Mural Limestone facies at Grassy Hill in Mule Mountains near Bisbee (from Scott, 1979). Sketch shows reefs, intertonguing, and pinchout of peloid-oid facies over a distance of 4.5 km. Formation symbols are: Kmu, upper Mural; Kml, lower Mural; Kcn, Cintura Formation.

Conglomerate outcrops on the south side of the circle and eastward to the exit. The vehicle caravan will stop and park near the intersection of U.S. 80 and Warren road, which enters from the south. This intersection is 1.8 miles (2.9 km) from the underpass and south of Grassy Hill, the highest point to the north.

The purpose of stop 1 is to study the Mural facies seen in cliffs and on slopes below Grassy Hill. In addition parts of the Morita and Cintura Formations may be studied. Figure 6 is a sketch of the geometry of the Mural facies below Grassy Hill. This stop also serves as an introduction to the scale of the facies seen in the Mural Limestone. A copy of the U.S. Geological Survey Map I-418 -- "Geologic Map of the Southern Part of the Mule Mountains, Arizona, Cochise County, Arizona" by P.T. Hayes and E.R. Landis (1964) -- is available for study. This is a short stop.

The upper Mural Limestone is easily recognized as the prominent cliff and bench former below the reddish-colored beds of the Cintura Formation, which also caps Grassy Hill. Several normal faults, which strike N. 20-30° E. and are all down to the northwest, offset the upper Mural beds. The upper Mural is about 82 m thick here (Warzeski, 1983). Slopes below the cliff contain the less resistant sandy limestone, sandstone, siltstone, and shale of the lower Mural, which is about 131 m thick here (Warzeski, 1983). Dips in the Mural at this location are 20-40° north-easterly, but only 1 mile eastward, where the Mural beds cross U.S. 80, the dip has steepened to 80° northeast to slightly overturned.

The prominent Mural cliff is formed by a thick peloid-oid grainstone shoal facies (Scott, 1979, p. 1112, 1116, 1117; see the complete lithologic description in the supplement). This facies is up to 31 m thick, pinches out to the north and south, overlies the dominantly clastic facies of the lower Mural, and underlies the thin-bedded mollusk-miliolid-orbitolinid facies comprising the upper part of the upper Mural. Warzeski (1983, p. 160) suggests a width of the shoal of 4 to 8 km, and perhaps even greater, but a more accurate determination is complicated by faulting. Figure 5 is a facies cross section of the upper Mural Limestone in which the peloid-oid grainstone facies may be seen grading into the coral-rudist fragment facies.

Figure 6 also shows the location of the two hillslopes to the east where the upper and lower Mural intertongue; these are Scott's (1979) localities 8323 and 8324.

GEOLOGIC HIGHLIGHTS EN ROUTE TO STOP 2

The trip route continues eastward on U.S. 80 and passes through the roadcut where the upper Mural beds are almost vertical to slightly overturned. At this point the road turns north and passes between hills made up of Cintura Formation outcrops for a distance of 3/4 mile (1.2 km). We exit Mule Gulch at a distance of 4.4 miles (7.1 km) from the underpass. Ahead is a good view of the Sulphur Springs Valley with the more distant Chiricahua, Swisshelm, and Pedregosa Mountains at about 11 o'clock.

The highway bends sharply southeast and is on Quaternary alluvium for the next 5.7 miles (9.2 km) to the point where the highway passes between two low hills or buttes of upper Mural Limestone. While en route to this point, outcrops of the Mural Limestone and Morita Formation can be seen in the hills to the right or southwest.

We are now at the Paul Spur locality of Scott and Brenckle (1977), Roybal (1979), and Scott (1979). Douglas is 12 miles (19.3 km) by highway to the east. The only nearby prominent landmark is the lime quarry at Paul Spur, which is located in the hill of upper Mural Limestone about 2 miles (3.2 km) to the south-southeast.

This is a long stop that actually begins at the south end of the southern butte. We therefore continue east on U.S. 80 for 0.9 mile (1.4 km) before turning right onto a gravel road that shortly turns right or west again to parallel the Phelps Dodge Corporation powerline. This road leads into Glance Creek. We park on the north side of the road opposite the south end of the butte.

STOP 2. PAUL SPUR PATCH REEFS

We are now located at the south end of the southern butte in the northeast corner of section 1, T. 24 S., R. 25 E., of the Bisbee quadrangle (15-minute series, 1958). The two buttes adjacent to U.S.

80, the smaller hill to the south, and the large hill farther south-southeast at the Paul Spur lime quarry are sometimes referred to as the Paul Spur ridge.

The purpose of stop 2 is to examine in some detail the three facies exposed in the two buttes. These facies include the coral-stromatolite-rudist (C-S-R) boundstone, the coral-rudist (C-R) fragment, and the mollusk-miliolid-Orbitolina (M-M-O) wackestone facies. Complete lithologic descriptions of these facies may be found in Scott (1979) in the supplement. These descriptions are supplemented later by some detailed observations of Warzeski (1983).

Southern Butte

The highest part of the southern butte displays two successive reefs of the C-S-R boundstone reef core facies in a cliff face. Height of the cliff face is about 15 m, but the upper reef is only about 5 m thick. The upper reef preserves chiefly reef core because of modern erosion. A photograph of the cliff is shown in Scott's Figure 9 (1979, p. 1114) along with two east-west cross sections that show relative abundance of fossils and a facies interpretation, respectively. The latter two sections are reproduced in Figure 7 of this field guide.

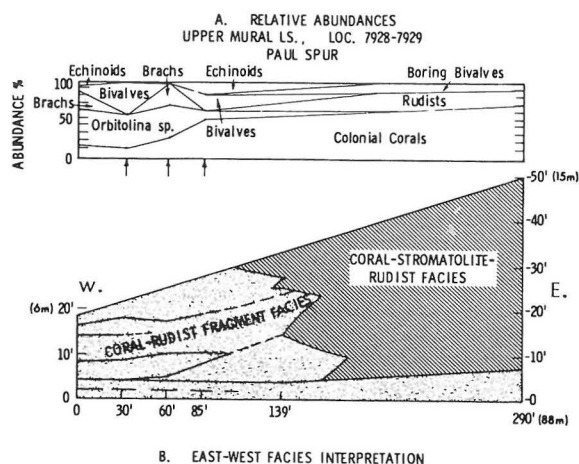


Figure 7. East-west cross section of south end of Paul Spur reef -- Scott's localities 7928 and 7929 (from Scott, 1979). A gives relative abundance of fossils; B is a facies interpretation. Footages at base of section are sampling points.

The lower reef, with its flanking facies, is more extensive. Figure 8 is a south-north cross section through the reefs at Paul Spur. These facies rest on lower Mural beds that make up the rubbly slope in the foreground. Actually, lower Mural beds are well exposed in outcropping beds on the slope and in several pits below the higher parts of the cliff.

Warzeski (1983) has shown the biotic makeup of Mural boundstone to be somewhat variable and has distinguished several distinct assemblages. This reef core is a coral-stromatolite boundstone with some rudists (caprinids). He describes this boundstone as follows (1983, p. 84):

Coral-stromatolite boundstone comprises platy, branching colonies of the coral Microsolena overlain by smooth, finely

laminated stromatolites a few mm to 15 cm in thickness Sparse caprinids are found nestled within or under the edges of Microsolena colonies. Small white dome-shaped bryozoans and pedunculate brachiopods are attached to the undersides of Microsolena plates. A second coral, Actinastrea, has a massive, irregular to tabular growth habit and occurs in the lower meter or two of coral-stromatolite boundstone reef cores. Coral-stromatolite boundstone grades upward into a more diverse faunal assemblage including Toucasia and Petalodontia (rudists), Calamophyllia and Ciadophyllia (branched corals), and Myriophyllia (a meandroid head coral), which contains only sparse stromatolites.

We will be able to recognize most of the components in the southern and northern buttes.

Microsolena has been misinterpreted in the past as a stromatoporoid, a hydrozoan, and even as a calcisponge (Scott, 1979, p. 1126; Warzeski, 1983, p. 87). Scott (1981) discusses in detail the growth forms and niches of corals (massive-tabular, lamellar, and branching forms), algae, and rudists, and the role of boring organisms (see the supplement).

Warzeski also describes in some detail the role of other organisms (1983, p. 86-87):

Common accessory organisms in all of these boundstone types include: bryozoans, pedunculate brachiopods, boring bivalves, boring sponges and laminar encrusting algae. Several types of bryozoans occur, notable [sic] a white, ball-like bryozoan which is found attached to undersides of platy corals and, in sizes up to 10 cm across, as loose balls. (Some of these may be Solenopora, a red algae). Pedunculate brachiopods were found in apparent growth position beneath platy corals. Numerous boring bivalves were found in their borings, and the distinctive galleries of boring clinoid sponges are common. Faceted, very fine sand- to silt-size chips produced by sponges as they excavate borings are a common constituent of sediment within and surrounding reefs, and in two cases were found

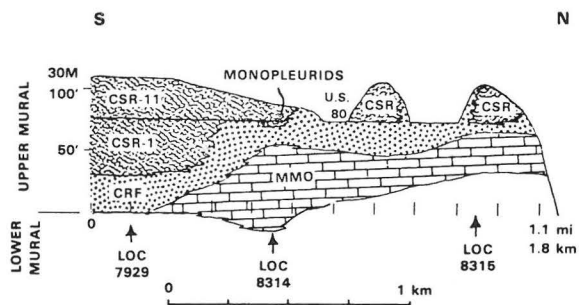


Figure 8. South-north cross section through reefs at Paul Spur -- Scott's localities 7929, 8314, and 8315 (from Scott, 1979). Facies are: CRF, coral-rudist fragment; CSR-1 and 11, coral-stromatolite-rudist reefs 1 and 2; MMO, mollusk-miliolid-orbitolinid wackestone-packstone.

filling internal cavities in shells (see also Petta, 1977). Laminar encrusting red algae, including squamariacean red algae ... are common, but generally thin and discontinuous. They may have played a minor binding role. Several varieties of problematic encrusting algae, encrusting oysters and worm tubes are all common. Sparse accessory organisms include branched and solitary corals, *Orbitolina*, *Coskinolina*, some miliolids, ostracods and gastropods. Stromatoporoids, an important component of other Lower Cretaceous reefs, are rare

Observations of many of these accessory organisms, borings, and sediment produced by sponges as they excavate borings require a good hand lens and an "elbows and knees-nose to the outcrop" position.

The *Microsolena*-stromatolite community is interpreted by Warzeski (1983, p. 136) to represent "an upper reef-slope framework stage in the large patch reefs at Paul Spur and elsewhere." He further interprets these communities to have formed below storm-wave base. His reasoning for this interpretation is as follows (1983, p. 136-137):

This interpretation is based upon 1) the consistent low position of coral-stromatolite framestone in the bank sequences, 2) the lack of breakage of the thin, fragile plates of *Microsolena*, and 3) pelagic microfossils found in flank sediments of the Paul Spur reefs. Close examination of the exceptional exposures at Paul Spur indicates that laminar *Microsolena* grew as large "bushes" with an overall conical form It branched in a pattern reminiscent of some of the bushier *Acropora palmata* encountered on Recent coral reefs. However, *Acropora palamata*, a shallow, high-energy coral, is seldom found to be in place in studies of the internal structure of recent reefs (Shinn, 1962), and in Pleistocene reefs exposed in Barbados. They are typically broken and often overturned or otherwise displaced. Yet the much thinner, presumably more fragile *Microsolena* branches are rarely found broken. *Microsolena* bushes clearly cannot have been exposed to significant wave energy.

The reef core facies grades into the flanking C-R fragment facies. This facies is well exposed to the west of the high part of the cliff. Scott sampled the flanking beds at five stations over a distance of 139 feet (42 m) to determine the relative abundance of fossils in the wackestones and packstones (Figure 7). At this locality the facies also includes contributions from mollusks, echinoids, brachiopods, and *Orbitolina*. Although not obvious in Figure 7, the C-R fragment facies may also grade into the M-M-O facies. See the complete lithologic description of the "Coral-Rudist Fragment Packstone -- Reef Flank" facies in the supplement (Scott, 1979).

The reef core and flanking facies can be studied up close in the lower cliff faces at the top of the slope. A short hike around the west side crosses the flanking beds and provides interesting fossil collecting and photography before one reaches U.S. 80.

Northern Butte

Three small fault blocks make up the northern butte (Figure 9). The upper Mural Limestone, which dips westerly at 15-35°, is readily visible on the backslope of each block from U.S. 80. This backslope is not a bedding surface, but instead, because of erosion, displays the subfacies that existed late in the development of the reef. The irregular surface contains some of the most spectacular views of organism-sediment relationships in the reef core. Just beyond the ridge top is a cliff that strikes north-northwest. Lower Mural Limestone beds form the slope below the cliff. The middle and south blocks provide the best views.

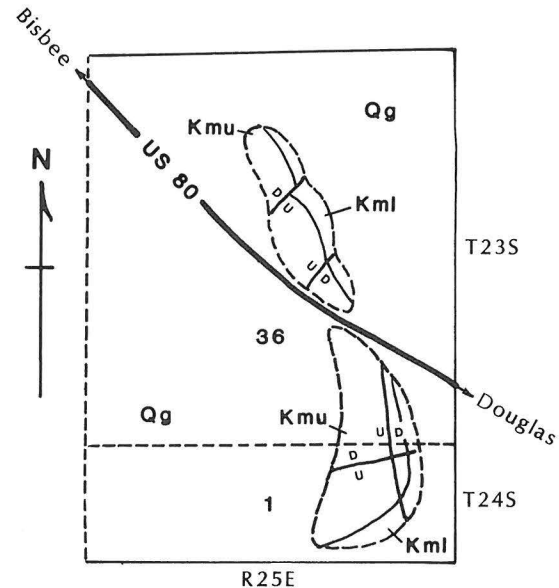


Figure 9. Stop 2. Geologic map of the north end of Paul Spur ridge adjacent to U.S. 80. Kml and Kmu = lower and upper Mural Limestone, respectively; Qg = Quaternary gravel, sand, and mudstone; strike and dip symbols purposely omitted, but bedding dips westerly at 15° to 35°; scale width of section 36 is 5016 feet (1529 m).

Roybal (1979, 1981) mapped the backslope of the middle block in detail and described four major facies (1981, p. 55):

- 1) The coral facies -- a reef front area dominated by a variety of corals. The corals acted as a baffle to the waves and created microhabitats in which other organisms, such as a single rudist, could live.
- 2) The *Microsolena*-stromatolite facies -- a solid framework of limited diversity. This laminar coral and algal buildup created the reef crest.
- 3) The two rudist subfacies, *Petalodontia* and caprinid-dominated by their respective rudists. These form thickets behind the *Microsolena*-stromatolite facies in protected areas of the reef flat and back reef.

- 4) The molluscan debris facies -- subrounded molluscan debris. This facies is present on almost every side of the reef core. Sediments were derived from the reef core.

The eroded surface exposes the facies ideally for photography. A trail has been flagged so that interested persons can take advantage of the afternoon sun. Use Figures 5, 6, and 13 from Roybal's 1981 paper (see the supplement) as an additional guide.

An equally spectacular view of the facies can be studied in the cliff face below the ridge top. To reach this cliff exposure, descend the slope trending northeast between the middle and south blocks and then follow the trail to the north to the flagged point. See Warzeski's (1983, p. 335) measured section in the supplement.

The south block is bounded on the east by low to high cliff exposures. However, the cliff can be climbed easily by following the flagged route. This route zigzags through the coral facies of the reef front and the *Microsolena*-stromatolite facies of the reef crest. The trail ends at the top of the cliff on the eroded backslope. Reef-flat and back-reef sediment-organism relations can be studied in three dimensions. Especially interesting are the thickets formed by the monopleurid and caprinid rudists. A short hike around the entire south block is recommended just to appreciate the transitional nature of the reef facies. In all locations, the photography is excellent.

Beds in the mollusk-miliolid-orbitolinid facies crop out along the base of the cliff on the east side of the butte and in the roadcut on the south side of U.S. 80 about 200 feet (61 m) east of stop 2.

From stop 2 we proceed directly to Douglas. The highway crosses the southern end of the Sulphur Springs Valley. To the south in Mexico the light-gray Mural Limestone beds stand out on the flanks of the Sierra Anibacachi. The intersection of U.S. 80 and U.S. 666 is 1 mile (1.6 km) west of Douglas; U.S. 666 traverses the Sulphur Springs Valley to the north and connects with I-10 just west of the Willcox Playa. The Phelps Dodge Corporation smelter, which is now closed, can be viewed on the south side of the highway.

GEOLOGIC HIGHLIGHTS -- DOUGLAS TO STOP 3

Stop 3 is located 25 miles (40 km) due east of Douglas in Guadalupe Canyon. The total road mileage is 34 miles (55 km) when measured from downtown Douglas. A mounted copy of the eastern half of the "Tectonic Map of Southeast Arizona" (Drewes, 1980) is available for review of the geology along the route. Because this is the first large organized field trip to travel the roads into Guadalupe Canyon, a road log (slightly modified from Schreiber, 1986) follows (all distances are given in miles).

- 0.0 Leave Gadsden Hotel parking lot; head east on 11th Street, crossing G Street (the main street in Douglas); proceed to A Avenue; turn left (north) on A Avenue and travel four blocks to 15th Street.

0.9

- 0.9 Turn right (east) on 15th Street, which becomes the Geronimo Trail; A Avenue School is on the left at the turn; two large water tanks are

ahead on the left side of the avenue after you make the turn; proceed east on 15th Street; WATCH FOR CHILDREN PLAYING -- this is a school and residential area.

1.9

- 2.8 Douglas Municipal Airport road on right. The Perilla Mountains fill the horizon at 10 to 11:30 o'clock. H. Drewes (1980) has mapped chiefly Cretaceous Bisbee Group sedimentary rocks, Tertiary volcanics, and Pleistocene to Pliocene basalts in the Perillas.

1.5

- 4.3 D-Hill on right at 1 o'clock is mapped by Drewes (1980) as Tertiary basalt(?). The road crosses Pennsylvanian-Permian sedimentary rocks behind D-Hill; Bisbee Group rocks and Laramide intrusives crop out south of road for the next 2.5 miles.

0.9

- 5.2 End of pavement. The Geronimo Trail is a well-maintained county road.

3.1

- 8.3 Knob/neck at 2 o'clock is a Laramide intrusive (Drewes, 1980).

1.7

- 10.0 Sharp curves and hills coming up -- SLOW DOWN! Watch for cattle guards and cattle on road or alongside road.

1.0

- 11.0 Hills to left or north include Bisbee Group sedimentary rocks and Tertiary volcanics. The road to the right leads into a drainage where Bisbee Group limestones and shales crop out.

1.8

- 12.8 A view of the San Bernardino Valley is coming up at 11 o'clock.

0.7

- 13.5 Entrance to Rocker M Ranch on left.

1.9

- 15.4 Good view of the San Bernardino volcanic field, which is composed of Pleistocene to Pliocene basalts. The road now descends into the Silver Creek drainage, which flows into Mexico.

1.1

- 16.5 Cattle guard; road to left or north leads into the malpais country.

1.4

- 17.9 Narrow bridge over Silver Creek. This bridge is a few hundred yards north of the U.S.-Mexico border. Basalt crops out north and south of

- road; to the south for the next 1/2 mile, modern floodplain sediments are in contact with the basalt.
- 0.9
- 18.8 Fork in road; keep left on Geronimo Trail. The road to the right leads to the old Slaughter Ranch which is now the San Bernardino National Historical Landmark. The road now heads north-east.
- 1.3
- 20.1 The hills at 2 o'clock are chiefly Pennsylvanian-Permian Earp Formation, Colina Limestone, and Epitaph Dolomite rocks. The hills from 12 to 2 o'clock are the southern end of the Peloncillo Mountains where Tertiary volcanics cover up Bisbee Group carbonate and clastic rocks.
- 1.4
- 21.5 Road to left leads to Malpais Ranch. The road ahead turns south towards the border and then east; basalt crops out on slopes, on small hills, and in wash.
- 0.8
- 22.3 Entering Black Draw; bridge ahead.
- 3.5
- 25.8 Road fork; keep right to enter Guadalupe Canyon; Geronimo Trail continues to the left; bench mark in V of road has an elevation of 3967 feet above MSL.
- 1.9
- 27.7 Entrance to Magoffin Ranch/Guadalupe Canyon Ranch.
- 0.2
- 27.9 Peloncillo Mountains are straight ahead. The gray cliffs are formed by the upper Mural Limestone.
- 1.5
- 29.4 Two exploration wells have been drilled adjacent to this road. The Thomson No. 2 State well was drilled to a depth of 802 feet (244 m) in December 1961 and bottomed in Permian(?) carbonates. The Guadalupe No. 1 State well was plugged and abandoned in December 1971 after penetrating the Bolsa Quartzite (Cambrian) at a depth of 5545 feet (1690 m).
- 0.3
- 29.7 Road to right leads to top of hill and the Guadalupe No. 1 State well location; watch for cattle guard ahead.
- 0.4
- 30.1 Ranch road to left leads into the Peloncillos. The Pickhandle Hills are at 11 o'clock.
- 0.9

- 31.0 Cattle guard; corral on right. The ranch road below cattle guard leads to the Earp-Colina-Epitaph outcrops on the hill to the south; south toe of hill is in Mexico.
- 0.8
- 31.8 Excellent view of the Pickhandle Hills. The Epitaph Dolomite is in thrust contact with the Earp Formation and Colina Limestone.
- 0.7
- 32.5 View of the Mexican Saddlehorn -- a Mural Limestone patch reef and the underlying lower Mural beds.
- 1.2
- 33.7 Stop 3. Cattle guard opposite the Mexican Saddlehorn. The Tertiary volcanics at 12 o'clock are in Arizona and New Mexico, whereas the hills at 2 o'clock are in old Mexico. Mural Limestone cliffs crop out at 11 o'clock. Park on right side of road.

STOP 3. MURAL LIMESTONE STRATIGRAPHY IN GUADALUPE CANYON

The Lower Cretaceous rocks in the extreme southeastern corner of Cochise County have been studied in detail only recently. In addition to the thesis research of Grocock (1975), Ferguson (1983), and Malvey (1985), Scott's (1979) localities 8326 and 8327 are located in the Guadalupe Canyon area. In an earlier study Stoyanow (1949, p. 27-29) briefly described sections exposed in the Guadalupe Canyon area near Baker Springs and on the McDonald Ranch near Sycamore Creek about 6 miles (9.7 km) north of stop 3. Cooper's (1959) "Reconnaissance Geologic Map of Southeastern Cochise County, Arizona" was the first useful geologic map of this corner of the state. Hayes (1982) refined the Cretaceous stratigraphy and faulting in the Guadalupe Canyon area as part of a larger mapping project along the Arizona-New Mexico border.

We are now located in the S 1/2 NE 1/4, sec. 17, T. 34 S., R. 32 E., Guadalupe Canyon quadrangle, Arizona-New Mexico (15-minute series, 1958) and but a few hundred feet north of Scott's (1979) locality 8326.

The Mexican Saddlehorn is actually a small erosional remnant of a coral-algal-rudist patch reef and associated facies (Figure 10). Steep cliffs surround the patch reef, but climbing is easy to mildly difficult in a few places so the rocks may be examined up close. Good exposures of the "oyster packstone" and "oolitic packstone" shown in Figure 10 may be found on the gentle north slope and in small drainages to the east and west. The contact between the lower and upper Mural is well exposed on three sides.

A partial section of the lower Mural Limestone crops out in many small drainages on the southeast-facing slope below the butte. The section is dominated by quartz sandstone and siltstone, but includes many thin to thick limestone beds; overall, the section is very fossiliferous. See the supplement for a measured section.

The main purpose of stop 3 is to study the entire Mural Limestone section in these outcrops because the lower to upper Mural transition can be viewed so clearly. A second purpose is to traverse the thick lower Mural section that lies to the south of the butte.

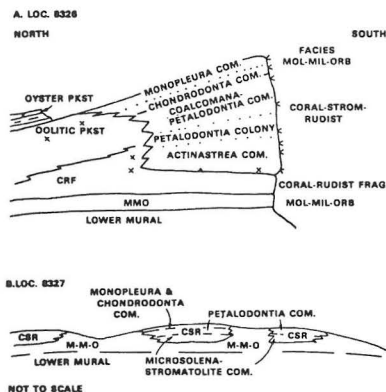


Figure 10. Schematic interpretation of facies and paleocommunities in the Guadalupe Canyon area (from Scott, 1979). Scott's (1979) locality 8326 is part of stop 3. Locality 8327 is 2-1/4 miles (3.6 km) to the northeast. The height of the south cliff face at locality 8326 is about 10 m.

Ferguson (1983) first recognized the greater thickness of this section relative to other sections to the west in the Bisbee area. He later commented as follows (Ferguson, 1986):

Exposures of Bisbee Group strata in the Guadalupe Canyon area consist predominantly of the Morita Formation and the Mural Limestone. The Mural Limestone section is greatly expanded from the type locale, and the boundaries of the upper and lower members as defined by Ransome (1904) are difficult to extend into the area. While the upper member remains uniform in thickness (50 meters), the lower member increases from 120 to 250 meters. Located within this expanded section is a prominent group of massive, cliff-forming, carbonate beds averaging 10 and locally exceeding 20 meters in thickness. The beds consist of fossiliferous and intra-clastic lime wackestone, and oncolite lime packstone. Hemispheroidal, ceroid corals (*Actinastrea?*) and large branching, ceroid corals are locally abundant. These massive carbonates crop out 32 kilometers to the west in the southern Perilla Mountains where they have thinned to 5 meters. The beds have not been described at the type section, and are inferred to pinch-out between the southern Perilla Mountains and the type locale 43 kilometers to the west. The areal extent of these carbonate beds is not known, but they would be expected to thicken south-eastward into the Chihuahua Trough. The similarity between these carbonates and those of the upper member of the Mural suggest that they represent two tongues that thicken and coalesce into a single unit to the southeast The thick, correlative, carbonate-dominated section in the Big Hatchet Mountains of southwestern New Mexico (U-Bar Formation) supports this inference.

Ferguson (1986) further pointed out that the massive carbonates "represent deposition in a marine environ-

ment, free of clastic influx, prior to such deposition at the type locale" and thus supports Hayes' (1970b) paleogeographic reconstructions "depicting the occurrence of a northwesterly migrating Aptian-Albian transgression through the region." See the supplement for measured sections of these massive carbonate beds.

This thick section stops near the south side of the Mexican Saddlehorn and appears to be continuous with the lower Mural beds on the east side, but outcrops do not exist to establish if this is the case.

In summary, stop 3 affords an unusual opportunity to view the transition from lower Mural mixed clastics and limestones to upper Mural limestones of a patch reef and associated facies. Outcrops are mostly well exposed and provide excellent collection opportunities of diverse rock types and fossils. The geology and Guadalupe Canyon are also very photogenic.

From stop 3 we head back a few miles to the Guadalupe Canyon Ranch -- a working cattle ranch -- for some western hospitality before returning to Douglas.

GEOLOGIC HIGHLIGHTS — DOUGLAS TO STOP 4

Stop 4 is located at the abandoned lime quarry at Lee Siding northeast of Douglas on U.S. 80. The distance to the locked gate on U.S. 80 via 11th Street-A Avenue-U.S. 80 is 8.9 miles (14.3 km). The Perilla Mountains are on the right or east as we travel northeast. To the northwest is the broad expanse of the southern half of the Sulphur Springs Valley.

The layered rocks of the higher slopes and peaks of the Perilla Mountains are principally Miocene and upper Oligocene extrusive rhyolite and rhyodacite (Drewes, 1980). These volcanics cover Upper Cretaceous "lowest Cordilleran (Laramide) sedimentary rocks," which include conglomerate, sandstone, and siltstone and "some red beds, fossiliferous black shale, and tuffaceous rocks" (Drewes, 1980). Less obvious are the Bisbee Group rocks that crop out on the lowest slopes and in the flatter grasslands adjacent to U.S. 80. The Bisbee Group rocks consist of typical lower and upper Mural lithologies.

STOP 4. MURAL PATCH REEF AT LEE SIDING QUARRY

The lime quarry at Lee Siding is located in the upper Mural Limestone. Quarrying activities ceased more than 50 years ago, and because entrance to the quarry was restricted during the years, the site is essentially as it was left. The remarkably clean quarry floor is in the mollusk-miliolid-orbitolinid facies of Scott (1979). Lower Mural beds make up the gentle slope around the steeper sides of the conical hill.

Although Grocock (1975) included a measured section from this locality in his thesis and discussed other aspects of the stratigraphy, Scott (1979) first described the reef core and flanking beds (Figure 11). More recently Monreal (1985) mapped the entire hill in detail and described the diagenesis of the upper Mural beds. We will drive up to the quarry floor to view the stratigraphy. This stop is a short but significant one because of the opportunity to view a vertical face that cuts across the reef core and flanking beds.

The quarry face exposes coral-stromatolite-rudist boundstone and packstone and coral-rudist packstone and grainstone facies on the north and northeast sides (Figure 12). Beds of the mollusk-miliolid-orbitolinid wackestone and packstone facies are exposed in the west-trending face and can be seen grading laterally into and overlying the coral-rudist packstone and

ACKNOWLEDGMENTS

We acknowledge with deep appreciation the contributions of past and recent researchers of Mural Limestone stratigraphy, paleontology, and petrography in southeastern Arizona. Philip T. Hayes, now retired from the U.S. Geological Survey, deserves credit for first building a sound foundation for subsequent researchers. Jo Ann Overs, premier word processor, contributed her skills to the final manuscript. Finally, we thank Mary, John, and Matt Magoffin, ranchers in Guadalupe Canyon, for their many courtesies over the years.

REFERENCES CITED

- Anderson, R.E., 1971, Thin skin distension in Tertiary rocks of southwestern Nevada: Geological Society of America Bulletin, v. 82, p. 43-58.
- Balcer, R.A., 1984, Stratigraphy and depositional history of the Pantano Formation (Oligocene-early Miocene), Pima County, Arizona [M.S. thesis]: Tucson, University of Arizona, 107 p.
- Bilodeau, W.L., and Lindberg, F.A., 1983, Early Cretaceous tectonics and sedimentation in southern Arizona, southwestern New Mexico, and northern Sonora, Mexico, *in* Reynolds, M.W., and Dolly, E.D., eds., Mesozoic paleogeography of the west-central United States: Society of Economic Paleontologists and Mineralogists, Rocky Mountain Section, Rocky Mountain Paleogeography Symposium 2, p. 173-188.
- Cooper, J.R., 1959, Reconnaissance geologic map of southeastern Cochise County, Arizona: U.S. Geological Survey Mineral Investigations Field Studies Map MF-213, scale 1:125,000.
- Damon, P.E., Lynch, D.J., and Shafiqullah, M., 1984, Cenozoic landscape development in the Basin and Range Province of Arizona, *in* Smiley, T.L., and others, eds., Landscapes of Arizona, the geological story: Lanham, University Press of America, p. 175-206.
- Dickinson, W.R., Fiorillo, A.R., Hall, D.L., Monreal, Rogelio, Potochnik, A.R., and Swift, P.N., 1987, Cretaceous strata of southern Arizona, *in* Reynolds, S.J., and Jenney, J.P., eds., Geology of Arizona: Arizona Geological Society Digest (in press).
- Dickinson, W.R., Klute, M.A., and Swift, P.N., 1986, The Bisbee Basin and its bearing on late Mesozoic paleogeographic and paleotectonic relations between the Cordilleran and Caribbean regions, *in* Abbott, P.L., ed., Cretaceous stratigraphy, western North America: Society of Economic Paleontologists and Mineralogists, Pacific Section, p. 51-62.
- Drewes, H., 1980, Tectonic map of southeast Arizona: U.S. Geological Survey Miscellaneous Investigations Series Map I-1109, scale 1:125,000.
- Dunham, R.J., 1962, Classification of carbonate rocks according to depositional texture, *in* Ham, W.E., ed., Classification of carbonate rocks: American Association of Petroleum Geologists Memoir 1, p. 108-121.
- Ferguson, R.C., 1983, Petrography, depositional environments, and diagenesis of Bisbee Group carbonates, Guadalupe Canyon area, Arizona [M.S. thesis]: Tucson, University of Arizona, 91 p.
- _____, 1986, Lower Cretaceous stratigraphy, Guadalupe Canyon area, Cochise County, Arizona [abs.], *in* Schreiber, J.F., Jr., ed., Frontiers in geology and ore deposits of the Southwest; Lower Cretaceous coral-algal-rudist reefs in southeast Arizona: Arizona Geological Society, Field Trip Guidebook #13, p. 55-57.
- Gray, R.S., 1967, Petrography of the upper Cenozoic non-marine sediments in the San Pedro Valley,

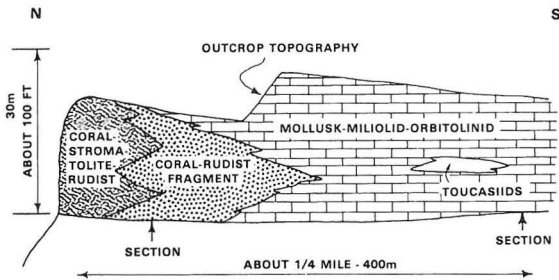


Figure 11. North-south cross section of reef at Lee Siding — Scott's locality 8325 (from Scott, 1979).

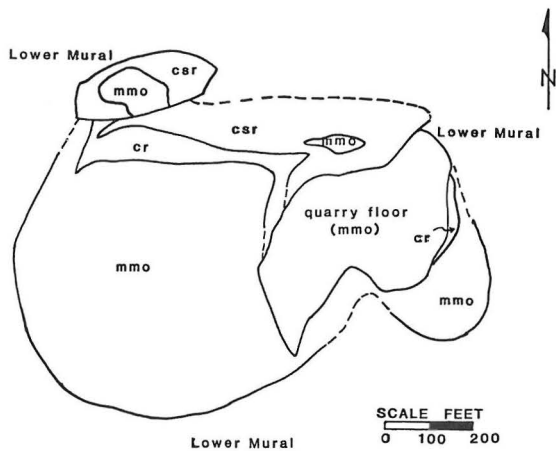


Figure 12. Generalized facies map of the upper Mural Limestone at the Lee Siding quarry (from Monreal, 1985). Facies are: csr - coral-stromatolite-rudist boundstone and packstone; cv - coral rudist packstone and grainstone; mmo - mollusk-miliolid-Orbitolina wackestone and packstone.

grainstone facies. Monreal (1985) measured a total thickness of 33 m for the mollusk-miliolid-orbitolinid wackestone and packstone facies.

Weathering of the quarry face and abandoned rock piles has emphasized the texture of the boundstones, wackestones, and packstones. We do not recommend climbing the steeper faces since the limestone is so broken up by numerous fractures, joints, and weathering along bedding planes and is thus very treacherous. Instead, limit your observations to the rock piles nearer the quarry floor.

GEOLOGIC HIGHLIGHTS — EXIT ROUTE TO TUCSON

The return trip to Tucson will be made via U.S. 80 through Tombstone to Benson and I-10. This route will permit viewing of the Bisbee Group rocks in the northern Mule Mountains and the extensive outcrops of upper Paleozoic rocks in the Government Butte and Tombstone Hills areas. Upon leaving Tombstone, we enter the San Pedro Valley again. The Dragoon Mountains will be on the right for most of the distance to Benson.

- Arizona: *Journal of Sedimentary Petrology*, v. 37, p. 774-789.
- Grocock, G.R., 1975, Stratigraphy and petrography of the upper member of the Mural Limestone in southeast Cochise County, Arizona [M.S. thesis]: Boulder, University of Colorado, 125 p.
- Hayes, P.T., 1970a, Mesozoic stratigraphy of the Mule and Huachuca Mountains, Arizona: U.S. Geological Survey Professional Paper 658-A, 28 p.
- _____ 1970b, Cretaceous paleogeography of southeastern Arizona and adjacent areas: U.S. Geological Survey Professional Paper 658-B, 42 p.
- _____ 1982, Geologic map of Bunk Robinson Peak and Whitmire Canyon Roadless Areas, Coronado National Forest, New Mexico and Arizona: U.S. Geological Survey Miscellaneous Field Studies Map MF-1425-A, scale 1:62,500.
- Hayes, P.T., and Landis, E.R., 1964, Geologic map of the southern part of the Mule Mountains, Cochise County, Arizona: U.S. Geological Survey Miscellaneous Geologic Investigations Map I-418, scale 1:48,000.
- Hayes, P.T., and Raup, R.B., 1968, Geologic map of the Huachuca and Mustang Mountains, southeastern Arizona: U.S. Geological Survey Miscellaneous Geologic Investigations Map I-509, scale 1:48,000.
- Izett, G.A., 1981, Volcanic ash beds; recorders of upper Cenozoic silicic pyroclastic volcanism in the western United States: *Journal of Geophysical Research*, v. 86, no. B11, p. 10200-10222.
- Johnson, N.M., Opdyke, N.D., and Lindsay, E.H., 1975, Magnetic polarity stratigraphy of Pliocene-Pleistocene terrestrial deposits and vertebrate faunas, San Pedro Valley, Arizona: *Geological Society of America Bulletin*, v. 86, p. 5-12.
- Kauffman, E.G., and Sohl, N.F., 1974, Structure and evolution of Antillean Cretaceous rudist frameworks: *Verhandlungen der Naturforschenden Gesellschaft in Basel*, v. 84, p. 399-467.
- Lindsay, E.H., 1978, Late Cenozoic vertebrate faunas, southeastern Arizona: New Mexico Geological Society, 29th Field Conference, Guidebook, p. 269-275.
- Lindsay, E.H., and Tessman, N.T., 1974, Cenozoic vertebrate localities and faunas in Arizona: *Journal of the Arizona Academy of Science*, v. 9, p. 3-24.
- Malvey, W.E., 1986, Depositional environments and diagenesis of the lower Mural Limestone (Lower Cretaceous), southeastern Arizona [abs.], in Schreiber, J.F., Jr., ed., *Frontiers in geology and ore deposits of the Southwest; Lower Cretaceous coral-algal-rudist reefs in southeast Arizona*: Arizona Geological Society, Field Trip Guidebook #13, p. 59-60.
- Monreal, R., 1985, Lithofacies, depositional environments, and diagenesis of the Mural Limestone (Lower Cretaceous), Lee Siding area, Cochise County, Arizona [M.S. thesis]: Tucson, University of Arizona, 100 p.
- _____ 1986, Lithofacies, depositional environments, and diagenesis of the Mural Limestone (Lower Cretaceous), Lee Siding area, Cochise County, Arizona [abs.], in Schreiber, J.F., Jr., ed., *Frontiers in geology and ore deposits of the Southwest; Lower Cretaceous coral-algal-rudist reefs in southeast Arizona*: Arizona Geological Society, Field Trip Guidebook #13, p. 58.
- Petta, T.J., 1977, Diagenesis and geochemistry of a Glen Rose patch reef complex, Bandera County, Texas, in Bebout, D.G., and Loucks, R.G., eds., *Cretaceous carbonates of Texas and Mexico, applications to subsurface exploration*: Texas Bureau of Economic Geology Report of Investigations Number 89, p. 138-167.
- Proffitt, J.M., 1977, Cenozoic geology of the Yerington district, Nevada: *Geological Society of America Bulletin*, v. 88, p. 247-266.
- Ransome, F.L., 1904, The geology and ore deposits of the Bisbee quadrangle, Arizona: U.S. Geological Survey Professional Paper 21, 168 p.
- Roybal, G.H., 1979, Facies relationships in a patch reef of the upper Mural Limestone in southeastern Arizona [M.S. thesis]: Tucson, University of Arizona, 76 p.
- _____ 1981, Facies development in a Lower Cretaceous coral-rudist reef (Mural Limestone, southeast Arizona): *The Mountain Geologist*, v. 18, p. 46-56.
- Schreiber, J.F., Jr., ed., 1986, *Frontiers in geology and ore deposits of the Southwest; Lower Cretaceous coral-algal-rudist reefs in southeast Arizona*: Arizona Geological Society, Field Trip Guidebook #13, 75 p.
- Scott, R.W., 1979, Depositional model of Early Cretaceous coral-algal-rudist reefs, Arizona: *American Association of Petroleum Geologists Bulletin*, v. 63, p. 1108-1127.
- _____ 1981, Biotic relations in Early Cretaceous coral-algal-rudist reefs, Arizona: *Journal of Paleontology*, v. 55, p. 463-478.
- Scott, R.W., and Brenckle, P.L., 1977, Biotic zonation of a Lower Cretaceous coral-algal-rudist reef, Arizona, in *Proceedings, 3rd International Coral Reef Symposium*: Miami, Rosentiel School of Marine and Atmospheric Science, University of Miami, p. 183-189.
- Shinn, E.A., 1962, Spur and groove formation on the Florida reef tract: *Journal of Sedimentary Petrology*, v. 33, p. 281-303.
- Stoyanow, A., 1949, Lower Cretaceous stratigraphy in southeastern Arizona: *Geological Society of America Memoir* 38, 169 p.
- Warzeski, E.R., 1979, Lower Cretaceous carbonate shelf in southeastern Arizona and northeastern Sonora, Mexico [abs.]: *American Association of Petroleum Geologists Bulletin*, v. 63, p. 547-548.
- _____ 1983, Facies patterns and diagenesis of a Lower Cretaceous carbonate shelf; northeastern Sonora and southeastern Arizona [Ph.D. thesis]: Binghamton, State University of New York, 401 p.
- _____ 1986, Stratigraphy of the Mural Limestone; a Lower Cretaceous carbonate shelf in Arizona and Sonora, in Rodriguez-Castaneda, J.L., and others, *Comite organizador, nuevas aportaciones a la geologia de Sonora*: Instituto de Geologia-UNAM, Estacion Regional del Noreste, Hermosillo, Sonora, p. 25.